UNIVERSIDADE DE SÃO PAULO

MUSEU DE ZOOLOGIA

Vinícius José Carvalho Reis

Diversity of the genus *Trichomycterus* Valenciennes, 1832 (Siluriforms, Trichomycteridae) in the Rio Doce basin: a systematic study integrating phenotypes, DNA and classical taxonomy

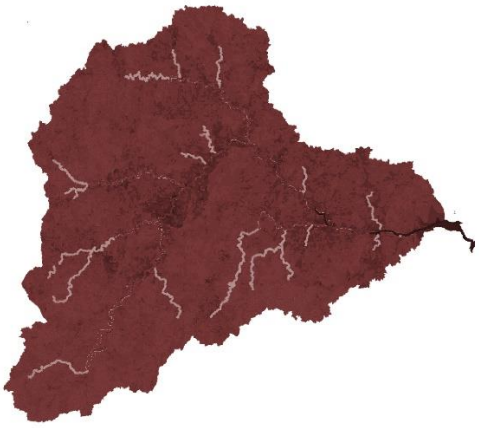

São Paulo

2018

Vinícius José Carvalho Reis

Diversity of the genus *Trichomycterus* Valenciennes, 1832 (Siluriforms, Trichomycteridae) in the Rio Doce basin: a systematic study integrating phenotypes, DNA and classical taxonomy

Dissertation Presented to the Graduate Program of the Museu de Zoologia da Universidade de São Paulo to obtain the degree of Master of Science in Systematics, Animal Taxonomy and Biodiversity

Advisor: Prof. Dr. Mário de Pinna

São Paulo

2018

I do not authorize the reproduction and dissemination of this work in part or entirely by any electronic or conventional means.

This work is not a publication in the sense of the International Code of Zoological Nomenclature (ICZN)

Catalogação na Publicação

Serviço de Biblioteca e Documentação

Museu de Zoologia da Universidade de São Paulo

Reis, Vinícius José Carvalho

Diversity of the genus *Trichomycterus* Valenciennes, 1832 (Siluriforms, Trichomycteridae) in the Rio Doce basin: a systematic study integrating phenotypes./ Vinícius José Carvalho Reis; orientador Mario Cesar Cardoso de Pinna. São Paulo, 2018. 303 p.

Dissertação de mestrado – Programa de Pós-Graduação em Sistemática, Taxonomia e Biodiversidade, Museu de Zoologia, Universidade de São Paulo, 2018.

Versão original

1. *Trichomycterus*. 2. Siluriformes. 3. Rio Doce - Siluriformes. I. dePinna, Mario Cesar Cardoso, orient. II. Título.

CDU 597.551.4

Name: Reis, Vinícius J. C.

Title: Diversity of the genus *Trichomycterus* Valenciennes, 1832 (Siluriforms, Trichomycteridae) in the Rio Doce basin: a systematic study integrating phenotypes, DNA and classical taxonomy. Dissertation Presented to the Post-Graduate Program of the Museu de Zoologia da Universidade de São Paulo to obtain the degree of Master Science in Systematics, Animal Taxonomy and Biodiversity

Comissão Julgadora

Prof. Dr._____ Instituição:_____

Julgamento: _____ Assinatura: _____

Prof. Dr._____ Instituição:_____

Julgamento: _____ Assinatura: _____

Prof. Dr._____ Instituição:_____

Julgamento: _____ Assinatura: _____

For all who fight for nature and knowledge

Acknowledgements

Aqui estou escrevendo os agradecimentos pelo prazer que me foi dado em construir essa dissertação junto de cada pessoa que, de alguma forma, deixou seu legado nesta obra. Obviamente eu seria um tanto egoísta e quiçá tolo em dizer que a autoria deste trabalho é somente e plenamente minha. Assim sendo o digo que cada letra, frase, parágrafo aqui redigido é o reflexo de cada um dos muitos que passaram em minha vida.

Logo de início eu gostaria de agradecer a toda minha família em especial aos meus pais, Hérica e José do Carmo, pelo apoio sentimental, e pelos legados que somente vocês dois poderiam me oferecer: a moral, a educação, e especialmente nesta ocasião, a persistência para atingir meus objetivos sejam eles quais forem. Sem suas asas eu certamente não conseguiria voos tão altos como hoje.

Possuir o privilégio de realizar o mestrado em uma das melhores instituições de pesquisa brasileira em zoologia, o Museu de Zoologia da Universidade de São Paulo (MZUSP), não seria possível caso, hoje, um grande amigo não tivesse me acolhido e confiado plenamente em meu potencial, mesmo incialmente, inúmeras vezes, eu ter demonstrado minha "leigacidade" sobre o assunto que eu iria por dois anos perseguir. Ao meu grande orientador e educador Mário de Pinna eu muito agradeço. Agradeço não apenas pela adoção acadêmica a qual você me teve, mas por todos os conselhos sobre a vida e mundos. Sob sua orientação eu não apenas me torno um melhor biólogo e mestre, mas também uma melhor pessoa.

A todos meus amigos e colegas do Museu de Zoologia da USP pelos inúmeros conselhos acadêmicos e pessoais entre os cafezinhos do dia a dia (Michel Gianeti, Manuela Marinho, Priscila

Camelier, Illana Fichberg, Igor Mourão, João Gênova, Paulo Presti, Vitor Abraão, Fábio Pupo, Vinícius Espíndola, Murilo Pastana, Verônica Slobodian, Gustavo Ballen, Arthur de Lima, Luíz Peixoto, Fernando D'agosta, Aline Staskowian, Jaqueline Battilana, Mônica Ulyssea, Juliana Gualda, Elias Araujo, Rafael Dell'erba, Joel Lastra, Ernesto Aranda, Natália Friol, Dione Seripierri). Em especial para Priscila Camelier, Fernando D'agosta, Luís Peixoto, Aline Staskowian, Jaqueline Battilana, e Mônica Ulyssea pelas diversas chacoalhadas e discussões preciosíssimas. Ao Vitor Abraão pelo grandioso apoio técnico-científico na edição das imagens desta dissertação. Ao Murilo Pastana pelas discussões sobre espécies e suas delimitações.

Igualmente agradeço ao corpo docente e técnico do Museu de Zoologia da USP, dos quais sem o apoio e discussões essa dissertação não possuiria a mesma qualidade. Meus sinceros agradecimentos ao prof. Aléssio Datovo pelas discussões sobre a diversidade dos *Trichomycterus*; ao Michel Gianetti e ao Osvaldo Oyakawa, preciosos técnicos da sessão de peixes do MZUSP, pela ajuda no tombamento e alocação dos espécimes de *Trichomycterus* obtidos ao longo desse estudo; a Jaqueline Battilana pelo apoio técnico prestado no laboratório de análises moleculares do MZUSP; e a grandiosa bibliotecaria Dione Seripierri, pela preciosa ajuda na confecção da bibliografia desta obra.

Meus sinceros agradecimentos a Dra. Lynne Parente do National Museum of Natural History (NMNH) – Smithsonian Institution, por me acolher em uma das maiores instituições de pesquisa em história natural do mundo, e pelas sábias discussões em diversos assuntos sobre ictiologia. Agradeço pela oportunidade de ter estado e conhecido o NMNH. Estar presente entre renomados pesquisadores muito me acrescentou e expandiu meu conhecimento a cerca da ictiologia.

Gostaria de agradecer as pesquisadoras Dra. Luisa Sarmento-Soares e Dra. Thaís Volpi, pelo vital apoio nessa dissertação através das riquíssimas discussões sobre a taxonomia e diversidade do gênero *Trichomycterus* e pelo empréstimo/doação de material representante da bacia do Rio Doce no estado do Espírito Santo. Sem suas contribuições, esse estudo estaria severamente comprometido. Por todo apoio e ajuda sou extremamente grato a vocês.

Fundamentais para a conclusão desse estudo, gostaria de agradecer a todos os docentes, pesquisadores, curadores e técnicos de outras grandes instituições de pesquisa pelo apoio prestado na forma de doação/empréstimo de material, orientações e discussões acadêmicas, uso de equipamentos e infraestrutura. Obrigado a todos do Laboratório de Ictiologia de Ribeirão Preto – (LIRP) USP-Ribeirão Preto (em especial para o prof. Flávio Bochmann, prof. Ricardo Cardoso, e Malu Araújo); a todos da UNESP-Botucatu (em especial para o prof. Cláudio Oliveira, Guilherme Costa e Silva, Luz Ochoa); a todos do Museu Nacional do Rio de Janeiro - (MNRJ) (em especial para o prof. Marcelo Britto, prof. Cristiano Moreira, e Sérgio Santos); a todos do Museu de Biologia Mello Leitão - (MBML), hoje Instituto Nacional da Mata Atlântica (em especial para a Dr. Luisa Samento-Soares, Dr. Thaís Volpi, Juliana da Silva, Mari Morais); a todos do Museu de História Natural e do Laboratório de Genética Comparada da Pontifícia Universidade Católica de Minas Gerais – (PUCMG) (em especial para o Tiago Pessali e prof. Daniel Carvalho); a todos do laboratório de Sistemática Molecular (Beagle) da Universidade Federal de Viçosa (UFV) (em especial para o prof. Jorge Dergam, Késsia Souza, e Simone Duarte); a todos do National Museum of Natural History (NMNH) of the Smithsonian Institution (em especial para a Dra. Sandra Raredon, Dr. Jeff Cleiton, Dr. David Santana, Dra. Lynne Parente, Dr. David Johnson); a todos do Museum of Comparative Zoology (MCZ) – Harvard University (em especial para o Dr. Chao Labbish, Dr. Karsten Hartel, Dr. Andrew Williston); a todos do Field Museum of Natural History

(em especial para o Dr. Caleb McMahan). Agradeço grandemente pela oportunidade de ter conhecido todos vocês. Muito obrigado pelas agradáveis conversas, discussões acadêmicas e amizade.

Outras pessoas, fora e dentro da academia, contribuíram para esta dissertação através da amizade e companheirismo, atitudes das quais me fortaleceram em todos os segundos de minha caminhada até a conclusão deste presente estudo. Desses destaco a minha família de Viçosa escolhida a dedo pelo companheirismo, amor, sinceridade e confiança. Assim sendo obrigado "Lavando Roupa" por fazer parte de minha história e me dar forças para perseguir meus objetivos. De todas as amizades eu não poderia deixar de mencionar um nome, Rodolfo Vieira. Muitíssimo obrigado pela sua preciosa amizade e companheirismo o qual levo por toda vida. Ao longo de meu mestrado sempre tive a certeza de poder encontrar em você a força que precisei para seguir adiante.

Por fim, esta revisão das espécies pertencentes ao gênero *Trichomycterus* na bacia do Rio Doce, teve o apoio financeiro através da concessão de bolsa de mestrado pela Coordenação de Aperfeiçoamento de Pessoal de Nível Superior (CAPESP; vigência 07/2016 à 04/2017), pela Fundação de Amparo à Pesquisa do Estado de São Paulo (FAPESP 2016/25467-7; vigência 05/2017 à 09/2018) e também pela Bolsa Estágio de Pesquisa no Exterior (BEPE-FAPESP 2017/17332-7; vigência 01/2018 à 04/2018). A bolsa de mestrado foi vinculada ao projeto de auxílio "Integrando dados morfológicos e moleculares na sistemática de três subgrupos de Siluriformes: subfamília Copionodontinae (Trichomycteridae), gênero *Pimelodella* (Heptapteridae) e família Cetopsidae" (FAPESP 2015/26804-4; vigência 08/2016 à 07/2018), sob coordenação do prof. Dr. Mário C. C. de Pinna, que forneceu grande parte da infraestrutura utilizada na condução do presente estudo.

Luto

MUSEU NACIONAL
RIO DE JANEIRO

Without memory, there is no culture. Without memory,

there would be no civilization, no society, no future.

Elie Wiesel

General Abstract

The diversity of the genus *Trichomycterus* Valenciennes 1832 in the Rio Doce basin is investigated using conventional and modern morphology and DNA analyses. The work is presented in two Chapters. Chapter One, entitled "Diversity of the genus *Trichomycterus* Valenciennes, 1832 (Siluriforms, Trichomycteridae) in the Rio Doce basin: a systematic study integrating phenotypes, DNA and classical taxonomy" integratively analyzes specimens of the genus from the entire Rio Doce drainage and adjacent basins, both from available world-wide collections and from active sampling efforts. A combination of phenotypic and DNA (COI barcoding analysis) provides evidence for the existence of 14 species in the basin, 10 of which are new: *T. alternatus* Eigenmann, 1917; *T. argos* Lezama *et al.*, 2012; *T. "astromycterus"* sp. nov.; *T. "barrocus"* sp. nov.; *T. "brucutu"* sp. nov.; *T. brunoi* Barbosa & Costa, 2010; *T. immaculatus* (Eigenmann & Eigenmann, 1889)] *T. "illuvies"* sp. nov.; *T. "melanopygius"* sp. nov.; *T. "ipatinguensis"* sp. nov.; *T. "pussilipygius"* sp. nov.; *T. "sordislutum"* sp. nov.; *T. "vinnulus"* sp. nov; and *T. "tantalus"* sp. nov. . In addition, a lectotype is designated for *T. immaculatus* and the species is considered as a senior synonym of *Trichomycterus pradensis* Sarmento-Soares *et al*., 2005. Although remarkable, such increase in species number of *Trichomycterus* in a single drainage matches similar recent increments in some other Southeastern Brazilian basins, such as the Paraíba do Sul and Iguaçu. The kind of differentiation among species herein recognized varies, with some of them being well-differentiated in morphology but not in barcoding data, and others showing the opposite phenomenon. The geographical distribution of each of the 14 species is plotted in the Rio Doce basin. The wide geographical distribution of some species (*T. alternatus* and *T. immaculatus*) is explained against data from geomorphological processes and comparative information on their biology. Chapter two, "The type specimens of *Trichomycterus alternatus*

(Eigenmann, 1917) and *T. zonatus* (Eigenmann, 1918), with elements for future revisionary work (Teleostei, Siluriformes, Trichomycteridae)" focuses on the complex taxonomy, nomenclature and type material status of *T. alternatus* and *T. zonatus*. The type series of the two species are analyzed in detail, both in morphology and locality data. Osteological information was obtained with conventional and a new technique of radiographic stereo-triplets. Our new data elucidates their species distinctiveness, diagnostic characteristics, type localities and show that *T. zonatus* does not occur in the Rio Doce basin.

Keywords: Integrative taxonomy; Neotropical catfish; barcoding; species delimitation; biogeographical dispertion.

Resumo Geral

A diversidade do gênero *Trichomycterus* Valenciennes 1832 na bacia do Rio Doce é investigada utilizando métodos convencionais e modernos em análises morfológicas e moleculares. Os resultados desta dissertação são apresentados em dois capítulos. Capítulo um, intitulado "Diversity of the genus *Trichomycterus* Valenciennes, 1832 (Siluriforms, Trichomycteridae) in the Rio Doce basin: a systematic study integrating phenotypes, DNA and classical taxonomy" examinou espécimes pertencentes a este gênero encontrados no Rio Doce e em bacias adjacentes disponíveis em coleções nacionais e internacionais e coletados durante esta dissertação. O conjunto de dados obtidos através de análises morfológicas e moleculares (COI, DNA barcoding) revelou a existência de 14 espécies na bacia do Rio Doce, das quais 10 novas: *T. alternatus* Eigenmann, 1917; *T. argos* Lezama *et al.*, 2012; *T. "astromycterus"* sp. nov.; *T. "barrocus"* sp. nov.; *T. "brucutu"* sp. nov.; *T. brunoi* Barbosa & Costa, 2010; *T. immaculatus* (Eigenmann & Eigenmann, 1889)] *T. "illuvies"* sp. nov.; *T. "melanopygius"* sp. nov.; *T. "ipatinguensis"* sp. nov.; *T. "pussilipygius"* sp. nov.; *T. "sordislutum"* sp. nov.; *T. "vinnulus"* sp. nov; and *T. "tantalus"* sp. nov. Além disso, é designado um lectótipo para *T. immaculatus*, espécie aqui proposta como sinônimo sênior de *Trichomycterus pradensis* Sarmento-Soares *et al*., 2005. O acentuado incremento em número de espécies de *Trichomycterus* para uma única bacia segue um padrão de crescimento em biodiversidade conhecida do gênero para outras drenagens do sudeste brasileiro a exemplo do rio Paraíba do Sul e Iguaçu. Os tipos de diferenciação detectada entre as espécies aqui tratadas variam, com algumas bem corroboradas morfologicamente, porém muito similares ou indiferenciáveis em análise de DNA *barcoding*, e outras apresentando o fenômeno oposto. As distribuições geográficas de cada uma das 14 espécies são mapeadas com base em todo o material examinado. A ampla distribuição geográfica de algumas espécies (*T.*

alternatus and *T. immaculatus*) é explicada através de processos geomorfológicos e informações comparativas sobre suas biologias. O capítulo dois, “The type specimens of *Trichomycterus alternatus* (Eigenmann, 1917) and *T. zonatus* (Eigenmann, 1918), with elements for future revisionary work (Teleostei, Siluriformes, Trichomycteridae)” se concentra em esclarecer a complexa taxonomia, nomenclatura e o status do material tipo de *T. alternatus* e *T. zonatus*. As séries tipos das duas espécies foram minuciosamente analisadas tanto para morfologia como para suas respectivas localidades de proveniência. Informações osteológicas foram obtidas através de técnicas de radiografia convencionais e uma nova metodologia chamada *stereo triplets*. Os dados obtidos corroboram as respectivas espécies como distintas, e permitem uma avaliação precisa de seus respectivos caracteres diagnósticos e localidades tipo. Também se chegou à conclusão que *T. zonatus* não ocorre na bacia do Rio Doce.

Palavras-chaves: Taxonomia integrativa; bagres neotropicais; barcoding; delimitação de espécies; dispersão biogeográfica.

Table list

Chapter 1

Table 01. Cytochrome Oxydase Sub-unity I (COI) primer used to produce distance analyses among species of *Trichomycterus* in the Rio Doce and adjacent basins in this dissertation.

Table 02. *Trichomycterus* specimens which the COI gene was successfully sequenced and used in this dissertation. Abbreviation: **URD**, upper Rio Doce; **MRD**, middle Rio Doce; **LRD**, lower Rio Doce; **MZUSP**, Museu de Zoologia da Universidade de São Paulo; **MZUFV**, Museu de Zoologia João Moojen da Universidade Federal de Viçosa; **MBML**, Museu de Biologia Melo Leitão; **UNESP**, Universidade Estadual Paulista; **PUCMG**, Pontifícia Universidade Católica de Minas Gerais; **MNRJ**, Museu Nacional do Rio de Janeiro.

Table 03. Morphometric data of *Trichomycterus alternatus* based on comparative materials.

Table 04. Average of conspecific barcoding divergence average (%) within *Trichomycterus* species analyzed in this dissertation, based on the model Kimura-Two-Parameters (K2P) using the COI data matrix.

Table 05. Morphometric data of *Trichomycterus argos* based on type materials.

Table 06. Morphometric data of *Trichomycterus "astromycterus"*, sp. nov. based on type materials.

Table 07. Morphometric data of *Trichomycterus "barrocus"*, sp. nov. based on type materials.

Table 08. Morphometric data of *Trichomycterus "brucutu"*, sp. nov. based on type materials.

Table 09. Morphometric data of *Trichomycterus brunoi* based on comparative materials.

Table 10. Morphometric data of *Trichomycterus "illuvies"*, sp. nov. based on type materials.

Table 11. Morphometric data of *Trichomycterus immaculatus* based on type and comparative materials.

Table 12. Average of congeneric barcoding divergence (%) between *Trichomycterus* species analyzed in this dissertation, based on the model Kimura-Two-Parameters (K2P) using the COI data matrix.

Table 13. Morphometric data of *Trichomycterus "ipatinguensis"*, sp. nov. based on type and comparative materials.

Table 14. Morphometric data of *Trichomycterus "melanopygius"*, sp. nov. based on type and comparative materials.

Table 15. Morphometric data of *Trichomycterus "pussilipygius"*, sp. nov. based on type materials.

Table 16. Morphometric data of *Trichomycterus "sordislutum"*, sp. nov. based on type materials.

Table 17. Morphometric data of *Trichomycterus "tantalus"*, sp. nov. based on type materials.

Table 18. Morphometric data of *Trichomycterus "vinnulus"***,** sp. nov. based on type materials.

Chapter 2 -

Table 1. – Morphometric and meristic data of *Trichomycterus alternatus* based on type materials.

Table 2. - Morphometric and meristic data of *Trichomycterus zonatus* based on type materials.

Figure list

Chapter 1

Fig. 01 – Hydrographic map of Rio Doce basin and the hydrographic region of Barra Seca river. Source: IBGE and Agência Nacional de Águas (ANA): Hidrografia e limites das bacias.

Fig. 02 – *Trichomycterus alternatus*, topotypes (right, lateral view; left, dorsal view): (A) MZUSP123764_IV, 42.97 mm SL; (B) MZUSP123764_III, 44,42 mm SL; (C) MZUSP123763, 45.42 mm SL; (D) MZUSP 123761, 50.98 mm SL. Brazil, State of Minas Gerais: Rio Doce municipality. Photos by V. J. C. Reis.

Fig. 03 – Color pattern and morphology variation in *Trichomycterus alternatus*: (A) MZUSP110937, 65.24 mm SL; (B) MZUSP87832, 58.18 mm SL; (C) MZUSP94564, 58.46 mm SL; (D) MZUSP109311, 49.30 mm SL; (E) MZUSP121719, 40.94 mm SL; (F) MZUSP 109302, 53.55 mm SL; (G) MBML6200, 47.00 mm SL. Photos by V. J. C. Reis.

Fig. 04 – Color pattern and morphology variation in *Trichomycterus "tantalus"*, sp. nov. (right, lateral view; left, dorsal view): (A) MZUFV2565, 154.01 mm SL; (B) MZUSP123369 (holotype), 75.98 mm SL; (C), MZUSP123369, 74.82 mm SL. Photos by V.J. C. Reis.

Fig. 05 - Color pattern and morphology variation in *Trichomycterus "ipatinguensis"*, sp. nov. (right, lateral view; left, dorsal view): (A) MZUSP104702, 67.57 mm SL; (B) MZUSP 112277 92.86 mm SL; (C) MBML6223, 68.68 mm SL. Photos by V.J. C. Reis.

Fig. 06 - Color pattern and morphology variation in *T. immaculatus* as represented in paratypes of *Trichomycterus pradensis* (right, lateral view; left, dorsal view): (A) MNRJ28484, 48.44 mm SL;

(B) MNRJ28485, 39.80 mm SL; (C) MNRJ28488, 67.42 mm SL; (D) MNRJ28490, 67.44 mm SL. Photos by V. J. C. Reis.

Fig. 07 - Color pattern and morphology variation in *Trichomycterus immaculatus* from the Rio Doce basin (right, lateral view; left, dorsal view): (A) MZUSP123368, 56.25 mm SL; (B) MZUSP123357, 69.41 mm SL; (C) MZUSP123762, 91.03 mm SL; MZUSP123353, 69.72 mm SL. Photos by V.J.C. Reis.

Fig. 08 - Color pattern and morphology variation in *Trichomycterus "pussilipygius"*, sp. nov. (A) MZUSP 123339, 33.7 mm SL; (B) MZUSP123339, 35.3 mm SL; (C) MZUSP123339, 70.0 mm SL. Photos by V.J. C. Reis.

Fig. 09 - Color pattern and morphology variation in *Trichomycterus "vinnulus"*, sp. nov. (right, lateral view; left, dorsal view): (A) MZUSP123750, 38.91 mm SL; (B) MZUSP123750, 47.07 mm SL; (C) MZUSP123750, 54.00 mm SL; (D) MZUSP123750, 60.60 mm SL. Photos by V.J.C. Reis.

Fig. 10 – Geographical distribution of *Trichomycterus alternatus* in the Rio Doce basin; Black circle - type locality; white circle – non-type localities.

Fig. 11 – *Trichomycterus argos.* MZUSP 106274, paratype, (A, lateral; B, dorsal; C, ventral) 56.75 mm SL and (D, lateral; E, dorsal; F, ventral) 90.81 mm SL. Brazil, State of Minas Gerais: Araponga municipality, Parque Estadual da Serra do Brigadeiro. Photo by V.J.C. Reis.

Fig. 12 - Dorsal views of the cranium and Weberian complex of a) *Trichomycterus argos* (DZUFMG 067, 101 mm SL, paratype) and b) *Trichomycterus brasiliensis* (DZUFMG 064, 102,1 mm SL). Abbreviations: **AP**, autopalatine; **EP**, epioccipital; **FF**, frontal fontanels; **FR**, frontal; **IO**, tendon-bone infraorbital; **LE**, lateral ethmoid; **ME**, mesethmoid; **MX**, maxilla; **PM**, premaxilla; **PS**, posttemporosupracleithrum; **PT**, pterotic; **RF**, foramen for the ramus lateralis accessorius

facialis; **SC**, cephalic sensory canal; **SO**, tendon-bone supraorbital; **SPP**, sphenotic-prootic-pterosphenoid compound bone; **SU**, parietosupraoccipital; **WC**, Weberian capsule. Scale bar = 1cm. From Lezama *et al*., 2012.

Fig. 13 – *Trichomycterus brunoi*. MBML4308, 41.83 mm SL. Brazil, State of Minas Gerais: Alto Caparaó. Photos by V.J.C.R Reis.

Fig. 14 - Geographical distribution of *Trichomycterus argos*, *Trichomycterus brasiliensis* and *T. brunoi* in the Rio Doce basin. Legend: **Red triangle -** type locality of *T. argos*; **white square -** non-type locality of *T. brasiliensis*; **red circle -** holotype and paratype locality of *T. brunoi*; **black circle -** paratype locality of *T. brunoi*; **white circle -** non-type localities of *T. brunoi*.

Fig. 15 – *Trichomycterus "astromycterus"*, sp. nov. MZUSP123760, holotype, 51.47 mm SL. Brazil, Minas Gerais: Rio Doce municipality. Photos by V.J.C. Reis.

Fig. 16 – CT-Scan images of maxilla and palatine of *Trichomycterus "astromycterus"*, sp. nov., paratype, MZUSP123341; dorsal view, left side. Abbreviation: MX, maxila; AP, autopalatine.

Fig. 17 – CT-Scan images of jaws of *Trichomycterus "astromycterus"*, sp. nov., paratype, MZUSP123341. Anteroventral view. Dentary teeth, first row mostly narrowly incisiform near symphysis, with remaining teeth conical. Abbreviation: DEN, dentary; PM, premaxilla.

Fig. 18 - Geographical distribution of *Trichomycterus "astromycterus"*, sp. nov. in the Rio Doce basin. Red circle – holotype (MZUSP123760) and paratypes (ex-MZUSP123760); black circle - paratypes MZUSP 123341.

Fig. 19 – *Trichomycterus "barrocus"*, sp. nov. MBML2238, holotype, 79.83 mm SL. Brazil, State of Espírito Santo, Afonso Cláudio municipality. Photos by V.J.C. Reis.

Fig. 20 – Geographical distribution of *Trichomycterus "barrocus"*, sp. nov. in the Rio Doce basin. Black circle - holotype (MBML 2238) and paratypes (ex-MBML 2238).

Fig. 21 - *Trichomycterus "brucutu"*, sp. nov. MZUSP 87834, holotype, 103 mm SL. Brazil, State of Minas Gerais, Santo Antônio de Itambé municipality. Photo by V. J. C. Reis.

Fig. 22 – Geographical distribution of *Trichomycterus "brucutu"*, sp. nov. in the Rio Doce basin. Legend: **Black circle** - holotype (MZUSP 87834) and paratype (1 ex. MZUSP 87834) localities.

Fig. 23 – (A) *Trichomycterus brunoi* (UFRJ5658); (B) *Trichomycterus fuliginosus* (MN18177); (C) *Trichomycterus claudiae* (UFRJ5685); (D) *Trichomycterus mariamole* (UFRJ5400); (E) *Trichomycterus novalimensis* (MZUSP37145); (F) *Trichomycterus rubiginosus* (MZUSP34168); (G) *Trichomycterus brasiliensis* (UFRJ4834). Left jaw suspensorium and opercular series, lateral view. Abbreviations: **H**, hyomandibula; **I**, interopercle; **M**, meta pterygoid; **0**, opercle; **P**, preopercle; **Q**, quadrate. Scale bar 1 mm. From Barbosa & Costa, 2010.

Fig. 24 - *Trichomycterus "illuvies"*, sp. nov. MZUSP 112750, holotype, 45.04 mm SL; Brazil, Minas Gerais, Ferros municipality. Photo by V. J. C. Reis.

Fig. 25 - Geographical distribution of *Trichomycterus "illuvies"*, sp. nov. in the Rio Doce basin. Legend: Red circle - holotype (MZUSP 112750) and paratype (ex-MZUSP 112750) localities; black circle – paratype (MZUSP 110720).

Fig. 26 - *Trichomycterus immaculatus* MCZ 8300_4, lectotype, 123.2mm SL; Brazil, Minas Gerais, Juiz de Fora municipality. Photo by V. J. C. Reis.

Fig. 27 – Neighbor-Joining (NJ) dendrogram with K2P distance of the *Trichomycterus* species from the Rio Doce and some related basins (Jucuruçu, Itaúna, São Mateus, São Francisco, and

Cubatão). Terminals composed by code of specimens and drainage origin (see Table 12). Abbreviations: **URD**, upper Rio Doce; **MRD**, middle Rio Doce; **LRD**, lower Rio Doce; **JU**, Jucuruçú; **ITN**, Itaúna; **SM**, São Mateus; **SF**, São Francisco; **CT**, Cubatão.

Fig. 28 - Geographical distribution of *Trichomycterus immaculatus* in the Rio Doce, Paraíba do Sul, São Mateus, and Jucuruçú basins. Legend: **Red triangle -** lectotype and paralectotype locality of *T. immaculatus*; **black triangle** - paralectotype locality of *T. immaculatus*; **red circle -** Jucuruçu locality of *T. immaculatus* (holotype of *T. pradensis*); **black circle -** Jucuruçu localities of *T. immaculatus* (paratypes of *T. pradensis*); **white circle -** Rio Doce localities of *T. immaculatus*.

Fig. 29 - *Trichomycterus "ipatinguensis"*, sp. nov. MZUSP 112279, holotype, 67.57 mm SL; Brazil, State of Minas Gerais, Conceição do Mato Dentro municipality. Photo by V. J. C. Reis.

Fig. 30 - Geographical distribution of *Trichomycterus "ipatinguensis"*, sp. nov. in the Rio Doce basin. Legend: Red circle - holotype and paratype localities; black circle – paratype localities; white circle - non-type localities.

Fig. 31 - *Trichomycterus "melanopygius"*, sp. nov. MZUSP 110936, holotype, 97.7 mm SL; Brazil, State of Minas Gerais, Mariana municipality. Photo by V. J. C. Reis.

Fig. 32 - Geographical distribution of *Trichomycterus "melanopygius"*, sp. nov. in the Rio Doce basin. Legend: **Red circle** - holotype and paratype localities; **black circle** – paratype localities; **white circle** - non-type localities.

Fig. 33 - *Trichomycterus "pussilipygius"*, sp. nov., holotype, MZUSP 123339, 68.8 mm SL; Brazil, State of Minas Gerais, Santa Rita de Minas municipality. Photo taken by V. J. C. Reis.

Fig. 34 - Geographical distribution of *Trichomycterus "pussilipygius"*, sp. nov. in the Rio Doce basin. Legend: Red circle - holotype and paratype localities.

Fig. 35 - *Trichomycterus "sordislutum"*, sp. nov., holotype, MZUSP 73162, 78.3 mm SL, Brazil, State of Minas Gerais, Conceição do Mato Dentro municipality. Photo by V. J. C. Reis.

Fig. 36 - Geographical distribution of *Trichomycterus "sordislutum"*, sp. nov in the Rio Doce basin. Legend: Red circle - holotype locality; black circle – paratype localities.

Fig. 37 – Trichomycterus "tantalus", sp. nov., holotype, MZUSP 123369, 75.98 mm SL; Brazil, Minas Gerais, Baguari municipality. Photo by V. J. C. Reis.

Fig. 38 - Geographical distribution of *Trichomycterus "tantalus"*, sp. nov. in the Rio Doce basin. Legend: Black circle - holotype (MZUSP123369) and paratype (1 ex. MZUSP123369) localities; white circle – paratype (MZUFV2565).

Fig. 39 - *Trichomycterus "vinnulus"*, sp. nov. MZUSP 123750, holotype, 54.0 mm SL; Brazil, State of Minas Gerais, Rio Doce municipality. Photo by V. J. C. Reis.

Fig. 40 - Geographical distribution of *Trichomycterus "vinnulus"*, sp. nov. in the Rio Doce basin. Legend: Red circle – holotype MZUSP 123750, and paratype ex-MZUSP 123750; black circle – paratype MZUSP 123757.

Fig. 41 – Mass concentration of *Trichomycterus* (*T. immaculatus*, *T. "tantalus"*, sp. nov, and *Trichomycterus* sp. 1) captured in the fish transposition system at the Baguari Hydroelectric plant, main channel of middle Rio Doce river. Photo by Tiago Pessali.

Fig. 42 – Hydrographic basin limits of 1 - Paraná; 2 - São Francisco; 5 - Rio Doce; 6 - Paraíba do Sul; showing the studied drainages that bordering 2 with 5, and 5 with 6. (A) Overview of studied

area; sampled streams along the (B) Cristiano Otoni Step and the (C) São Geraldo Step. Modified figure extracted from Cherem *et al.*, 2012.

Chapter 2 –

Fig. 01. - Geographical distribution of *Trichomycterus alternatus* and *Trichomycterus zonatus* type material. Legend: **Red star** – *T. alternatus*, holotype FMNH 58082 and paratype FMNH 58083; **yellow star** – *T. zonatus*, holotype FMNH58573 and paratype FMNH 58574; **yellow circle** - *T. zonatus* paratype FMNH 58572.

Fig. 02. - *Trichomycterus alternatus*. Lateral view of FMNH 58082, holotype, (A) 65.57 mm SL and FMNH 58083, paratype, (B - K) 42.53 - 57.12 mm SL. Brazil, Minas Gerais: Rio Doce municipality. Photo by V. J. C. Reis.

Fig. 03 - *Trichomycterus alternatus*. Dorsal head view of FMNH 58082, holotype, (K) 65.57 mm SL and FMNH 58083, paratype, (A-J) 42.53 - 57.12 mm SL. Brazil, Minas Gerais: Rio Doce municipality. Photo by V. J. C. Reis.

Fig. 04 - Stereo triplet of *Trichomycterus alternatus* holotype FMNH 58082. 3D image of ventral view formed on the right side and 3D image of dorsal view formed on the left side.

Fig. 05. - *Trichomycterus zonatus*. Lateral view of FMNH58573, holotype, (A) 52.31 mm SL; FMNH 58574, paratype, (B and C) 42.83 - 46.85 mm SL, (both holotype and paratype from Água Quente); and FMNH 58572, paratype, (D) 50.69 mm SL., Cubatao, 7 miles west of Santos, São Paulo, Brazil. Photo by V. J. C. Reis.

Fig. 06. - *Trichomycterus zonatus*. Dorsal head view of FMNH58573, holotype, (A) 52.31 mm SL; FMNH 58574, paratype, (B and C) 42.83 - 46.85 mm SL, (both holotype and paratype from

Água Quente); and FMNH 58572, paratype, (D) 50.69 mm SL., Cubatao, 7 miles west of Santos, São Paulo, Brazil. Photo by V. J. C. Reis.

Fig. 07 - Stereo triplet of *Trichomycterus zonatus* holotype FMNH58573. 3D image of ventral view formed on the right side and 3D image of dorsal view formed on the left side.

Fig. 08 – Sensory pores of head in (A) - *Trichomycterus alternatus* (holotype FMNH58082), and in (B) - *Trichomycteus zonatus* (holotype FMNH58573). Abbreviations: **i1**, infraorbital sensory pore 1; **i3**, infraorbital sensory pore 3; **i10-11**, infraorbital sensory pore 10 and 11; **ll1-2**, lateral line sensory pore 1 (supracleithral sensory branch) and 2; **po1-2**, postotic sensory pore 1 and 2; **s1**, supraorbital sensory pore 1; **s3**, supraorbital sensory pore 3; **s6**, supraorbital sensory pore 6 (epiphyseal branch).

Summary

Chapter 1- Diversity of the genus *Trichomycterus* Valenciennes, 1832 (Siluriforms, Trichomycteridae) in the Rio Doce basin: a systematic study integrating phenotypes, DNA and classical taxonomy. 1

Introduction 2

Material and Methods 8

Fieldwork and Species sampling 8

Field expeditions and sampling methodology 8

Morphology 9

Meristics and morphometrics 9

Osteology 10

Pigmentation analyses 10

Cartography and image records 11

Molecular analyses 11

Extraction and sequencing 11

In the Laboratory of Molecular Biology of the MZUSP 11

In the Laboratory of Analytical Biology of the Smithsonian Institution 12

Sequence analysis 13

Species delimitation 14

From operational taxonomic units to species taxa 16

Results 18

Taxonomic accounts 18

Key to species of *Trichomycterus* in the Rio Doce basin 18

Species accounts 22

Trichomycterus alternatus (Eigenmann, 1917) 22

Trichomycterus argos Lezama *et al.*, 2012 38
Trichomycterus "astromycterus", sp. nov. 44
Trichomycterus "barrocus", sp. nov. 51
Trichomycterus "brucutu", sp. nov. 57
Trichomycterus brunoi Barbosa & Costa, 2010. 62
Trichomycterus "illuvies", sp. nov. 69
Trichomycterus immaculatus (Eigenmann & Eigenmann, 1889) 74
Trichomycterus "ipatinguensis", sp. nov. 89
Trichomycterus "melanopygius", sp. nov. 96
Trichomycterus "pussilipygius", sp. nov. 102
Trichomycterus "sordislutum", sp. nov. 107
Trichomycterus "tantalus", sp nov. 112
T*richomycterus "vinnulus"*, sp nov. 118
Barcoding results 124
Discussion 126
Can genetic divergence be used as a proxy for taxonomic differentiation? 126
Diversity and distribution of *Trichomycterus* in the Rio Doce basin 130
Taxonomic situation in *Trichomycterus* 134
References 137
Table List 156
Figure List 185

Chapter 2. – The type specimens of *Trichomycterus alternatus* (Eigenmann, 1917) and *Trichomycterus zonatus* (Eigenmann, 1918), with elements for future revisionary work (Teleostei, Siluriformes, Trichomycteridae). 231

Introduction 234

Material and Methods 235

Meristics and morphometrics 235

Osteology and the Stereo Triplet 236

Research institutions 237

Material examined 237

Cartography and image records 238

Results 239

Type localities 239

Taxonomical accounts 242

Trichomycterus alternatus (Eigenmann, 1917) 242

Trichomycterus zonatus (Eigenmann, 1918) 246

Discussion 251

References 256

Table List 263

Figure List 268

Chapter 1- Diversity of the genus *Trichomycterus* Valenciennes, 1832 (Siluriforms, Trichomycteridae) in the Rio Doce basin: a systematic study integrating phenotypes, DNA and classical taxonomy.

Introduction

The Neotropical region comprises 5,000 freshwater fish species and is the richest ichthyofauna on the planet (Reis *et al.*, 2003). This diversity is due to the high heterogeneity of present and past environments in that region, which allied with geologic and ecological factors, caused lineage diversification and ensuing increased biodiversity. Vari & Malabarba (1998) estimate a total number of 8000 neotropical fish species, a figure larger than present records.

Trichomycteridae is one of the richest families of Siluriformes. According to de Pinna (1998), it is a monophyletic group with eight subfamilies, Copionodontinae, Glanapteryginae, Sarcoglanidinae, Stegophilinae, Trichogeninae, Trichomycterinae, Tridentinae and Vandellinae. Fishes from this family are characterized, among others particularities, by a highly modified opercular apparatus, adapted to locomotion in rocky environments and, in the case of parasite species (Stegophilinae and Vandellinae), used to attach into the host gill cavity (de Pinna, 1998; Adriaens *et al.*, 2010). Due to the ability to climb waterfalls in some family members, many species are found in high altitudes, resulting in pronounced endemism (Eigenmann, 1918; Santos, 2012).

Among Trichomycteridae subfamilies, Trichomycterinae has a very confusing systematics. Baskin (1973), de Pinna (1998) and Costa & Bockmann (1993) affirm that the subfamily is not a natural group. On the other hand, Arratia (1990) found four morphological characters that are candidates as putative synapomorphies for the group: (1) vomer with a large and unique posterior process; (2) Enarthrodial joint between the opercle and preopercle in adults; (3) pronounced notch in the posteromedial margin of the third ceratobranchial; and (4) anterior membranous process of basioccipital well developed, extending ventro-laterally to the parasphenoid and prootic. Wosiacki (2002), utilizing 61 Trichomycterinae species and 13 out-group species, corroborated the non-

monophyletic hypothesis for the group. Lastly, Datovo & Bockmann (2010) found a unique myological trait in trichomycterine taxa included in their study, the posterior portion of the levator internus 4 originating by the dorsal face of posttemporo-supracleitrum, and suggested this character as a possible synapomorphy for the subfamily.

Currently, there are eight genera in Trichomycterinae: *Bullockia*, *Eremophilus*, *Hatcheria*, *Ituglanis*, *Rhizosomichthys*, *Scleronema*, *Silvinichtys*, and *Trichmycterus* (de Pinna, 1998). Among those, *Trichomycterus* has the largest number of nominal species, 184 (Eschmeyer & Fong, 2018), and it is currently the most complex taxon in the family due to its geographical distribution, non-monophyletic status and confusing taxonomic history (de Pinna, 1989; 1998).

The genus *Trichomycterus* was described by Valenciennes in 1832, having as type species *T. nigricans* Valenciennes, 1832, from the State of Santa Catarina, Brazil. Since then, many species have been described, and today this genus is one of the most diverse from the neotropics. Many taxonomists throughout time have described species from this genus based mostly on external features, such as number of fin rays, body proportion, and pigmentation. However, starting with Tchernavin (1944) such characters have been gradually shown not to constitute reliable taxonomic proxies for species differentiation due to intraspecific and ontogenetic variation and allometric effects.

For most of the first half of the 20th century, there was no uniform taxonomic standard followed by the majority of ichthyologists. Descriptions of *Trichomycterus* species from that time are not uniform, resulting in difficulties comparing data among different pecies. As observed by Tchernavin (1944), to identify or compare species was sometimes impossible due to the lack of taxonomic uniformity. After his publication the awareness about the consequences on the lack of taxonomy standard and the use of intraspecific variable characters in genus lighted up the attention

of taxonomists, who started to more rigorously state taxonomy methodology and to avoid the use of unreliable characters (Baskin, 1973; de Pinna, 1992b; Costa, 1992; Barbosa, 2000; Bockmann & Sazima, 2004). Tchernavin (1944) was one of the first publications to describe and clearly explain the characters used to diagnose Trichomycterinae species and is in fact used as a standard to the present.

As mentioned above, *Trichomycterus* as a whole has a wide geographic range, and its species are found throughout South and part of Central America on both sides of the Andes (de Pinna, 1989). Many species of *Trichomycterus* have been described from the eastern coastal basins of Brazil. Among those, one of the largest is the Rio Doce.

The Rio Doce basin spans the Brazilian States of Minas Gerais and Espírito Santo (Fig. 01). It has the one of the most diverse fish faunas in Eastern Brazilian drainages, including a significant proportion of endemics (Barros *et al*., 2012; Dergam *et al*., 2017; Sales *et al*., 2018). However, the Rio Doce is at present severely degraded by anthropic impacts such as damming, seweage discharge, and the recent burst of Samarco SA ore tailing dam, and its biodiversity is critically endangered. There are currently six *Trichomycterus* species reported for in the Rio Doce: *T. alternatus* Eigenmann, 1917; *T. argos* Lezama, Triques & Santos, 2012; *T. auroguttatus* Costa, 1992; *T. brasiliensis* Lutken, 1874; 2010, *T. immaculatus* Eigenmann & Eigenmann, 1889; *T. pradensis* Sarmento-Soares, 2005 (Sato *et al*., 2004; Vieira, 2010; Lezama, 2012; Da Silva, 2013; Sales *et al*., 2018). Of those, only *T. alternatus* and *T. argos* were originally described from that basin, with the former also reported widely from other eastern basins of Brazil. Those records, however, are highly questionable, because a thorough investigation into the applicability of those names have never been made to the Rio Doce *Trichomycterus* species and the underlying taxonomy is widely recognized as precarious. Examination of material available in museum

collections, done in association with this work, has revealed an unexpected diversity of *Trichomycterus* in the waters of the Rio Doce, with many forms that clearly do not fit currently known taxa. It has also shown that the applicability of available names is largely arbitrary and poorly supported by data. Resolution of this issue requires both a systematic investigation into the biological reality of the specific entities assignable to *Trichomycterus* in the Rio Doce and also a taxonomic investigation into the applicability of available taxon names.

Neotropical hyperdiverse fish taxa commonly have old and complex taxonomies and to diagnose species from those taxa is usualy laborious and sometimes impossible (Wosiacki, 2002; Costa-Silva *et al*., 2015; Sales *et al*., 2018). From the middle of the 20th century until now the number of *Trichomycterus* species from Southeastern Brazil has more than tripled, from nine valid species to 33 (Eschmeyer & Fong, 2018). The abrupt increase in biodiversity of this taxon is a consequence of a new generation of Brazilians ichthyologists. Although the diversity of *Trichomycterus* is gradually being revealed and it is helping to create conservation strategies for the taxon, diagnosing of species of the genus has become a problem when allied with their high morphological plasticity (e.g color pattern and morphometry) as has been demonstrated in *Trichomycterus davisi* (Haseman 1911) and *T. brasiliensis* (Bockmann & Sazima, 2004; Barbosa & Costa, 2010; and Nascimento *et al*., 2017).

Molecular analyses using mitochondrial DNA have often been employed alongside morphological data in order to diagnose taxonomic groups and their phylogenetic relationship in fish species (Avise et al., 1998; Avise & Wlaker, 1999; Martin & Bermingham, 2000; Chiachio *et al.*, 2008; Cardoso & Montoya-Burgos, 2009; Carvalho *et al*., 2015, Costa-Silva *et al*., 2015, Sales *et al*., 2018). DNA barcoding, in particular, has been applied to help discriminate species of Trichomycteridae in Southeastern Brazil, as a test of the efficiency of alfa taxonomy studies.

(Pereira *et al*., 2010 and 2013; Ochoa et al., 2017; Sales *et al*., 2018). Those particular genes have been widely used in this sort of studies because of their advantages in species-level applications in comparison with nuclear genes, such as absence of introns, limited recombination and haploid mode of inheritance (Saccone *et al*., 1999).

Of multiple mitochondrial markers, cytochrome oxidase sub-unity I (COI) has been the most used to diagnose species. That gene stands out because of its fast evolutionary rate (in comparison with other commonly used mitochondrial markers such as 16S and Cyt-b, and its low conspecific variation relative to its congeneric variation. (Hebert *et al*., 2003). Since Hebert *et al*., (2003) this gene has been used to diagnose all kinds of animal species from invertebrates to vertebrates, such as springtails (Hogg & Hebert, 2004a), butterflies (Hebert *et al*., 2004a; Elias *et al*., 2007), crustaceans (Costa *et al*., 2007; Lefebure *et al.*, 2006), fish (Ward *et al.*, 2005; Hubert *et al*., 2008; Valdez-Moreno *et al*., 2009; Carvalho *et al*., 2011; Rosso *et al.*, 2012), birds (Hebert *et al*., 2004b; Yoo *et al.*, 2006) and mammals (Clare *et al*., 2007). COI has also been used to other puporses such as identification of invasive species (Corin *et al*. 2007), wildlife forensics investigations (Pons, 2006; Dawnay *et al*., 2007; Nelson *et al*., 2007), diagnosis of cryptic communities (Pfenninger *et al*. 2007; Costa-Silva *et al*., 2015), and fisheries strategies (Metcalf *et al*., 2007).

Despite all its advantages, the use of COI in systematic studies has some caveats, such as the occasional inability to seggregate otherwise well-diferenciated species and the possibility of mitochondrial introgression (Rubinoff *et al*., 2006). However, such cases are the exception rather than the rule and affect only 5% to 10% of cases (Ward *et al*. 2005; Hubert *et al*. 2008; Valdez-Moreno *et al.* 2009; Pereira *et al*., 2013). For all its net benefits, the Fish DNA Barcoding of Life Campaign was created as an international and cost-effective iniciative to gather all COI sequence

and associated taxonomic information in a database organized as a web-plataform http://www.fishbol.org/ (Ward *et al*., 2009).

This chapter intends to study the diversity of the genus *Trichomycterus* in the Rio Doce using both COI data and phenotypic characteristics, including those traditionally employed in the taxonomy of the genus. We make a special effort to provide information on intraspecific and ontogenetic variation, as well as detailed assessments on geographical distribution. Results demonstrate that *Trichomycterus* in the Rio Doce was poorly understood on all aspects, including previously entirely unknown species, cryptic species, poorly-defined species and species described multiple times (junior synonyms). We also use our data on taxonomy and geographical distribution to offer insights on biogeography and offer possible explanations on why some species are so widespread while others are narrowly endemic.

Material and Methods

Fieldwork and Species sampling

A total of 1.921 specimens utilized in this study included both museum and newly-collected material. The latter were obtained in fieldwork done by the author and concentrated on poorly sampled locations and type localities. Examined material is listed under each species account.

Institutional acronyms are: collection from the Universidade Federal de Viçosa - Viçosa (MZUFV); collection from the Universidade Estadual Paulista - Botucatu (LBP); Field Museum of Natural History - Chicago (FMNH); Museu de Biologia Melo Leitão - Instituto Nacional da Mata Atlântica - Santa Teresa (MBML); Museum of Comparative Zoology – Harvard University, Cambridge (MCZ); Museu de História Natural and Laboratório de Genética Comparada of the Pontifícia Universidade Católica of Minas Gerais – Belo Horizonte (LGC); Museu de Zoologia da Universidade de São Paulo – São Paulo (MZUSP); Museu Nacional do Rio de Janeiro - Rio de Janeiro (MNRJ); National Museum of Natural History – Smithsonian Institution, Washington, DC (NMNH).

Field expeditions and sampling methodology

Trichomycterus samples were taken from the Rio Doce and adjacent basins in areas with limited or no sampling of *Trichomycterus* material. Locations thus chosen were in the upper and middle Rio Doce and respective adjacent tributaries. Comparative material included representatives also from other Southeastern Brazilian basins.

Sampling methodology included active methods (e.g sieve scan, and gillnets), in headwaters areas with lotic water and with rocky floor or litter accumulation (Uieda & Castro,

1999). The sampling sites in the sub-basin of the Rio Doce were chose by previous ichthyofaunal wildlife survey (Lezama, 2012; Sato *et al*., 2004; Vieira, 2010; da Silva *et al*., 2013) together with the specimen locality data in museums collections.

The sampled fishes were euthanized emerging them into eugenol solution, as recommended by the Conselho Nacional de Controle de Experimentação Animal (CONCEA, 2013). Tissue samples were taken from the right side in the posterior region of the flanks and immediately preserved in 98% ethanol. After that, the fishes were fixed in 10% formalin for one week and then transferred to 70% ethanol. All specimens collected directly for this study are deposited in the MZUSP ichthyological collection.

Morphology

Meristics and morphometrics

The morphometric data was taken with digital caliper (0.1 mm). The morphometric measurement definitions and meristic data were obtained according to de Pinna (1992b) and Bockmann & Sazima (2004). Following the latter, fin-rays counts discriminated rays in three groups (1st, unsegmented and unbranched represented by lower-case Roman numeral; 2nd, segmented and unbranched represented by upper-case Roman numeral; 3rd segmented and branched represented by Arabic numeral), the last posterior closely-set two rays in dorsal and anal-fins were counted as branched rays (thus part of the Arabic figure). Principal caudal-fin ray counts included all branched rays plus one unbranched ray in each lobe, counts given for each lobe (upper first) separated by a plus sign. Vertebrae numbers did not include those involved in the Weberian complex, and the compound caudal centrum was counted as one element. Vertebrae counts were

taken from cleared and stained or radiographed material. Meristic and morphometric data were taken on the left side of specimens whenever possible.

Osteology

Osteology data were obtained from specimens cleared and stained according to Taylor & van Dyke (1985), radiographs and computerized tomography in a few cases. Computerized tomography imaging was done in the Micro CT scans done with a Phoenix v|tome|x M – General Electric Company, belonging to Museu de Zoologia, Universidade de São Paulo, using voxel size X=0.02370301 microns, number of images 5000, voltage 60Kv, and current 220mA. Specimen dissection followed Weitzman (1974) with small changes to fit anatomical peculiarities of the Siluriformes. Additional dissection was implemented to expose some difficult-to-access regions in Siluriformes, like the Weberian apparatus and the posterior part of the neurocranium. Osteological nomenclature followed de Pinna (1989), Lundberg (1982).

Pigmentation analyses

Pigmentation in the entire body was examined by region distribution and shape on the body. The pigment regions were described in the following order: dorsum, lateral surface of the body (divided into dorsal and ventral to lateral midline, when pertinent) ventral side of the body, head and fins. Pigment pattern can vary markedly within species of *Trichomycterus* and this variation is accounted for in the descriptions. Ontogenetic variation can also be extreme in species of the genus. In a few cases where such information was available, it was also covered in the color descriptions of each species.

Cartography and image records

Photographs of dorsal, lateral and ventral view of all species were done by a NIKON P700 camera. Images were edited using software photoshop. Global Positioning System (GPS) data from specimens of *Trichomycterus* reported to the Rio Doce basin were clustered into species group and plotted into GoogleEarth Pro® in order to create a KML file for each species. These files were then used within the free software QGIS 2.16 to create maps showing geographical distributions of each species.

Molecular analyses

Extraction and sequencing

This study amplified mitochondrial gene Cytochrome Oxidase Sub-unity I (COI) (Hebert *et al*., 2003) from 162 specimens of *Trichomycterus* from Rio Doce and adjacent basins. Total DNA extraction was done from different kinds of tissue (muscle and gills). DNA extraction was made using the Invitrogen PureLink™ Genomic DNA Kit (Thermor Fisher) according to the fabricant protocol in the molecular biology laboratory of the MZUSP and in the Laboratory of Analytical Biology (LAB) of the Smithsonian Institution. When in the LAB, quantification used Qubit 2.0 fluorometer Invitrogen (Thermo Fisher).

In the Laboratory of Molecular Biology of the MZUSP

The primers used of Cytochrome C Oxidase subunit I is described in Table 01. Amplification by the Polymerase Chain Reaction (PCR) technique (Ward *et al*., 2005; Ochoa *et al*., 2017) was performed in a final volume of 20 μL. The PCR mix was composed by 1 μL of total

DNA sample, 0.4 µL of FishF1 and FishR1 (5 mM) primers, 2 µL of Taq buffer (10X), 0,6 µL of MgCl2 (50mM), 0,4 µL of dNTPs (10 mM) and 0,05 µL of Taq (PlatinumR *Taq* DNA Polymerase) (5 U/uL), plus 15,15 µL of ultrapure water to complete the final volume. The PCR reactions were performed on Verity (Applied System) thermaoycler according to the following schedule: first cycle at 95^0C for 5'; 35 cycles of 95^0C during 45", 54^0C during 30", and 72^0C for 1'; final extension of 72^0C for 7'. Each PCR reaction was checked by electrophoresis in agarose at 1%. Only those reactions which had shown a considerable success were purified using ExoSAP-IT (GE Health-care, Bucks, UK), and sent to be sequenced at the Centro de Pesquisa sobre o Genoma Humano e Células–Tronco –USP or whenever possible, sent without purification to Macrogen Inc. When in the latter, the sequences were obtained, in both directions, in ABI 3530 DNA Automatic Sequencer (Applied Biosystems Inc., USA), with Big Dye Terminator v3.1 Cycle Sequencing Kit, according to its protocol.

In the Laboratory of Analytical Biology of the Smithsonian Institution.

The primers used of Cytochrome C Oxidase subunit I is described in Table 01. Amplification was performed in a total volume of 10 µL with 5µL of 10x Promega Go Taq G2 Hot Start Master Mix (M7833), 0.3µL of each primer (0.01mM), 0.1µL BSA (New England Biolabs B9000S), 4.3µL of nuclease-free water and 1µL of template DNA. The thermal-cycler profile consisted of an initial denaturation step at 95ºC for 5 minutes, followed by 35 cycles of chain denaturation (95ºC for 30s), annealing (48ºC for 30s) and nucleotide extension (72ºC 45s) each, plus a final extension step at 72ºC for 5 minutes (modification of Ward *et al*., 2005).

Each PCR reaction was checked by electrophoresis in agarose at 1,5%. Only those reactions which had shown successful amplification were purified using ExoSAP-IT (Affymetrix)

(0,5 µL ExoSap enzyme, 1,5 µL nuclease-free water per reaction). The thermal-cycler profile for PCR purification was 36ºC for 30 minutes followed by 80ºC for 20 minutes.

Sequencing reactions were performed using 1 µL of purified PCR product in a 10 µL reaction containing 0.5 µL primer, 1.75 µL Big Dye buffer and 0.5 µL Big Dye (Life Technologies). The thermal-cycler profile consisted of 35 cycles of denaturation (95ºC 30s), annealing (50ºC 30s), and extension (60ºC 4 min). The BigDye products were purified with Sephadex G-50 (Sigma-Aldrich) in Millipore Sephadex plates (MAHVN-4550) to remove unincorporated ddNTPs, and dried at 95ºC for 15 minutes. The purified products were then loaded on an automatic sequencer ABI 3730XL in the Laboratory of Analytical Biology at National Museum of Natural History, Smithsonian Institution.

The successfully sequenced specimens are presented in Table 02.

Sequence analysis

Alignments and sequence editing were performed in a non-commercial license of Geneious 7.1.9 software. In order to analyze the genetic distance, Kimura 2-parameter model (K2P, Kimura, 1980) was calculated in the MEGA-X software (Kumar *et al*., 2018). COI sequences were used to estimate Neighbor-Joining phenogram in Geneious and MEGA-X with the following parameters: substitution model was K2P, including transitions + transversions, rates among sites in gama distribution, gaps/missing data treatment was pairwise delection, and the codon positions excluded the noncoding ones. The results were compared with those presented by Pereira *et al*. (2013) and Sales *et al*., (2018) which they found genetic divergences below 2% among the *Trichomycterus* species. These analyzes are serving as comparative parameter to evaluate these model inside the genus, as well as to test the method efficiency in the intraspecific limits identification.

Species delimitation

The general theoretical framework for species delimitation is that observable traits, phenotypic or molecular, are simply consequences of the process of speciation and differentiation. Thus, evidences for the existence of species-level taxa are just proxies for evolutionary divergence, useful for identifying final products of multidimensional processes operating in evolutionary time and whose details are usually intangible. In accordance with that, species delimitations were performed synergistically with molecular and morphological data. All specimens available were included in comparisons and descriptions in order to estimate intra-specific variation. The species concept followed de Pinna (1999), in which species is a "diagnosable sample of (observed or inferred) life cycles represented by exemplars all of which are hypothesized to attach to the same node in a cladogram, and which are not structured into other similarly diagnosable clusters". The concept of species proposed by Nixon and Wheeler (1990; adapted from a similar concept by Nelson & Platnick, 1981) is also compatible with the general procedure adopted here: "the smallest aggregations of populations (sexual) or lineages (asexual) diagnosable by a unique combination of character states in comparable individuals (semaphoronts)". No fixed threshold value was defined as a standard limit for species differentiation in barcoding data. A value of 2% or higher has been applied as indicative of species-level differentiation in animal species, such as in bony fish species (Hebert *et al*., 2003, 2004; Ward *et al*., 2009; Carvalho *et al*., 2011; and Pereira *et al*., 2011a and 2011b, 2013; Sales *et al*., 2018). However, such fixed thresholds have been repeatedly shown to violate species boundaries in actual situations (Vinas & Tudela, 2009; Carvalho *et al*., 2011; Costa-Silva *et al*., 2015; Shum *et al*., 2017). Clearly, each taxon has its own evolutionary rate, and the application of a fixed threshold for all fish species is unrealistic (Krieger & Fuerst, 2002). As a corollary, we did not adopt an automated procedure for delimiting species boundaries on the basis

of barcoding data. All such protocols rely on assumptions parameters which are potentially violated in real situations. They also imply that certain parameters are homogeneously distributed in trees (i.e., that a general model exists), a constraint that we did not wish to impose on our data. The assemblage of *Trichomycterus* species in the Rio Doce is not a monophyletic group and therefore cannot be treated as an evolutionarily meaningful unit. Some species therein are obviously more closely related to species outside of the Doce basin than to species within it (e.g., *T. argos* and *T. brunoi* are related to *T. brasiliensis* from the Rio São Francisco; *T. pradensis* to *T. immaculatus* in the Paraíba do Sul; and *T. alternatus* to several nominal forms from the Paraíba do Sul and other coastal basins such as *T. auroguttatus*, *T. caudofasciatus* Alencar & Costa 2004, *T. florensis* (Eigenmann 1917), *T. gasparinii* Barbosa 2013, T. *longibarbatus* Costa 1992, *T. mimosensis* Barbosa 2013, *T. pantherinus* Alencar & Costa 2004, *T. travassosi* (Miranda Ribeiro 1949). So, we preferred to use corrected distances (expressed as a simple NJ dendrogram) as a guide to observed divergence, rather than as a map of species limits. Our use of COI data (and in fact morphological as well) can be characterized as a discovery procedure that helps to locate species boundaries, rather than as a species-delimiting procedure. Final taxonomic decisions were based on a combination of COI, morphological, geographical and other biological variables. Such strategy yields a more realistic picture of the complexity of actual situations, with problems such as incomplete taxonomic representation and species known from morphology only. While this certainly adds an element of subjectivity in our analysis, our proposals about species limits and composition are presented as testable hypotheses.

For morphological data, species-level differentiation was determined by the presence a unique combination of character states verifiable in all specimens of an examined sample, permitting diagnosability from all other clusters. Divergence based on statistical frequency alone

was not considered sufficient to diagnose a specie. Continuous characters (both morphometric and meristic) were taken as evidence of differentiation only when associated with gaps in their distribution values.

Each species recognized is provided with synonymy, diagnosis, description, etymology, remarks, and geographic distribution, when pertinent. All the nomenclatural procedures followed rules and recommendations of the International Code of Zoology Nomenclature (ICZN, 2000). An identification key is provided for all valid species recognized, both new and old.

Geography was an important element in the process of species-level boundaries. Sympatry among species-candidates was considered as a test of their integrity as lineages and evidence of isolation even in face of close contact which might otherwise cross reproductive barriers (this is so-called non-dimensional species; Mayr, 1969). Similarly, differentiation in sympatry was a flag for potential cases of sexual dimorphism, polymorphism and, in presence of different sizes, ontogenetic variation. Such cases were examined in more detail in order to remove those potential misleading factors from final conclusions about species boundaries.

From operational taxonomic units to species taxa

The procedure for detecting taxonomic differentiation was based on a stepwise mutual-illuminating strategy. The general idea was to search for discontinuities in intrinsic biological attributes which were then subject to various tests and cross-references in order to isolate those differences indicative of lineage isolation. The process started with a circumscription of phenotypic categories characterized by an overlap of diagnostic characteristics from various morphological systems (color pattern, meristics, morphometrics, osteology etc). The existence of

gaps in one or more of those variables among phenotypes were considered as suggestive of species-level limits. The entities thus delimited were then tested for consistency and taxonomic integrity against supplemental information on possible sexual dimorphism, ontogenetic changes, polymorphism, sympatry, geographically intermediate populations and intermediate phenotypes. After such potential causative factors were properly considered and discarded, the entities still maintaining their integrity were considered as likely candidates for individual lineages representing species-level taxa. Genetic analyses utilized samples representing a broad range of the phenotypic variation detected and multiple representatives of each potential lineage were used whenever possible. This assured that species undetected phenotypically could be disclosed by genetic distances and then reexamined in more detail for subtle morphological divergence not detected in previous examination.

The strategy adopted here did not assume intra-basin endemism, because some species of *Trichomycterus* are known to be distributed across more than one hydrographic system. Therefore, although the scope of this paper is the Rio Doce, resolution of the taxonomic and nomenclatural situation of the species therein relied on information extrapolating the boundaries of that basin. In fact, most decisions on species limits and names resorted to a comparative scope encompassing the entire genus.

Results

Taxonomic accounts

Key to species of Trichomycterus in the Rio Doce basin

1a. I+6 pectoral-fin rays; two lateral line pores. _____2

2a. 26 – 31 interopercular odontodes. _____***Trichomycterus brunoi*.**

2b. 39 – 40 interopercular odontodes. _____***Trichomycterus argos*.**

1b. I+7 or I+8 pectoral-fin rays; two or three lateral line pores _____3

3a - Caudal-fin with a dark macula at base of middle caudal-fin rays, extending posteriorly as dark horizontal band to margin of fin; 7 branchiostegal rays. _____4

4a - I+7 pectoral-fin rays; chromathophores always forming round dark maculae mostly bigger than eye diameter randomly distributed on the body.

_____ ***Trichomycterus "ipatinguensis".***

4b - I+7 or I+8 pectoral-fin rays; chromathophores usually homogeneously distributed on body and not forming dark maculae. _____5

5a – Three lateral-line pores; caudal-fin deeply forked_____***Trichomycterus "tantalus".***

5b – Two lateral-line pores; caudal-fin subtruncate or slightly forked_____6

6a - I+7 or I+8 (rarely) pectoral-fin rays; 39-40 post-Weberian vertebrae _____***Trichomycterus "melanopygius".***

6b - I+8 pectoral-fin rays; 34-36 post-Weberian vertebrae _____***Trichomycterus immaculatus.***

3b - Caudal-fin without a dark macula at base of middle caudal-fin rays, extending posteriorly as dark horizontal band to margin of fin; 6 to 8 branchiostegal rays. _____7

7a - Nasal barbel short, posteriorly not surpassing eye; 6 or 7 branchiostegal rays. _____8

8a – 38 – 63 opercular odontodes; maculae in the mid-lateral line of body usually fused, creating a wide stripe extending between posterior border of opercle to base of middle caudal-fin rays. _____9

9a – Three lateral-line pores; 6 branchiostegal rays. _____***Trichomycterus "sordislutum".***

9b – Two lateral-line pores; 7 branchiostegal rays. _____***Trichomycterus "barrocus".***

8b – 25 – 35 interopercular odontodes; round and dark maculae, rarely fused to each other (occasional fusion usually in region between posterior margin of opercle to base of dorsal-fin). forming file along mid-lateral line of body.

_____10

10a – Three lateral-line pores; caudal fin slightly forked to deeply forked; I+7 or I+8 pectoral-fin rays.

_____***Trichomycterus "astromycterus".***

10b – Two lateral-line pores; caudal fin round to sub-truncated; I+7 pectoral-fin rays. _____***Trichomycterus alternatus.***

7b - Nasal barbel posteriorly surpassing eye; 7 or 8 number of branchiostegal rays. _____11

11a - Dark maculae in the mid-lateral portion of body partly or totally fused to each other and forming a stripe from posterior border of opercle to base of dorsal fin or to base of caudal-fin rays; absence of small round dark maculae randomly distributed in all body

_____12

12a - Six branchiostegal rays; I+7 or I+8 pectoral-fin rays; head length 19.8 - 22.1% SL; prepelvic length 51.9 - 55.2% SL.

_____***Trichomycterus "illuvies".***

12b – Seven branchiostegal rays; I+7 pectoral-fin rays; head length 16.6 - 18.8% SL; prepelvic length 58.5% - 59.0% SL.

_____***Trichomycterus "pussilipygius".***

11b – Absence of dark maculae in the mid-lateral portion of body partly or totally fused to each other and forming a stripe from posterior border of opercle to base of dorsal fin or to base of caudal-fin rays; Presence of small, round and dark maculae randomly distributed in all body resembling *T. brasiliensis* species complex.

_____13

13a – Three lateral line pores; 7 branchiostegal rays; pelvic-fin rays surpassing urogenital opening.

_____***Trichomycterus "vinnulus".***

14b – Two lateral line pores; 8 branchiostegal rays; pelvic-fin rays not surpassing urogenital opening.

_____***Trichomycterus "brucutu".***

Species accounts

Trichomycterus alternatus (Eigenmann, 1917)

(Fig. 02)

Pygidium alternatum Eigenmann, 1917: 700, Rio Doce, Brazil [holotype**:** FMNH 58082 (ex CM 7079), paratypes**:** CAS 64575 (4), FMNH 58083 (62)]; Henn 1928:79 [type catalog]; Ibarra & Stewart 1987:72 [type catalog]; Ferraris 2007:414 [checklist];

Trichomycterus alternatum; Burgess 1989:321 [list];

Trichomycterus alternatus; Costa, 1992:104 [comparisons]; Bizerril 1994:623 [list]; Miquelarena & Fernández 2000:44 [list]; de Pinna & Wosiacki, 2003:279 [checklist]; Wosiacki, 2004 [type catalog]; Wosiacki & Garavello 2004:5 [list]; Triques & Vono 2004:170 [comparisons]; Bockmann & Sazima 2004:71 [comparisons]; Bockmann *et al*. 2004:227 [cited]; Alencar & Costa 2004:3 [comparisons]; Wosiacki, 2005:51 [comparisons]; Lima *et al.*, 2008 [comparisons]; Barbosa & Costa 2010:120 [comparisons]; Sarmento-Soares *et al.*, 2011:262 [comparisons]; Roldi *et al.*, 2011:02 [comparisons]; Barbosa & Costa 2011:308 [comparisons]; Barbosa & Costa 2012:155 [comparisons]; Barbosa 2013:274 [comparisons], DoNascimiento *et al.*, 2014a:709 [comparisons]; García-Melo *et al.* 2016:238 [comparisons]; Sales *et al.*, 2018 [comparisons].

Diagnosis – *Trichomycterus alternatus* is distinguished from all species from the Rio Doce basin by its color pattern consisting in three lines of usually round maculae on the trunk and one line of usually round maculae, from same size to bigger than eye diameter, in the midline of body, could be fusing or not with others. Distinguished from *T. caipora* Lima, Lazzarotto & Costa 2008, *T. immaculatus*, *T. pradensis*, *T. giganteus* Lima & Costa 2004, *T. "tantalus"*, and *T.*

"melanopygius", from all species from the *T. brasiliensis* complex and *T. zonatus* (Eigenmann, 1918) by the number of pectoral-fin rays, I+7 (vs. I+8 in *T. "astromycterus", T. caipora, T. immaculatus, T. pradensis, T. giganteus, T. "tantalus", T. "melanopygius"* and I+6 in *T. brasiliensis* spececies complex, and *T. zonatus*). Distinguished from T. "astromycterus", *T. "tantalus", T. "ipatinguensis", T. "vinnulus"* and *T. "sordislutum"* by the number of sensory pores in the lateral line, two (vs. three in *T. "astromycterus", T. "tantalus", T. "ipatinguensis", T. "vinnulus"* and *T. "sordislutum"*). Distinguished from *T. "barrocus"* by depth of body, preanal and prepelvic length, 18.31% - 14.89%, 82.91% - 63.84%, 70.86% - 52.82%, respectively (vs. 13.85% - 8.97%, 69.03% - 48.98%, 52.51% - 41.87%, respectively, in *T. "barrocus"*).

Description – Morphometric data for specimens examined in Table 03. Body long and almost totally straight, trunk roughly round in cross-section near head, then slightly deeper than broad and softly compressed to caudal peduncle, tapering to Caudal-fin. Dorsal profile of body gently convex to dorsal-fin origin, then straight or slightly concave along caudal peduncle to caudal-fin origin. Ventral profile convex from gular region to vent, due partly to abdominal distension, then straight or slightly concave along anal-fin origin to caudal-fin base. Caudal peduncle almost deep such as body at beginning of anal-fin base.

Head approximately one-fifth of SL, pentagonal, slightly longer than wide and depressed. Mouth sub-terminal. Upper jaw slightly longer than lower. Upper lip wider than lower lip, and laterally continuous with base of maxillary barbel. Lower lip small, approximately 2/3 width of upper one, partly divided into right and left portions by with median concavity. Lower lip with uniform covering of tiny vilii, resulting in velvet-like surface and not clustered into large papillae. Region between upper and lower lips with slender fleshy lobe.

Dentary and premaxillary teeth similar to each other in shape. Dentary teeth conical, arranged in four irregular rows, first row with 9 - 11 teeth, extending from base to slightly up of coronoid process, with size of individual teeth increasing markedly towards symphysis and from posterior to anterior rows. Total area of premaxilary teeth slightly smaller than that of dentary, with teeth arranged irregularly in four rows, first row with approximately 8 - 10 teeth, over entire ventral surface of premaxilla. Premaxilary teeth conical.

Eye medium-sized, slightly protruding, positioned latero-dorsally on head, without free orbital rim and covered with transparent skin. Eye located on anterior half of HL, closer to lateral border of the head than to the midline in dorsal view. Infraorbital latero-sensory canal incomplete, extending from sphenotic posteriorly to terminal pore located ventroposteriorly to eye. Anterior nares surrounded by tube of integument directed anterolaterally, continuous posterolaterally with nasal barbel. Posterior nares closer to anterior nares than to the eyes, surrounded by tube of integument incomplete posteriorly. Maxillary barbel tubular narrowing markedly towards fine tip, reaching from anteromesial side of interopercle until 1/4 from base of pectoral-fin. Rictal barbel inserted immediately ventral to maxillary barbel. Its tip reaching from posterior border of eyes to base of pectoral-fin. Nasal barbel originating on posterolateral region of anterior nares, reaching anywhere from posterior border of eyes to anterior portion of opercle. Interopercular patch of odontodes medium to large, oval in shape and with well-developed odontodes, prominent in ventral aspect of head. Interopercular patch of odontodes extending from vertical through ventroposterior border of eye to ventroanterior to opercle. Odontodes arranged in three or four irregular series, with those on mesial series much longer than those on lateral one; odontodes gradually larger posteriorly in both series, with those posteriorly on mesial row largest. Interopercular odontodes 25 – 34. Opercular patch of odontodes on dorsolateral surface of

posterior part of head, positioned anterodorsally to pectoral-fin base, roundish in shape and larger than eye in dorsal aspect of head. Opercular odontodes 12 – 16, sunk in individual slits of integument, progressively larger posteriorly, all with fine tips, with largest ones curved distally and claw-like. Entire patch surrounded by specialized rim of integument.

Pectoral-fin medium-sized, its base immediately posterior and ventral to opercular patch of odontodes. Pectoral-fin rays I+7. First pectoral-fin ray (unbranched) longer than all others, prolonged as filament beyond fin web, varing in length. Other rays progressively less long, their tips following continuous line along fin margin. Pelvic-fin with convex distal profile, its origin slightly posterior to middle of SL and anterior to vertical through dorsal-fin origin, to slightly covering anal and urogenital openings in adults. Base of Pelvic-fins positioned one eye diameter to each other. Pelvic-fin rays I+4, first ray unbranched. Sciatic process of basipterygium lomg, and thin. Dorsal-fin long, its distal profile sinusoidal. Dorsal-fin origin closer to base of caudal-fin than to tip of snout. Dorsal-fin rays (ii or iii)+II+7, two or three unsegmented and unbranched rudimentary rays, commonly present in *Trichomycteru*s, two segmented and unbranched procurrent rays and seven branched and segmented rays (therein included two posterior closely-set rays). Anal fin slightly smaller than dorsal-fin, its distal profile gently convex. Anal-fin origin posterior to vertical through end of dorsal-fin base. Anal-fin rays (i, ii, or iii) +II+5, one to three unsegmented and unbranched rudimentary rays, two segmented and unbranched procurrent rays and five branched and segmented rays. Caudal-fin from rounded to truncated shape, with 6+7 principal rays. Adipose-fin absent or modified into low integument fold extending between end of dorsal-fin and caudal-fin origin. Post-Weberian vertebrae 34 (1), 35 (10), 36 (09), 37 (01). First dorsal-fin pterygiophore immediately anterior to neural spine of 15^{th} (05), 16^{th} (15), 17^{th} (02), vertebra, first anal-fin pterygiophore immediately anterior to neural spine of 19^{th} (02); 20^{th} (13),

21th (07) vertebra. Caudal-fin procurrent rays plus one segmented non-principal ray dorsally and ventrally. Procurrent caudal-fin rays, 18 - 25 dorsally and 11 - 15 ventrally, beginning anteriorly at 28th to 32th vertebrae. Pleural ribs 10 (01), 11 (10), 12(09), 13 (04). Branchiostegal rays 6(02) to 7 (18), some specimens have both six and seven branchiostegal rays in each side. Dorsal-fin pterygiophores 8. Anal-fin pterygiophores 6.

Cephalic lateral line canals with simple, non-dendritic tubes ending in single pores. Supraorbital canal mostly within frontal bone. Supraorbital pores invariably present: s1 mesial to nasal-barbel base and autopalatine, s3 mesial to posterior nostril and anterior to frontal, and single or paired s6 posteromedial to eye and at midlength of frontal. Infraorbital canal with four pores, i1 and i2 anteriorly and i10 and i11 posteriorly. Canal not ossified. Infraorbital pore i1 located ventro-lateral to nasal-barbel base and autopalatine, i2 ventro-lateral to posterior nostril and anterior to frontal, i10 and i11 posterior to eye. Otic canal without pores. Postotic pores po1, anteromedial to opercular patch of odontodes), and po2, mesial to opercular patch of odontodes. Lateral line of trunk anteriorly continuous with postotic canal and reduced to short tube. Lateral line pores ll1 and ll2 present dorsomedial to pectoral-fin base.

Coloration in ethanol. – Dark chromatophores distributed into inner and outer skin layers. Those on inner skin layer forming large roundish maculae responsible for the main color features of the body. Basic arrangement of maculae in four variably-arranged rows. One row along mid-dorsal line from occiput, through entire dorsum, into dorsal edge of caudal peduncle and to base of Caudal-fin. Second row ventrolateral to that, extending from base of head through upper part of flanks, dorsal portion of caudal peduncle, to base of caudal-fin. Third row running along mid-lateral line, from immediately posterior to opercle to base of caudal-fin. Fourth and ventralmost row shorter, extending from mid-length of abdomen through ventral margin of caudal peduncle to

base of caudal-fin. Basic four-row pattern disrupted by fusions (mostly along anterior part of body) and unaligned maculae, resulting in varied configurations. Mid-lateral line mostly independent but occasionally fused on dorsum. Head darkest on region corresponding to neurocranium, outlined by brain pigment seen by transparency. Dark spot normally at base of opercular patch of odontodes, with additional dark markings on cheeks. Light teardrop-shade area extending from posterior margin of eye to base of opercular patch of odontodes, corresponding to levator operculi muscle. Base of nasal barbels surrounded with concentration of dark pigment, extending posteriorly as elongate dark field to anterior margin of eyes. Distal margin of integument fold of opercular patch of odontodes darkly-pigmented. Interopercular patch of odontodes white. Ventral side of the body lacking dark pigment. Fins with small brownish spots randomly distributed on fin-rays.

Remarks – *Trichomycterus alternatus* was described from the upper Rio Doce basin at the town of Rio Doce, State of Minas Gerais (cf. Chapter 2 of this Dissertation). Research associated with the present work shows that the species is distributed throughout the Rio Doce basin and probably adjacent basins as well. Such conclusion is corroborated by both morphological and molecular data, which fail to detect structuring and character segregation indicative of specific differentiation across its range. Such result is not unexpected and representatives of the species have been reported from numerous Southeastern Brazilian localities in the literature, both in the Rio Doce and elsewhere (Barbosa, 2004; Volpi, 2017; Lima, 2008).

Different populations of *T. alternatus* in the Rio Doce may show specific local morphological peculiarities which at first glance may seem to distinguish them from typical specimens of *T. alternatus*. For example, some populations can have very long barbels resembling the phenotype described for *T. longibarbatus*. At the other extreme, barbels are very short in some

other populations, similarly to those considered typical of *T. auroguttatus*. Similar patterns of apparent differentiation occur also in the first pectoral-fin ray, which can form a filament which can vary widely in length. Similar variation is observed in the degree to which the pelvic-fin reaches or covers the urogenital opening and the color pattern (Fig. 03). Such variation can be geographically correlated, and comparisons between the extreme conditions may lead to erroneous conclusions about taxonomic differentiation. However, examination of intermediary populations clearly demonstrates that such variation is clinal, thus blurring any clear-cut boundaries which might be indicative of different species. Such conclusion is supported also by the lack of significant structuring in COI sequences analyzed here.

As an example of the situation described above, comparisons between a population of *T. alternatus* from the Piranga river (upper Rio Doce basin) and another from Santa Maria do Rio Doce river (lower Rio Doce basin), reveal pronounced differences in characters such as barbel length, first pectoral-fin ray length and pigmentation pattern. The differences are so striking that might seem to suggest separate species. However, there are intervening populations with intermediary conditions which bridge the apparent morphological gap. That fact, plus the low genetic divergence among various populations (> 1.73% DNA Barcoding) (Table 04), demonstrate that the two phenotypically divergent populations cannot represent distinct lineages at the species level. A similar situation was reported by Nascimento *at al*. (2017) in *Trichomycterus davisi* Haseman, 1911. That species shows wide variation in morphology and color pattern (Nascimento *at al*., 2017). Although color pattern has been shown to be conservative in some *Trichomycterus* species (Bockmann & Sazima, 2004), this is by no means the rule in species of the genus, where color pattern may be subject to pronounced polymorphism (Arratia *et al*., 1978; Triques & Vono, 2004; Castellanos-Morales, 2007; Lima *et al*., 2008; Silva *et al*., 2010; Ferrer & Malabarba, 2013

and Buckup *et al*. 2014). Marked degrees of intraspecific variation in color pattern and other morphological traits exist in several *Trichomycterus* species in the Rio Doce, such as, *T. alternatus*, *T. "tantalus"*, *T. "ipatinguensis"*, *T. immaculatus*, *T. "pussilypigyus"*, and *T. "vinnulus"* (Fig. 03; 04; 05; 06; 07; 08; 09). In agreement with such hypotheses about intraspecific color variation, COI sequences of samples of *T. "tantalus"*, *T. "ipatinguensis"*, *T. pradensis* and *T. "vinnulus"* lack any significant intraspecific barcoding divergence (Table 04). *Trichomycterus alternatus* has 1.75% intraspecific divergence. Ward *et al*. 2009 suggested that a group of related specimens of fish with barcoding divergence below 2% have 95% probability to be the same species. Similar results were reported in several other papers (Mabragaña *et al*., 2011; Hubert *et al*., 2008; Carvalho *et al*., 2011; Pereira *et al*., 2011a, 2011b; and Ward, 2009). However, Pereira *et al*. (2011a, 2013) suggest that 2% barcoding divergence may be an unrealistic high threshold for species of *Trichomycterus* and thus underestimate its real diversity.

Geographical distribution – *Trichomycterus alternatus* is distributed throughout the entire Rio Doce (Fig. 10). It also occurs have been reported to several other basins in Southeastern Brazil (Barbosa, 2004; Volpi, 2017).

Meterial examined – Type material: Holotype FMNH 58082, 65.57 mm SL; Rio Doce, near the village of Rio Doce, Minas Gerais, Brazil, Rio Doce basin; col. J. Haseman, 25 May 1908; **Paratype FMNH 58083**, 62, 30.44 - 57.90 mm SL; same data from holotype. **Topotipic material - MZUSP 123761**, 01, 50.87 mm SL; Rio Doce, Córrego da Laje creek near town of Rio Doce, tributary of main channel of Rio Doce basin (20°14'13.05"S 42°56'53.65"W); col. V. J. C. Reis, M. C. C. de Pinna, G. F. de Pinna & G. Ballen, 23 Jun 2018. **MZUSP 123763**, 1, 46.25 mm SL; Rio Doce, creek bordering the hidropower dam resevouir Risoleta Neves, Rio Doce basin (20°12'21.63"S 42°52'56.24"W); col. V. J. C. Reis, M. C. C. de Pinna, G. F. de Pinna & G. Ballen,

24 Jun 2018. **MZUSP 123764**, 4, 47.29 – 42.65 mm SL; Rio Doce, creek bordering the hidropower dam resevouir Risoleta Neves, Rio Doce basin (20°12'22.03"S 42°52'57.44"W); col. V. J. C. Reis, M. C. C. de Pinna, G. F. de Pinna & G. Ballen, 24 Jun 2018.

Non-type material - All from Brazil, State of Espírito Santo, Rio Doce hydrographic basin. **MBML 607**, 2, 56.13 – 39.23 mm SL; Itarana, Limoeiro creek, tributary of Santa Joana basin (19°52'26"S 40°52'31"W); col. R. L. Teixeira & P. S. Miller, 18 Oct 2000. **MBML 646**, 7, 50.67 – 21.12 mm SL; Itarana, Jatibocas creek, Santa Joana basin (19°52'26"S 40°52'31"W); col. R. L. Teixeira & P. S. Miller 19 Apr 2001. **MBML 690**, 6, 62.33 – 24.96 mm SL; Itarana, Jatibocas creek, Santa Joana basin (19°52'26"S 40°52'31"W); col. R. L. Teixeira & P. S. Miller 10 Aug 2000. **MBML 727**, 1, 33.56 mm SL; Itarana, Santa Joana basin (19°52'26"S 40°52'31"W); col. R. L. Teixeira & P. S. Miller, 18 Oct 2000. **MBML 755**, 9, 47,98 – 28,96 mm SL; Itarana, Jatibocas creek, Santa Joana river (19°52'26"S 40°52'31"W); col. R. L. Teixeira & P. S. Miller, 18 Oct 2000. **MBML 811**, 1, 32.97 mm SL; Itarana, Jatibocas creek, tributary of Santa Joana river (19°52'26"S 40°52'31"W); col. R. L. Teixeira & P. S. Miller, 08 Feb 2001. **MBML 1051**, 3, 76.33 – 55.43 mm SL; Santa Teresa, Vinte e Cinco de Julho creek, at headwaters of Santo Antônio river, tributary of Santa Maria do Rio Doce basin (19°56'08"S 40°36'01"W); col. R. L. Teixeira, 19 Mar 2005. **MBML 1339**, 2, 57.39 – 46.54 mm SL; Santa Teresa, Rio Cinco de Novembro river, Santa Maria do Rio Doce basin (19°56'08"S 40°36'01"W); col. R. L. Teixeira, 11 May 2005. **MBML 1361**, 3, 37.74 – 26.83 mm SL; Itarana, Córrego Sossego creek, tributary of Santa Joana river (19°52'26"S 40°52'31"W); col. R. L. Teixeira, 20 Aug 2000. **MBML 2230**, 11, 59.55 – 28.84 mm SL; Afonso Cláudio, Córrego do Cedro creek, Guandu basin (20°11'42"S 41°03'42"W); col. L. M. Sarmento-Soares, R. F. Martins-Pinheiro, A. T. Aranda, R. L. Teixeira, M. M. C. Roldi & M. M. Lopes, 12 Jun 2009. **MBML 2234**, 12, 84.13 – 26.83 mm SL; Afonso Cláudio, Guandu basin (20°09'16"S

41°05'59"W); col. L. M. Sarmento-Soares, R. F. Martins-Pinheiro, A. T. Aranda, R. L. Teixeira, M. M. C. Roldi & M. M. Lopes, 12 Jun 09. **MBML 2237**, 3, 39.60 – 26.41 mm SL; Laranja da Terra, Ribeirão Lagoa stream, tributary of Guandu basin (19°59'26"S 41°03'54"W); col. L. M. Sarmento-Soares, R. F. Martins-Pinheiro, A. T. Aranda, R. L. Teixeira, M. M. C. Roldi & M. M. Lopes, 12 Jun 2009. **MBML 4306**, 6, 56.79 – 20.87 mm SL; Iúna, Rio Claro river, tributary of Manhuaçu riber (20°22'24,2"S 41°49'39,7"W); col. L. M. Sarmento Soares, M. R. Britto, V. C. Espindula, F. M. R. S. Pupo, R. F. M. Pinheiro & M. M. C. Roldi, 09 Sep 2011. **MBML 4309**, 2, 28.10 – 21.38 mm SL, Iúna, Ribeirão do Brás creek, Manhuaçu basin (20°20'33,9"S 41°48'55,6"W); col. L. M. Sarmento Soares, M. R. Britto, V. C. Espindula, F. M. R. S. Pupo, R. F. M. Pinheiro & M. M. C. Roldi, 10 Sep 2011. **MBML 4338**, 7, 38.48 – 26.99 mm SL; Júna, José Pedro riuver, tributary of Manhuaçu basin (20°22'09,5"S 41°51'27,5"W); col. L. M. Sarmento Soares, M. R. Britto, V. C. Espindula, F. M. R. S. Pupo, R. F. M. Pinheiro & M. M. C. Roldi, 10 Sep 2011. **MBML 4438**, 2, 40 – 26.3 mm SL; Santa Teresa, near Milanesi municipality, Santa Maria do Rio Doce basin (19°47'02,1"S 40°38'52,0"W); col. R. B. Soares, J. Gurtler & V. R. Bada, 24 Sep 2011. **MBML 4642**, 2, 47.47 – 38.16 mm SL; Santa Teresa, Santo Antônio creek, Santa Maria do Rio Doce basin (19°53'17,1"S 40°34'27,1"W); col. L. M. Sarmento Soares, R. F. M. Pinheiro, M. M. C. Roldi & R. B. Soares 12 Feb 2012. **MBML 6160**, 8, 56.16 – 27.05 mm SL; Santa Teresa, Espanhol creek, Santa Maria do Rio Doce basin (19°52'41,6"S 40°36'48,5"W); col. C. J. Cunha, J. P. Silva & R. B. Soares, 20 Aug 2012. **MBML 6161**, 13, 50.08 – 17.79 mm SL; Santa Teresa, Rio 5 de Novembro, bacia do rio Santa Maria do Rio Doce (19°53'49,2" S 40°36'10,9" W); col. C. J. Cunha, J. P. Silva & R. B. Soares, 20 Aug 12. **MBML 6207**, 2, 36.45 – 32.10 mm SL; Santa Teresa, Cinco de Novembro river, at the left side of ES-080, straigth Santo Antônio do Canaã to Santa Teresa, Rio Santa Maria do Rio Doce (19°50'26,0"S 40°37'47,3"W);

col. C. J. Cunha, J. P. Silva & R. B. Soares, 20 Aug 2012. **MBML 6210**, 2, 37.09 - 36.26 mm SL; Santa Teresa, Espanhol creek near to the mouth of Cinco de Novembro river, tributary of Santa Maria do Rio Doce basin (19°52'41,6"S 40°36'48,5"W); col. C. J. Cunha, J. P. Silva & R. B. Soares, 20 Aug 2012. **MBML 6211**, 1, 38.60 mm SL; Santa Teresa, Cinco de Novembro river, tributary of Santa Maria do Rio Doce basin (19°53'49,2" S 40°36'10,9" W); col. C. J. Cunha, J. P. Silva & R. B. Soares, 20 Aug 2012. **MBML 6228**, 12, 76,69 – 36,15 mm SL, Brejatuba, Córrego da Passagem creek, Guandu river (20° 7'33.00"S 41°16'47.00"W); col. Biodiverses Project staff, 11 Aug. 2012. **MBML 6627**, 2, 39.63 – 26.88 mm SL; Pancas, Cachoeira do Bassini waterfall, Pancas basin (19°50'26,0"S 40°37'47,3"W); col. C. J. Cunha, J. P. Silva & R. B. Soares 20 Aug 2012. **MBML 6822**, 14, 55.28 – 33.32 mm SL; Santa Teresa, Vinte cinco de Julho river, tributary of Santa Maria do Rio Doce basin (19°50'20,7"S 40°34'04,3"W); col. L. M. Sarmento Soares, R. F. Martins Pinheiro, M. M. C. Roldi & R. Becalli, 05 May 13. **MBML 6833**, 4, 49.12 – 35.10 mm SL; Santa Teresa, Santo Antônio creek, Santa Maria do Rio Doce basin (19°53'04,4"S 40°34'30"W); col. L. M. Sarmento Soares, R. F. Martins Pinheiro, M. M. C. Roldi & R. Becalli, 05 May 2013. **MBML 6841**, 5, 40.6 – 34.82 mm SL; Santa Teresa, Santo Antônio creek, Santa Maria do Rio Doce basin (19°53'20,3"S 40°34'32,8"W); col. L. M. Sarmento Soares, R. F. Martins Pinheiro, M. M. C. Roldi & R. Becalli, 05 May 2013. **MBML 6860**, 6, 63.52 – 34.48 mm SL; Santa Teresa, Santo Antônio river, tributary of Santa Maria do Rio Doce basin (19°53'20,3"S 40°34'32,8"W); col. L. M. Sarmento Soares, R. F. Martins Pinheiro, M. M. C. Roldi & R. Becalli, 05 May 2013. **MBML 7598**, 4, 74.07 – 43.06 mm SL; Afonso Cláudio, Córrego do Cedro creek, tributary of Guandu river (20°11'42"S 41°03'43"W); col. T. A. Volpi & M. M. Lopes, 09 Dec 2013. **MBML 7641**, 42, 57.85 – 23.75 mm SL; Afonso Cláudio, Córrego do Cedro creek, Guandu basin (20°11'42"S 41°03'43"W); col. T. A. Volpi & M. M. Lopes, 09 Dec 13. **MBML 7642**, 6,

68.47 – 35.55 mm SL; Afonso Cláudio, Boa Sorte river, tributary of Guandu basin (20°10'59" S 41°04'46" W); col. T. A. Volpi & M. M. Lopes 09 Dec 2013. **MBML 7665**, 7, 39.06 – 19.79 mm SL; Pancas, Panquinhas stream, tributary of Pancas basin (19°13'00"S 40°52'01"W); col. T. A. Volpi & M. M. Lopes 10 Dec 2013. **MBML 7672**, 2, 30.91 – 36.09 mm SL; Pancas, São Luís creek, Pancas basin (19°13'46"S 40°48'52"W); col. T. A. Volpi & M. M. Lopes 11 Dec 2013. **MBML 7681**, 10, 32.23 – 24.64 mm SL; Santa Teres, Tabocas river, tributary of Pancas basin (19°52'57"S 40°41'24"W); col. T. A. Volpi & M. M. Lopes 11 Dec 2013. **MBML 8191**, 1, 39.27 mm SL; Iúna, José Pedro stream, Manhuaçu basin (20°22'10,4"S 41°51'28,4"W); col. T. A. Volpi, K. B. S. de Paula & E. L. Muhl, 10 May 2014.**MBML 8426**, 7, 47.41 – 28.75 mm SL; Santa Teresa, Santa Maria do Rio Doce basin, near to its spring (19°57'52,5"S 40°44'20,4"W); T. A. Volpi, M. M. Lopes, K. B. S. de Paula & E. L. Muhl, 18 May 2014. **MBML 8502**, 2, 53.99 – 53.55 mm SL; Santa Teresa, Santa Maria do Rio Doce basin (19°57'52,5"S 40°44'20,4"W); col. T. A. Volpi, M. M. Lopes, K. B. S. de Paula & E. L. Muhl, 18 May 2014. **MBML 9977**, 2, 44.51 – 34.34 mm Sl; Santa Teresa, Tabocas river, tributary of Santa Maria do Rio Doce basin (19º52'57"S 40º41'24"W); col. T. A. Volpi & M. M. Lopes, 11 Dec 2013.

All from Bazil, State of Minas Gerais, Rio Doce hydrographic basin. **MZUSP 58474**, 1, 46.09 mm SL; Braúnas, Córrego do Gaspar creek, Santo Antônio basin (18°58'60.00"S 42°44'21.00"W); col. P. M. C. Araujo & F. A. Bockmann, 04 Oct. 1997. **MZUSP 69366**, 14, 51.71 – 31.8 mm SL; Coroaci, Suaçuí basin (18°41'38.00"S 42°12'50.00"W); col. A. M. Zanta, 29 Apr. 2001. **MZUSP 72962**, 81, 48.22 – 23.48 mm SL; Santa Teresa, Reserva de Nova Lombardia (19°54'23.91"S 40°33'38.66"W); col. J. L. Helmer, 08 Jan. 1993. **MZUSP 73148**, 8, 31.93 – 19.89 mm SL; Conceição do Mato Dentro, Rio do Peixe river, Santo Antônio basin (19°11'14.20"S 43° 8'45.31"W); col. F. Di Dario & S. Kakinami, 13 Sep 2001. **MZUSP 73163**, 7, 29.93 – 16.57mm

SL; Conceição do Mato Dentro, Rio do Peixe, Santo Antônio basin (19°11'40.04"S 43° 8'43.99"W); col. F. Di Dario & S. Kakinami, 14 Sep. 2001. **MZUSP 75254**, 3, 85,70 – 81.54mm SL; Ouro Preto, Tripuí creek, tributary of Piranga basin (20°23'45.63"S 43°34'11.92"W); col. M. R. Silvério, D. C. Oliveira & A. Oliveira, 01 Mar. 2001. **MZUSP 82369**, 5, 58.38 – 50.03 mm SL; Caranaíba, Papagaio river (20°51'12.00"S 43°43'12.00"W); col. J. C. Oliveira, A. L. Alves, L. R. Sato, 13 Oct. 2001. **MZUSP 82371**, 1, 66,69 mm SL; Caranaíba, Piranga basin (20°58'17.00"S 43°42'33.00"W); col. J. C. Oliveira, A. L. Alves & L. R. Sato, 12 Oct. 2001. **MZUSP 82370**, 1, 42.94 mm SL; Desterro de Melo, Xopotó river, tributary of Piranga river (21° 9'34.00"S 43°24'37.00"W); col. J. C. Oliveira, A. L. Alves, L. R. Sato, 12 Oct. 2001. **MZUSP 87825**, 4, 61,6 – 47.98 mm SL; Santo Antônio do Itambé, Santo Antônio basin (18°30'0.00"S 43°17'60.00"W); col. Alfredo Carvalho Filho, 09 Aug 2004. **MZUSP 87832**, 5, 57.73 – 36.27 mm SL; Santo Antonio de Itambé, Lageado creek, Mão D`água river, Santo Antônio basin (18°28'27.12"S 43°17'29.27"W); col. Alfredo Carvalho Filho, 30 Aug. 2004. **MZUSP 94485**, 3, 42.28 –34.54 mm SL; Alto Rio Doce, Xopotó river, tributary of Piranga river (21°4'4.00"S 43°27'50.00"W); col. Oyakawa, Baena & Loeb, 11 Jul. 2007. **MZUSP 94486**, 1, 27.75 mm SL; Alto Rio Doce Rio, Xopotó river, tributary of Piranga river (21° 4'4.00"S 43°27'50.00"W); col. Oyakawa, Baena & Loeb, 11 Jul. 2007. **MZUSP 94503**, 3, 50.75 – 42.8 mm SL; Caranaiba, Piranga river (20°51'37.00"S 43°43'11.00"W); col. Oyakawa, Baena & Loeb, 09 Jul. 2007. **MZUSP 94512**, 4, 38.97 – 34.32 mm SL; Alto Rio Doce, Xopotó river, Piranga river (21° 3'11.00"S 43°26'46.00"W); col. Oyakawa, Baena & Loeb, 11 Jul. 2007. **MZUSP 94518**, 2, 62.58 – 54.32 mm SL; Desterro de Melo; Xopotó river, tributary of Piranga river (21° 9'29.00"S 43°32'34.00"W); col. Oyakawa, Baena & Loeb, 10 Jul. 2007. **MZUSP 94520**, 2, 43.18 – 60.19 mm SL; Caranaiba, Piranga river (20°52'52.00"S 43°44'15.00"W); col. Oyakawa, Baena & Loeb, 09 Jul. 2007. **MZUSP 94522**, 7,

62.11 – 43.04 mm SL; Caranaiba, Piranga basin (20°52'52.00"S 43°44'15.00"W); col. Oyakawa, Baena & Loeb, 09 Jul. 2007. **MZUSP 94531**, 3, 48.12 – 29.24 mm SL; Desterro de Melo, Xopotó river, tributary of Piranga basin (21°9'10.00"S 43°31'49.00"W); col. Oyakawa, Baena & Loeb, 10 Jul. 2007. **MZUSP 94536**, 2, 35.47 – 26.24 mm SL; Desterro de Melo, Xopotó river, Piranga basin (21° 9'10.00"S 43°31'28.00"W); col. Oyakawa, Baena & Loeb, 09 Jul. 2007. **MZUSP 94538,** 3, 47.11 – 43.97 mm SL; Desterro de Melo, Xopotó river, tributary of Piranga basin (21° 9'10.00"S 43°31'28.00"W); col. Oyakawa, Baena & Loeb, 10 Jul. 2007. **MZUSP 94547**, 14, 39.69 – 22.81 mm SL; Carandaí, Piranga basin (20°57'45.00"S 43°41'48.00"W); col. Oyakawa, Baena & Loeb, 09 Jul. 2007. **MZUSP 94548**, 6, 58.45 – 32.26 mm SL; Carandaí, Piranga river (20°57'45.00"S 43°41'48.00"W); col. Oyakawa, Baena & Loeb, 09 Jul. 2007. **MZUSP 94564**, 75, 55.71 – 36.96 mm SL; Desterro de Melo, Xopotó river, tributary of Piranga river (21° 8'53.00"S 43°30'46.00"W); col. Oyakawa, Baena & Loeb, 10 Jul 2007. **MZUSP 109302**, 5, 53.1 – 33.3 mm SL; Conceição do Mato Dentro, Santo Antônio basin (18°43'50.00"S 43°26'8.00"W); col. T. C. Pessali, Dec. 2010. **MZUSP 109304**, 4, 40.63 – 21.28 mm SL; Conceição do Mato Dentro, Santo Antônio basin (18°53'18.00"S 43°27'7.00"W); col. T. C. Pessali, Dec. 2010. **MZUSP 109311**, 4, 49.04 – 33.83 mm SL; Conceição do Mato Dentro, Santo Antônio basin (18°49'44.00"S 43°24'25.00"W); col. T. C. Pessali, Dec. 2010. **MZUSP 109313**, 2, 49.66 – 49.15 mm SL; Conceição do Mato Dentro, Santo Antônio basin (18°48'16.00"S 43°26'16.00"W); col. T. C. Pessali, Dec. 2010. **MZUSP 109319**, 3, 33.31 – 30.98 mm SL; Conceição do Mato Dentro, Santo Antônio basin (18°59'25.00"S 43°26'47.00"W); col. T. C. Pessali, Dec. 2010. **MZUSP 109352**, 1, 38,95mm SL; Catas Altas, Paracatu creek, tributary of Piracicaba basin (20° 6'53.00"S 43°24'31.00"W); col. B. Maia, 31 Mar 2010. **MZUSP 109391**, 3, 64,08 – 42,68 mm SL; Santa Bárbara, Ribeirão Preto creek, tributary of Piracicaba basin (20° 3'57.00"S 43°40'16.00"W); col.

B. Maia, 31 Jul. 2010. **MZUSP 109392**, 1, 59.00 mm SL; Santa Barbara, Ribeirão Preto, tributary of Piracicaba basin (20° 3'57.00"S 43°40'16.00"W); col. Bruno Maia, Aug. 2010. **MZUSP 110933**, 1, 37.08 mm SL; Mariana, Gualaxo do Sul river (20°30'16.97"S 43°24'39.28"W); col. L.F. Salvador Jr. & L.A.C. Missiaggia, 05 Jul. 2012. **MZUSP 110937**, 1, 66,61 mm SL; Mariana, Piracicaba basin (20°13'48.93"S 43°27'14.34"W); col. L. F. Salvador Jr. & L. A. C. Missiaggia, 05 Oct. 2012. **MZUSP 112753**, 4, 41.81 – 35.91mm SL; Ferros, Santo Antônio basin (19°13'34.50"S 43° 1'9.50"W); col. O. T. Oyakawa & T. F. Teixeira, 16 Aug. 2012. **MZUSP121709**, 1, 48.53 mm SL; Coronel Fabriciano, Cachoeira do Escorrega waterfall, tributary of Piracicaba basin (19°25'0.42"S 42°43'20.68"W); col. V. J. C. Reis, 22 Mar. 2017. MZUSP 69333, 1, 63.02 mm SL; Coroací, Suaçuí basin (18°36'45.93"S 42°16'52.91"W); col. A. M. Zanata, 28 Apr. 2001. **MZUSP 121710**, 1, 48.88 mm SL; Coronel Fabriciano, Cachoeira do escorrega waterfall, Piracicaba basin (19°25'0.42"S 42°43'20.68"W); col. V. J. C. Reis, 22 Mar. 2017. **MZUSP 121719**, 4, 52.09 – 40.91 mm SL; Santana do Paraíso, Piracicaba basin (19°19'20.24"S 42°31'38.49"W); col. V. J. C. Reis, 23 Mar. 2017. **MZUSP 123393**, 1, 43.51; Baguarí, main stream of Rio Doce (19° 1'14.00"S 42° 7'14.40"W); col. V.J.C. Reis & T. Pessali, 12 Nov. 2017.

LBP 1013, 1, 62,09 mm SL; Caranaíba, Piranga river (21° 8'56.82"S 43°23'58.38"W); col. J. C. Oliveira, A. L. Alves, L. R. Sato, 12 Oct. 2001. **LBP 1016**, 3, 56,49 – 44,32 mm SL; Caranaíba, Piranga river (20°58'10.26"S 43°42'19.86"W); col. JC Oliveira, A. L. Alves, L. R. Sato, 13 Oct. 2001. **LBP 1020**, 12, 51.07 – 36.18 mm SL; Caranaíba, Papagaio river (20°51'7.74"S 43°43'7.62"W); col. J. C. Oliveira, A. L. Alves, L. R. Sato, 13 Oct. 2011. **LBP 8350**, 1, 38,95 mm SL; Ferros, Piçarrão river (19°16'43.87"S 42°53'53.40"W); col. C. Oliveira, G. J. C. Silva, F. F. Roxo, T. N. A. Pereira, 18 May 2009. **LBP 12259**, 15, 56.77 – 35.13 mm SL; Desterro de Melo,

Xopotó river (21° 9'9.70"S 43°31'37.90"W); col. A. Ferreira, F. F. Roxo, G. J. Costa e Silva, 19 Jun. 2011.

MNRJ 1152, 16, 66.17 – 31.58 mm SL; Viçosa, Piranga river (20°44'51.10"S 42°51'35.95"W); col. J. Moojen Oliveira, no date. **MNRJ 22400**, 6, (56.32 – 32.75 mm SL); Caparaó, Grumarim creek, tributary of Capim Roxo river (20°31'38.69"S 41°53'33.83"W); col. A. T. Aranda, F. A. G. Melo & F. P. Silva, 07 Aug. 2001. **MNRJ 30980**, 2, 76.01 – 62.8 mm SL; Senhora dos Remédios, Piranga river (21° 2'13.69"S 43°35'46.63"W); col. M. Britto, N. Tamaio & I. Tamaio, 30 Dec. 2006. **MNRJ 39468**, 9, 40.07 – 25.16 mm SL; Alto Caparaó, Caparaó river, tributary of Manhuaçu basin (20°27'38.26"S 41°52'5.40"W); col. L. M. Sarmento-Soares, M. R. Britto, 09 Sep. 2011. **MNRJ 42745**, 1, 68.34 mm SL; Caparaó, Caparaó river, tributary of Manhuaçu river (20°32'0.17"S 41°54'34.70"W); col. P. Buckup, M. Britto & D. F. Moraes Junior, 14 Apr. 2014. **MNRJ 43174**, 1, 60.59 mm SL; Alto Caparaó, Caparaó river, tributary of Manhuaçu basin (20°28'39.58"S 41°52'25.50"W); col. E. Pauls, 08 May 1997. **MNRJ 50893**, 3, 43.53 – 43.84 mm SL; Serra Azul, main stream of Suaçuí Grande basin (123357); col. S. A. Santos & T. C. Pessali, 16 Feb. 2018.

Trichomycterus argos Lezama *et al.*, 2012

(Fig. 11)

Trichomycterus argos Lezama, Triques & Santos, 2012:62, Figs. 2, 3a. Parque Estadual da Serra do Brigadeiro, Córrego Nova, headwaters of the Rio Casca, right bank tributary of Rio Doce at the limits of Rio Doce and Rio Paraíba do Sul basins, 20°43'19"S, 42°28'43"W, Minas Gerias State, Brazil [Holotype: AZUFMG 103. Paratypes: DZUFMG 058 (1), 059 (14), 067 (1, c&s); MZUSP 106274 (3)]; DoNascimiento *et al.*, 2014b [list]; García-Melo *et al*. 2016:237 [cited (discussion on its relationships)].

Diagnosis - *Trichomycterus argos* is distinguished from all congeners from Southeastern Brazil except from the *T. brasiliensis* species complex, by the number of pectoral-fin rays, I+6, (vs. I+8 or I+7). Lezama, Triques & Santos (2012) distinguished *T. argos* from *T. brasilienis* by the absence of series of spots, as well as absence of confluent spots forming elongated marks or vermiculations (vs. presence of series of large [three times eye-diameter or more] spots dorsolaterally, laterally and ventrolaterally on flank in *T. brasiliensis*, more clearly visible in small specimens), by a transverse and straight border between the parietosupraoccipital and frontal bones (Fig. 12a) (vs. oblique and irregular border, in *T. brasiliensis*; Fig. 12b) and by a large foramen for the ramus lateralis accessorius facialis, visible in dorsal view, in the parietosupraoccipital bone (vs. foramen for the ramus lateralis accessorius facialis minute, at least four times smaller than in the new species, located on a ridge of the bone, and visible only in lateral view, in *T. brasiliensis*; Fig. 12b). Distinguished from *T. brunoi* by a longer snout/HL, and by the number of interopercle odontodes, 39 - 40 (vs. shorter snout and 26 – 31interopercle odontodes in *T. brunoi*).

Description – Morphometric data for specimens examined in Table 05. Body long and almost totally straight, trunk roughly round in cross-section near head, then slightly deeper than broad and softly compressed to caudal peduncle, tapering to Caudal-fin. Dorsal profile of body gently convex to dorsal-fin origin, then straight or slightly concave along caudal peduncle to caudal-fin origin. Ventral profile convex from gular region to vent, due partly to abdominal distension, then straight or slightly concave along anal-fin origin to caudal-fin base. Caudal peduncle turns as deep as body at beginning of anal-fin base slightly right at the base of caudal-fin rays.

Head approximately one-fifth to one-fourth of SL, pentagonal, longer than wide and depressed, with a long snout. Mouth sub-terminal. Upper jaw slightly longer than lower. Upper lip wider than lower lip, and laterally continuous with base of maxillary barbel. Lower lip small, approximately 2/3 width of upper one, partly divided into right and left portions by with median concavity. Lower lip with uniform covering of tiny vilii, resulting in velvet-like surface and not clustered into large papillae. Region between upper and lower lips with slender fleshy lobe.

Dentary and premaxillary teeth similar to each other in shape. Dentary teeth conical with size of individual teeth increasing markedly towards symphysis and from posterior to anterior rows. Total area of premaxillary teeth slightly smaller than that of dentary, with teeth arranged irregularly in four rows, over entire ventral surface of premaxilla. Premaxillary teeth conical.

Eye small-sized, protruding, positioned dorsally on head, without free orbital rim and covered with transparent skin. Eye located on anterior half of HL, closer to lateral border of the head than to the midline in dorsal view. Infraorbital latero-sensory canal incomplete, extending from sphenotic posteriorly to terminal pore located ventroposteriorly to eye. Anterior nares surrounded by tube of integument directed anterolaterally, continuous posterolaterally with nasal barbel. Posterior nares closer to anterior nares than to the eyes, surrounded by tube of integument

incomplete posteriorly. Maxillary barbel tubular narrowing markedly towards fine tip, reaching base of pectoral-fin. Rictal barbel inserted immediately ventral to maxillary barbel. Its tip goes until lateroposterior border of interopercle. Nasal barbel originating on posterolateral region of anterior nares, reaching from slightly anterior to anterior border of opercle to touching, but not surpassing, anterior border of opercle. Interopercular patch of odontodes, oval in shape and with well-developed odontodes, prominent in ventral aspect of head. Interopercular patch of odontodes extending from vertical through ventroposterior border of eye to ventroanterior to opercle. Odontodes arranged in three irregular series, with those on mesial series much longer than those on lateral one; odontodes gradually larger posteriorly in both series, with those posteriorly on mesial row largest. Interopercular odontodes 39 - 40. Opercular patch of odontodes on dorsolateral surface of posterior part of head, positioned anterodorsally to pectoral-fin base, roundish in shape slightly smaller than eye in dorsal aspect of head. Opercular odontodes 14 - 18, sunk in individual slits of integument, progressively larger posteriorly, all with fine tips, with largest ones curved distally and claw-like. Entire patch surrounded by specialized rim of integument.

Pectoral-fin medium-sized, its base immediately posterior and ventral to opercular patch of odontodes. Pectoral-fin rays I+6. First pectoral-fin ray (unbranched) longer than all others, prolonged as filament beyond fin web, with short filament. Other rays progressively less long, their tips following continuous line along fin margin. Pelvic-fin with convex distal profile, its origin slightly posterior to middle of SL and anterior to vertical through dorsal-fin origin, surpassing anal and urogenital openings in adults. Pelvic-fin rays I+4, first ray unbranched, its bases are very close to each other. Dorsal-fin long, its distal profile sinusoidal. Dorsal-fin origin closer to base of caudal-fin than to tip of snout. Dorsal-fin rays II+7, two segmented and unbranched procurrent rays and seven branched and segmented rays (therein included two

posterior closely-set rays). Anal fin slightly smaller than dorsal-fin, its distal profile gently convex. Anal-fin origin posterior to vertical through end of dorsal-fin base. Anal-fin rays II+5 two segmented and unbranched procurrent rays and five branched and segmented rays. Caudal-fin rounded with 6+7 principal rays. Adipose-fin absents or modified into low integument fold extending between end of dorsal-fin and caudal-fin origin. Due to the absence of specimens that were no type-material and just three paratypes available to analyze, this description does not have osteological descriptions.

Cephalic lateral line canals with simple, non-dendritic tubes ending in single pores. Supraorbital canal mostly within frontal bone. Supraorbital pores invariably present: s1 mesial to nasal-barbel base and autopalatine, s3 mesial to posterior nostril and anterior to frontal, paired s6, posteromedial to eye and at midlength of frontal, and distance to orbits being the same that distance to mesial line. Infraorbital canal with four pores, i1 and i2 anteriorly and i10 and i11 posteriorly. Canal lacking associated ossification. Infraorbital pore i1 located ventro-lateral to nasal-barbel base and autopalatine, i2 ventro-lateral to posterior nostril and anterior to frontal, i10 and i11 posterior to eye. Otic canal without pores. Postotic pores po1, anteromedial to opercular patch of odontodes), and po2, mesial to opercular patch of odontodes. Lateral line of trunk anteriorly continuous with postotic canal and reduced to short tube. Lateral line pores ll1 and ll2 present dorsomedial to pectoral-fin base.

Coloration in ethanol. – *Trichomycterus argos* has two basic types of pigmentation patterns, which one probably turning into the other along ontogeny. Contrary to the original description of *T. argos*, a small paratype of this species has chromatophores forming round dark maculae bigger than eye diameter organized in a line along the mid-lateral portion of body. That line beigins right posterior to the opercle and extends to the end of dorsal-fin base. Dorsally to that mid-lateral line,

there are several smaller, round to amoeboid in shape, dark blurred maculae that can be coalescent or not and with mid-lateral line maculae. Those maculae or spots are randomly distributed dorsally in the body. Ventrally to the mid-lateral line, there are randomly distributed round dark maculae, fewer and bigger than dorsal maculae. In larger and bigger specimens of *T. argos* the pigmentation pattern changes considerably from the one described above. The mid-lateral line maculae fade or disappear and the pigmentation pattern agrees with that in the original description. However, in both young and adult specimens the pigmentation concentration still follows the same pattern. In both young and adult specimens, the caudal peduncle has fewer chromatophores in comparison with the rest of the body. Ventrally in the abdomen there few or no dark pigmentation. Fins with few spots or none, except on the caudal-fin which has a vertical dark bar. Mid-dorsum of the trunk with dark chromatophores forming small round to amoeboid blurred and partly coalescent maculae. The concentration of chromatophores seems to increase with size. In the head of young specimens there are several dark round variably-sized, widely-spaced maculae, while in adult specimens these maculae change in shape and size, becoming small and vermiculate to amoeboid. Head with agglutinated brownish chromatophores. Tip of snout, cheeks, and ventroposterior region of the eye with fewer chromatophores in comparison with the rest of head. Opercular odontodes with dark pigment, mainly in the surrounding integument fold. Interopercular odontodes lightly pigmented.

Remarks – *Trichomycterus argos* Lezama *et al.*, 2012 and its presumably close relative *T. brunoi* Barbosa & Costa, 2010 are the only species resembling *T. brasiliensis* known to occur in the Rio Doce basin. *Trichomycterus brunoi* and *T. argos* belong as part of the *Trichomycterus brasiliensis* complex (Bockmann & Sazima, 2004; Barbosa & Costa, 2010) indeed sharing many character

conditions such as number of pectoral-fin rays I+6, similar color pattern, and pelvic-fin bases in close proximity.

Lezama *et al.* (2012) reported that *T. argos* is distinguished from *T. brunoi* exclusively by its color pattern (presence of stripes, vermiculations or reticulations in the former and their absence in the latter). However, color pattern is not a reliable proxy for diagnosing most species in *Trichomycterus*, and within samples examined referable to the two species, the range of variation shows overlap, thus blurring the apparent limits between the two taxa (Fig. 11 and 13). Indeed, color pattern has been reported to vary considerably within species of the *T. brasiliensis* complex (Barbosa & Costa, 2010). The scant evidence available suggests that *T. argos* is probably a junior synonym of *T. brunoi*. A conclusive solution to this issue, however, requires additional research and more numerous specimens from both species.

Geographical distribution – *Trichomycterus argos* is known only from the type material, collected in the Rio Casca, tributary of Rio Doce basin at the State Park Serra do Brigadeiro. Intersting both type locality of *T. argos* and *T. brunoi* is considerably close to each other (about 50 km) with many small tributaries between them (Fig. 14). With this in mind, and even without empiric data, it is possible to suppose that both species could coinhabit the same stream somewhere else in this region.

Examined material – Paratype **MZUSP 106274**, 3, 90.80 – 56.10 mm SL; Brazil, State of Minas Gerais, Araponga municipality, Parque Estadual da Serra do Brigadeiro, Córrego Serra Nova, headwaters of the Rio Casca, right bank tributary of Rio Doce at the limits of Rio Doce and Rio Paraíba do Sul basins (20°43'19"S 42°28'43"W); col. P. S. Santos, 7 October 2001.

Trichomycterus ‘‘astromycterus’’, sp. nov.

(Fig. 15)

Holotype. – MZUSP 123760, 51.98 mm SL, Brazil, Minas Gerais, Rio Doce; Rio do Peixe river tributary of Piranga river (20°11'40.32"S 42°51'8.47"W); col. VJC Reis, M de Pinna, G. Ballen & GF de Pinna.

Paratype. – MZUSP 123341, 1, 46.11mm SL, Brazil, Minas Gerais, Naque municipality; Santo Antônio river, tributary of Rio Doce basin (19°14'0.76"S 42°19'26.52"W); col. T. Pessali, 01 Sep 2017. **ex - MZUSP 123760**, 37, 51.66 - 11.81 mm SL, (C&S, 2, 45.76 - 44.09 mm SL), Brazil, Minas Gerais, Rio Doce; Rio do Peixe river tributary of Piranga river (20°11'40.32"S 42°51'8.47"W); col. VJC Reis, M de Pinna, G. Ballen & GF de Pinna. **MZUSP 123361**, 13, 38.46 - 29.33 mm SL, (C&S, 2, 35.66 – 34.29); Brazil, Minas Gerais, Naque municipality; Santo Antônio river, tributary of Rio Doce basin (19°14'0.76"S 42°19'26.52"W); col. T. Pessali & VJC Reis 25 Oct 2017.

Diagnosis.- Autapomorphically diagnosed by the following characters, unique within Trichomycteridae: 1- the distally expanded maxilla (Fig. 16); 2- the t-shaped, short and thick mesethmoid cornua; 3- the hypertrophied anterior process of the vomer. The slightly hypocercal Caudal-fin further distinguishes the new species from all congeners. Distinguished from all congeners from the Rio Doce basin by the number of branched and segmented dorsal-fin rays and dorsal pterygiophores, having six to nine rays (more commum eight and nine) and seven to nine pterygiophores (vs. strictly seven branched and segmented dorsal-fin rays and strictly eight pterygiophores from all species from the Rio Doce). Distinguished from all congeners from the Rio Doce basin by the number of dorsal and ventral proccurent caudal-fin rays, which the number of dorsal proccurent caudal-fin rays usually is the doble of ventral proccurent caudal-fin rays (vs.

more similar number of dorsal and ventral procurrent caudal-fin rays). The combination of narrow caudal peduncle (9.30% SL), the long head (22.33%SL), the very short barbels, and the protruding dorsal eyes further distinguish the new species from all other Trichomycterinae in southeastern Brazil.

Description.- Morphometric data for specimens examined in Table 06. Body short and stout, trunk roughly round in cross-section near head, then slightly deeper than broad and abruptly compressed at caudal peduncle, tapering to Caudal-fin. Dorsal profile of body gently convex to dorsal-fin origin, then straight or slightly convex along caudal peduncle to caudal-fin origin. Ventral profile convex from gular region to vent, due partly to abdominal distension, then straight to anal-fin origin and straight or slightly concave along caudal peduncle to caudal-fin base. Caudal peduncle region markedly less deep than rest of body. Dorsal profile of caudal peduncle including vestigial fin fold or Adipose-fin, poorly defined and confluent with Caudal-fin.

Head longer than wide and depressed. Mouth inferior, located distant from anterior margin of snout. Upper jaw markedly longer than lower, with premaxillary dentition almost entirely exposed in ventral view. Upper lip broad, wide and fleshy in ventral view, its ventral surface covered with numerous large papillae. Each papilla formed by cluster of small vilii. Lateral portion of upper lip continuous with base of rictal barbel. Lower lip small, approximately half as wide as upper one, with median concavity slightly dividing it into right and left portions. Lower lip with uniform coveling of tiny vilii, velvet-like in aspect and not clustered into large papillae. Region between upper and lower lips with well-differentiated fleshy lobe, adpressed posteriorly to cheek musculature.

Dentary and premaxillary teeth similar to each other in shape and size. Dentary teeth approximately 45-55 in number, arranged in three irregular rows extending to base of coronoid

process, with size of individual teeth increasing markedly towards symphysis and from posterior to anterior rows, with medialmost anterior tooth approximately seven times the length of lateralmost posterior tooth. In cleared and stained paratypes, dentary teeth of first row mostly narrowly incisiform near symphysis, with remaining teeth conical (Fig. 17). Area of premaxilary teeth smaller than that of dentary, with 30-40 teeth arranged irregularly over entire ventral surface of premaxilla. In cleard and stained paratypes, teeth near symphysis mostly narrowly incisiform, especially anteriorly, with remaining teeth conical. In considerably larger holotype, most jaw teeth incisiform.

Eyes large, protruding, positioned dorsally on head, without free orbital rim and covered with transparent skin. Eyes located slightly posterior to half of HL, closer to midline than to lateral border of head in dorsal view. Infraorbital latero-sensory canal incomplete, extending from sphenotic posteriorly to endpore located ventroposteriorly to eye. Anterior nares surrounded by tube of integument directed anterolaterally, continuous posterolaterally with nasal barbel. Part of integument rim extending along posterior margin of barbel forming conspicuous flap for proximal 25% of barbel. Posterior nares slightly closer together than anterior ones, surrounded by tube of integument incomplete posteriorly. Maxillary barbel extremely wide at base and narrowing markedly towards fine tip, reaching slightly beyond middle of eye when completely extended. Rictal barbel inserted immediately ventral to maxillary barbel but with base one-third as wide, its tip not reaching base of interopercular patch of odontodes when completely extended. Nasal barbel keel-like, originating on posterolateral region of anterior nares, reaching about 60% of distance between its base and anterior margin of eye. Interopercular patch of odontodes small in overall size, slightly larger than eye in lateral aspect, oval in shape and with well-developed odontodes, visible in ventral aspect of head but not conspicuously so. Interopercular patch of odontodes

extending from vertical through posterior border of eye anteriorly to slightly to anterior to vertical through pectoral-fin base posteriorly. Odontodes arranged in two irregular series, with those on mesial series much larger than those on lateral one; odontodes gradually larger posteriorly in both series, with those posteriorly on mesial row largest. Interopercle odontodes 23 -24. Opercular patch of odontodes on dorsolateral surface of posterior part of head, anterodorsally to pectoral-fin base, roundish in shape and slightly smaller than eye in dorsal aspect of head. Opercular odontodes 11 - 16, each one sunk in individual slit of integument, progressively larger posteriorly, all with fine tips, with largest ones curved distally and claw-like. Entire patch surrounded by specialized rim of integument typical of that complex in most other trichomycterids.

Pectoral-fin large (tip of first ray extending to middle of distance between occiput and pelvic-fin base), gently convex or sinusoidal in distal profile, its base immediately posterior and ventral to opercular patch of odontodes. Pectoral-fin rays I+7 or I+8 with counts asymmetrical in some specimens. First pectoral-fin ray (unbranched) longer than all others, prolonged as filamente beyond fin web. Other rays progressively less long, their tips following continuous line along fin margin. Second ray sometimes longer than more posterior rays. Pelvic-fin with convex distal profile, its origin slightly posterior to middle of SL, and anterior to vertical through dorsal-fin origin, surpassing anal and urogenital openings by approximately half-fin length, but falling short of anal-fin origin also by half-fin length. Pelvic-fin rays I+4, first ray (unbranched) shorter than others. Long fine pelvic splint extending for almost half-length of first pelvic-fin ray. Dorsal-fin long, its distal profile sinusoidal. Dorsal-fin origin closer to base of Caudal-fin than to tip of snout. Dorsal-fin rays ii+II+6 (01), ii+II+7 (02), ii+II+8 (02) or ii+II+9 (02), plus two anterior unsegmented procurrent rays. Anal fin smaller and shorter than dorsal-fin, its distal profile gently convex. Anal-fin origin slightly anterior to vertical through end of dorsal-fin base. Anal-fin rays

i+II+5 (06) and ii+II+5 (01), plus one anterior unsegmented procurrent ray. Caudal-fin bilobed with round corners, with lower lobe longer than upper one and 6+7 principal rays. Caudal-fin procurrent rays 20-23 dorsally and 9-13 ventrally, plus one segmented non-principal ray ventrally in some specimens. Adipose-fin absent or modified into low integument fold extending between end of dorsal-fin and caudal-fin origin. Vertebrae 32(02), 33(03), 34(01), 35(01). First dorsal-fin pterygiophore immediately anterior to neural spine of 12^{th} (03), 13^{th} (02), 14^{th} (02) vertebra, first anal-fin pterygiophore immediately anterior to neural spine of 17^{th} (03), 18^{th} (02), 19^{th} (02) vertebra. Pleural ribs 8 (02), 9 (04), 10 (01). Branchiostegal rays 7. Dorsal-fin pterygiophores 7 (01), 8 (02), 9 (04). Anal-fin pterygiophores 6 (07).

Cephalic lateral line canals with simple, non-dendritic tubes ending in single pores. Supraorbital canal mostly within frontal bone. Supraorbital pores invariably present: s1 mesial to nasal-barbel base and autopalatine, s3 elongated and mesial to posterior nostril and anterior to frontal, and s6 single or very close together posteromedial to eye and at midlength of frontal. Infraorbital canal consisting of four pores, two anterior-most, i1 and i2, and two posteriormost, i10 and i11, lacking associated ossifications. Infraorbital pores: i1 ventro-lateral to nasal-barbel base and autopalatine, i2 ventro-lateral to posterior nostril and anterior to frontal, with its anterior border open, i10 and i11 posterior to eye, and anterolateral to anterior process of sphenotic. Otic canal without pores. Postotic pores po1 (anteromedial to opercular patch of odontodes and lateral to joint between sphenotic-prootic-pterosphenoid and pterotic), and po2 (medial to opercular patch of odontodes and lateral to joint between pterotic and posttemporo-supracleithrum). Lateral line of trunk anteriorly continuous with postotic canal and reduced to short, non-ossified tube in all four type specimens. Lateral line pores ll1, ll2 and ll3 present dorsomedially to pectoral-fin base and posterior to posttemporo-supracleithrum.

Coloration in ethanol. - Dorsum and sides of body with large roundish marks roughly arranged in files, 12-15 laterally and 7-9 dorsally, progressively smaller and less orderly posteriorly. Narrow scattering of smaller spots ventral to large lateral ones, roughly following interface between myomeres and abdominal cavity and extending posteriorly onto ventral part of caudal peduncle. Conspicuous dark spot dorsal to base of Pelvic-fin. Abdominal region white.

Overall color of head similar to, and slightly denser than, that of dorsum. Cheeks and snout with closely-set dark fields. Dorsal part of opercular patch of odontodes surrounded with dark field. Integument amidst opercular odontodes interspersed with dark streaks, contrasting with white odontode slits. Region of head corresponding to skull roof almost continuously dark. Sensory pores on head white. Bases of nostrils extremely dark. Ventral surface of head white, except for sparse irregular melanophores close to angle of mouth. Dorsal surface of upper lip less dark than rest of head. Ventral part of uper lip and lower lip white. Base of maxillary barbel darky-pigmented dorsally, especially posteriorly. Dark fields extending onto basal third of dorsal surface of barbel, with remainder of barbel white on both sides. Rictal barbel mostly white, with few small elongate dark fields near base. Nasal barbel dark along nearly its entire length, on both sides. Base of pectoral-fin with dense dark spots on dorsal surface, extending to half of fin as elongate fields along fin rays. Ventral surface of pectoral-fin lacking dark pigment. Dorsal and anal fins with heavy dark covering over basal third or half of individual rays, fading distally. Fin web lacking dark chromatophores. Pelvic-fins white. Basal two-thirds of caudal-fin rays darkly dashed, with individual dashes vertically-aligned and forming pattern of three or four vertical stripes on fin, progressively less pronounced distally. Margin of Caudal-fin white.

Etymology.- A compound noun formed from *Astroblepus* (Astroblepidae) and *Trichomycterus* (Trichomycteridae) in reference to the superficially similar aspect of the new taxon to the former genus.

Remarks. - *Trichomycterus "astromycterus"* is a remarkable species differing from all trichomycterinaes in many morphological aspects (cf. Diagnosis above). Its external morphology superficially resembles species of *Microcambeva* (Sarcoglanidinae) but detailed study of its anatomy and COI sequences leave no doubt that it is not a member of the Sarcoganidinae but a Trichomycterinae instead. The numerous and conspicuous autapomorphies of *T. "astromycterus"* distinguish it not just from all *Trichomycterus* in the Doce basin, but in fact from all other congeners in the Eastern coast of South America. Such high degree of phenotypic divergence might suggest that it represents a new genus under traditional generic concepts in Trichomycteridae. Nevertheless, no conspicuous morphological evidence was found that might place it outside of the phylogenetic range currently circumscribed to species of *Trichomycterus* (de Pinna, 1998, 2017; Wosiacki, 2002). Because phylogenetic principles dictate that higher taxa are to be justified on grounds of relative phylogenetic position, rather than merely lineage divergence, we think that the best placement for *T. "astromycterus"* is within the genus *Trichomycterus*. This is corroborated by our COI data, which place the species internested within *T. alternatus* (see Dicussion below). *Trichomycterus "astromycterus"* is definitely a taxon which deserves more study, first of all because of its combination of pronounced phenotypic divergence associated with no COI divergence (see Discussion).

Interestingly, material collected of *T. "astromycterus"* came from quite two different habitats. At Rio do Peixe locality, adult specimens were found among rocks in an extremely fast-running water sector. At the Santo Antônio locality, specimens were collected deeply buried in

sand banks, in sectors with moderate current. Juvenile specimens in the Rio do Peixe locality were found in quiet sectors over sand banks.

Geographical distribution - *Trichomycterus "astromycterus"* was collected in the upper and middle Rio Doce basin. In both localities this species was very close to the main channel of Rio Doce river, which suggest this species is probably distributed in all basin (Fig. 18).

Trichomycterus "barrocus", sp. nov.

(Fig. 19)

Holotype - MBML 2238, 79.83 mm SL, (X-rayed); Brazil, Espírito Santo, Afonso Cláudio; Boa Sorte river, Guandú river; 20°10'57.00"S 41° 4'50.00"W; L. M. Sarmento-Soares, R. F. Martins-Pinheiro, A. T. Aranda, R. L. Teixeira e M. M. C. Roldi and M. M. Lopes; 12 Jun 2009.

Paratype – ex-**MBML 2238**, 5, 79.83 – 54.90 mm SL, (C&S 1, 55.86 mm Sl), (Rafiografed, 1, 78.74 – 55.86 mm SL); Brazil, Espírito Santo, Afonso Cláudio; Boa Sorte river, Guandú river; 20°10'57.00"S 41° 4'50.00"W; L. M. Sarmento-Soares, R. F. Martins-Pinheiro, A. T. Aranda, R. L. Teixeira e M. M. C. Roldi and M. M. Lopes; 12 Jun 2009.

Diagnosis. - *Trichomycterus "barrocus"* is distinguished from all congeners in Southeastern Brazil by its color pattern, composed of two rows of unfused dark maculae. First row, dark and broad stripe in the mid-dorsum of trunk running from posterior border of head until caudal-fin, merged with amorphous dark maculae that resemble drops of dark ink in an unpigmented background. Second row of large and round dark maculae, which can fuse creating a broad stripe in some specimens. Row running in the lateral midline of body from posterior to opercle until base of caudal-fin. Ventral to second row, lateral in the abdomen, presence of small round to amorphous

dark maculae, mainly from middle of body to caudal-fin. *Trichomycterus "barrocus"* is further distinguished from all congeners in Rio Doce basin, except *T. "sordislutum"* and some morphs of *T. alternatus*, by the short barbels, with the nasal barbel barely crossing the eyes, and maxilary and rictal barbels not reaching the interopercle and by the large urhoyal with long and thin wings (vs. curved urhoyal with short and wide wings).

Description.- Morphometric data for specimens examined in Table 07. Body long and almost totally straight, trunk roughly round in cross-section near head, then slightly deeper than broad and softly compressed to caudal peduncle, tapering to Caudal-fin. Dorsal profile of body gently convex to dorsal-fin origin, then straight or slightly concave along caudal peduncle to caudal-fin origin. Ventral profile convex from gular region to vent, due partly to abdominal distension, then straight or slightly concave along anal-fin origin to caudal-fin base. Caudal peduncle long and less as deep as body at end of anal-fin base.

Head approximately one-fifth of SL, pentagonal, longer than wide and depressed. Mouth sub-terminal. Upper jaw slightly longer than lower. Upper lip wider than lower lip, and laterally continuous with base of maxillary barbel. Lower lip small, approximately 2/3 width of upper one, partly divided into right and left portions by with median concavity. Lower lip with uniform covering of tiny vilii, resulting in velvet-like surface and not clustered into large papillae. Region between upper and lower lips with slender fleshy lobe.

Dentary and premaxillary teeth similar to each other in shape. Dentary teeth conical, arranged in four irregular rows, first row with 12 teeth, extending from base to slightly up of coronoid process, with size of individual teeth increasing markedly towards symphysis and from posterior to anterior rows. Total area of premaxilary teeth slightly smaller than that of dentary,

with teeth arranged irregularly in four rows, first row with approximately 13 teeth, over entire ventral surface of premaxilla. Premaxilary teeth conical.

Eye medium-sized, slightly protruding, positioned dorsally on head, without free orbital rim and covered with transparent skin. Eye located on anterior half of HL, closer to lateral border of the head than to the midline in dorsal view. Infraorbital latero-sensory canal incomplete, extending from sphenotic posteriorly to terminal pore located ventroposteriorly to eye. Anterior nares surrounded by tube of integument directed anterolaterally, continuous posterolaterally with nasal barbel. Posterior nares closer to anterior nares than to the eyes, surrounded by tube of integument incomplete posteriorly. Maxillary barbel tubular narrowing markedly towards fine tip, barely reaching from vertical posterior border of eye. Rictal barbel inserted immediately ventral to maxillary barbel. Its tip reaching until vertically posterior border of eye, not reaching the interopercle. Nasal barbel originating on posterolateral region of anterior nares, reaching anywhere from posterior border of eye, not reaching the interopercle. Interopercular patch of odontodes large, oval in shape and with well-developed odontodes, prominent in ventral aspect of head. Interopercular patch of odontodes extending from vertical through ventroposterior border of eye to ventroanterior to opercle. Odontodes arranged in two or three irregular series, with those on mesial series much longer than those on lateral one; odontodes gradually larger posteriorly in both series, with those posteriorly on mesial row largest. Interopercular odontodes 38 – 49. Opercular patch of odontodes on dorsolateral surface of posterior part of head, positioned anterodorsally to pectoral-fin base, roundish in shape and larger than eye in dorsal aspect of head. Opercular odontodes 15 - 25, sunk in individual slits of integument, progressively larger posteriorly, all with fine tips, with largest ones curved distally and claw-like. Entire patch surrounded by specialized rim of integument.

Pectoral-fin medium-sized, its base immediately posterior and ventral to opercular patch of odontodes. Pectoral-fin rays I+7. First pectoral-fin ray (unbranched) longer than all others, prolonged as filament beyond fin web. Other rays progressively less long, their tips following continuous line along fin margin. Pelvic-fin with convex distal profile, its origin slightly posterior to middle of SL and anterior to vertical through dorsal-fin origin, slightly covering anal and urogenital openings in adults. Base of pelvic-fins positioned close to each other. Pelvic-fin rays I+4, first ray unbranched. Ischiatic process of basipterygium short and thin. Dorsal-fin long, its distal profile sinusoidal. Dorsal-fin origin closer to base of Caudal-fin than to tip of snout. Dorsal-fin rays ii+II+6 (01), iii+II+7 (03), two or three unsegmented and unbranched rudimentary rays, commonly present in *Trichomycterus*, two segmented and unbranched procurrent rays and six (rare in *Trichomycterus* from Southeasten Brazil) or seven branched and segmented rays (therein included two posterior closely-set rays). Anal fin slightly smaller than dorsal-fin, its distal profile gently convex. Anal-fin origin posterior to vertical through end of dorsal-fin base. Anal-fin rays ii+I+7 (01) or iii+II+5 (03), two or three unsegmented and unbranched rudimentary rays, two segmented and unbranched procurrent rays (one specimen with one, though it is probably a demormity) and five branched and segmented rays (one specimen with seven, though it is probably a deformity). Caudal-fin sub-truncated shape, with 6+7 principal rays. Adipose-fin absent or modified into low integument fold extending between end of dorsal-fin and caudal-fin origin. Post-Weberian vertebrae 36 (03), 37 (01). First dorsal-fin pterygiophore immediately anterior to neural spine of 16th (01), 17th (01) 18th (01) vertebra, first anal-fin pterygiophore immediately anterior to neural spine of 21th (03) and 22th (01) vertebra. Caudal-fin procurrent rays plus one segmented non-principal ray dorsally and ventrally. Procurrent caudal-fin rays, 15 - 17 dorsally and 12 - 13 ventrally, beginning anteriorly at 31th (01), 32th (01), 33th (01*) vertebrae. Pleural ribs 11 (01), 12

(01), 13 (02). Branchiostegal rays 7 (04). Dorsal-fin pterygiophores 7 (01), 8 (03). Anal-fin pterygiophores 6 (04).

Cephalic lateral line canals with simple, non-dendritic tubes ending in single pores. Supraorbital canal mostly within frontal bone. Supraorbital pores invariably present: s1 mesial to nasal-barbel base and autopalatine, s3 mesial to posterior nostril and anterior to frontal, paired s6, though very close to each other, posteromedial to eye and at midlength of frontal. Infraorbital canal with four pores, i1 and i2 anteriorly and i10 and i11 posteriorly. Canal not ossified. Infraorbital pore i1 located ventro-lateral to nasal-barbel base and autopalatine, i2 ventro-lateral to posterior nostril and anterior to frontal, i10 and i11 posterior to eye. Otic canal without pores. Postotic pores po1, anteromedial to opercular patch of odontodes), and po2, mesial to opercular patch of odontodes. Lateral line of trunk anteriorly continuous with postotic canal and reduced to short tube. Lateral line pores ll1 and ll2 present dorsomedial to pectoral-fin base.

Coloration in ethanol. – Head with agglutinated brownish chromatophores. Tip of snout (from the anterior nares to the tip of upper lip), cheeks (right ventral to obits) and ventroposterior region of eye (not including the anterior portion in front of opercle) with little or no dark pigment. Opercular odontodes with dark pigment, interopercular odontodes white. Body with two rows of unfused dark maculae. First row a dark and broad stripe in the mid-dorsum of trunk running from posterior margin of head to caudal fin, merged with amorphous dark maculae resembling drops of dark ink in a white background. Second row formed by large and round dark maculae, occasionally fusing and forming a broad stripe in some specimens. Row running along the lateral midline of body from posteriorly to opercle until base of caudal-fin. Ventral to second row, small round to amorphous dark maculae, mainly from middle of body to caudal-fin. Ventral part of the body with

no dark pigmentation. Pectoral, pelvic, dorsal and anal fins with brownish spots mainly along bases. Caudal-fin with a vertical dark stripe across its base and spots amongst rays.

Etymology – The epithet "barrocus" comes from the historical art period, the baroque. This epithet was chosen to represent the beauty of this species.

Remarks –*Trichomycterus "barrocus"* is a distinctive and readily diagnosable species, endemic to lower Rio Doce basin. Some meristic values in this species are highly variable (number of Post-Werberian vertebrae, position of first dorsal and ventral pterygiophores, number of ribs and anal-fin rays; cf. Description above). Despite such surprising intraspecific variation in only three specimens available for osteological examination, they fall within the limits of variation in species of *Trichomycterus* represented by more abundant material. Because other diagnostic characters do not vary significantly, it seems likely that the type material represents a single species. Moreover, this species presents a distinct color pattern distinguished from all congeners (cf. pigmentation pattern in this description). Such dorsal color pattern has not been seeing in any other species. Although its mid-lateral color pattern can resemble some species such as *T. reinhardti (Eigenmann 1917)*, *T. itatiayae* Miranda Ribeiro 1906, *T. giganteus*, *T. nigroauratus* Barbosa & Costa 2008 and some morphs of *T. caipora*, the combination of morphology characters distinguishes this species from all formers.

Geographical distribution – *Trichomycterus "barrocus"* is endemic to the lower Rio Doce basin, at the Boa Sorte river, tributary of Rio Guandu (Fig. 20).

Trichomycterus "brucutu", sp. nov.

(Fig. 21)

Holotype - MZUSP 87834, 103 mm SL, radiographed; Brazil, State of Minas Gerais, Santo Antônio de Itambé, Lajeado creek, tributary of rio Mão D'água (18°30'0.00"S 43°17'60.00"W); col. A. Carvalho-Filho, 30 Aug 2004.

Paratype – Same data of holotype **– ex - MZUSP 87834 -** 2, 24.6 - 71.8 mm SL, radiographed; Brazil, State of Minas Gerais, Santo Antônio de Itambé, Lajeado creek, tributary of rio Mão D'água (18°30'0.00"S 43°17'60.00"W); col. A. Carvalho-Filho, 30 Aug 2004.

Diagnosis.- *Trichomycterus "brucutu"* is distinguished from all Southeastern Brazilian congeners by the deepest body, 19% - 19.94% (vs. 10.53% – 18.31% in all species analyzed from Southeast Brazil); by a long and wide dorsal and ventral integument fold from end of dorsal and anal- fin to base of caudal-fin, presenting long proccurent rays (vs. dorsal and ventral membrane beginning from middle of caudal peduncle length). Distinguished from all congeners from Rio Doce basin by its color pattern consisted by tiny, light brown, round to vermiculate spots homogeneous distributed into entire body. Distinguished from *T. "astromycterus", T. caipora, T. "tantalus", T. immaculatus, T. giganteus, T. "melanopygius"* and from all species from *T. brasiliensis* complex by number of pectoral-fin rays, strictly I+7 (vs. I+8 and I+6 or less, respectively).

Description.-

Morphometric data for specimens examined in Table 08. Body long and almost totally straight, trunk roughly round in cross-section near head, then slightly deeper than broad and softly compressed to caudal peduncle, tapering to Caudal-fin. Dorsal profile of body gently convex to dorsal-fin origin, then straight or slightly concave along caudal peduncle to caudal-fin origin.

Ventral profile convex from gular region to vent, due partly to abdominal distension, then straight or slightly concave along anal-fin origin to caudal-fin base. Caudal peduncle long, wide and as deep as body at beginning of anal-fin base, with a long and wide dorsal and ventral membrane from end of dorsal and anal- fin to caudal-fin, presenting long proccurent rays

Head approximately one-sixth of SL, pentagonal, longer than wide and depressed. Mouth sub-terminal. Upper jaw slightly longer than lower. Upper lip wider than lower lip, and laterally continuous with base of maxillary barbel. Lower lip small, approximately 2/3 width of upper one, partly divided into right and left portions by with median concavity. Lower lip with uniform covering of tiny vilii, resulting in velvet-like surface and not clustered into large papillae. Region between upper and lower lips with slender fleshy lobe.

Dentary and premaxillary teeth similar to each other in shape. Dentary teeth conical, arranged in four irregular rows extending from base to slightly up of coronoid process, with size of individual teeth increasing markedly towards symphysis and from posterior to anterior rows. Total area of premaxilary teeth slightly smaller than that of dentary, with teeth arranged irregularly in four rows over entire ventral surface of premaxilla. Premaxilary teeth conical.

Eye small sized-sized, protruding, positioned dorsally on head, without free orbital rim and covered with transparent skin. Eye located on anterior half of HL, closer to lateral border of the head than to the midline in dorsal view. Extensor tentaculi and dilatator opercula seems well-hypertrophied, creating a crest-like elevation dorsal to eyes. Infraorbital latero-sensory canal incomplete, extending from sphenotic posteriorly to terminal pore located ventroposteriorly to eye. Anterior nares surrounded by tube of integument directed anterolaterally, continuous posterolaterally with nasal barbel. Posterior nares closer to anterior nares than to the eyes, surrounded by tube of integument incomplete posteriorly. Maxillary barbel tubular narrowing

markedly towards fine tip, reaching the base of pectoral-fin. Rictal barbel inserted immediately ventral to maxillary barbel. Its tip reaching lateroposterior border of interopercle. Nasal barbel originating on posterolateral region of anterior nares, reaching anterior border of opercle. Interopercular patch of odontodes small, about 3/2 size of opercle, oval in shape and with well-developed odontodes, prominent in ventral aspect of head. Interopercular patch of odontodes extending from vertical through ventroposterior border of eye to ventroanterior to opercle. Odontodes arranged in two or three irregular series, with those on mesial series much longer than those on lateral one; odontodes gradually larger posteriorly in both series, with those posteriorly on mesial row largest. Interopercular odontodes 37 - 45. Opercular patch of odontodes on dorsolateral surface of posterior part of head, positioned anterodorsally to pectoral-fin base, roundish in shape in dorsal aspect of head and same size of eye diameter. Opercular odontodes 18 - 21, sunk in individual slits of integument, progressively larger posteriorly, all with fine tips, with largest ones curved distally and claw-like. Entire patch surrounded by specialized rim of integument.

Pectoral-fin medium-sized, its base immediately posterior and ventral to opercular patch of odontodes. Pectoral-fin rays I+7. First pectoral-fin ray (unbranched) longer than all others, prolonged as filament beyond fin web. Other rays progressively less long, their tips following continuous line along fin margin. Pelvic-fin with convex distal profile, its origin slightly posterior to middle of SL and anterior to vertical through dorsal-fin origin, touching the anterior border of anal and urogenital openings in adults, but not crossing it. Base of Pelvic-fins positioned one eye diameter close to each other. Pelvic-fin rays I+4, first ray unbranched. Dorsal-fin long, its distal profile sinusoidal. Dorsal-fin origin closer to base of Caudal-fin than to tip of snout. Dorsal-fin rays ii+II+7 (02), two unsegmented and unbranched rudimentary rays, commonly present in

Trichomycterus, two segmented and unbranched procurrent rays and seven branched and segmented rays (therein included two posterior closely-set rays). Anal fin slightly smaller than dorsal-fin, its distal profile gently convex. Anal-fin origin posterior to vertical through end of dorsal-fin base. Anal-fin rays ii+II+5 (02), two unsegmented and unbranched rudimentary rays, two segmented and unbranched procurrent rays and five branched and segmented rays. Caudal-fin sub-truncated shape, with 6+7 principal rays. Adipose-fin modified into high integument fold extending between end of dorsal-fin and caudal-fin origin. Post-Weberian vertebrae, 37 (02). First dorsal-fin pterygiophore immediately anterior to neural spine of 17th (02), vertebra, first anal-fin pterygiophore immediately anterior to neural spine of 21th(02) vertebra. Caudal-fin procurrent rays plus one segmented non-principal ray dorsally and ventrally. Procurrent caudal-fin rays, 24 - 25 (02) dorsally and 14 - 17 (02) ventrally, beginning anteriorly at 28th (02) vertebra. Pleural ribs 12 (01) - 13 (01). Branchiostegal rays 8 (02). Dorsal-fin pterygiophores 8. Anal-fin pterygiophores 6.

Cephalic lateral line canals with simple, non-dendritic tubes ending in single pores. Supraorbital canal mostly within frontal bone. Supraorbital pores invariably present: s1 mesial to nasal-barbel base and autopalatine, s3 mesial to posterior nostril and anterior to frontal, paired s6, closer to mesial line than to eyes, posteromedial to eye and at midlength of frontal. Infraorbital canal with four pores, i1 and i2 anteriorly and i10 and i11 posteriorly. Canal not ossified. Infraorbital pore i1 located ventro-lateral to nasal-barbel base and autopalatine, i2 ventro-lateral to posterior nostril and anterior to frontal, i10 and i11 posterior to eye. Otic canal without pores. Postotic pores po1, anteromedial to opercular patch of odontodes), and po2, mesial to opercular patch of odontodes. Lateral line of trunk anteriorly continuous with postotic canal and reduced to short tube. Lateral line pores ll1 and ll2 present dorsomedial to pectoral-fin base.

Coloration in ethanol. – Dark chromatophores distributed into inner and outer skin layers. Head darkest on region corresponding to neurocranium, outlined by brain pigment seen by transparency. Area of the *levator operculi* and *aductor operculi* muscles on the cheeks with few chromathofores. Laterally on the head rounded dark and tiny spots, mainly located anterolaterally to opercle. Similar maculae pattern found on all body. Margin of integument fold of opercular patch of odontodes darkly-pigmented. Interopercular patch of odontodes white (no pigmentation). Base of nasal barbels surrounded with concentration of dark pigment, extending posteriorly as elongate dark field to anterior margin of eyes. Through all body, excluding the ventral part, presence of tiny brownish round to amoeboid maculae shortly spaced among others, rarely fusing to others. Spots restricted to base of fins, though rays are usually dark pigmented.

Etymology – The epithet "Brucutu" comes from a Brazilian slang for rustic, gross and brute, as well as the deep body and caudal peduncle of this species. This name derives from an American cartoon about a rustic and brute cave man who lives in a pre-history time. Brucutu is also the second largest iron cave in Brazil, located in the State of Minas Gerais, which its hydrographical area belongs to the Rio Doce basin.

Remarks – *Trichomycterus "brucutu"* has a remarkably deep body when adult, however a small specimen (24.7 mm SL) collected together with the holotype does not show this particularity. Although this character is definitely helpful to identify adult specimens, it is not useful for diagnosing small ones. A second conspicuous diagnostic character for *T. "brucutu"* is the length and depth of dorsal and ventral integument fold on the caudal peduncle. Such trait accentuates the depth of the caudal peduncle and makes it externally even (in depth) from the level of dorsal and anal-fin ends to slightly beyond caudal-fin base. Such condition is unique among species of *Trichomycterus* in Southeastern Brazil. In all other species with deep caudal peduncles (e.g., *T.*

brasiliensis), the posterior part of the that region flares towards its fusion with the caudal fin. *Trichomycterus "brucutu"* is most similar in general body shape and pigmentation to *T. vermiculatus* and from species belonging to *T. brasiliensis* complex. However, the former can be readily distinguished by the number of pectoral-fin ray, I+7 (vs. I+5 or 6 in *T. vermiculatus* and in all species belonging to *T. brasiliensis* complex); and distinguished by the distance between pelvic-fin bases, one eye diameter between both bases (vs. pelvic-fin bases in very close proximity). In sum, *T. "brucutu"* is not just promptly distinguished from *T. vermiculatus*, but from all species fitting in the *T. brasiliensis* complex.

Geographical distribution – *Trichomycterus "brucutu"* is endemic to the Lajeado creek, in the headwaters of Rio Santo Antônio, a tributary of the middle Rio Doce basin (Fig. 22).

Trichomycterus brunoi Barbosa & Costa, 2010.

(Fig. 13)

Trichomycterus brunoi - Barbosa M. A. & Costa W. J. E. M., 2010, 97-122, fig. 1 and 3; Brazil: State of Minas Gerais: Alto Caparaó municipality: lateral channel of Rio Caparaó, Rio Itabapoana basin, Alto Caparaó, 20° 25' 54"S 41° 51' 57" W, altitude 1047 m; [Holotype - UFRJ 6030, 58.0 mm SL; Paratypes - UFRJ 5649, 11,35.8-110.2 mm SL; same locality as holotype; UFRJ 5658, 5, c&s, 37.0- 60.7 mm SL; same data as holotype. UFRJ 5650, 2, 26.28-43.4 mm SL; cachoeira do Chiador, tributary of Rio São Domingos, approximately 17 km N of Espera Feliz, 20° 33' 25"S 41° 51' 27" W, altitude 957 m]; Barbosa 2013:274 [cited (discussion on its relationships)]; García-Melo *et al*. 2016:237 [cited (discussion on its relationships)]; Barbosa & Katz 2016:262 [cited (discussion on its relationships)].

Diagnosis.- *Trichomycterus brunoi* is distinguished from all congeners from Southeastern Brazil except from the *T. brasiliensis* species complex, by the number of pectoral-fin rays, I+6, (vs. I+8 or I+7). Distinguished from *T. argos* by the presence of stripes, vermiculations or reticulations (vs. absence of this color pattern), and by a shorter snout (vs. longer snout). Barbosa & Costa (2010) distinguish *T. brunoi* by from all species of the *T. brasiliensis* species complex, except *T. fuliginosus* Barbosa & Costa 2010, by the unique morphology of the metapterygoid, in which there is a distinct posterior process directed to the anterior tip of the hyomandibula (Fig. 23 A, B) (vs. process absent; Fig. 23 C - G). *Trichomycterus brunoi* differs from *T. fuliginosus* by having eight branchiostegal rays (vs. nine), the pelvic-fin origin at a vertical through the centrum of the 18th vertebra (vs. 17th vertebra), the Caudal-fin rounded (vs. sub-truncated), the caudal peduncle slenderer (caudal peduncle depth 12.0-13.6 % SL vs. 13.6-15.0 % SL), and deep posterior articulation of the quadrate (Fig. 23A) (vs. slender; Fig. 23B).

Description.- Morphometric data for specimens examined in Table 09. Body long and almost totally straight, trunk roughly round in cross-section near head, then slightly deeper than broad and softly compressed to caudal peduncle, tapering to Caudal-fin. Dorsal profile of body gently convex to dorsal-fin origin, then straight or slightly concave along caudal peduncle to caudal-fin origin. Ventral profile convex from gular region to vent, due partly to abdominal distension, then straight or slightly concave along anal-fin origin to caudal-fin base. Caudal peduncle as deep as body at end of anal-fin base.

Head approximately one-fifth to one-fourth of SL, pentagonal, longer than wide and depressed, with a long snout. Mouth sub-terminal. Upper jaw slightly longer than lower. Upper lip wider than lower lip, and laterally continuous with base of maxillary barbel. Lower lip small, approximately 2/3 width of upper one, partly divided into right and left portions by with median

concavity. Lower lip with uniform covering of tiny vilii, resulting in velvet-like surface and not clustered into large papillae. Region between upper and lower lips with slender fleshy lobe.

Dentary and premaxillary teeth similar to each other in shape. Dentary teeth conical, arranged in four irregular rows, first row with 12 teeth, extending from base to slightly up of coronoid process, with size of individual teeth increasing markedly towards symphysis and from posterior to anterior rows. Total area of premaxilary teeth slightly smaller than that of dentary, with teeth arranged irregularly in four rows, first row with approximately 13 teeth, over entire ventral surface of premaxilla. Premaxilary teeth conical.

Eye small-sized, protruding, positioned dorsally on head, without free orbital rim and covered with transparent skin. Eye located on anterior half of HL, closer to lateral border of the head than to the midline in dorsal view. Infraorbital latero-sensory canal incomplete, extending from sphenotic posteriorly to terminal pore located ventroposteriorly to eye. Anterior nares surrounded by tube of integument directed anterolaterally, continuous posterolaterally with nasal barbel. Posterior nares closer to anterior nares than to the eyes, surrounded by tube of integument incomplete posteriorly. Maxillary barbel tubular narrowing markedly towards fine tip, reaching until half of pectoral-fin length. Rictal barbel inserted immediately ventral to maxillary barbel. Its tip reaching the opening gill. Nasal barbel originating on posterolateral region of anterior nares, reaching until posterior region of the opercle, not crossing it. Interopercular patch of odontodes small, oval in shape and with well-developed odontodes, prominent in ventral aspect of head. Interopercular patch of odontodes extending from vertical through ventroposterior border of eye to ventroanterior to opercle. Odontodes arranged in two or three irregular series, with those on mesial series much longer than those on lateral one; odontodes gradually larger posteriorly in both series, with those posteriorly on mesial row largest. Interopercular odontodes 26 - 31. Opercular

patch of odontodes on dorsolateral surface of posterior part of head, positioned a interodorsally to pectoral-fin base, roundish in shape slightly smaller than eye in dorsal aspect of head. Opercular odontodes 13 - 16, sunk in individual slits of integument, progressively larger posteriorly, all with fine tips, with largest ones curved distally and claw-like. Entire patch surrounded by specialized rim of integument.

Pectoral-fin medium-sized, its base immediately posterior and ventral to opercular patch of odontodes. Pectoral-fin rays I+6. First pectoral-fin ray (unbranched) longer than all others, prolonged as filament beyond fin web. Other rays progressively less long, their tips following continuous line along fin margin. Pelvic-fin with convex distal profile, its origin slightly posterior to middle of SL and anterior to vertical through dorsal-fin origin, slightly surpassing anal and urogenital openings in adults. Pelvic-fin rays I+4, first ray unbranched. Dorsal-fin long, its distal profile sinusoidal. Dorsal-fin origin closer to base of Caudal-fin than to tip of snout. Dorsal-fin rays ii+II+7 (03), two unsegmented and unbranched rudimentary rays, commonly present in *Trichomycterus*, two segmented and unbranched procurrent rays and seven branched and segmented rays (therein included two posterior closely-set rays). Anal-fin slightly smaller than dorsal-fin, its distal profile gently convex. Anal-fin origin posterior to vertical through end of dorsal-fin base. Anal-fin rays ii+II+5 (01) or iii+II+5 (01), two or three unsegmented and unbranched rudimentary rays, two segmented and unbranched procurrent rays and five branched and segmented rays. Caudal-fin rounded with 6+7 principal rays. Adipose-fin absent or modified into low integument fold extending between end of dorsal-fin and caudal-fin origin. Post-Weberian vertebrae 36 (01) and 38 (02). First dorsal-fin pterygiophore immediately anterior to neural spine of 18th (03) vertebra, first anal-fin pterygiophore immediately anterior to neural spine of 21th (03) vertebra. Caudal-fin procurrent rays plus one segmented non-principal ray dorsally and ventrally.

Procurrent caudal-fin rays, 16 dorsally and 13 ventrally, beginning anteriorly at 32th (01) vertebrae. Pleural ribs 12 (02), 13 (01). Branchiostegal rays 8. Dorsal-fin pterygiophores 8. Anal-fin pterygiophores 6.

Cephalic lateral line canals with simple, non-dendritic tubes ending in single pores. Supraorbital canal mostly within frontal bone. Supraorbital pores invariably present: s1 mesial to nasal-barbel base and autopalatine, s3 mesial to posterior nostril and anterior to frontal, paired s6 but very close to each other, posteromedial to eye and at midlength of frontal. Infraorbital canal with four pores, i1 and i2 anteriorly and i10 and i11 posteriorly. Canal lacking associated ossification. Infraorbital pore i1 located ventro-lateral to nasal-barbel base and autopalatine, i2 ventro-lateral to posterior nostril and anterior to frontal, i10 and i11 posterior to eye. Otic canal without pores. Postotic pores po1, anteromedial to opercular patch of odontodes), and po2, mesial to opercular patch of odontodes. Lateral line of trunk anteriorly continuous with postotic canal and reduced to short tube. Lateral line pores ll1 and ll2 present dorsomedial to pectoral-fin base.

Coloration in ethanol. – White to light yellowish dermis with dark chromathophores agglutinating and forming round to vermiculated maculae. Small and slender maculae with same or smaller diameter of eye. Maculae randomly distributed in all body, from the head to base of middle caudal-fin rays. Antero-laterally at the midline of body, maculae can agglutinate creating broken stripes or being slightly organized in a line. Ventrally to lateral midline of body maculae are more spaced among others and commonly with rounded shape, while dorsally to lateral midline of body there are more maculae and they are more vermiculated and fused with others. Ventral portion of the body there is no pigmentation. Presence of dark spots on the base of fins.

Remarks – *Trichomycterus brunoi* is a member of the *T. brasiliensis* species complex, once it has I+6 pectoral-fin rays, similar color pattern, a slender posterior tip of posterior ceratohyal, and

pelvic-fin bases in close proximity (Barbosa & Costa, 2003; Bockmann & Sazima, 2004; Barbosa & Costa, 2010). The type locality of *T. brunoi* is at the upper Rio Itabapoana, near the divide with the headwaters of the Rio Manhuaçu (a tributary to Rio Doce), (Fig. 14), and nontype specimens were actually collected in the latter. The species most similar to *T. brunoi* in the Rio Doce basin is *Trichomycterus argos*, described from the Rio Casta, tributary of the Upper Rio Doce in the Serra do Brigadeiro State Park. *Trichomycterus argos* probably also belongs to the *Trichomycterus brasiliensis* complex. The species is known exclusively from the types and probably endemic to its type locality.

As mentioned before (see Remarks on *T. argos*) *Trichomycterus brunoi* is very similar to *T. argos*, and the two species may be synonyms.

Barbosa & Costa (2010) distinguish *Trichomycterus brunoi* from all species of the *T. brasiliensis* species complex, except *T. fuliginosus*, by the unique morphology of the metapterygoid, which has a distinct posterior process directed towards the anterior tip of the hyomandibula. However, the shape of the metapterygoid varies intraspecifically in *Trichomycterus*. The same posterior process of the metapterygoid described in Barbosa & Costa (2010) as diagnostic for *T. brunoi* is also present in [(*T. fuliginosus*, *T. claudiae*, *T. mariamole*, *T. novalimensis*, *T. rubiginosus*) Barbosa & Costa 2010] and *T. brasiliensis*. Even in *T. claudiae*, it is possible to see a small posterior process on the metapterygoid directed to the anterior tip of the hyomandibula (Fig. 23). The condition of this character varies considerably, with wide overlap among species in the *T. brasiliensis* complex and does not seem to clearly diagnose *T. brunoi*. Although our observations are not intended to invalidate the use of metapterygoid shape as a taxonomically-relevant character in general, they show that pronounced intraspecific variation exists which must be accounted for.

Geographical distribution – *Trichomycterus brunoi* was described to the Itabapoana basin in the Caparaó State Park and is also present in the Rio Doce at Rio Manhuaçu (Fig. 14).

Material examined - MBML 4304, 4, 55.12 – 29.63 mm SL; Brazil, Espírito Santo, Iúna; Rio Claro river, Manhuaçu river; 20°22'22.00"S 41°49'40.90"W; L.M.Sarmento Soares, M.R.Britto, V.C.Espindula, F.M.R.S.Pupo, R.F.M.Pinheiro e M.M.C.Roldi; 09 Sep 2011. **MBML 4307**, 1, 32.49 mm SL; Brazil, Espírito Santo, Iúna; Rio Claro river, Manhuaçu river; 20°22'24.20"S 41°49'39.70"W; L.M.Sarmento Soares, M.R.Britto, V.C.Espindula, F.M.R.S.Pupo, R.F.M.Pinheiro e M.M.C.Roldi; 9 Sep 2011. **MBML 4308**, 2, 41.68 – 30.20 mm SL, C&S 31.93 mm SL; Brazil, Espírito Santo, Iúna; Ribeirão do Brás creek, Manhuaçu river; 20°20'33.90"S 41°48'55.60"W; L.M.Sarmento Soares, M.R.Britto, V.C.Espindula, F.M.R.S.Pupo, R.F.M.Pinheiro e M.M.C.Roldi; 10 Sep 2011. **MBML 4337**, 4, 83.60 – 31.04 mm SL; Brazil, Espírito Santo, Iúna; José Preto river, Manhuaçu river 20°22'9.50"S 41°51'27.50"W; L.M.Sarmento Soares, M.R.Britto, V.C.Espindula, F.M.R.S.Pupo, R.F.M.Pinheiro e M.M.C.Roldi; 10 Sep 2011. **MNRJ 22401**, 2, 33.64 - 74.99 mm SL; Brazil, Minas Gerais, Caparaó; Grumarim creek, tributary of Capim Roxo river (20º30’48’’S 42º1’19” W); col. A. T. Aranda, F. A. G. Melo, & F. P. Silva, 07 Aug. 2001.

Trichomycterus "illuvies", sp. nov.

(Fig. 24)

Holotype. – MZUSP 112750, 45.04 mm SL, Brazil, State of Minas Gerais, Ferros, Santo Antônio river on the bridge at the downtown of Ferros, river tributary of Rio Doce basin (19°13'34.50"S 43° 1'9.50"W); col. O. T. Oyakawa & T. F. Teixeira, 16 Aug 2012.

Paratypes. – All from Brazil, state of Minas Gerais. **MZUSP 110720**, 1, (37.64 mm SL), Bom Jesus do Galho; Ribeirão Sacramento creek, tributary of Rio Doce basin (19°47'50.00"S 42°18'9.00"W); col. A. Netto-Ferreira & R. Pádua, 03 Aug 2010. ex-**MZUSP 112750**, 10, 43.74 - 32.17 mm SL, (C&S, 3, 40.79 – 31.90 mm SL); collected together with the holotype.

Diagnosis.- Disntinguished from all Southeastern Brazil congener, except from *T. reinhardti*, *T. itatiayae*, *T. giganteus*, and *T. nigroauratus* by its color pattern, with a broad dark stripe running in the mid-lateral line of body from immediately posterior to opercle to base of caudal-fin. Distinguished from all congeners from Rio Doce basin, except from *T. alternatus*, *T. immaculatus* and *T. "sordislutum"* by the number of branchiostegal rays, strictly six (vs. seven or eight). Distinguished from *T. immaculatus*, *T. giganteus*, *T. caipora*, *T. reinhardti* and *T. itatiayae* by the number of pectoral-fin ray, I+7 (vs. strictly I+8 in *T. immaculatus*, *T. giganteus* and *T. caipora* and I+6 in *T. reinhardti* and *T. itatiayae*). Distinguished from *T. nigroauratus* by the absence of a golden spots on the snout, flank, above and below the midline, and the dorsum (vs. presence of this color patter in *T. nigroauratus*) and by the absence of a maculae row ventrolateral to the mid-lateral stripe on the body (vs. presence of this row in *T. nigroauratus*).

Description.- Morphometric data for specimens examined in Table 10. Body long and almost totally straight, trunk roughly round in cross-section near head, then slightly deeper than broad and softly compressed to caudal peduncle, tapering to Caudal-fin. Dorsal profile of body gently convex to dorsal-fin origin, then straight or slightly concave along caudal peduncle to caudal-fin origin. Ventral profile convex from gular region to vent, due partly to abdominal distension, then straight or slightly concave along anal-fin origin to caudal-fin base. Caudal peduncle medium-sized, as deep as body at end of anal-fin base.

Head approximately one-fifth of SL, pentagonal, longer than wide and depressed. Mouth sub-terminal. Upper jaw slightly longer than lower. Upper lip wider than lower lip, and laterally continuous with base of maxillary barbel. Lower lip small, approximately 2/3 width of upper one, partly divided into right and left portions by with median concavity. Lower lip with uniform covering of tiny vilii, resulting in velvet-like surface and not clustered into large papillae. Region between upper and lower lips with slender fleshy lobe.

Dentary and premaxillary teeth similar to each other in shape. Dentary teeth conical, arranged in four irregular rows extending from base to slightly up of coronoid process, with size of individual teeth increasing markedly towards symphysis and from posterior to anterior rows. Total area of premaxilary teeth slightly smaller than that of dentary, with teeth arranged irregularly in four rows over entire ventral surface of premaxilla. Premaxilary teeth conical.

Eye medium-sized, protruding, positioned dorsally on head, without free orbital rim and covered with transparent skin. Eye located on anterior half of HL, closer to lateral border of the head than to the midline in dorsal view. Infraorbital latero-sensory canal incomplete, extending from sphenotic posteriorly to terminal pore located ventroposteriorly to eye. Anterior nares surrounded by tube of integument directed anterolaterally, continuous posterolaterally with nasal

barbel. Posterior nares closer to anterior nares than to the eyes, surrounded by tube of integument incomplete posteriorly. Maxillary barbel tubular narrowing markedly towards fine tip, until the lateroposterior border of interopercle. Rictal barbel inserted immediately ventral to maxillary barbel. Its tip reaching lateroanterior border of interopercle. Nasal barbel originating on posterolateral region of anterior nares. Its tips surpass eye, but do not touch anterior border of opercle. Interopercular patch of odontodes small, oval in shape and with well-developed odontodes, prominent in ventral aspect of head. Interopercular patch of odontodes extending from vertical through ventroposterior border of eye to ventroanterior to opercle. Odontodes arranged in two or three irregular series, with those on mesial series much longer than those on lateral one; odontodes gradually larger posteriorly in both series, with those posteriorly on mesial row largest. Interopercular odontodes 30 - 44. Opercular patch of odontodes on dorsolateral surface of posterior part of head, positioned anterodorsally to pectoral-fin base, roundish to oval in shape in dorsal aspect of head and same size of eye diameter. Opercular odontodes 18 - 24, sunk in individual slits of integument, progressively larger posteriorly, all with fine tips, with largest ones curved distally and claw-like. Entire patch surrounded by specialized rim of integument.

Pectoral-fin large-sized, its base immediately posterior and ventral to opercular patch of odontodes. Pectoral-fin rays I+7 or rarely I+8. First pectoral-fin ray (unbranched) longer than all others, prolonged as short filament beyond fin web. Other rays progressively less long, their tips following continuous line along fin margin. Pelvic-fin with convex distal profile, its origin slightly posterior to middle of SL and anterior to vertical through dorsal-fin origin, its tip reach from anterior border of urogenital opening to posterior border of it. Base of Pelvic-fins positioned slightly close to each other. Pelvic-fin rays I+4, first ray unbranched. Dorsal-fin long, its distal profile sinusoidal. Dorsal-fin origin closer to base of Caudal-fin than to tip of snout. Dorsal-fin

rays iii+II+7 (03), three unsegmented and unbranched rudimentary rays, commonly present in *Trichomycteru*s, two segmented and unbranched procurrent rays and seven branched and segmented rays (therein included two posterior closely-set rays). Anal fin slightly smaller than dorsal-fin, its distal profile gently convex. Anal-fin origin posterior to vertical through end of dorsal-fin base. Anal-fin rays iii+II+5 (03), three unsegmented and unbranched rudimentary rays, two segmented and unbranched procurrent rays and five branched and segmented rays. Caudal-fin rounded shape, with 6+7 principal rays. Adipose-fin absent or modified into low integument fold extending between end of dorsal-fin and caudal-fin origin. Post-Weberian vertebrae, 37 (02) and 38 (01). First dorsal-fin pterygiophore immediately anterior to neural spine of 18th (03), vertebra, first anal-fin pterygiophore immediately anterior to neural spine of 23th (03) vertebra. Caudal-fin procurrent rays plus one segmented non-principal ray dorsally and ventrally. Procurrent caudal-fin rays, 12 - 14 (03) dorsally and 11 - 13 (03) ventrally, beginning anteriorly at 34th (02) vertebra. Pleural ribs 13 (03). Branchiostegal rays 6 (03). Dorsal-fin pterygiophores 8. Anal-fin pterygiophores 6.

Cephalic lateral line canals with simple, non-dendritic tubes ending in single pores. Supraorbital canal mostly within frontal bone. Supraorbital pores invariably present: s1 mesial to nasal-barbel base and autopalatine, s3 mesial to posterior nostril and anterior to frontal, single or paired s6, closer to mesial line than to eyes, posteromedial to eye and at midlength of frontal. Infraorbital canal with four pores, i1 and i2 anteriorly and i10 and i11 posteriorly. Canal not ossified. Infraorbital pore i1 located ventro-lateral to nasal-barbel base and autopalatine, i2 ventro-lateral to posterior nostril and anterior to frontal, i10 and i11 posterior to eye. Otic canal without pores. Postotic pores po1, anteromedial to opercular patch of odontodes), and po2, mesial to

opercular patch of odontodes. Lateral line of trunk anteriorly continuous with postotic canal and reduced to short tube. Lateral line pores ll1 and ll2 present dorsomedial to pectoral-fin base.

Coloration in ethanol. – Dark chromatophores distributed into inner and outer skin layers. Those on inner skin layer forming broad dark stripes or faded maculae responsible for the main color features of the body. Basic arrangement of stripes and maculae in two stripes and one maculae row. First stripe along mid-dorsal line from occiput, through entire dorsum, into dorsal edge of caudal peduncle and to base of Caudal-fin. Maculae row ventrolateral to that, extending from base of head through upper part of flanks, dorsal portion of caudal peduncle, to base of caudal-fin. Secound stripe running along mid-lateral line, from immediately posterior to opercle to base of caudal-fin. In some specimens there is a secound shorter, ventralmost maculae row, extending from mid-length of abdomen through ventral margin of caudal peduncle to base of caudal-fin. Dorsal stripe and row disrupted by fusions (mostly along anterior part of body). Mid-lateral stripe independent and never fused on dorsum. Head darkest on region corresponding to neurocranium, outlined by brain pigment seen by transparency. Umpigmented circular area extending from posterior margin of eye to base of opercular patch of odontodes. Base of nasal barbels surrounded with concentration of dark pigment, extending posteriorly as elongate dark field to anterior margin of eyes. Distal margin of integument fold of opercular patch of odontodes darkly-pigmented. Interopercular patch of odontodes white. Ventral side of the body lacking dark pigment. Fins with small brownish spots randomly distributed on fin-rays.

Etymology – The epithet “illuvies” means inundation or filthy condition as the same as the environmental condition let from the mining company Samarco SA into the Rio Doce. This epithet is a critic and an eternal reminder of the catastrophe suffered by this hydrographic basin.

Geographical distribution – *Trichomycterus "illuvies"* was found in two drainages belonging to Rio Doce basin, the Santo Antônio river (holotype locality) and Ribeirão Sacramento (paratype locality) (Fig. 25). Despite this species is found in just two localities, the distance between them is large enough to propose that it is not restricted to their type localites, probably distributed in more drainages into this basin.

Trichomycterus immaculatus (Eigenmann & Eigenmann, 1889)

(Fig. 06, 07, 26)

Pygidium immaculatum Eigenmann & Eigenmann, 1889:52; Juiz de Fora, Parahybuna River; São Matheos river; Juiz de Fora, Paraíba do Sul river; Goiás, Brazil [Syntypes: MCZ 8266, 8300, 8302, 8305, 8307].

Trichomycterus immaculatum; Burgess 1989:322 [list]

Trichomycterus immaculatus (Eigenmann & Eigenmann, 1889); Bizerril 1994:623 [list]; Triques & Vono 2004:82 [list and discussion on relationships]; Bockmann & Sazima 2004 [comparisons]; Bockmann *et al*. 2004:227 [comparisons]; Maldonado-Ocampo & Albert 2004:5 [comparisons]; Lima & Costa 2004:3 [comparisons]; Sarmento-Soares *et al.*, 2005:209 [comparisons]; Wosiacki 2005:52 [comparisons]; Ferraris 2007:419 [check list]; Lima *et al.*, 2008:316 [comparisons]; Barbosa & Costa 2010:121 [comparisons]; Roldi *et al.*, 2011:02 [comparisons]; Sarmento-Soares *et al.*, 2011:262 [comparisons]; DoNascimiento *et al.*, 2014 [comparisons]; García-Melo *et al*. 2016:237 [comparisons]; Sales *et al.*, 2018 [comparisons].

Trichomycterus pradensis Sarmento-Soares *et al.*, 2005; Jucuruçu, rio Jucuruçu, 2 kilometers before the city of Jucuruçu on road Itamaraju-Jucuruçu, middle of rio Jucuruçu basin, 16°50'10"S,

40°08'40"W, Bahia, Brazil; [Holotype: MNRJ 28483; - Paratypes: Jucuruçu basin (MNRJ 28484, AUM 42724, MNRJ 28486, MNRJ 28487, MNRJ 28488, MNRJ 28489), Peruípe basin (MNRJ 28485), Itanhém basin (AMNH 236101, ANSP 188703, AUM 42733, FLMNH 148993, MNRJ 28490, MNRJ 28491)]; Ferraris 2007:422 [comparisons]; Barbosa & Costa 2011:308 [comparisons]; García-Melo *et al.* 2016:237 [comparisons].

Diagnosis – *Trichomycterus immaculatus* is distinguished from its congeners from Southeastern Brazil, except from *T. caipora*, *T. "tantalus"* and *T. giganteus* by strictly I+8 pectoral-fin rays (vs. I+7 or less in all congeners from Southeastern Brazil). Distinguished from *T. "tantalus"* and *T. "vinnulus"* by the number of lateral line pores, two (vs. three in *T. "tantalus"* and *T. "vinnulus"*). Distinguished from *T. giganteus*, and all its congeners from Southeastern Brazil, except from *T. itatiayae*, *T. reinhardti*, and *T. pauciradiatus*, by absence of dark and broad stripe running from lateral midline of body from head to caudal peduncle. Distinguished from *T. caipora* by the color pattern, homogeneous color pattern to spoted body with many round dark maculae (vs. the presence of four irregular longitudinal rows of rounded blotches on trunk in *T. caipora*).

Description - Morphometric data for specimens examined in Table 11. Body long and almost totally straight, trunk roughly round in cross-section near head, then slightly deeper than broad and softly compressed to caudal peduncle, tapering to Caudal-fin. Dorsal profile of body gently convex to dorsal-fin origin, then straight or slightly concave along caudal peduncle to caudal-fin origin. Ventral profile convex from gular region to vent, due partly to abdominal distension, then straight or slightly concave along anal-fin origin to caudal-fin base. Caudal peduncle varying from nearly as deep as body at the beginning of dorsal-fin base to as deep as body at the end of anal-fin base.

Head length approximately one-fifth of SL, pentagonal, longer than wide and depressed. Mouth sub-terminal. Upper jaw slightly longer than lower. Upper lip wider than lower lip, and

laterally continuous with base of maxillary barbel. Lower lip small, approximately 2/3 width of upper one, partly divided into right and left portions by with median concavity. Lower lip with uniform covering of tiny vilii, resulting in velvet-like surface and not clustered into large papillae. Region between upper and lower lips with slender fleshy lobe.

Dentary and premaxillary teeth similar to each other in shape and size. Dentary teeth conical, arranged in four irregular rows, first row 09 – 12 extending from base to slightly up of coronoid process, with size of individual teeth increasing markedly towards symphysis and from posterior to anterior rows. Total area of premaxilary teeth smaller than that of dentary, with conical teeth arranged irregularly in four rows, first row 10 – 16 over entire ventral surface of premaxilla.

Eye medium-sized, slightly protruding, positioned dorsally on head, without free orbital rim and covered with transparent skin. Eye located on anterior half of HL, closer to lateral border of head than to the midline in dorsal view. Infraorbital latero-sensory canal incomplete, extending from sphenotic posteriorly to terminal pore located ventroposteriorly to eye. Anterior nares surrounded by tube of integument directed anterolaterally, continuous posterolaterally with nasal barbel. Posterior nares closer to anterior nares than to the eyes, surrounded by tube of integument incomplete posteriorly. Length of all barbels variable. Maxillary barbel tubular narrowing markedly towards fine tip, variably reaching from middle of interopercle to the base of pectoral-fin. Rictal barbel inserted immediately ventral to maxillary barbel. Its tip reaching from anterolateral to posterolateral border of interopercle. Nasal barbel originating on posterolateral region of anterior nares, reaching anywhere from middle of eye to anterior border of opercle. Interopercular patch of odontodes large, oval in shape and with well-developed odontodes, prominent in ventral aspect of head. Interopercular patch of odontodes extending from vertical through ventroposterior border of eye to ventroanterior to opercle. Odontodes arranged in two or

three irregular series, with those on mesial series much longer than those on lateral one; odontodes gradually larger posteriorly in both series, with those posteriorly on mesial row largest. Interopercular odontodes 37 – 46. Opercular patch of odontodes on dorsolateral surface of posterior part of head, positioned anterodorsally to pectoral-fin base, roundish in shape and larger than eye in dorsal aspect of head. Opercular odontodes 15 – 25, sunk in individual slits of integument, progressively larger posteriorly, all with fine tips, with largest ones curved distally and claw-like. Entire patch surrounded by specialized rim of integument.

Pectoral-fin medium-sized, its base immediately posterior and ventral to opercular patch of odontodes. Pectoral-fin rays strictly I+8. First pectoral-fin ray, unbranched, longer than all others, and prolonged as filament beyond fin web. Other rays progressively less long, their tips following continuous line along fin margin. Pelvic-fin with convex distal profile, its origin slightly posterior to middle of SL and anterior to vertical through dorsal-fin origin, its length varying from not touching to touching but never covering completely anal and urogenital openings in adults. Base of Pelvic-fins positioned close to each other. Pelvic-fin rays I+4, first ray unbranched. Dorsal-fin long, its distal profile sinusoidal. Dorsal-fin origin closer to base of Caudal-fin than to tip of snout. Dorsal-fin rays iii+II+7 (12); iii+III+6 (01) or iv+II+7 (02), three - four unsegmented and unbranched rudimentary rays, commonly present in *Trichomycteru*s, two or three segmented and unbranched procurrent rays and six (rare) or seven branched and segmented rays (therein included two posterior closely-set rays). Anal fin slightly smaller than dorsal-fin, its distal profile gently convex. Anal-fin origin posterior to vertical through end of dorsal-fin base. Anal-fin rays ii+II+5 (2) or iii+II+5 (13), two - three unsegmented and unbranched rudimentary rays, two segmented and unbranched procurrent rays and five branched and segmented rays. Caudal-fin from sub-truncated to slightly forked, with 6+7 (14) or 5+7 (01) principal rays. Adipose-fin absents or

modified into low integument fold extending between end of dorsal-fin and caudal-fin origin. Post-Weberian vertebrae 34 (02), 35 (05) or 36 (08). First dorsal-fin pterygiophore immediately anterior to neural spine of 16th (09) or 17th (06) vertebra, first anal-fin pterygiophore immediately anterior to neural spine of 20th (01); 21th (09) or 22th (04) vertebra. Caudal-fin procurrent rays plus one segmented non-principal ray dorsally and ventrally in some specimens. Procurrent caudal-fin rays, 13 – 17 dorsally and 12 - 14 ventrally, beginning anteriorly at 31th or 32th vertebrae. Pleural ribs 10 (05), 11 (09) or 12 (01). Branchiostegal rays 6 (01) or 7 (14). Dorsal-fin pterygiophores 8. Anal-fin pterygiophores 6.

Cephalic lateral line canals with simple, non-dendritic tubes ending in single pores. Supraorbital canal mostly within frontal bone. Supraorbital pores invariably present: s1 mesial to nasal-barbel base and autopalatine, s3 mesial to posterior nostril and anterior to frontal, from single to more common paired s6 posteromedial to eye and at midlength of frontal. Infraorbital canal with four pores, i1 and i2 anteriorly and i10 and i11 posteriorly. Canal partly ossified in some specimens. Infraorbital pore i1 located ventro-lateral to nasal-barbel base and autopalatine, i2 ventro-lateral to posterior nostril and anterior to frontal, i10 and i11 posterior to eye. Otic canal without pores. Postotic pores po1, anteromedial to opercular patch of odontodes), and po2, mesial to opercular patch of odontodes. Lateral line of trunk anteriorly continuous with postotic canal and reduced to short tube, partially ossified in some specimens. Lateral line pores ll1 and ll2 present dorsomedial to pectoral-fin base.

Coloration in ethanol. – *Trichomycterus immaculatus* is variable in pigmentation pattern, with two extreme color morphs bridged by intermediate conditions (Figs. 06, 07). At one extreme, the entire body is covered with a uniform scattering of dark chromatophores in inner and outer layers of skin, not forming maculae or spots. Specimens with this color pattern usually have dusky fins

with transparent margins. At the other extreme, chromathophores usually are uniformly-distrituted in inner skin layer. In outer layer, chromathophores are darker and agglutinate to form round maculae, as large as, or larger than, eye diameter. Maculae cover dorsum to the midlateral line of body, being completely absent ventral to that limit. Maculae are randomly distributed in adults. Fins, except Caudal-fin, are mostly transparent. In young specimens, maculae are more evident and arranged along midline of body, from dorsoposterior of opercle to base of caudal-fin (resulting in pattern similar to that of *T. alternatus*). In specimens intermediate between two extreme color morphs, chromathophores can agglutinate to create faded maculae with almost same tonality of background skin pigmentation, turning harder their observation in alive and fixed specimens. When these maculae are present, they are restricted to the dorsum, never extending ventrally beyond lateral midline. Color pattern of head, caudal-fin and ventral part of body are invariable in all specimens. Head lacks maculae or blotches, with area corresponding to neurocranium darker than rest of head. Integument surrounding opercular odontodes darkly-pigmented. Interopercular patch of odontodes white. Cheeks less darkly-pigmented than rest of head. Caudal-fin rays from dusky with hyaline margins to middle caudal-fin rays darkly pigmented. In young specimens dark caudal stripe more evident and gradually fading or masked by adjacent caudal-fin pigmentation. Ventral part of body without pigmentation, white in color.

Remarks – *Trichomycterus immaculatus* stands out as the most complex taxonomic case in this paper. Our results show that *T. immaculatus* is a senior synonym of *T. pradensis*. Moreover, two new species, *T. "melanopygius"* and *T. "tantalus"*, are very similar to *T. immaculatus*.

Trichomycterus immaculatus was described on the basis of 14 syntypes from three different basins: Paraíba do Sul (MZC 8300, 10 ex.; MCZ 8305, 1 ex.; MCZ 8307, 1 ex.), São Mateus (MCZ

8302, 1 ex.), and some drainage in the State of Goiás (perhaps the Tocantins; MCZ 8298, 1 ex.). The latter is obviously a different species from the remaining syntypes. That small single specimen has I+7 pectoral-fin rays (vs. I+8 in remaining syntypes), depth of body 12% SL (vs. 14% to 17.9%); caudal peduncle depth 9.2% SL (vs. 11.3% to 14.9%) and a paired S6 cephalic latero-sensory pore (vs. single). Such non-conspecificity among syntypes is potentially risky for nomenclatural stability and requires a lectotype designation. Since the majority of syntypes are from the Paraíba do Sul basin, this paper designates specimen MCZ 8300_4 (Fig. 26) as the lectotype of *Trichomycterus immaculatus*. This specimen is a particularly well-preserved and allows observation of all characters included in the original description.

Two other species in the Rio Doce are very similar to *T. immaculatus*: *T. "melanopygius"*, and *T. "tantalus"*. *Trichomycterus pradensis* was described from three adjacent but independent basins in southern Bahia and northern Minas Gerais States: Jucuruçu (locality of the holotype), Peruípe and Itanhém. almost all of them from Southern State of Bahia Brazil. The original diagnosis states that the species is distinguished from all other congeners by a combination of three characters: closely-set S6 pores, a small patch of robust opercular odontodes (with 8 to 10 odontodes) and eight branched pectoral-fin rays. Examination of the holotype and 52 paratypes shows that those traits need reevaluation. First, the spacing between S6 pores is variable in the type series and no different from conditions in several other species of *Trichomycterus* from the Rio Doce. Second, the number of odontodes actually varies between 13 and 26 in the type specimens, with no specimen in the reported 8-10 range. Finally, eight branched pectoral-fin rays can be found in other *Trichomycterus* species (e.g. *T. immaculatus*; *T. "astromycterus"*, *T. "tantalus"* in the Doce basin). The combination of the three characteristics (considering the corrected values for odontode number) is matched in at least two species in the Rio Doce basin, *T.*

immaculatus and *T. "tantalus"*. The latter species is diagnosable by a number of other characters (cf. Diagnosis above) and is surely not conspecific with type specimens of *T. pradensis*. With *T. immaculatus*, on the other hand, there seem to be no additional distinguishing traits once all evidence is taken into consideration. The latter species matches the specimens of *T. pradensis* in all observable characteristics. The spotted color pattern of the holotype of *T. pradensis* (cf. Sarmento *et al.*, 2005, fig. 1) might superficially seem to distinguish it from the homogeneous-colored *T. immaculatus*. However, the color pattern varies in the range between those two extremes in the type series of *T. pradensis* (as mentioned in the original description; Sarmento et al, 2005: 296) (Fig. 06), with such variation also seen within *T. immaculatus* (Fig. 07). Careful examination of specimens referrable to both *T. pradensis* and *T. immaculatus*, including type material of the two species and both internal and external anatomy, fails to reveal any other phenotypic characteristics possibly diagnostic. Barcoding analysis shows little genetic divergence (1.22%) between specimens referrable to *T. pradensis* (including topotypic material) and forms referrable to *T. immaculatus* from throughout the Rio Doce. Therefore, both phenotypic and barcoding evidence demonstrates that *T. pradensis* is conspecific with forms identifiable with *T. immaculatus* from the Rio Doce (a conclusion also reached by Volpi, 2017).

The question that remains is whether the form referrable to *T. immaculatus* in the Rio Doce is actually conspecific with the real *T. immaculatus*. The species has indeed been reported from the Rio Doce numerous times in the past, including by Eigenmann himself (the specimen illustrating the species in Eigenmann, 1918, plate 52 is from the Rio Doce), but its type locality (as defined in the present paper; see above) is the Rio Paraíba do Sul. We examined specimens from both Eigenmann´s reported locality in the Rio Doce (including a molecular sample) and several localities in the Paraíba do Sul, and again failed to disclose evidence of separate species.

Thus, forms referrable to *T. immaculatus* in both the Rio Doce and the Paraíba do Sul are also conspecific. In view of the other considerations presented above, *T. immaculatus* seems to be a widespread species occurring throughout the entire Rio Doce, Rio Paraíba do Sul, Rio São Mateus, Rio Itaúna and Rio Jucuruçu (the latter type locality of *T. pradensis*). In such scenario, *T. pradensis* is herein proposed as a junior synonym of *T. immaculatus*. As discussed below (see Discussion), such wide distributions can be associated with geomorphological processes known to have occurred in the region (Cherem *et al*., 2012).

In the Rio Doce basin, *Trichomycterus "melanopygius"* is the species most similar to *T. immaculatus*, especially in its homogeneous color pattern and the presence of a dark horizontal stripe along the central caudal-fin rays (visible in all specimens of the former and small specimens of the latter; the characteristic becomes obscured by additional pigmentation in large specimens of the latter). In fact, the two species look so similar in external aspect that they may easily be mistaken in superficial examination and can be considered as cryptic species. However, examination of details (given in the respective Diagnoses) readily distinguishes them. This conclusion is corroborated by their significant genetic distances (cf. Molecular Results, Table 12 and Fig. 27).

Trichomycterus "tantalus" is another species which is similar to *T. immaculatus*, though not to the same degree as *T. "melanopygius"*. Many specimens of *T. "tantalus"* are different from *T. immaculatus* in color pattern, because of the abrupt fading of dark coloration ventral to the lateral midline. However, such difference is not absolute, and some specimens are well within the range of color patterns seen in *T. immaculatus* (Fig. 04A). But the two species are otherwise easily distinguishable on the basis of several other traits, including a very evident concave or forked caudal fin and hypertrophied opercle in *T. "tantalus"* (vs. a truncate caudal fin and regular-sized

opercle in *T. immaculatus*), among other characters listed in their Diagnoses. The species-level differentiation between the two species is also reflected in their barcoding divergence (Table 12, fig. 27).

Geographical distribution – *Trichomycterus immaculatus* is widely distributed in the entire Rio Doce and many other Southeastern basins such as Paraíba do Sul, Jucuruçu and isolated coastal basins in the State of Espírito Santo (such as Itaúnas and São Mateus) (Fig. 28).

Material examined – Type material – Lectotype (designated herein): MCZ 8300_4, 123.2 mm SL, Juiz de Fora, State of Minas Gerais, Brazil, Parahybuna river; col. H. W. Halfeld, 01 Jan. 1854 to 31 Dec. 1854. **Paralectotypes**: **MCZ 8300**, 4, 123.2 - 164.97 mm SL, collected with lectotype. **MCZ 8302**, 01, 121.38 mm SL; São Mateus, State of Espírito Santo, São Mateus river; col. C. F. Hartt & E. Copeland in Thayer Expedition to Brazil, 01 Jan. 1865 to 31 Dec. 1965. **MCZ 8305**, 01, 117.64 mm SL; Juiz de Fora State of Minas Gerais, Brazil, Parahyba river; col. L. Agassiz & J. Whitaker, in Thayer Expedition to Brazil ,21 Jun. 1865 to 27 Jun. 1865. **MCZ 8307**, 01, 116.17 mm SL; Juiz de Fora State of Minas Gerais, Brazil, Parahyba river; col. L. Agassiz & J. Whitaker, in Thayer Expedition to Brazil, 21 Jun. 1865 to 27 Jun. 1865. **MCZ 8296**, 01, 51.55 mm SL; Senhor Honorio, Goiás; col. Senhor Honorio, in Thayer Expedition to Brazil, 01 Jan. 1865 to 31 Dec. 1865 (specimen not conspecific with lectotype and remaining paralectotypes)..

Types of examined material – Paratypes of *Trichomycterus pradensis* **- MNRJ 28484**, 09, 39.44 – 108.95 mm SL, Jucuruçu, rio Jucuruçu. **MNRJ 28485**, 05, 39.99 – 66.53 mm SL, Bahia, riacho a 500 m do ponto anterior, bacia do rio Peruípe; **MNRJ 28488**, 07, paratypes, 49.09 – 99.03 mm SL, Palmópolis, rio Dois de Abril, bacia do rio Jucuruçu; **MNRJ 28490**, 09, paratypes, 46.70 – 74.05 mm SL, Itanhém, córrego Água Fria, rio Itanhém. **Non-type material - MZUSP 41738**, 02, 71.56 – 48.41 mm SL; Brazil, State of Espitiro Santo, Ibatiba; São João river basin (20°23'60.00"S

41°25'0.00"W); col. C. A. S. Lucena & P.V.Azevedo, 06 Sep. 1989. **All further MZUSP from Brazil, State of Minas Gerais - MZUSP 58479**, 29, 115.21 – 47.49 mm SL; Brazil, State of Minas Gerais, Joanésia; Guacho creek, tributary of Santo Antônio river basin (19° 7'37.86"S 42°39'48.93"W); col. F. A. Bockmann & P. M. C. Araujo, 05 Oct. 1997. **MZUSP 69333**, 01, 63.02 mm SL; Coroaci; Suaçuí Pequeno river (18°36'45.93"S 42°16'52.91"W); col. A. M. Zanata, 28 Apr. 2001. **MZUSP 69359**, 1, 77.77 mm SL; Coroaci; Suaçuí Pequeno river (18°37'20.29"S 42°16'16.34"W); col. A. M. Zanata, 29 Apr. 2001. **MZUSP 69367**, 1, 83.5 mm SL; Coroaci Suaçuí Pequeno river (18°41'38.00"S 42°12'50.00"W); col. A. M. Zanata, 29 Apr. 2001. **MZUSP 75034**, 2, 66.98 mm SL; Sarduá Tronqueiras river, tributary Suaçuí river basin (18°46'44.29"S 42°23'41.00"W); col. F. Di Dario & B. Di Dario, 08 Dec. 2001. **MZUSP 75059**, 8, 78.57 – 48.75 mm SL; Coroaci, Suaçuí river basin (18°36'45.57"S 42°16'18.73"W); col. F. Di Dario & B. Di Dario, 06 Dec. 2001. **MZUSP 81028**, 9, 133.76 – 55.75 mm SL; Manhuaçu, Manhuaçu river (20°15'24.00"S 42° 7'2.00"W); col. Carlos B.M. Alves, 23 Apr. 2002. **MZUSP 81029**, 6, 113.98 – 58.95 mm SL; Manhuaçu, Manhuaçu river (20°15'24.00"S 42° 7'2.00"W); col. Carlos B.M. Alves, 22 Apr. 2002. **MZUSP 81032**, 8, 79.68 – 37.07 mm SL; São Luiz, Manhuaçu river (20°20'12.00"S 42° 4'48.00"W); col. Carlos B.M. Alves, 21 Apr. 2002. **MZUSP 94488**, 2, 82.27 – 65.9 mm SL; Alto Rio Doce, Xopotó river, Piranga river basin (21° 4'4.00"S 43°27'50.00"W); col. Oyakawa, Baena e Loeb, 11 Jul. 2007. **MZUSP 123334**, 45, 38.54 – 85.25 mm SL; Bom Jesus do Manhuaçu, Manhuaçu river (20°17'34.24"S 42° 8'50.88"W); col. T. Pessali, 07 Sep. 15. **MZUSP 123335**, 10, 45.27 – 55.91 mm SL; Bom Jesus do Manhuaçu, Manhuaçu river, Rio Doce basin (20°17'34.24"S 42° 8'50.88"W); col. T. Pessali, 22 Apr. 2015. **MZUSP 123336**, 22, 53.06 – 105.29 mm SL; Realeza, Manhuaçu river, Rio Doce basin (20°14'49.13"S 42° 5'2.18"W); col. T. Pessali, 21 Abr 2015. **MZUSP 123337**, 92, 52.15 – 98.25 mm SL; Realeza, Manhuaçu river,

tributary of Rio Doce basin (20°14'49.13"S 42° 8'26.17"W); col. T. Pessali, 08 Sep. 2015. **MZUSP 123342**, 1, 67.46 mm SL; Naque, Main channel of Rio Doce river (19°14'19.42"S 42°18'22.65"W); col. T. Pessali, 19 Jul. 2017. **MZUSP 123344**, 7, 45.56 – 84.55 mm SL, Açucena, Corrente Grande river, Rio Doce basin (18°57'9.86"S 42°21'38.20"W); col. T. Pessali, 31 Jul. 2017. **MZUSP 123345**, 123, 48.35 – 112.85 mm SL, Baguari, Main channel of Rio Doce river (19° 1'3.06"S 42° 7'16.31"W); col. T. Pessali, 12 Dec. 2016. **MZUSP 123347**, 12, 39.20 – 77.72 mm SL; Açucena, Corrente Grande river, Rio Doce basin (18°57'9.86"S 42°21'38.20"W); col. T. Pessali, 31 May 2017. **MZUSP 123348**, 83, 50.22 – 111.43 mm SL; Baguari, Main channel of Rio Doce river (19° 1'27.83"S 42° 7'34.40"W); col. T. Pessali, 20 Dec. 2016. **MZUSP 123349**, 74, 43.66 – 76.68 mm SL, Itambacuri, Suaçui Grande river, tributary of Rio Doce basin (18° 5'42.17"S 41°41'22.16"W); col. T. Pessali, 09 Sep. 2015. **MZSUP 123352**, 4, 41 – 67.25 mm SL, Açucena, Corrente Grande river, Rio Doce basin (18°57'9.86"S 42°21'38.20"W); col. T. Pessali, 31 May 2017. **MZUSP 123353**, 23, 40.3 – 70.25 mm SL; Baguari, São Mateus creek, tributary of Corrente Grande river (18°59'24.54"S 42°18'57.98"W); col. T. Pessali & V. Reis, 17 Nov. 2017. **MZUSP 123354**, 1, 43.65 mm SL; Açucena, São Mateus creek, tributary of Corrente Grande river (18°59'24.54"S 42°18'57.98"W); col. T. Pessali, Aug. 2013. **MZUSP 123356**, 15, 46.94 – 79.42 mm SL; Açucena, São Mateus creek, tributary of Corrente Grande river (18°57'10.39"S 42°21'39.81"W); col. T. Pessali, 02 Sep. 2017. **MZUSP 123357**, 3, 69.27 – 80.19 mm SL; Baguari, Suaçui Pequeno, tributary of Rio Doce basin (18°56'2.50"S 42° 5'2.18"W); col. T. Pessali & V. Reis, 16 Nov. 2017 – MG. **MZUSP MZUSP 123367**, 1, 51.8 mm SL; Bom Jesus do Manhuaçu, Manhuaçu river, Rio Doce basin (20°17'34.24"S 42° 8'50.88"W); col. T. Pessali, 27 Abr. 2015. **MZUSP 123368**, 18, 45.62 – 85.67 mm SL; Baguari, Main channel of Rio Doce river (19° 1'14.68"S 42° 7'6.81"W); col. T. Pessali, 13 Dec. 2016. **MZUSP 123370**, 8, 44.54 – 56.03 mm

SL; Itambacuri, Suaçui Grande river, Rio Doce basin (18° 5'42.17"S 41°41'22.16"W); col. T. Pessali, 09 Sep. 2015 – MG.

LBP 1019, 2, 114.90 – 68.80 mm SL; Brazil, State of Minas Gerais, between Capela Nova and Caranaíba, Piranga river, tributary of Rio Doce basin (20°58'10.26"S 43°42'19.86"W); col. JC Oliveira, AL Alves, LR Sato, 13 Oct. 2001.

All lots from Brazil, State of Minas Gerais - **MZUFV 3335**, 3, 109.35 - 118.28 mm SL; Guaraciaba, UHE Brecha, Piranga river, Rio Doce basin (20°29'42.01"S 43° 0'15.59"W); col. J.A. Dergam & Tottola, A.H., 23 Mar. 2003. **MZUFV 3348**, 2, 100.69 - 105.5 mm SL; Ponte Nova, UHE Brito, Rio Piranga river (20°23'22.43"S 42°54'9.23"W); col. J.A. Dergam & Tottola, A.H., 24 Mar. 2003. **MZUFV 3378**, 3, 82.54 - 99.69 mm SL; Guaraciaba, UHE Brecha, Piranga river, Rio Doce basin (20°29'34.47"S 43° 0'24.18"W); col. J.A. Dergam & Tottola, A.H., 10 Apr. 2003. **MZUFV 3393**, 10, 91 - 110.51 mm SL; Ponte Nova, UHE Brito, Rio Piranga river (20°23'42.38"S 42°54'9.36"W); col. J.A. Dergam & Tottola, A.H., 12 Apr. 2003 , – MG.

All from Brazil, State of Espírito Santo - **MBML 55**, 1, 49.68 mm SL; Colatina, Santa Maria do Rio Doce basin (19°36'14.00"S 40°37'13.00"W); col. R. L. Teixeira & J. A. P. Scheneider, 29 Aug. 1996. **MBML 438**, 12, 53.16 – 34.22 mm SL; Santa Teresa, Rúdio Waterfall, Santa Maria do Rio Doce basin (19°50'11.00"S 40°41'27.00"W); col. R. L. Teixeira, 30 Jun. 2000. **MBML 636**, 3, 100.53 – 69.99 mm SL; Itaguaçu, Fazenda Coser, Santa Joana basin (19°48'6.00"S 40°51'20.00"W); col. R.L.Teixeira & P.S.Miller, 08 Sep. 2000**. MBML 648**, 5, 85.26 – 66.16 mm SL; Itarana, Jatibocas stream, Santa Joana basin (19°52'26.00"S 40°52'31.00"W); col. R.L.Teixeira & P.S.Miller, 19 Apr. 2001. **MBML 672**, 2, 74.84 – 66.61 mm SL; Itaguaçu, Fazenda Coser, Santa Joana basin (19°48'6.00"S 40°51'20.00"W); col. R.L.Teixeira & P.S. Miller, 21 May 2001. **MBML 695,** 24, 104.59 – 44.4 mm SL, Itarana, Jatibocas stream, Santa Joana basin

(19°52'26.00"S 40°52'31.00"W); col. R. L. Teixeira & P. S. Miller, 10 Aug. 2000. **MBML 701**, 13, 71.89 – 36.47 mm SL; Itarana, Santa Joana basin (19°52'26.00"S 40°52'31.00"W); col. R. L. Teixeira & P. S. Miller, 19 Aug. 2000. **MBML 753**, 10, 117.52 – 62.06 mm SL; Itarama, Jatiboca stream, Santa Joana basin (19°52'26.00"S 40°52'31.00"W); col. R. L. Teixeira & P. S. Miller, 18 Oct. 2000. **MBML 765**, 1, 94.72 mm SL; Itarana, Santa Joana river (19°52'26.00"S 40°52'31.00"W); col. R. L. Teixeira & P. S. Miller, 08 Feb. 2002. **MBML 788**, 1, 79.59 mm SL; Itarana, Jatibocas stream, Santa Joana basin (19°52'26.00"S 40°52'31.00"W); col. R. L. Teixeira, 12 Oct. 2000. **MBML 805**, 4, 93.08 – 71.66 mm SL; Itarana, Jatibocas stream, Santa Joana basin (19°52'26.00"S 40°52'31.00"W); col. R. L. Teixeira & P. S. Miller, 21 Jun. 2001. **MBML 807**, 7, 80.52 – 65.54 mm SL; Itarana, Jatibocas stream, Santa Joana basin (19°52'26.00"S 40°52'31.00"W); col. R. L. Teixeira & P. S. Miller, 08 Feb. 2001. **MBML 999**, 4, 51.11 – 40.39 mm SL; Itarana, Santa Joana river, tributary of Rio Doce basin (19°52'26.00"S 40°52'31.00"W); col. R. L. Teixeira & P. C. M. Mili, 21 Jun. 2001. **MBML 1014**, 1, 43.80 mm SL; Itarana, Limoeiro creek, Santa Joana river (19°52'26.00"S 40°52'31.00"W); col. R. L. Teixeira, 19 Apr. 2001. **MBML 1357**, 3, 66.44 – 43.43 mm SL; Colatina, Cachoeira do oito waterfall, Pancas river basin (19°27'21.00"S 40°37'29.00"W); col. R. L. Teixeira & G. I. Almeida, 08 Dec. 2005. **MBML 1395**, 1, 57.74 mm SL; Colatina, Santa Maria do Rio Doce basin (19°32'55.00"S 40°38'7.00"W); col. R. L. Teixeira & Borlute, 11 Oct. 2005. **MBML 2243**, 1, 71.69 mm SL; Laranja da Terra e Serra Pelada, Timbuva stream, Gandu river basin (19°54'55.00"S 41° 5'18.00"W); col. L. M. Sarmento-Soares, R. F. Martins-Pinheiro, A. T. Aranda, R. L. Teixeira, M. M. C. Roldi & M. M. Lopes, 12 Jun. 2009. **MBML 2274**, 3, 118.89 – 50.15 mm SL; Laranja da Terra, Lagoa stream, Gandu river basin (19°59'26.00"S 41° 3'55.00"W); col. L. M. Sarmento-Soares, R. F. Martins-Pinheiro, A. T. Aranda, R. L. Teixeira, M. M. C. Roldi & M. M. Lopes, 12 Jun. 2009. **MBML 2290**, 11, 85,55 –

27,55 mm SL; Afonso Cláudio, Rio do Cobre river, tributary of Guandu basin (20° 9'19.00"S 41° 8'31.00"W); L. M. Sarmento-Soares, R. F. Martins-Pinheiro, A. T. Aranda, R. L. Teixeira, M. M. C. Roldi & M. M. Lopes, 14 Jun. 2009. **MBML 2295**, 2, 38.15 – 34.72 mm SL; Afonso Claudio Rio do Peixe river, Gandu river basin (20° 7'39.00"S 41° 8'9.00"W); col. A. T. Aranda, R. F. Martins-Pinheiro, R. L. Teixeira & M. M. C. Roldi, 14 Jun. 2009. **MBML 2304**, 18, 58.13 – 34.21 mm SL; Afonso Cláudio, Rio da Cobra river, tributary of Guandu river (20°12'4.00"S 41° 8'7.00"W); col. A. T. Aranda, R. F. Martins-Pinheiro, R. L. Teixeira & M. M. C. Roldi, 14 Jun. 2009. **MBML 2312**, 13, 76,47 - 33,08 mm SL; Afonso Cláudio, Rio da Cobra river, Guandu basin (20°10'57.00"S 41° 4'50.00"W); col. A. T. Aranda, R. F. Martins-Pinheiro, R. L. Teixeira & M. M. C. Roldi, 14 Jun. 2009. **MBML 2974**, 10, 99.18 – 50.86 mm SL; Colatina, Santa Maria do Rio Doce basin (19°32'21.00"S 40°37'50.00"W); col. R. L. Teixeira & E. C. Perrone, 06 Nov. 1988. **MBML 3465**, 4, 103.51 – 53.08 mm SL; Baixo Gandu, Mutum Preto river, Mutum Preto river (19°23'7.00"S 40°53'52.00"W); col. L. M. Sarmento-Soares, R. F. Martins-Pinheiro, M. R. Britto & F. M. R. S. Pupo, 01 Oct. 2010. **MBML 3571**, 9, 61.53 – 31.18 mm SL; Águia Branca, Águas Claras stream, São José river (18°57'17.00"S 40°45'19.00"W); col. L. M. Sarmento-Soares, R. F. Martins-Pinheiro, M. R. Britto & F. M. R. S. Pupo, 05 Oct. 2010. **MBML 3878**, 1, 46.95 mm SL; Colatina, São João Pequeno river (19°28'45.00"S 40°44'15.00"W); col. M. M. Martinelli, 27 Sep. 2010. **MBML 4274**, 3, 42.12 mm – 32.27 mm SL; Águia Branca, Braço Azul river, São José basin (19° 3'44.00"S 40°34'21.00"W); col. J. L. Helmer, 12 Aug. 2011. **MBML 4385**, 1, 49.35 mm SL; Santa Teresa, Santa Maria do Rio Doce river (19°46'21.10"S 40°38'2.70"W); col. R. B. Soares, J. Gurtler & V. R. Bada, 24 Sep. 2011. **MBML 4431**, 1, 39.91 mm SL; Santa Teresa, Santa Maria do Rio Doce river (19°46'21.10"S 40°38'2.70"W); col. R. B. Soares, J. Gurtler & V. R. Bada, 24 Sep. 2011. **MBML 6139**, 1, 66.2 mm SL; Santa Teresa, Cinco de Novembro river, Santa Maria

do Rio Doce basin (19°49'42.90"S 40°38'18.40"W); col. C. J. Cunha, J. P. Silva & R. B. Soares, 20 Aug. 2012. **MBML 6153**, 8, 84.35 – 23.67 mm SL; Santa Teresa, Cinco de Novembro river, Santa Maria do Rio Doce river (19°50'26.00"S 40°37'47.30"W); col. C. J. Cunha, J. P. Silva & R. B. Soares, 20 Aug. 2012.

Trichomycterus "ipatinguensis", sp. nov.

(Fig. 05, 29)

Holotype – MZUSP 112279, 67.57 mm SL; Brazil, Minas Gerais, Conceição do Mato Dentro, Meloso Creek, Santo Antônio creek (19° 4'35.98"S 43°20'28.84"W); col. M. V. Loeb, 12 Jan 2011.

Paratype – All from Brazil, state of Minas Gerais. **MZUSP 112234**, 1, 29.29 mm SL; Brazil, Minas Gerais, Conceição do Mato Dentro; Espírito Santo creek, Santo Antônio river; 19° 7'3.06"S 43°17'43.07"W; M. V. Loeb; 05 Jan 2011. **MZUSP 112237**, 5, 31.59 - 26.5 mm Sl; Brazil, Minas Gerais, Conceição do Mato Dentro; Axupé creek, Santo Antônio river; 19° 6'44.10"S 43°16'4.65"W; M. V. Loeb; 06 Jan 2011. **MZUSP 112241**, 2, 32.59 - 27.79 mm SL; Brazil, Minas Gerais, Conceição do Mato Dentro; Axupé creek, Santo Antônio river, 19° 6'44.47"S 43°16'44.68"W, M. V. Loeb; 06 Jan 2011. **MZUSP 112250**, 1, 24.21 mm SL; Brazil, Minas Gerais, Conceição do Mato Dentro; Faia creek, Santo Antônio river; 19° 3'0.16"S 43°21'45.45"W; M. V. Loeb; 09 Jan 2011. **MZUSP 112253**, 1, 25.66 mm SL; Brazil, Minas Gerais, Conceição do Mato Dentro; Ponte Nova Creek, Santo Antônio river; 18°59'24.67"S 43°23'1.62"W; M. V. Loeb; 10 Jan 2011. **MZUSP 112260**, 7, 58.41 – 29.66 mm SL; Brazil, Minas Gerais, Conceição do Mato Dentro; Antonieta creek, Santo Antônio river; 19° 0'42.07"S 43°22'20.42"W; M. V. Loeb; 10 Jan 2011. **MZUSP 112270**, 7, 63.94 – 28.82 mm Sl, 3 c&s (41.2 – 28.98 mm SL); Brazil Minas Gerais,

Conceição do Mato Dentro; São João river, Santo Antônio river; 19° 2'30.77"S 43°20'34.02"W; M. V. Loeb; 11 Jan 2011. **MZUSP 112271**, 4, 103.75 – 39.26 mm SL, 1 c&s (39.05 – mm SL); Brazil, Minas Gerais, Conceição do Mato Dentro; São João creek, Santo Antônio river; 19° 1'21.73"S 43°20'38.60"W; M. V. Loeb; 11 Jan 2011.

Diagnosis.- *Trichomycterus "ipatinguensis"* is distinguished from all congeners from the Rio Doce basin except from *T. "tantalus"*, and *T. "melanopygius"* by a dark stripe extending from the base of middle caudal-fin rays to nearly margin of this fin (vs. absent dark stripe). Distinguished from all congeners from Rio Doce basin except from *T. brunoi*, *T. "brucutu"* and *T. "ipatinguensis"* by number of branchiostegal rays, eight (vs. seven or six). Distinguished from *T. caipora*, *T. immaculatus*, *T. giganteus*, and from *T. brasiliensis* species complex by the number of pectoral-fin rays, I+7 (vs. I+8 to *T. immaculatus*, *T. giganteus*, *T. caipora* and I+6 to *T. brasiliensis* complex species).

Description.- Morphometric data for specimens examined in Table 13. Body long and almost totally straight, trunk roughly round in cross-section near head, then slightly deeper than broad and softly compressed to caudal peduncle, tapering to Caudal-fin. Dorsal profile of body gently convex to dorsal-fin origin, then straight or slightly concave along caudal peduncle to caudal-fin origin. Ventral profile convex from gular region to vent, due partly to abdominal distension, then straight or slightly concave along anal-fin origin to caudal-fin base. Caudal peduncle nearly as deep as body at end of anal-fin base.

Head approximately one sixth to one-fifth of SL, pentagonal, longer than wide and depressed. Mouth sub-terminal. Upper jaw slightly longer than lower. Upper lip wider than lower lip, and laterally continuous with base of maxillary barbel. Lower lip small, approximately 2/3 width of upper one, partly divided into right and left portions by with median concavity. Lower lip

with uniform covering of tiny vilii, resulting in velvet-like surface and not clustered into large papillae. Region between upper and lower lips with slender fleshy lobe.

Dentary and premaxillary teeth similar to each other in shape. Dentary teeth conical, arranged in four irregular rows, first row with 10 -14 teeth, extending from base to slightly up of coronoid process, with size of individual teeth increasing markedly towards symphysis and from posterior to anterior rows. Total area of premaxilary teeth slightly smaller than that of dentary, with teeth arranged irregularly in four rows, first row with approximately 11 – 14 teeth, over entire ventral surface of premaxilla. Premaxilary teeth conical.

Eye medium-sized, slightly protruding, positioned dorsally on head, without free orbital rim and covered with transparent skin. Eye located on anterior half of HL, closer to lateral border of the head than to the midline in dorsal view. Infraorbital latero-sensory canal incomplete, extending from sphenotic posteriorly to terminal pore located ventroposteriorly to eye. Anterior nares surrounded by tube of integument directed anterolaterally, continuous posterolaterally with nasal barbel. Posterior nares closer to anterior nares than to the eyes, surrounded by tube of integument incomplete posteriorly. Maxillary barbel tubular narrowing markedly towards fine tip, reaching from lateroposterior side of interopercle until base of pectoral-fin. Rictal barbel inserted immediately ventral to maxillary barbel. Its tip reaching from anterolateral to the middle of interopercle. Nasal barbel originating on posterolateral region of anterior nares, reaching anywhere from posterior border of eyes to anterior portion of opercle. Interopercular patch of odontodes large, oval in shape and with well-developed odontodes, prominent in ventral aspect of head. Interopercular patch of odontodes extending from vertical through ventroposterior border of eye to ventroanterior to opercle. Odontodes arranged in two or three irregular series, with those on mesial series much longer than those on lateral one; odontodes gradually larger posteriorly in both

series, with those posteriorly on mesial row largest. Interopercular odontodes 25 – 38. Opercular patch of odontodes on dorsolateral surface of posterior part of head, positioned anterodorsally to pectoral-fin base, roundish in shape and larger than eye in dorsal aspect of head. Opercular odontodes 13 - 18, sunk in individual slits of integument, progressively larger posteriorly, all with fine tips, with largest ones curved distally and claw-like. Entire patch surrounded by specialized rim of integument.

Pectoral-fin medium-sized, its base immediately posterior and ventral to opercular patch of odontodes. Pectoral-fin rays I+7. First pectoral-fin ray (unbranched) longer than all others, prolonged as filament beyond fin web. Other rays progressively less long, their tips following continuous line along fin margin. Pelvic-fin with convex distal profile, its origin slightly posterior to middle of SL and anterior to vertical through dorsal-fin origin, anteriorly touching anal and urogenital openings in adults but never covering it. Base of Pelvic-fins positioned less than eye diameter close to each other. Pelvic-fin rays I+4, first ray unbranched. Ischiatic process of basipterygium long and laterally curved. Dorsal-fin long, its distal profile sinusoidal. Dorsal-fin origin closer to base of Caudal-fin than to tip of snout. Dorsal-fin rays ii+II+7 (02); iii+II+7 (05), two or three unsegmented and unbranched rudimentary rays, commonly present in *Trichomycteru*s, two segmented and unbranched procurrent rays and seven branched and segmented rays (therein included two posterior closely-set rays). Anal fin slightly smaller than dorsal-fin, its distal profile gently convex. Anal-fin origin posterior to vertical through end of dorsal-fin base. Anal-fin rays ii+II+5 (2) or iii+II+5 (05), two or three unsegmented and unbranched rudimentary rays, two segmented and unbranched procurrent rays and five branched and segmented rays. Caudal-fin rounded shape, with 6+7 principal rays. Adipose-fin absent or modified into low integument fold extending between end of dorsal-fin and caudal-fin origin. Post-

Weberian vertebrae 37 (07). First dorsal-fin pterygiophore immediately anterior to neural spine of 17th (05) or 18th (02) vertebra, first anal-fin pterygiophore immediately anterior to neural spine of 21th (04) or 22th (03) vertebra. Caudal-fin procurrent rays plus one segmented non-principal ray dorsally and ventrally. Procurrent caudal-fin rays, 16 - 21 dorsally and 11 - 15 ventrally, beginning anteriorly at 32th (07) vertebrae. Pleural ribs 12 (05), 13 (02). Branchiostegal rays 7 (01), 8 (06). Dorsal-fin pterygiophores 8. Anal-fin pterygiophores 6.

Cephalic lateral line canals with simple, non-dendritic tubes ending in single pores. Supraorbital canal mostly within frontal bone. Supraorbital pores invariably present: s1 mesial to nasal-barbel base and autopalatine, s3 mesial to posterior nostril and anterior to frontal, and paired s6 posteromedial to eye and at midlength of frontal. Infraorbital canal with four pores, i1 and i2 anteriorly and i10 and i11 posteriorly. Canal not ossified. Infraorbital pore i1 located ventro-lateral to nasal-barbel base and autopalatine, i2 ventro-lateral to posterior nostril and anterior to frontal, i10 and i11 posterior to eye. Otic canal without pores. Postotic pores po1, anteromedial to opercular patch of odontodes), and po2, mesial to opercular patch of odontodes. Lateral line of trunk anteriorly continuous with postotic canal and reduced to short tube. Lateral line pores ll1 and ll2, in some specimens the ll3 is present, present dorsomedial to pectoral-fin base.

Coloration in ethanol. – *Trichomycterus "ipatinguensis"* is randomly covered with round to amoeboid dark maculae. These maculae rarely fuse with each other, sharply varying in size and number creating two extreme of color pattern (Fig. 05). At one extreme, most of all maculae are bigger or same size of twice eye diameter. In the other extreme maculae are much smaller, size of eye diameter, and higher in number. Head and base of all fins, except for caudal-fin, fallow the color pattern of body. Color pattern of caudal-fin and ventral part of body are invariable in this species. Caudal-fin with dark stripe extending from the base of middle caudal-fin rays to nearly

margin of fin. Caudal stripe more evident in young specimens and gradually fading or masked by adjacent caudal-fin pigmentation. Ventral part of body without pigmentation, white in color.

Etymology – The epithet "ipatinguensis" is in honor to Ipatinga, a city located in the State of Minas Gerais where the Piracicaba river turns into the Rio Doce basin.

Remarks – *Trichomycterus "ipatinguensis"* is highly variable in color pattern, a situation common in species of the genus (Arratia *et al*., 1978; Triques & Vono, 2004; Castellanos-Morales, 2007; Lima *et al*., 2008; Silva *et al*., 2010; Ferrer & Malabarba, 2013; Buckup *et al*. 2014; Cardoso *at al*., 2017). The overall color pattern of *T. "ipatinguensis"* can resemble the well-known *T. brasiliensis* or species from the *T. brasiliensis* complex. However, the species is highly divergent from *T. brasiliensis* both morphologically and molecularly (Table 12). *T. "tantalus"* and *T. "melanopygius"*, on the other hand, display low DNA barcoding divergence with *T. "ipatinguensis"*. Those species are nevertheless very distinct phenotypically from each other and from *T. "ipatinguensis"* (for further information on *T. "ipatinguensis"*, cf. *T. "tantalus"* Remarks).

Geographical distribution – *Trichomycterus "ipatinguensis"* is distributed through all Rio Doce basin in its headwaters (Fig. 30). Although it is interesting to note that despite this species was found in all basin, any specimen was not collected in the main channel of Rio Doce river.

Material examined- All MZUSP from Brazil, State of Minas Gerias. **MZUSP 87814**, 11, 103.45 – 39.24 mm SL, 2 c&s (114.92 – 102.45 mm SL); Serro, Creek tributary of Rio Doce basin (18°34'50.11"S 43°23'31.49"W); A. Carvalho Filho; 27 Aug 2004. **MZUSP 104700**, 2, 45.34 – 41.93 mm SL; Conceição do Mato Dentro; Creek between Conceição do Mato Dentro and Meloso municipality (19^{0}02'58" S 49^{0}21'45"W); col. I. Fichberg, 18 Mar 2009. **MZUSP 104701**, 10,

39.66 – 26.38 mm SL; Conceição do Mato Dentro, creek on the road that cross the Meloso municipality, Rio Doce basin (18°58'21.37"S 43°17'51.30"W); col. I Fichberg & M. V. Loeb, 21 Mar, 2009. **MZUSP 104702**, 6, 78.92 – 27.03 mm SL, 2 c&s (50.13 – mm SL); Conceição do Mato Dentro, Faia creek, tributary of São João river (19^{o}01'19''S 49^{o} 20'39"W); col. I Fichberg & M. V. Loeb, 19 Mar 2009. **MZUSP 104706**, 1, 52.67 mm SL; Conceição do Mato Dentro, Creek tributary of Axupé river (19^{0}06'36"S 49^{0}17'55"W); col. I. Fichberg & M. Loeb, 18 Mar 2009. **MZUSP 109370**, 2, 56.36 – 47.84 mm SL, 1 c&s (56.02– mm SL); Brazil, Minas Gerais, Santa Barbara; Ribeirão Preto creek, Piracicaba river; 20° 5'36.00"S 43°39'26.00"W; W; B. P. Maia; 31 Jul 2010. **MZUSP 109385**, 1, 100.53 mm SL; Brazil, Minas Gerais, Santa Barbara; São João river, Piracicaba river; 20° 2'28.00"S 43°40'2.00"W; B. P. Maia; 31 Jul 2010. **MZUSP 109393**, 2, 112.64 – 50.09 mm SL; Brazil, Minas Gerais, Santa Barbara; Ribeirão Preto creek, Piracicaba river; 20° 3'57.00"S 43°40'16.00"; W; B. P. Maia; 31 Jul 2010.

All MBML from Brazil, State of Espírito Santo. **MBML 4340**, 1, 73.71 mm SL; Iúna, Córrego Feio creek, Manhuaçu basin (20°22'9.40"S 41°51'28.70"W); col. L. M. Sarmento Soares, M. R. Britto, V. C. Espindula, F. M. R. S. Pupo, R. F. M. Pinheiro & M. M. C. Roldi, 10 Sep. 11. **MBML 4337**, 4, 60.86 – 31.04 mm SL; Iúna, José Preto river in the National Park of Caparaó, Manhuaçu river (20°22'9.50"S 41°51'27.50"W); col. L.M.Sarmento Soares, M.R.Britto, V.C.Espindula, F.M.R.S.Pupo, R.F.M.Pinheiro & M.M.C.Roldi, 10 Sep 2011. **MBML 6223**, 13, 95.36 – 30.10 mm SL; Afonso Cláudio, Rio Guandu river (20° 4'12.00"S 41°13'44.00"W); Researches from the BIOdiversES Project, 11 Aug 2012. **MBML 6825**, 1, 52.42 mm SL; Santa Teresa, 25 de Julho river, Santa Maria do Rio Doce river (19°50'14.60"S 40°33'18.80"W); col. L. M. Sarmento Soares, R. F. Martins Pinheiro, M. M. C. Roldi and R. Becalli, 5 May 2013. **MBML 6844**, 34, 100.51 – 40.67 mm SL; Santa Teresa, Vince e Cinco de Julho river, tributary of Santa Maria do Rio Doce

(19°50'20.70"S 40°34'4.30"W); col. L. M. Sarmento Soares, R. F. Martins Pinheiro, M. M. C. Roldi & R. Becalli, 05 May 2013.

Trichomycterus "melanopygius", sp. nov.

(Fig. 31)

Holotype – MZUSP 110936, 97.7 mm SL; Brazil, State of Minas Gerais, Mariana, Gualaxo do Sul river, tributary of Rio Doce basin (20°25′59.995″S 43°23′46.756″W); col. L. F. Salvador Jr. & L. A. C. Missiaggia, 05 Jun 2012.

Paratypes – All from Brazil, State of Minas Gerais. **MZUSP 94508**, 1, 34.7 mm SL; Desterro de Melo, Xopotó stream, at bridge in town of Desterro de Melo (21°8′53″S 43°30′46″W); col. O. T. Oyakawa, E. Baena & M. Loeb, 10 Jul 2007. **MZUSP 94537**, 1, 41.1 mm SL; Desterro de Melo, Xopotó creek at entrance of town of Desterro de Melo (21°9'10.00"S 43°31' 28.00"W); col. O. T. Oyakawa, E. Baena & M. Loeb, 10 Jul 2007. **MZUSP 110714**, 1, 69.1 mm SL; Itambé do Mato Dentro, rio Tanque, Rio Doce basin (19°25'28.00"S 43°12'1.00"W); col. A. de Castro & R. Pádua, 05 Aug 2010. **MZUSP 110720**, 1, 36.5 mm SL; Bom Jesus do Galho, Sacramento creek, middle of Rio Doce basin (19°47'50.00"S 42°18'9.00"W); col. A. de Castro & R. Pádua, 03 Aug 2010. **MZUSP 110932**, 2, 28.3-100.7 mm SL; Mariana; Gualaxo do Sul river, Rio Doce basin (20°30'16.97"S 43° 24' 39.28"W); col. L. F. Salvador Jr. & L. A. C. Missiaggia, 05 Jul 2012. **MZUSP 112748**, 4, 37.2-49.2 mm SL, 2 c&s (42.84 - 48.89 – mm SL); Ferros, rio Santo Antônio, at bridge in downtown Ferros, Rio Doce basin, (19°13′34.5″S 43°1′9.5″W); col. O. T. Oyakawa & T. F. Teixeira, 16 Aug 2012. **MZUSP 123762**, 1, 64.0 mm SL; Rio Doce; stream on the left

side and running into Risoleta Neves reservoir (20°12'21.63"S 42°52'56.24"W); col. V. J. C. Reis, M. C. C. de Pinna, G. F. de Pinna & G. Ballen, 24 Jun 2018.

Non-type material examined. - All MBML from Brazil, State of Espírito Santo. **MBML 54**, 2, 44.8 - 46.0 mm SL; Colatina; rio Santa Maria do Rio Doce, Rio Doce basin (19°36'14.00"S 40°37'13.00"W); col. R .L. Teixeira & J. A. P. Scheneider, 29 Aug 1996. **MBML 701**, 3, 36.5 - 71.9 mm SL; Itarana, rio Santa Joana, Rio Doce basin (19°52'26.00"S 40°52'31.00"W); col. R. L. Teixeira & P. S. Miller, 19 Aug 2000. **MBML 1049**, 1, 107.0 mm SL; Santa Teresa; Córrego Vinte e Cinco de Julho, rio Santa Maria do Rio Doce (19°56'8.00"S 40°36'1.00"W); col. R. L. Teixeira, 19 Mar 2005. **MBML 6151**, 1, 65.3 mm SL; Santa Teresa; rio Cinco de Novembro, next to road ES-080 to Santo Antônio do Canaã, tributary of rio Santa Maria do Rio Doce, Rio Doce basin (19°50'26.00"S 40°37'47.30"W); col. C. J. Cunha, J. P. Silva & R. B. Soares, 20 Aug 2012. **LBP 22843**, 1, 36.23 mm SL; Brazil, Minas Gerais, Morro do Pilar, Rio Doce basin (20°57'22.45"S 43°46'45.48"W); col. unkown, 25 Jan. 2017.

Diagnosis.- *Trichomycterus "melanopygius"* is distinguished from its congeners from Southeastern Brazil by 49-50 Post-Weberian vertebrae (vs. maximally until 47). Distinguished by an unpigmented area longitudinally crossing the middle portion of dorsal and anal-fin. Distinguished by uniform color pattern, except for *T. immaculatus* and *T. "tantalus"*. Distinguished from *T. "tantalus"*, *T. giganteus*, *T. immaculatus*, *T. pradensis* by majority I+7 pectoral-fin rays (vs. strictly I+8). Distinguished from all species of Rio Doce basin, except for *T. "ipatinguensis"* and *T. "tantalus"* by dark maculae extending from base of caudal-fin rays until the tip (vs. absence or dusky caudal-fin rays).

Description.- Morphometric data for specimens examined in Table 14. Body long and almost totally straight, trunk roughly round in cross-section near head, then slightly deeper than broad and

softly compressed to caudal peduncle, tapering to Caudal-fin. Dorsal profile of body gently convex to dorsal-fin origin, then straight or slightly concave along caudal peduncle to caudal-fin origin. Ventral profile convex from gular region to vent, due partly to abdominal distension, then straight or slightly concave along anal-fin origin to caudal-fin base. Caudal peduncle as deep as body at beginning of anal-fin base.

Head approximately one-fourth of SL, pentagonal, longer than wide and depressed. Mouth sub-terminal. Upper jaw slightly longer than lower. Upper lip wider than lower lip, and laterally continuous with base of maxillary barbel. Lower lip small, approximately 2/3 width of upper one, partly divided into right and left portions by with median concavity. Lower lip with uniform covering of tiny vilii, resulting in velvet-like surface and not clustered into large papillae. Region between upper and lower lips with slender fleshy lobe.

Dentary and premaxillary teeth similar to each other in shape. Dentary teeth conical, arranged in four irregular rows, first row with 12-13 teeth, extending from base to slightly up of coronoid process, with size of individual teeth increasing markedly towards symphysis and from posterior to anterior rows. Total area of premaxilary teeth slightly smaller than that of dentary, with teeth arranged irregularly in four rows, first row with approximately 9 – 11 teeth, over entire ventral surface of premaxilla. Premaxilary teeth conical.

Eye medium-sized, protruding, positioned dorsally on head, without free orbital rim and covered with transparent skin. Eye located on anterior half of HL, closer to lateral border of the head than to the midline in dorsal view. Infraorbital latero-sensory canal incomplete, extending from sphenotic posteriorly to terminal pore located ventroposteriorly to eye. Anterior nares surrounded by tube of integument directed anterolaterally, continuous posterolaterally with nasal barbel. Posterior nares closer to anterior nares than to the eyes, surrounded by tube of integument

incomplete posteriorly. Maxillary barbel tubular narrowing markedly towards fine tip, reaching from lateroposterior side of interopercle until base of pectoral-fin. Rictal barbel inserted immediately ventral to maxillary barbel. Its tip reaching from anterolateral to the middle of interopercle. Nasal barbel originating on posterolateral region of anterior nares, reaching anywhere from posterior border of eyes to anterior portion of opercle. Interopercular patch of odontodes large, oval in shape and with well-developed odontodes, prominent in ventral aspect of head. Interopercular patch of odontodes extending from vertical through ventroposterior border of eye to ventroanterior to opercle. Odontodes arranged in two or three irregular series, with those on mesial series much longer than those on lateral one; odontodes gradually larger posteriorly in both series, with those posteriorly on mesial row largest. Interopercular odontodes 39 – 51. Opercular patch of odontodes on dorsolateral surface of posterior part of head, positioned anterodorsally to pectoral-fin base, roundish in shape and larger than eye in dorsal aspect of head. Opercular odontodes 18 - 19, sunk in individual slits of integument, progressively larger posteriorly, all with fine tips, with largest ones curved distally and claw-like. Entire patch surrounded by specialized rim of integument.

Pectoral-fin medium-sized, its base immediately posterior and ventral to opercular patch of odontodes. Pectoral-fin rays I+7 or I+8 (rare). First pectoral-fin ray (unbranched) longer than all others, prolonged as filament beyond fin web. Other rays progressively less long, their tips following continuous line along fin margin. Pelvic-fin with convex distal profile, its origin slightly posterior to middle of SL and anterior to vertical through dorsal-fin origin, covering anal and urogenital openings in adults. Base of pelvic-fins positioned close to each other. Pelvic-fin rays I+4, first ray unbranched. Ischiatic process of basipterygium short, and thin. Dorsal-fin long, its distal profile sinusoidal. Dorsal-fin origin closer to base of Caudal-fin than to tip of snout. Dorsal-

fin rays iii+II+7 (01) or iii+II+6 (01), three unsegmented and unbranched rudimentary rays, commonly present in *Trichomycterus*, two segmented and unbranched procurrent rays and six or seven branched and segmented rays (therein included two posterior closely-set rays). Anal fin slightly smaller than dorsal-fin, its distal profile gently convex. Anal-fin origin posterior to vertical through end of dorsal-fin base. Anal-fin rays ii+II+5 (2), two unsegmented and unbranched rudimentary rays, two segmented and unbranched procurrent rays and five branched and segmented rays. Caudal-fin from round to sub-truncated shape, with 6+7 principal rays. Adipose-fin absent or modified into low integument fold extending between end of dorsal-fin and caudal-fin origin. Post-Weberian vertebrae 39 (01), 40 (01). First dorsal-fin pterygiophore immediately anterior to neural spine of 20th (02) vertebra, first anal-fin pterygiophore immediately anterior to neural spine of 23th (01); 24th (01) vertebra. Caudal-fin procurrent rays plus one segmented non-principal ray dorsally and ventrally. Procurrent caudal-fin rays, 17 - 18 (02) dorsally and 14 - 15 (02) ventrally, beginning anteriorly at 34th (01) or 35th (01) vertebrae. Pleural ribs 13 (02). Branchiostegal rays 7 (01), 8 (01). Dorsal-fin pterygiophores 8. Anal-fin pterygiophores 6.

Cephalic lateral line canals with simple, non-dendritic tubes ending in single pores. Supraorbital canal mostly within frontal bone. Supraorbital pores invariably present: s1 mesial to nasal-barbel base and autopalatine, s3 mesial to posterior nostril and anterior to frontal, and paired s6 posteromedial to eye and at midlength of frontal. Infraorbital canal with four pores, i1 and i2 anteriorly and i10 and i11 posteriorly. Canal not ossified. Infraorbital pore i1 located ventro-lateral to nasal-barbel base and autopalatine, i2 ventro-lateral to posterior nostril and anterior to frontal, i10 and i11 posterior to eye. Otic canal without pores. Postotic pores po1, anteromedial to opercular patch of odontodes), and po2, mesial to opercular patch of odontodes. Lateral line of trunk

anteriorly continuous with postotic canal and reduced to short tube. Lateral line pores ll1 and ll2 present dorsomedial to pectoral-fin base.

Coloration in ethanol. – Dorsal and lateral parts of body covered with uniform scattering of dark chromatophores on inner and outer layers of skin, not forming maculae or spots. Ventral part of body, from lower lip to anal-fin base, without pigment. Dorsal and anal fins darkly-pigmented, but each with conspicuous unpigmented band longitudinally along their middle portion. Caudal-fin with broad longitudinal dark stripe from base of middle caudal-fin rays nearly to margin of fin. Caudal stripe more evident in young specimens and gradually fading or masked by adjacent caudal-fin pigmentation in larger specimens (a pattern similar to that in *Trichomycterus "ipatinguensis"* and *Trichomycterus "tantalus"*). Integument surrounding opercular odontodes darkly-pigmented. Interopercular patch of odontodes without dark pigment.

Etymology - A compound noun formed from "Melano" (dark, black in ancient greek) and "Pygidium" (caudal part of an animal in new latin or greek, pugē rump) in reference to its notable dark maculae from base of middle caudal-fin rays slightly to its margin.

Remarks. - *Trichomycterus "melanopygius"* is usually diagnosed as *Trichomycterus immaculatus*, due to some overlapped characters such as general color pattern, and first pectoral-fin ray with a segmented, unbranched, and long filament. However, *T. "melanopygius"* is distinguished from the latter by other morphological and molecular features, such as number of pectoral-fin rays, I+7 (vs. strictly I+8 for *T. immaculatus*), number of post-werberian vertebrae range, 39 – 40 (vs. 34 to 37 for *T. immaculatus*), and by position of first dorsal and ventral-fin pterygiophore immediately anterior to neural spine, 20^{th} dorsally and 23^{th} - 24^{th} ventrally (vs. 16^{th} - 17^{th} dorsally, and 20^{th} - 22^{th} ventrally for *T. immaculatus*). Additionally, *T. "melanopygius"* species is well-corroborated by DNA barcoding, 0.26% of intraspecific divergence, and presents

3.80% of DNA barcoding divergence between *T. immaculatus*. Once for Neotropical fishes 2% is considered a well-corroborated threshold (De Carvalho *et al*., 2011; Pereira *et al*., 2010, 2011a and 2013), this genetic distance between both species is big enough to confirm their validity.

Geographical distribution – *Trichomycterus "melanopygius"* is distributed through all Rio Doce basin, mainly in its headwaters (Fig. 32). The unique specimen collected at the main channel was at Rio Doce municipality in the State of Minas Gerais. The presence of this specimen in the main channel justifies the why *T. "melanopygius"* is found in the whole basin. Holotype is from Gualaxo do Sul river a tributary of Rio Doce basin.

Trichomycterus "pussilipygius", sp. nov.

(Fig. 33)

Holotype – MZUSP 123339, 68.84 mm SL; Brazil, State of Minas Gerais, Santa Rita de Minas; Caratinga river, tributary of Rio Doce basin (19°51'20.22"S 42° 8'24.63"W); col. T. Pessali, 08 Sep. 2015.

Paratype – Same data from holotype **ex-MZUSP 123339**, 14, 30.76 - 68.64 mm SL, (C&S), 3, 33.18 - 34.93 mm SL.

Diagnosis – *Trichomycterus "pussillipygius"* is distinguished from all congeners from the Rio Doce basin by a large metapterygoid with an antero-ventral acute process (vs. absence of this process in species from Rio Doce), by the average size of head, except from *T. "brucutu"*, small one 17.62, (vs. 18% and larger), and by the size of fins, shortest/SL (vs. longer fins/SL). Distinguished from *T. "brucutu"* by the color pattern, presence of three broad and dark stripes

running through all body (vs. absence of stripes or maculae forming lines in *T. "brucutu"*), and by the height of caudal peduncle, 9.48% - 11.57% (vs.14.76% – 15% in T. "brucutu").

Description – Morphometric data for specimens examined in Table 15. Body long and almost totally straight, trunk roughly round in cross-section near head, then slightly deeper than broad and softly compressed to caudal peduncle, tapering to Caudal-fin. Dorsal profile of body gently convex to dorsal-fin origin, then straight or slightly concave along caudal peduncle to caudal-fin origin. Ventral profile convex from gular region to vent, due partly to abdominal distension, then straight or slightly concave along anal-fin origin to caudal-fin base. Caudal peduncle short, depth smaller than depth at the end of anal-fin base.

Head approximately one-sixth of SL, pentagonal, slightly longer than wide and depressed. Mouth sub-terminal. Upper jaw longer than lower. Upper lip wider than lower lip, and laterally continuous with base of maxillary barbel. Lower lip small, approximately 3/2 width of upper one, partly divided into right and left portions by with median concavity. Lower lip with uniform covering of tiny vilii, resulting in velvet-like surface and not clustered into large papillae. Region between upper and lower lips with slender fleshy lobe.

Dentary and premaxillary teeth similar to each other in shape. Dentary teeth conical, arranged in four irregular rows, first row with 9 - 11 teeth, extending from base to slightly up of coronoid process, with size of individual teeth increasing markedly towards symphysis and from posterior to anterior rows. Total area of premaxillary teeth slightly smaller than that of dentary, with teeth arranged irregularly in four rows, first row with approximately 11 - 12 teeth, over entire ventral surface of premaxilla. Premaxillary teeth conical.

Eye large-sized, slightly protruding, positioned latero-dorsally on head, without free orbital rim and covered with transparent skin. Eye located on anterior half of HL, closer to lateral border of the head than to the midline in dorsal view. Infraorbital latero-sensory canal incomplete, extending from sphenotic posteriorly to terminal pore located ventroposteriorly to eye. Anterior nares surrounded by tube of integument directed anterolaterally, continuous posterolaterally with nasal barbel. Posterior nares closer to anterior nares than to eyes, surrounded by tube of integument incomplete posteriorly. Maxillary barbel tubular narrowing markedly towards fine tip, reaching the base of pectoral-fin. Rictal barbel inserted immediately ventral to maxillary barbel. Its tip reaching latero-posterior border of interopercle. Nasal barbel originating on posterolateral region of anterior nares, reaching anterior border of opercle. Interopercular patch of odontodes small, oval in shape and with well-developed odontodes, prominent in ventral aspect of head. Interopercular patch of odontodes extending from vertical through ventroposterior border of eye to ventroanterior to opercle. Odontodes arranged in three irregular series, with those on mesial series much longer than those on lateral one; odontodes gradually larger posteriorly in both series, with those posteriorly on mesial row largest. Interopercular odontodes 34 -36. Opercular patch of odontodes on dorsolateral surface of posterior part of head, positioned anterodorsally to pectoral-fin base, roundish in shape and very small, smaller than eye diameter in dorsal aspect of head. Opercular odontodes 14 - 20, sunk in individual slits of integument, progressively larger posteriorly, all with fine tips, with largest ones curved distally and claw-like. Entire patch surrounded by specialized rim of integument.

Pectoral-fin medium-sized, its base under posterior and ventral to opercular patch of odontodes. Pectoral-fin rays I+7. First pectoral-fin ray (unbranched) slightly longer than all others, prolonged as filament beyond fin web. Other rays progressively less long, their tips following

continuous line along fin margin. Pelvic-fin with convex distal profile, its origin slightly posterior to middle of SL and anterior to vertical through dorsal-fin origin, covering anal and urogenital openings in adults. Base of Pelvic-fins positioned one eye diameter to each other. Pelvic-fin rays I+4, first ray unbranched. Ischiatic process of basipterygium short, hook-like, and latero-curved. Dorsal-fin long, its distal profile sinusoidal. Dorsal-fin origin closer to base of Caudal-fin than to tip of snout. Dorsal-fin rays ii+II+7, two unsegmented and unbranched rudimentary rays, commonly present in *Trichomycteru*s, two segmented and unbranched procurrent rays and seven branched and segmented rays (therein included two posterior closely-set rays). Anal fin slightly smaller than dorsal-fin, its distal profile gently convex. Anal-fin origin posterior to vertical through end of dorsal-fin base. Anal-fin rays ii +II+5, two unsegmented and unbranched rudimentary rays, two segmented and unbranched procurrent rays and five branched and segmented rays. Caudal-fin sub-truncated, with 6+7 principal rays. Adipose-fin absents or modified into low integument fold extending between end of dorsal-fin and caudal-fin origin. Post-Weberian vertebrae 35 (01) - 36 (02). First dorsal-fin pterygiophore immediately anterior to neural spine of 17th (03), vertebra, first anal-fin pterygiophore immediately anterior to neural spine of 20th (02) and 21th (01) vertebra. Caudal-fin procurrent rays plus one segmented non-principal ray dorsally and ventrally. Procurrent caudal-fin rays, 15 - 16 dorsally and 11 ventrally, beginning anteriorly at 32th vertebrae. Pleural ribs 12 (03). Branchiostegal rays 7 (03). Dorsal-fin pterygiophores 8. Anal-fin pterygiophores 6.

Cephalic lateral line canals with simple, non-dendritic tubes ending in single pores. Supraorbital canal mostly within frontal bone. Supraorbital pores invariably present: s1 mesial to nasal-barbel base and autopalatine, s3 mesial to posterior nostril and anterior to frontal, paired s6 posteromedial to eye and at midlength of frontal. Infraorbital canal with four pores, i1 and i2 anteriorly and i10 and i11 posteriorly. Canal partially ossified in adults. Infraorbital pore i1 located

ventro-lateral to nasal-barbel base and autopalatine, i2 ventro-lateral to posterior nostril and anterior to frontal, i10 and i11 posterior to eye. Otic canal without pores. Postotic pores po1, anteromedial to opercular patch of odontodes), and po2, mesial to opercular patch of odontodes. Lateral line of trunk anteriorly continuous with postotic canal and reduced to short tube. Lateral line pores ll1, ll2 present dorsomedial to pectoral-fin base.

Coloration in ethanol. – Presence of two dark broad stripes located in the mid-dorsum and lateral-dorsum of trunk; presence of one line, partially stripe and partially round maculae, in the mid-lateral portion of body; and presence of a line of round dark maculae variable in size located dorsally to abdomen and ventrally to mid-lateral line of body. All stripes and lines of maculae running from posterior border of head until base of caudal-fin not fusing with each other. Base of fins with dark pigments. Caudal-fin base with a transversal dark stripe. Head darkest on region corresponding to neurocranium, outlined by brain pigment seen by transparency. Dark spot normally at base of opercular patch of odontodes, with additional dark markings on cheeks. Light teardrop-shade area extending from ventral margin of eye to base of opercular patch of odontodes, corresponding to *levator operculi* muscle. Base of nasal barbels surrounded with concentration of dark pigment, extending posteriorly as elongate dark field to anterior margin of eyes. Distal margin of integument fold of opercular patch of odontodes darkly-pigmented. Interopercular patch of odontodes white. Ventral side of the body lacking dark pigment.

Epistemology – The epithet "pussilipygius" comes from the junction of two latim words, *pussili* that means small, and *pigyus* that means tail, caudal or terminal portion of an animal body. This epithet was chosen to reinforce the short fins and mainly caudal-fin that this species has.

Geographical distribution – *Trichomycterus "pussilipygius"* was found just in the headwaters of Caratinga river in a unique locality (Fig. 34), probably being an endemic species from this river.

Trichomycterus "sordislutum", sp. nov.

(Fig. 35)

Holotype - MZUSP 73162, 78.28 mm SL, Brazil, Minas Gerais, Conceição do Mato Dentro municipality, Rio do Peixe river, tributary of Santo Antônio river (19°12'1.83"S 43° 8'32.41"W); col. F. Di Dario & S. Kakinami, 14 Jan 2001.

Paratypes - All from Brazil, state of Minas Gerais. **MZUSP 80309**, 2, 92.41 - 82.55 mm SL, Suaçuí Grande river, Rio Doce basin (18°29'48.86"S 42°19'53.66"W); col. C B M Alves, 16 Mar 2001. **MZUSP 123340**, 1, 92.77 mm SL, Iapú municipality, Caratinga river, Rio Doce basin (19°28'36.41"S 42° 7'44.44"W); col. T. Pessali, 08 Oct 2015.

Diagnosis- *Trichomycterus "sordislutum"* is distinguished from all Southeastern Brazil congeners except for *T. "astromycterus", T. "tantalus", T. "vinnulus"* and *T. nigricans* by number of pores in lateral line, three pores (vs. two pores in lateral line). Distinguished from *T. "tantalus", T. giganteus, T. immaculatus*, and *T. caipora* by number of pectoral-fin rays, I+7 (vs. strictly I+8 pectoral-fin rays). Distinguished from all Southeastern Brazil congeners except for *T. caipora* by its color pattern, big and round maculae blurred by dark chromathophores in all body. Distinguished from all Rio Docer congeners except for some morphs of *T. alternatus* and *T. "barrocus"* by length of barbels, all short, nasal barbel barely crossing posterior border of eyes, maxilar and rictal barbel barely touching anteromesial border of interopercle.

Description - Morphometric data for specimens examined in Table 16. Body long and almost totally straight, trunk roughly round in cross-section near head, then slightly deeper than broad and softly compressed to caudal peduncle, tapering to Caudal-fin. Dorsal profile of body gently convex to dorsal-fin origin, then straight or slightly concave along caudal peduncle to caudal-fin origin.

Ventral profile convex from gular region to vent, due partly to abdominal distension, then straight or slightly concave along anal-fin origin to caudal-fin base. Caudal peduncle slightly as deep as body at end of anal-fin base.

Head approximately one-fifth of SL, pentagonal, longer than wide and depressed. Mouth sub-terminal. Upper jaw slightly longer than lower. Upper lip wider than lower lip, and laterally continuous with base of maxillary barbel. Lower lip small, approximately 2/3 width of upper one, partly divided into right and left portions by with median concavity. Lower lip with uniform covering of tiny vilii, resulting in velvet-like surface and not clustered into large papillae. Region between upper and lower lips with slender fleshy lobe. Dentary teeth conical. Total area of premaxilary teeth slightly smaller than that of dentary. Premaxilary teeth conical.

Eye medium-sized, one-seventh of head length, protruding, positioned dorsally on head, without free orbital rim and covered with transparent skin. Eye located on anterior half of HL, closer to lateral border of the head than to the midline in dorsal view. Infraorbital latero-sensory canal incomplete, extending from sphenotic posteriorly to terminal pore located ventroposteriorly to eye. Anterior nares surrounded by tube of integument directed anterolaterally, continuous posterolaterally with nasal barbel. Posterior nares closer to anterior nares than to the eyes, surrounded by tube of integument incomplete posteriorly. Maxillary barbell short, wide in its base, tubular, narrowing markedly towards fine tip, reaching until anteromesial border of interopercle. Rictal barbel very short, inserted immediately ventral to maxillary barbel. Its tip goes until the most anteromesial portion of interopercle. Nasal barbell short and wide in its base, originating on posterolateral region of anterior nares. Its tip goes until slightly beyond eyes. Interopercular patch of odontodes very large, oval in shape and with well-developed odontodes, prominent in ventral aspect of head. Interopercular patch of odontodes extending from vertical through ventroposterior

border of eye to ventroanterior to opercle. Odontodes arranged in three to four irregular series, with those on mesial series much longer than those on lateral one; odontodes gradually larger posteriorly in both series, with those posteriorly on mesial row largest. Interopercular odontodes 47 - 63. Opercular patch of odontodes on dorsolateral surface of posterior part of head, positioned anterodorsally to pectoral-fin base, roundish in shape and larger than eye in dorsal aspect of head. Opercular odontodes 24 - 28, sunk in individual slits of integument, progressively larger posteriorly, all with fine tips, with largest ones curved distally and claw-like. Entire patch surrounded by specialized rim of integument.

Pectoral-fin large-sized, its base immediately posterior and ventral to opercular patch of odontodes. Pectoral-fin rays I+7. First pectoral-fin ray (unbranched) longer than all others, prolonged as filament beyond fin web. Other rays progressively less long, their tips following continuous line along fin margin. Pelvic-fin with convex distal profile, its origin slightly posterior to middle of SL and anterior to vertical through dorsal-fin origin, its bases are close together, and their tips touch but not cover anal and urogenital openings. Pelvic-fin rays I+4, first ray unbranched. Dorsal-fin long, its distal profile sinusoidal. Dorsal-fin origin closer to base of Caudal-fin than to tip of snout. Dorsal-fin rays iii+II+7 (01), three unsegmented and unbranched rudimentary rays, commonly present in *Trichomycteru*s, two segmented and unbranched procurrent rays and seven branched and segmented rays (therein included two posterior closely-set rays). Anal fin slightly smaller than dorsal-fin, its distal profile gently convex. Anal-fin origin posterior to vertical through end of dorsal-fin base. Anal-fin rays iii+II+5 (01), three unsegmented and unbranched rudimentary rays, two segmented and unbranched procurrent rays (one specimen with one, though it is very rare) and five branched and segmented rays (one specimen with seven, though it is very rare). Caudal-fin from rounded shape, with 6+7 principal rays. Adipose-fin absent

or modified into low integument fold extending between end of dorsal-fin and caudal-fin origin. Post-Weberian vertebrae 37 (01). First dorsal-fin pterygiophore immediately anterior to neural spine of 18th (01) vertebra, first anal-fin pterygiophore immediately anterior to neural spine of 22th (01) vertebra. Caudal-fin procurrent rays plus one segmented non-principal ray dorsally and ventrally. Procurrent caudal-fin rays, 12 (01) dorsally and 11 (01) ventrally, beginning anteriorly at 33th (01) vertebrae. Pleural ribs 13 (01). Branchiostegal rays 6 (01). Dorsal-fin pterygiophores 8. Anal-fin pterygiophores 6.

Cephalic lateral line canals with simple, non-dendritic tubes ending in single pores. Supraorbital canal mostly within frontal bone. Supraorbital pores invariably present: s1 mesial to nasal-barbel base and autopalatine, s3 mesial to posterior nostril and anterior to frontal, and single or paired s6 posteromedial to eye and at midlength of frontal. Infraorbital canal with four pores, i1 and i2 anteriorly and i10 and i11 posteriorly. Canal not ossified. Infraorbital pore i1 located ventro-lateral to nasal-barbel base and autopalatine, i2 ventro-lateral to posterior nostril and anterior to frontal, i10 and i11 posterior to eye. Otic canal without pores. Postotic pores po1, anteromedial to opercular patch of odontodes), and po2, mesial to opercular patch of odontodes. Lateral line of trunk anteriorly continuous with postotic canal and reduced to short tube. Lateral line pores ll1, ll2 and ll3 present dorsomedial to pectoral-fin base.

Coloration in ethanol. - Dark chromatophores distributed into inner and outer skin layers and dermis. Chromatophores on inner skin layer form large roundish blotches, bigger than eye diameter. These botches can be aligned and fused with others creating strips along the body. Outer skin layer pigmentation follows no pattern, shadowing the inner pigmentation. In the dorsum, on the inner layer, presence of two aligned dark blotches from head to Caudal-fin. These lines are laterally positioned in the dorsum, bordering the right and left side of dorsum. Between the lateral

blotch line of dorsum and the medium line of body, there is almost absence of pigmentation in the inner layer of dermis, creating a pattern of unpigmented line from dorsal of opercle to dorsal of caudal-fin rays. In the medium line of body there is a thick and dark strip that come from dorsolateral of opercle to middle caudal-fin ray. This line can be uninterrupted or interrupted from dorsal-fin origin to Caudal-fin ray. Ventral to medium line of body there are chromatophores organized in ducky blotches pattern, sometimes forming rounded maculae. All fins are well pigmented with dark chromatophores. Tip of fins not pigmented, creating a white band. Ventrally in the body there is no pigmentation. Head darkest on region corresponding to neurocranium, outlined by brain pigment seen by transparency. Light teardrop-shade area extending from posterior margin of eye to base of opercular patch of odontodes, corresponding to levator operculi muscle. Base of nasal barbels surrounded with concentration of dark pigment, extending posteriorly as elongate dark field to anterior margin of eyes. Distal margin of integument fold of opercular patch of odontodes darkly-pigmented. Interopercular patch of odontodes white.

Etymology – The epithet "sordislutum" comes from the junction of two latin words. The first is *sordidus*, which means nasty, sordid. The second is *lutum*, which means mud and dirt. The junction of both make reference to the ore mud from Samarco SA that was dumped into the Rio Doce basin polluting almost its entirely.

Remarks - *Trichomycterus "sordislutum"* is a large-sized *Trichomycterus* species when compared to its congeners. This species is very similar to *Trichomycterus caipora* from the Macabu river basin (a small isolated drainage opening into the Lagoa Feia, a coastal lagoon in the State of rio de Janeiro), yet distinguishing from the latter by the number of pectoral-fin rays and number of sensory pores in the lateral line. Although there are few morphological characters distinguishing

both species, they are particularly consistent, fully discriminating the two taxa with no overlap. The two species are isolated in distinct hydrografic basins without any known connection.

Note.- This species is currently under description by S. Santos (MNRJ) and will be published separately.

Geographical distribution - *Trichomycterus "sordislutum"* is present in the headwaters of the Rio Santo Antônio, Rio Suaçuí Grande and Rio Caratinga river (Fig. 36). This species was not found in the main channel of Rio Doce river despite its rather broad distribution.

Trichomycterus "tantalus", sp nov.

(Fig. 37)

Holotype - MZUSP 123369, 75.98 mm SL; Brazil, State of Minas Gerais, Baguari, Main streen of Rio Doce basin (19° 1' 33.62"S 42° 7' 29.12"W); V. J. C. Reis & T. Pessali, 12 Nov. 2017.

Paratypes – All from Brazil, State of Minas Gerais. **MZUFV 2565**, 01, 154.01 mm SL; Raul Soares, Matipó river, downstream UHE Emboque (20° 7' 25.71"S 42°23' 6.07"W); col. J. Dergam, 27 Aug. 1998. **ex-MZUSP 123369**, 23, 68.44 – 80.23 mm SL, Same data in holotype.

Diagnose – *Trichomycterus "tantalus"* is distinguished from all congeners from Southeastern Brazil by a large opercle with 25 to 33 odontodes (vs. 13 to 25 opercular odontodes in all *Trichomycterus* species from the Southeastern Brazil). Distinguished from all Southeastern Brazilian congeners, except from T. astromycterus, *T. caipora*, *T. melanopygius*, *T. nigricans*, *T. immaculatus*, and *T. giganteus* by having strictly I+8 pectoral-fin rays (vs. I+7), distinguished

from all congeners from Rio Doce basin by a strongly forked caudal-fin (vs. rounded, truncated or slightly forked); distinguished from all congeners from Rio Doce basin, except from *T. vinnulus* by three pores in the lateral line (vs. two pores in the lateral line).

Description – Morphometric data for specimens examined in Table 17. Body long and almost totally straight, trunk roughly round in cross-section near head, then slightly deeper than broad and softly compressed to caudal peduncle, tapering to Caudal-fin. Dorsal profile of body gently convex to dorsal-fin origin, then straight or slightly concave along caudal peduncle to caudal-fin origin. Ventral profile convex from gular region to vent, due partly to abdominal distension, then straight or slightly concave along anal-fin origin to caudal-fin base. Caudal peduncle long, beginning almost 1/2 of body depth at beginning of dorsal-fin base and fastly expanding until 1/4 of caudal-fin rays

Head approximately one-fifth of SL, pentagonal, slightly longer than wide and depressed. Mouth sub-terminal. Upper jaw longer than lower. Upper lip wider than lower lip, and laterally continuous with base of maxillary barbel. Lower lip small, in many specimens from MZUSP 123369 it is atrophied, approximately 1/2 width of upper one, partly divided into right and left portions by with median concavity. Lower lip with uniform covering of tiny vilii, resulting in velvet-like surface and not clustered into large papillae. Region between upper and lower lips with slender fleshy lobe.

Dentary and premaxillary teeth similar to each other in shape. Dentary teeth conical, arranged in four irregular rows, first row with 15 teeth, extending from base to slightly up of coronoid process, with size of individual teeth increasing markedly towards symphysis and from posterior to anterior rows. Total area of premaxilary teeth slightly smaller than that of dentary,

with teeth arranged irregularly in four rows, first row with approximately 15 teeth, over entire ventral surface of premaxilla. Premaxilary teeth conical.

Eye medium-sized, slightly protruding, positioned latero-dorsally on head, without free orbital rim and covered with transparent skin. Eye located on anterior half of HL, closer to lateral border of the head than to the midline in dorsal view. Infraorbital latero-sensory canal incomplete, extending from sphenotic posteriorly to terminal pore located ventroposteriorly to eye. Anterior nares surrounded by tube of integument directed anterolaterally, continuous posterolaterally with nasal barbel. Posterior nares closer to anterior nares than to the eyes, surrounded by tube of integument incomplete posteriorly. Maxillary barbel tubular narrowing markedly towards fine tip, reaching from anterior border of eyes until anteromesial border of interopercle. Rictal barbel inserted immediately ventral to maxillary barbel. Its tip reaching from posterior border of posterior nares until posterior border of eyes, not touching the interopercle. Nasal barbel originating on posterolateral region of anterior nares, reaching anywhere from posterior border of posterior nares to slightly posterior to eyes. Interopercular patch of odontodes large, oval in shape and with well-developed odontodes, prominent in ventral aspect of head. Interopercular patch of odontodes extending from vertical through ventroposterior border of eye to ventroanterior to opercle. Odontodes arranged in three or four irregular series, with those on mesial series much longer than those on lateral one; odontodes gradually larger posteriorly in both series, with those posteriorly on mesial row largest. Interopercular odontodes 40 - 52. Opercular patch of odontodes on dorsolateral surface of posterior part of head, positioned anterodorsally to pectoral-fin base, roundish in shape and very large, 2 times or more eye diameter in dorsal aspect of head. Opercular odontodes 25 - 33, sunk in individual slits of integument, progressively larger posteriorly, all with

fine tips, with largest ones curved distally and claw-like. Entire patch surrounded by specialized rim of integument.

Pectoral-fin medium-sized, its base under posterior and ventral to opercular patch of odontodes. Pectoral-fin rays I+8. First pectoral-fin ray (unbranched) longer than all others, prolonged as filament beyond fin web. Other rays progressively less long, their tips following continuous line along fin margin. Pelvic-fin with convex distal profile, its origin slightly posterior to middle of SL and anterior to vertical through dorsal-fin origin, slightly covering anal and urogenital openings in adults. Base of Pelvic-fins positioned close to each other. Pelvic-fin rays I+4, first ray unbranched. Ischiatic process of basipterygium long, hook-like, and latero-curved. Dorsal-fin long, its distal profile sinusoidal. Dorsal-fin origin closer to base of Caudal-fin than to tip of snout. Dorsal-fin rays iii+II+7 (01) or iv+II+7 (01), three or four unsegmented and unbranched rudimentary rays, commonly present in *Trichomycteru*s, two segmented and unbranched procurrent rays and seven branched and segmented rays (therein included two posterior closely-set rays). Anal fin slightly smaller than dorsal-fin, its distal profile gently convex. Anal-fin origin posterior to vertical through end of dorsal-fin base. Anal-fin rays iii+II+5 or iv+II+5, three or four unsegmented and unbranched rudimentary rays, two segmented and unbranched procurrent rays and five branched and segmented rays. Caudal-fin deeply forked, with 6+7 principal rays. Adipose-fin absent or modified into low integument fold extending between end of dorsal-fin and caudal-fin origin. Post-Weberian vertebrae 36 (02). First dorsal-fin pterygiophore immediately anterior to neural spine of 16^{th} (01), 17^{th} (01), vertebra, first anal-fin pterygiophore immediately anterior to neural spine of 21^{th} (01) and 22^{th} (01) vertebra. Caudal-fin procurrent rays plus one segmented non-principal ray dorsally and ventrally extending until 1/4 on caudal-fin rays. Procurrent caudal-fin rays, 16 - 17 dorsally and 14 - 13 ventrally, beginning

anteriorly at 32th vertebrae. Pleural ribs 11 (01), 12 (01). Branchiostegal rays 7 (02). Dorsal-fin pterygiophores 8. Anal-fin pterygiophores 6.

Cephalic lateral line canals with simple, non-dendritic tubes ending in single pores. Supraorbital canal mostly within frontal bone. Supraorbital pores invariably present: s1 mesial to nasal-barbel base and autopalatine, s3 mesial to posterior nostril and anterior to frontal, and single s6 posteromedial to eye and at midlength of frontal. Infraorbital canal with four pores, i1 and i2 anteriorly and i10 and i11 posteriorly. Canal partially ossified in adults. Infraorbital pore i1 located ventro-lateral to nasal-barbel base and autopalatine, i2 ventro-lateral to posterior nostril and anterior to frontal, i10 and i11 posterior to eye. Otic canal without pores. Postotic pores po1, anteromedial to opercular patch of odontodes), and po2, mesial to opercular patch of odontodes. Lateral line of trunk anteriorly continuous with postotic canal and reduced to short tube. Lateral line pores ll1, ll2 and ll3 present dorsomedial to pectoral-fin base.

Coloration in ethanol. – Yellowish body with dark chromathophores not forming maculae. Dark chromatophores homogeneously distributed in all trunk dorsally from head until posterior-most caudal peduncle, laterally until mid-line of body. Pigmentation interspecifically vary from almost absence of dorsal and lateral pigmentation to fully pigmented as described above. Head darkest on region corresponding to neurocranium, outlined by brain pigment. Cheeks less pigmented than neorocranium on the dilatactor operculi muscle region, probably due its contraction. Base of nasal barbels surrounded with concentration of dark pigment, extending posteriorly as elongate dark field to anterior margin of eyes. Distal margin of integument fold of opercular patch of odontodes darkly-pigmented. Interopercular patch of odontodes white. Ventral side of the body lacking dark pigment. Base of pectoral and dorsal-fins darkly pigmented. Presence of dark and broad maculae

backgrounded by hyaline caudal-fin rays from base of middle caudal-fin rays to nearly margin of fin.

Etymology – The epithet *tantalus* comes from the ancient Greek word, *tantalos* which means symbol of eternal torment. This name was chosen once this species has a very large patch of odontodes in the opercle, the biggest among species of the Rio Doce basin, which gives the ideia of a feared creature that torments all.

Remarks – *Trichomycterus "tantalus"* is a most distinctive species among its congeners, not only from the Rio Doce, but across the entire Southeastern Brazilian region. This is a reophilic species, found so far only in the main channel of the Rio Doce and the main channel of the Rio Matipó. In both cases, specimens were collected near hydropower plants during fish transposition activities. The species has obvious reophilic characters such as a deeply forked caudal-fin. Its extremely tough, resilient integument is also suggestive of an adaptation to withstand attriction among boulders in strong currents. Numerous specimens of *T. "tantalus"* display severe head abnormalities, such as deformed and asymmetrical metapterygoids, quadrate and autopalatines; bent mesethmoid and other deformities in cranial bones. Those abnormalities are perhaps caused by repeated trauma in their turbulent habitat, where specimens supposely collide often to rocks, causing growth aberrations in bones. Interestingly, other species such as *T. immaculatus* and *Trichomycterus* sp. collected syntopically with *T. "tantalus"* do not show such skeletal alterations. Despite such morphological variation, the species displays very low intraspecific DNA barcoding divergence (> 0.01%).

Although readily diagnosable morphologically among congeners in the Rio Doce basin, *Trichomycterus "tantalus"* differs little in barcoding data from *T. "ipatinguensis"* (1.84%) and *T. "melanopygius'* (1,47%). Low genetic distance among morphologically distinct Neotropical

freshwater fish species is a common phenomenon (see Discussion below and Montoya-Burgos, 2003; Hubert *et al*., 2007; Perdices *et al*., 2002, 2005; and Ornelas-Gacia *et al*., 2008; Costa-Silva *et al*., 2015).

Geographical distribution. - *Trichomycterus "tantalus"* occurs in the main channel of the Rio Doce in its middle and upper sectors (Fig. 38).

Trichomycterus "vinnulus", sp nov.

(Fig. 39)

Holotype – MZUSP 123750, 54.00 mm SL; Brazil, State of Minas Gerais, Rio Doce municipality; Creek by the margin of the Hydroelectric Hydropower dam reservoir (20°12'21.63"S 42°52'56.24"W); col. VJC Reis, M de Pinna, G Ballen, GF de Pinna, 24 Jun 2018.

Paratype – ex-MZUSP 123750, 42, 60.73 – 28.76 mm SL; Same data from holotype. **MZUSP 123757**, 7, 59.33 – 32.28 mm SL; Rio Doce, Rio do Peixe river, Piranga basin (20°11'40.32"S 42°51'8.47"W); col. VJC Reis, M de Pinna, G Ballen, GF de Pinna, 24 Jun 2018.

Diagnosis – *Trichomycterus "vinnulus"* is distinguished from all congeners from Southeastern Brazil, excepted for *T. "tantalus"* and *T. "sordislutum"* by the number of lateral pores, three (vs. two pores). Distinguished from *T." tantalus"* by the number of pectoral-fin rays, I+7 (vs. I+8 in *T. "tantalus"*) and by the size of opercle, smaller than eye diameter (vs. three times bigger than eye diameter in *T. "tantalus").* Distinguished from *T. "sordislutum"* by the color pattern, several randomly distributed round and dark maculae through all body (vs. few, large and aligned dark and faded maculae aligned in the mid-lateral line portion of body in *T. "sordislutum"*). Distinguished from Southeastern Brazil congeners, excepted from *T. brasiliensis* species complex

by its color pattern, dark round maculae randomly distributed into entire body. However, *T. "vinnulus"* is distinguished from this complex by the number of pectoral-fin rays, I+7 (vs. I+6 in *T. brasiliensis* species complex). Distinguished from *T. alternatus* by body proportions, slender and long body (vs. short to medium body, less deep than in *T. "vinnulus"* in *T. alternatus*).

Description - Morphometric data for specimens examined in Table 18. Body long and almost totally straight, trunk roughly round in cross-section near head, then slightly deeper than broad and softly compressed to caudal peduncle, tapering to Caudal-fin. Dorsal profile of body gently convex to dorsal-fin origin, then straight or slightly concave along caudal peduncle to caudal-fin origin. Ventral profile convex from gular region to vent, due partly to abdominal distension, then straight or slightly concave along anal-fin origin to caudal-fin base. Caudal peduncle long, depth similar to body depth, and slightly expanding at the beginning of caudal-fin rays.

Head approximately one-fifth of SL, pentagonal, slightly longer than wide and depressed. Mouth sub-terminal. Upper jaw longer than lower. Upper lip wider than lower lip, and laterally continuous with base of maxillary barbel. Lower lip small, approximately 3/2 width of upper one, partly divided into right and left portions by with median concavity. Lower lip with uniform covering of tiny vilii, resulting in velvet-like surface and not clustered into large papillae. Region between upper and lower lips with slender fleshy lobe.

Dentary and premaxillary teeth similar to each other in shape. Dentary teeth conical, arranged in four irregular rows, first row with 8 teeth, extending from base to slightly up of coronoid process, with size of individual teeth increasing markedly towards symphysis and from posterior to anterior rows. Total area of premaxilary teeth slightly smaller than that of dentary, with teeth arranged irregularly in four rows, first row with approximately 9 – 10 teeth, over entire ventral surface of premaxilla. Premaxilary teeth conical.

Eye large-sized, slightly protruding, positioned latero-dorsally on head, without free orbital rim and covered with transparent skin. Eye located on anterior half of HL, closer to lateral border of the head than to the midline in dorsal view. Infraorbital latero-sensory canal incomplete, extending from sphenotic posteriorly to terminal pore located ventroposteriorly to eye. Anterior nares surrounded by tube of integument directed anterolaterally, continuous posterolaterally with nasal barbel. Posterior nares closer to anterior nares than to eyes, surrounded by tube of integument incomplete posteriorly. Maxillary barbel tubular narrowing markedly towards fine tip, reaching the base of pectoral-fin. Rictal barbel inserted immediately ventral to maxillary barbel. Its tip reaching from posterior border of posterior nares until antero-mesial border of interopercle. Nasal barbel originating on posterolateral region of anterior nares, reaching from posterior border of eyes until slightly further posterior border of eyes, never touching opercle. Interopercular patch of odontodes small, oval in shape and with well-developed odontodes, prominent in ventral aspect of head. Interopercular patch of odontodes extending from vertical through ventroposterior border of eye to ventroanterior to opercle. Odontodes arranged in three irregular series, with those on mesial series much longer than those on lateral one; odontodes gradually larger posteriorly in both series, with those posteriorly on mesial row largest. Interopercular odontodes 25 - 26. Opercular patch of odontodes on dorsolateral surface of posterior part of head, positioned anterodorsally to pectoral-fin base, roundish in shape and very small, smaller than eye diameter in dorsal aspect of head. Opercular odontodes 11 - 14, sunk in individual slits of integument, progressively larger posteriorly, all with fine tips, with largest ones curved distally and claw-like. Entire patch surrounded by specialized rim of integument.

Pectoral-fin medium-sized, its base under posterior and ventral to opercular patch of odontodes. Pectoral-fin rays I+7. First pectoral-fin ray (unbranched) slightly longer than all others,

prolonged as filament beyond fin web. Other rays progressively less long, their tips following continuous line along fin margin. Pelvic-fin with convex distal profile, its origin slightly posterior to middle of SL and anterior to vertical through dorsal-fin origin, covering anal and urogenital openings in adults. Base of Pelvic-fins positioned one eye diameter to each other. Pelvic-fin rays I+4, first ray unbranched. Ischiatic process of basipterygium long, hook-like, and latero-curved. Dorsal-fin long, its distal profile sinusoidal. Dorsal-fin origin closer to base of Caudal-fin than to tip of snout. Dorsal-fin rays iii+ II+7 or iv+ II+7, three or four unsegmented and unbranched rudimentary rays, commonly present in *Trichomycteru*s, two segmented and unbranched procurrent rays and seven branched and segmented rays (therein included two posterior closely-set rays). Anal fin slightly smaller than dorsal-fin, its distal profile gently convex. Anal-fin origin posterior to vertical through end of dorsal-fin base. Anal-fin rays ii+II+5 or iii+II+5, two or three unsegmented and unbranched rudimentary rays, two segmented and unbranched procurrent rays and five branched and segmented rays. Caudal-fin sub-truncated, with 6+7 principal rays. Adipose-fin absents or modified into low integument fold extending between end of dorsal-fin and caudal-fin origin. Post-Weberian vertebrae 36 (01) – 37 (01). First dorsal-fin pterygiophore immediately anterior to neural spine of 16^{th} (01), 17^{th} (01), vertebra, first anal-fin pterygiophore immediately anterior to neural spine of 20^{th} (01) and 21^{th} (01) vertebra. Caudal-fin procurrent rays plus one segmented non-principal ray dorsally and ventrally extending until 1/4 on caudal-fin rays. Procurrent caudal-fin rays, 19 - 21 dorsally and 12 - 13 ventrally, beginning anteriorly at 32^{th} vertebrae. Pleural ribs 9 (01), 12 (02). Branchiostegal rays 7 (03). Dorsal-fin pterygiophores 8. Anal-fin pterygiophores 6.

Cephalic lateral line canals with simple, non-dendritic tubes ending in single pores. Supraorbital canal mostly within frontal bone. Supraorbital pores invariably present: s1 mesial to

nasal-barbel base and autopalatine, s3 mesial to posterior nostril and anterior to frontal, paired s6 posteromedial to eye and at midlength of frontal. Infraorbital canal with four pores, i1 and i2 anteriorly and i10 and i11 posteriorly. Canal partially ossified in adults. Infraorbital pore i1 located ventro-lateral to nasal-barbel base and autopalatine, i2 ventro-lateral to posterior nostril and anterior to frontal, i10 and i11 posterior to eye. Otic canal without pores. Postotic pores po1, anteromedial to opercular patch of odontodes), and po2, mesial to opercular patch of odontodes. Lateral line of trunk anteriorly continuous with postotic canal and reduced to short tube. Lateral line pores ll1, ll2 and ll3 present dorsomedial to pectoral-fin base.

Coloration in ethanol. – *Trichomycetus "vinnulus"* has a wide range of color pattern with two more distinct morphs. The first morph color pattern is consisted by, round and dark maculae organized in four rows. The size, shape and number of maculae vary from specimens. First row along mid-dorsal line from occiput, through entire dorsum, into dorsal edge of caudal peduncle and to base of caudal-fin. Second row ventrolateral to that, extending from base of head through upper part of flanks, dorsal portion of caudal peduncle, to base of caudal-fin. Third row running along mid-lateral line, from immediately posterior to opercle to base of caudal-fin. Fourth and ventralmost row shorter, extending from antero-length of abdomen through ventral margin of caudal peduncle to base of caudal-fin. Fourth row usually composed by unaligned maculae. Rows are mostly independent rarely fusing. As described before the number of maculae considerably increase allied with shortening and lack of difined shape in some specimens. This modification of pigmentation creates the second morph which is defined by the following pattern: Body entirely, except for the ventral side, covered with dark, small than eye diameter and amorphous maculae. Some specimens with. absence of well difined rows observed in the latter pattern. Maculae decreasing in size from the mid-dorsum to ventrolateral side of body. Maculae mostly independent

rarely fusing. Head entirely covered by small dark spots or with dark blotches probably resulted by the fusion of smaller maculae. Head darkest on region corresponding to neurocranium, outlined by brain pigment. Cheeks less pigmented than neorocranium on the protactor opercule muscle region. Base of nasal barbels surrounded with concentration of dark pigment, extending posteriorly as elongate dark field to anterior margin of eyes. Distal margin of integument fold of opercular patch of odontodes darkly-pigmented. Interopercular patch of odontodes white. Ventral side of the body lacking dark pigment. Fin-rays covered by small dark spots.

Etymology – The epithet "*vinnulus*" is a latin word to designate wine or something graceful, and beautiful as the specimens belonging to this taxon.

Remarks – *Trichomycterus "vinnulus"* is a distinctive and readily diagnosable species. However, DNA barcoding shows low divergence relative to its sympatric species *T. alternatus*, 1.88% (Table 12, Fig. 27). Low genetic distance among morphologically distinct Neotropical freshwater fish species can be explained by many factors, including recent speciation or mitochondrial introgression due to hybridization (Montoya- Burgos, 2003; Hubert *et al*., 2007; Perdices *et al*., 2002, 2005; and Ornelas-Gacia *et al*., 2008; Costa-Silva *et al*., 2015). *Trichomycterus "vinnulus"* and *T. alternatus* coinhabit the same creek and were collected in the same microhabitat in one of the localities and in the absence of any knowledge at present about their divergence times, the possibility of mitochondrial introgression by hybridization cannot be ruled out. Similar situations were reported in various other fish groups, for example *Mobula alfredi* (Krefft 1868) vs. *Mobula birostris* (Walbaum 1792) (Kashiwagi *et al*., 2012) and *Rineloricaria langei* Ingenito *et al*. 2008 vs. *Rineloricaria kronei* (Miranda Ribeiro 1911) (Costa-Silva *et al*., 2015). In the present case, analyses using nuclear DNA markers would necessary to determine the reasons for low barcode divergence in association with pronounced phenotypic divergence between *T. "vinnulus"* and *T.*

alternatus. However, *T. "vinnulus"* differs from its congeners by phenotypic divergence as large as, or larger than, that normally seen among other *Trichomycterus* species.

Geographical distribution - *Trichomycterus "vinnulus"* is known from two localities in the Upper Rio Doce basin near the Risoleta Neves Hydropower reservoir: an unnamed creek on the left margin of the reservoir and the Rio do Peixe river, left tributary of Rio Doce, downstream from the Risoleta Neves Hydropower reservoir (Fig. 40).

Barcoding results

Of 14 morphologically diagnosed species reported to the Rio Doce basin, molecular data was available for eight (*T. alternatus, T. "astromycterus", T. "tantalus", T. immaculatus, T. "ipatinguensis", T. "vinnulus", T. "melanopygius"*. and *T. "sordislutum"*). Three additional species were included in this analysis for an expansion of taxonomical range (*T. brasiliensis, Trichomycterus* sp.1 and *Trichomycterus* sp. 2).

In sum, a total of 152 COI barcodes were obtained from 11 species of *Trichomycterus* mostly from theRio Doce basin (Table 02). The maximum length of amplified sequences ranged from 684 to 702 bp. No insertions, deletions, or stop codons were observed. *Trichomycterus alternatus* was the species most densely represented, with 75 sequenced specimens, while *Trichomycterus* sp.1 was represented by just one sequenced individual. Species represented by samples from outside of the Rio Doce basin were *T. brasiliensis* (four specimens from Rio das Velhas river, tributary of São Francisco basin), *T. immaculatus* (one from Itauna river, two from Jucuruçu basin and two from São Mateus), and *Trichomycterus sp.* 2 (four specimens from the Cubatão river).

Nearly all 11 species in this analysis (91.66%), show conspecific Kimura 2 Parameters (K2P) divergence lesser than 1%, which closely matches species boundaries defined by morphological diagnoses. Only *Trichomycterus alternatus* has high intraspecific genetic divergence (1.73%), overlapping conspecific and congeneric K2P distances (0.00% to 1.73% among conspecific, and 0.8% to 7.86% congeneric species) (Table 04). The lowest congeneric species divergence was 0.08% between *T. "melanopygius"* and *T. "ipatinguensis"*, two morphologically well-distinct species, while the highest congeneric species divergence was 7.86% between *T. brasiliensis* and *Trichomycterus* sp. 2. Despite DNA barcoding divergence below 2% among many species pairs such as *T. immaculatus* and *T. pradensis* (1.22%); *T. alternatus* and *T. "astromycterus"* (1.49%); *T. alternatus* and *T. "vinnulus"* (1.87%); *T. "tantalus"* with *T. "ipatinguensis"* (1.84%); *T. "tantalus"* and *T. "melanopygius"* (1.45%); and *T. "melanopygius"* and *T. "ipatinguensis"* (0.08%), the average congeneric divergence was 4.3% among all *Trichomycterus* species in this study. Considering only specimens from the Rio Doce, this value drops to 3.7% (Table 12).

Two species among originally assignable to *T. alternatus* were found to be highly divergent from the latter, *Trichomycterus* sp. 1 (3.06%) and *Trichomycterus* sp. 2 (3.17%). Those forms likely represent distinct species but the limited material available does not allow their diagnosis at present. At the other extreme, three other species that are unambigously diagnosable as distinct species (*T. "astromycterus"* and *T. "vinnulus"*) were clustered within *T. alternatus*, with low K2P genetic interspecific divergence (Table 12, Fig. 27). *Trichomycterus alternatus* has the highest conspecific generic divergence and several sub-clusters. Although extreme sub-clusters within this species present high K2P divergence among them, there are several intermediate sub-clusters

bridging such molecular divergence. This makes it unlikely that there is more than a single species in the complex (Fig. 27, Discussion).

Trichomycterus immaculatus is the most homogenous species analyzed in this paper, especially in view of its wide geographical range and number of representative specimens (36 COI sequences). This species is morphologically well-defined and also molecularly corroborated, with low conspecific genetic divergence, 0.1% (Table 04 and Fig. 27). Moreover *T. immaculatus* is distinguished from all analyzed species by high congeneric divergence, ranging from 3.77% to 6.21% (Table 12).

Discussion

Can genetic divergence be used as a proxy for taxonomic differentiation?

Results of the present work show an amazing congruence between the results from phenotypic analysis and divergence in COI sequence data. Among the species with both morphological and molecular data available, four display both morphological and barcoding differentiation and a neatly segregated into clustersin the NJ tree (Fig. 27). This is the case with *T. "tantalus"*, *T. immaculatus*, *T. "ipatinguensis"*, and *T. "sordislutum"*. While the degree of COI divergence is not always large, the similarity clusters agree with those based on morphological delimitation. Such cases are straightforward and simply indicate that differentiation in those lineages is expressed in both levels of their organization. A remarkable exception involves *T. alternatus* and its closest relatives. For example, *T. "astromycterus"* is one of the best-characterized species morphologically, with an impressive array of distinguishing characteristics from various body systems (in both internal and external anatomy), some of which unique and

probably autapomorphic. Further corroborating its condition as a separate lineage, there are no morphologically intermediate specimens between *T. "astromycterus"* and *T. alternatus*. Still, such pronounced phenotypic divergence is not reflected at all in COI sequences. Samples of *T. "astromycterus"* are randomly internested within a vast cluster composed of *T. alternatus* representatives (Fig. 27). Without morphological information, this species is virtually impossible to diagnose by barcoding alone. Such situation is not without parallel, and similar cases have been reported in a number of other fishes, both neotropical and otherwise (Carvalho *et al*., 2011; Pereira *et al*., 2010, 2013, 2015; Costa-Silva *et al*., 2015). Still tangled within the *T. alternatus* complex, another species which is also well-differentiated morphologically yet identical in COI sequences is *T. "vinnulus"*. Other similar case happens with *T. "melanopygius"* and *T. "ipatinguensis"* in the Rio Doce basin. In the case of of *T. "melanopygius"*, samples available do not even cluster together. But the degree of COI divergence is very small at those levels and little relevance attaches to such details. The phenomenon of lineage differentiation without equivalent mitochondrial divergence is common in neotropical fishes (Montoya-Burgos, 2003; Hubert *et al*., 2007; Perdices *et al*., 2002, 2005; and Ornelas-Gacia *et al*., 2008; Costa-Silva *et al*., 2015) and is usually attributed to two causes: recently-split lineages and mitochondrial introgression. At present, it is not possible to definitely decide which of the two causes is responsible for the cases reported here. However, the fact that *T. "astromycterus"*, *T. "vinnulus"* are sympatric with *T. alternatus* suggests mitochondrial introgression may be a relevant factor. This is not the case with *T. "melanopygius" and T. "ipatinguensis"*, which are entirely allopatric. Of course, both introgression and recent divergence are not mutually exclusive and the two factors may be at play. Resolution of this issue requires further research and additional data from nuclear markers.

Another interesting case involves the opposite situation: species with pronounced COI divergence but little or no morphological differentiation. This has been reported within many nominal species such as *Piabina argentea* Reinhardt 1867 (Pereira *et al*., 2011b) *Hoplias malabaricus* (Bloch 1794) (Marques *et al*., 2013 and Nascimento *et al*., 2017), *Rineloricaria* Bleeker 1862 (Costa-Silva *et al*., 2015) and *Curimatopsis* Steindachner 1876 (Melo *et al*., 2016)**.** This phenomenon is the most commonly-reported result from barcoding studies, which refer to such cases as revealing of hidden diversity. Often, species thus disclosed are considered to be cryptic species. Although common in fishes in general, this is a much rarer phenomenon among the *Trichomycterus* from the Rio Doce and we have identified only two such cases, both within the *T. alternatus* complex**.** One is a sample from the Rio Cubatão, an isolated basin and thus outside of the Rio Doce drainage altogether. The four specimens examined of that locality display great morphological resemblance to *T. alternatus* yet show 3.15% differentiation from other samples of this species in the Rio Doce. Such information in combination with the geographical discontinuity, strongly suggests that they represent a different species. Another case of mitochondrial divergence without apparent morphological differentiation is a single specimen (MZict 3132) from the Rio Doce at Baguari, district of Governador Valadares, MG, which is again similar to *T. alternatus* as defined here yet shows 3.10% COI divergence relative to other samples of the species. Unfortunately, there is a single specimen in that sample and it does not allow detailed morphological studies. Still, barcoding divergence in this case is so pronounced that it suggests the existence of another, yet unrecognized, species in the *T. alternatus* complex. Additional specimens are necessary to resolve this question.

Our analyses show that *T. alternatus* is the most complex species among those recognized from the Rio Doce, with the highest average intraspecific genetic distance (1.73%) among

recognized species in that basin. The divergence dendrogram (Fig. 27) shows a number of small clusters, ranging from 2.76% to 0.72%, which seem to be somewhat differentiated but not to a degree enough for recognition of separate specific status. This is clearly an indication of a broadly-distributed species with several partly-isolated populations in early stages of differentiation as observed in other Neotropical fishes (Pereira *et al*., 2010; Costa-Silva *et al*., 2015; Sales *et al*., 2018). Considering the limited COI divergence, in combination with the lack of any decisive phenotypic differentiation, we believe none of those (except the two cases mentioned above) warrant separate specific status at this point. Although our dendrograms are simply distance schemes and not hypotheses of relationships, it seems likely that *T. alternatus* is in fact not a historically cohesive unit. Subsections of it (*T. "astromycterus"* and *T. "vinnulus"*) have differentiated into full species while the remaining assemblage retained taxonomic uniformity. This scenario implies that *T. alternatus* is a metaspecies, i.e., an entity which retains some degree of reproductive continuity, genetic and phenotypic uniformity, but lacks historical cohesiveness. (Donoghue, 1985; de Queiroz & Donoghue, 1990)

In sum, it is clear that barcoding and morphological data are largely congruent in our results. This is strong indication that the taxonomic decisions implemented here are supported by separate types of biological data and thus robust from an ontological perspective. Such reasoning implies that congruent conclusions from independent sources of evidence provide empirical support for lineage differentiation. Also, the degree of barcode differentiation cannot be translated into a single cutoff value. Initial proposals of barcoding taxonomy expected a rather uniform divergence rate as a general standard for specific differentiation (Hebert *et al*., 2003; Ward *et al*., 2009). Later research quickly demonstrated that those initial expectations were naive and that taxonomic differentiation reflective of specific distinctiveness varies widely among different

groups of organisms (Pereira *et al*., 2013; Costa-Silva *et al*., 2015; Sales *et al*., 2018) and even within closely related clades (Costa-Silva *et al*., 2015; Carvalho *et al*., 2015; Sales *et al*., 2018). But beyond questions of congruence or incongruence, the most interesting situations are in fact those where the separate types of data mutually illuminate each other. Cases such as those of *T. "astromycterus", T. "vinnulus", T. "melanopygius"* and *T. "ipatinguensis"* on the one hand, and the population of *T. alternatus* from Rio Cubatão and the specimen from Rio Doce at Baguari, on the other, show that no single type of data can be taken as *prima facie* evidence of taxonomic differentiation. In the former two cases, COI differentiation alone would be utterly incapable to detect the existence of those two well-differentiated and readily diagnosable species. In the latter, morphological data have as yet failed to reflect pronounced barcoding distinctiveness most likely reflective of - yet unrecognized - taxonomic distinctiveness.

Diversity and distribution of *Trichomycterus* in the Rio Doce basin

The present paper has identified 14 species of *Trichomycterus* in the Rio Doce basin, including 10 new ones. The pronounced increase in number of species is not unexpected, because some of its neighboring basins, such as the Paraíba do Sul, the most intensely-studied basin for *Trichomycterus* diversity in Southeastern Brazil, has 18 species reported so far: *T. immaculatus* (Eigenmann & Eigenmann, 1889); *T. goeldii* (Boulenger, 1896); *T. itatiayae* Miranda Ribeiro, 1906; *T. vermiculatus* (Eigenmann, 1917); *T. santaritae* (Eigenmann, 1918); *T. paquequerense* (Miranda Ribeiro, 1943); *T. albinotatus* Costa, 1992; *T. auroguttatus* Costa, 1992; *T. mimonha* Costa, 1992; *T. mirissumba* Costa, 1992; *T. caipora* Lima, Lazzarotto & Costa, 2008; *T. nigroauratus* Barbosa & Costa, 2008; *T. claudiae* Barbosa & Costa, 2010; *T. fuliginosus* Barbosa & Costa, 2010; *T. maculosus* Barbosa & Costa, 2010; *T. mariamole* Barbosa & Costa, 2010; *T. macrophthalmus* Barbosa & Costa, 2012; *T. puriventri*s Barbosa & Costa, 2012. Next comes the

São Francisco basin, the largest basin in Southeastern Brazil but not yet as well studied as the Paraíba do Sul, with 10 valid species: *T. brasiliensis* Lütken, 1874; *T. reinhardti* (Eigenmann, 1917); *T. concolor* Costa, 1992; *T. variegatus* Costa, 1992; *T. itacarambiensis* Trazano & de Pinna, 1996; *T. trefauti* Wosiacki, 2004; *T. macrotrichopterus* Barbosa & Costa, 2010; *T. novalimensis* Barbosa & Costa, 2010; *T. rubbioli* Bichuette & Rizzato, 2010; and *T. rubiginosus* Barbosa & Costa, 2010. Additional species are known from lesser basins adjacent to the Rio Doce: Itabapoana basin (*T. brunoi* Barbosa & Costa, 2010; *T. mimosensis* Barbosa, 2013; *T. caudofasciatus* Alencar & Costa, 2004); Coastal drainages (*T. potschi* Barbosa & Costa, 2003; *T. longibarbatus* Costa, 1992; *T. gasparinii* Barbosa, 2013; *T. pantherinus* Alencar & Costa, 2004); Rio Grande basin (*T. maracaya* Bockmann & Sazima, 2004; *T. pirabitira* Barbosa & Azevedo-Santos, 2012); Jequitinhonha basin [Triques & Vono, 2004 (*T. landinga*; *T. itacambirusu*; *T. jequitinhonhae*)]. Thus, the pronounced increase in species number here reported for the Rio Doce does not depart from the figure expected for a drainage of that magnitude and in fact matches that reported for similar basins in the same region.

Most of the species of *Trichomycterus* recognized for the Rio Doce are narrowly endemic in distribution, with some known from but a single locality, e.g., *T. argos*, *T. "barrocus"*, *T. brunoi*, *T. "brucutu"*, *T. "pussilipygius"*, and *T. "vinnulus"*. Of course, some of those may in part be simply a result of collection gaps, because sampling in the Rio Doce is still far from exhaustive. But in any event it is likely that those species are not widely distributed because existing collections are sufficient to reveal a number of widely-distributed species so far. Other species occur in wider areas within the Rio Doce basin, such as *T. "astromycterus"*, *T. "tantalus"*, *T. "illuvies"*, *T. "melanopygius"*, and *T. "sordislutum"*. Finally, a few species are widely distributed throughout the Rio Doce basin, like *T. alternatus*, *T. immaculatus* and *T. "ipatinguensis"*. The great diversity

and often narrow geographical distribution of species of *Trichomycterus* in Southeastern Brazil supports past proposals of pronounced endemism in the genus (Tchernavin, 1944; Costa, 1992; de Pinna, 1992a; Bizerril, 1994; Barbosa & Costa, 2003). Species of the genus do indeed tend to inhabit headwaters, a fact which in itself agrees with high levels of isolation and endemism. However, some species of *Trichomycterus* are reported to migrate up and down watercourses and even undergo mass migrations (Dahl, 1960; de Pinna, 1998; Miranda-Chumacero *et al*., 2015). In the present case, this seems to be the explanation for the broad distribution of some species, like *T. immaculatus*, which is regularly collected both in streams and in the main channel of the Rio Doce, indicating that specimens of the species are capable of living and moving throughout a large gradient of river conditions as part of their life cycle. The species has also been reported to congregate in large numbers suggestive of some sort of migratory behavior (pers. comm. T. Pessali; Fig. 41). The lack of significant morphological or genetic divergence among populations (cf. Table 12). strongly agrees with such scenario.

The situation with *Trichomycterus immaculatus*, however, is more complex than that, because its distribution covers also the Paraíba do Sul drainage. In this case, the explanation seems to involve factors additional to simply the vagility of the species. Geological processes are possibly an important factor in the trans-basin distribution of *T. immaculatus*. According to Cherem *et al*. (2012) the São Geraldo steps (escarpment dividing the Rio Doce from the Paraíba do Sul) have been constantly denudated by geological process and weathering in an inland direction. As a result, the Paraíba do Sul is abducting 15.68 m/My from the Rio Doce, a process which has resulted in stream capture events from the Rio Doce into the Paraíba do Sul (Fig. 42) [such processes are quite general and have also been reported in other parts of the world such as the Drakenberg escarpment in Southeastern Africa (Fleming *et al.,* 1999), the Namibia escarpment in Southwestern Africa

(Bierman & Caffee, 2001), the Great Escarpment Southeastern Australia (Heimsath *et al*., 2001; 2006), the Blue Ridge escarpment Eastern North America (Sullivan *et al*., 2007), and the Sri Lankan escarpment Oceania (Vanacker *et al*., 2007)]. In such scenario, *T. immaculatus* might have dispersed into the Paraíba do Sul from the Rio Doce. Although the details and chronology of such an event are yet unknown and certainly need further study, it is at least a first plausible explanation for the observed distribution of *T. immaculatus*. The same explanation may account for the distribution of *T. alternatus*, which also occurs in the Doce and Paraíba do Sul (with several close relatives described as separate species in the latter basin, such as *T. auroguttatus*, *T. albinotatus*, and *T. goeldii*). Preliminary evidence suggests that *T. alternatus* has reduced vagility potential when compared to *T. immaculatus*, with rare reports of specimens from the main channel, no reported sightings of mass migration so far (pers. obs.). Still, within the Rio Doce, *T. alternatus* has a broad distribution, in fact as wide as that of *T. immaculatus*. However, an important additional difference exists between the two species. The genetic divergence and structuring in *T. alternatus* is significantly larger than that of *T. immaculatus* (cf. Tables 12, Fig. 27). Perhaps, as commented above, this is a result of the comparatively reduced vagility of the former in relation to the latter, which favors isolation, even if incomplete. Still, the wide distribution of *T. alternatus* in the Rio Doce is a precondition which may positively influence its dispersal probability into the Paraíba do Sul via stream capture caused by the same denudation phenomenon described above.

The same basin-abducting phenomenon described above for the Paraíba do Sul and Doce occurs also between the latter and the Rio São Francisco. The Rio Doce is invading 8.77 m/My into the São Francisco basin (Cherem *et al*., 2012) with presumably associated stream capture events. (Fig. 42). Although few species of *Trichomycterus* is so far reported to co-occur in those two basins (Ferraris 2007 and Sales *et al*., 2018), such as *T. argos* seems to be a close relative of

T. brasiliensis, from the São Francisco, (Lezama *et al*., 2012). It is possibly a result of biotic dispersal from the São Francisco into the Rio Doce by the denudation process, in this case with subsequent divergence. This is an interesting topic for further investigation once more specimens and data on both *T. argos* and *T. brasiliensis* become available.

In sum, the scenario described above implies that *T. immaculatus* invaded the Paraíba do Sul from the Doce. This hypothesis can be tested by an investigation into the genetic variability of the species in the two basins. The colonization event necessarily implies a bottleneck effect which results in reduced genetic variability of the founding population (Nei *et al*., 1975). Our hypothesis thus predicts that *T. immaculatus* in the Paraíba do Sul will have reduced genetic variability relative to its conspecifics in the Rio Doce. This can easily be tested with additional samples and analyses from throughout the distribution range of *T. immaculatus*. The same reasoning applies to similar conjectures about *T. alternatus* and *T. argos*/*T. brasiliensis* discussed above. The alternative hypothesis, naturally, is classical vicariance, where the ancestor of *T. immaculatus* was broadly distributed in both basins, perhaps by past hydrographic conjoining, and became isolated once the drainages separated.

Taxonomic situation in *Trichomycterus*

Trichomycterus is a hyper diverse and non-monophyletic taxon (de Pinna, 1989, 1998; Wosiacki, 2002; Ochoa *et al*., 2017). Its taxonomic history is complex, with many cases of synonymy and heterogeneous descriptive methodology (Eigenmann, 1918; Tchernavin, 1944; Baskin, 1973; de Pinna, 1989; Wasiacki, 2002; Bochmann & Sazima, 2004; Barbosa, 2004). Of 14 species found in the Rio Doce, only four were previously described. Of those, *T. immaculatus* and *T. alternatus*, are particularly illustrative cases to demonstrate the ill-effects of poor taxonomic standards.

Although published by the same author, C. Eigenmann, descriptions of *T. immaculatus* and *T. alternatus* adopt very different methodologies. Their subsequent redescriptions (Eigemann, 1918) follow still a third set of parameters. While the multiplicity of descriptive standards is in itself undesirable, the real problem is the lack of objectivity in their methodology. Often it is not clear how simple information like fin-ray counts and proportional measurements were taken. This makes meaningful comparisons impossible in subsequent work. Such difficulties were reported and harshly criticized by Tchernavin (1944). Despite such warnings, the same caveats still plague the taxonomy of *Trichomycterus* to the present date.

As discussed above (see Remarks on *T. immaculatus*), the lack of unified taxonomic standards allied with the use of taxonomically unsound characters can lead to erroneous species identification and redundant new species descriptions. A particularly complex situation happens with *Trichomycterus alternatus*. This species is widely distributed into the Rio Doce and adjacent basins. In the course of more than one hundred years since its description, several species very closely resembling *T. alternatus* have been described from the Rio Doce and other adjacent basins. Some of those have already been synonymized into *T. alternatus*, such as *T. florensis* (Miranda Ribeiro 1943) and *T. travassosi* (Miranda Ribeiro 1949). However, these two junior synonyms are probably just the tip of the iceberg. Other species such as *T. longibarbatus*, *T. caudofasciatus*, *T. auroguttatus*, *T. albinotatus*, *T. pantherinus*, *T. gasparinii*, *T. mimosensis* are all obviously part of the *T. alternaus* gestalt. They still await a careful evaluation of their distinctiveness from *T. alternatus* on the basis of realistic estimates of intraspecific variation and resort to information from type material.

Further compounding the problem, *Trichomycterus alternatus* happens not to be the oldest name available for a *Trichomycterus* species from Southeastern Brazil with those general

characteristics. *Trichomycterus goeldii* Boulenger 1896, from a tributary of Paraíba do Sul basin, was described with a brief diagnosis without any illustration. The identity of that species is still a mystery and the resolution of its status may have significant consequences for the nomenclature of *Trichomycterus* in the region. Resolution of this issue must rely on information from specimens from the type locality in combination with information on the type material, and will be the subject of a separate contribution (in collaboration with S. Santos, M. Britto and M. de Pinna).

Another situation that deserves mention is *Trichomycterus brasiliensis* Lütken, 1874, described to Rio das Velhas, in the São Francisco basin. Taxonomic misattention, in combination with poor descriptions resulted in the creation of many similar taxonomic entities and even a proposed species complex (Barbosa & Costa, 2003). In the Rio Doce basin, *T. argos* Lezama *et al.*, 2012 and *T. brunoi* Barbosa & Costa, 2010 are closely related, if not junior synonyms of *T. brasiliensis* (see Remarks on *T. argos* and *T. brunoi*). Resolution of this problem relies on further work on the identity and delimitation of *T. brasiliensis*, a rather complex subject which lies beyond the scope of this work.

In sum, our experience with the *Trichomycterus* of the Rio Doce demonstrates that contingent factors in the history of the systematics of the genus have paved the way for standards which may be resulting in taxonomic inflation of the diversity of the genus in Southeastern Brazil. A concerted effort must be undertaken in order to attain uniformity of taxonomic practices in *Trichomycterus* descriptions on the basis of wide-ranging and objectively standardized sources of data. Attention to intraspecific and geographic variation is also tantamount in this process. Although a hard-to-reach objective, this is a necessary precondition for significant progress in understanding the diversity and evolution of the genus and to forestall the creation of newborn synonyms. Once applied, the tempestuous cloud on this genus can finally start to dissipate.

References

Adriaens, D.; Baskin, J. N. & H. Coppens. 2010. Evolutionary morphology of trichomycterid catfishes: about handing on and digging. *In*: Nelson J. S.; Schultze H. P. & Wilson M. V. H. (Eds.). **Origin and phylogenetic interrelationships of Teleosts**. Munchen, Verlag Dr. Friedrich Pfeil. p. 337-362.

Arratia, G. 1990. The South American Trichomycterinae (Teleostei: Siluriformes), a problematic group. *In*: Peters, G. & Hutterer, R. (Eds.). **Vertebrates in the tropics**. Bonn, Museum Alexander Koening. p. 395–403.

Arratia, G.; Chang, A.; Menu-Marque, S. & Rojas, G. 1978. About Bullockia gen. nov., Trichomycterus mendozensis n. sp. and revision of the family Trichomycteridae (Pisces, Siluriformes). **Studies on Neotropical Fauna and Environment**, 13(3–4):157–194. https://doi.org/10.1080/01650527809360539

Avise, J. C.; Walker, D. & Glenn, C. J. 1998. Speciation durations and Pleistocene effects on vertebrate phylogeography. **Proceedings Royal Society of London, B**, 265: 1707-1712.

Avise, J. C. & Walker, D. 1999. Species realities and numbers in sexual vertebrates: Perspectives from an asexually transmitted genome. Proceedings National Academy of Science, 96: p. 992–995.

Barbosa, M.A. 2000. **Revisão Sistemática do Complexo de Espécies *Trichomycterus* brasiliensis (Silurifonnes: Trichomycteridae)**. Rio de Janeiro, 126p. Dissertation not published (Mestrado em Zoologia), Programa de Pós-Graduação em Ciências Biológicas/Zoologia, Museu Nacional/UFRJ.

Barbosa, V. M. A. S. 2004. **Revisão Sistemática do gênero Trichomycterus Valenciennes do Sudeste do Brasil (Siluriformes: Loricarioidea: Trichomycteridae)**. Rio de Janeiro, UFRJ/ Museu Nacional. Phd tesis not published.

Barbosa, M. A. 2013. Description of two new species of the catfish genus *Trichomycterus* (Teleostei: Siluriformes: Trichomycteridae) from the coastal river basins, southeastern Brazil. **Vertebrate Zoology**, 63 (3): 269 – 275.

Barbosa, M.A. & Costa, W.J. E.M. 2003a. Trichomycterus potschi (Siluriformes: Loricarioidei): a new trichomycterid catfish from coastal streams of southeastern Brazil. **Ichthyological Exploration of Freshwaters**, 14: 281-287.

Barbosa, M. A. & Costa, W. J. E. M. 2003b. Validade, relações filogeneticas e redescrição de Eremophilus candidus (Ribeiro, 1949) (Siluriformes: Trichomycteridae). **Arquivos do Museu Nacional**, 61: 179- 188.

Barbosa, M.A. & Costa, W.J.E.M. 2010. Seven new species of the catfish genus *Trichomycterus* (Teleostei: Siluriformes: Trichomycteridae) from Southeastern Brazil and redescription of *T. brasiliensis*. **lchthyological Exploration of Freshwaters**, 21(2): 97-122.

Barbosa, M. A. & Costa, W. J. E. M. 2011. Description of a new species of the catfish genus *Trichomycterus* (Teleostei: Siluriformes: Trichomycteridae) from the rio de Contas basin, northeastern Brazil. **Vertebrate Zoology**, 61 (3): 307-312.

Barbosa, M. A. & Costa, W. J. E. M. 2012. *Trichomycterus puriventris* (Teleostei: Siluriformes: Trichomycteridae), a new species of catfish from the rio Paraíba do Sul basin, southeastern Brazil. **Vertebrate Zoology**, 62 (2): 155-160.

Barbosa, M. A. & Katz, A. M. 2016. A new species of the catfish genus *Trichomycterus* (Teleostei: Siluriformes: Trichomycteridae) from the Paranaíba basin, Central Brazil. **Vertebrate Zoology**, 66 (3): 261-265.

Barros, L. C.; Santos, U.; Zanuncio, J. C. & Dergam, J. A. 2012. *Plagioscion squamosissimus* (Sciaenidae) and *Parachromis managuensis* (Cichlidae): a threat to native fishes of the Doce River in Minas Gerais, Brazil. **PloS one,** 7(6): e39138.

Baskin J. N. 1973. **Structure and relationships of the Trichomycteridae**. Tese de Doutorado, New York, City University of New York. 389 p.

Bierman, P.R. & Caffee, M. 2001. Slow rates of rock surface erosion and sediment production across the Namib Desert and escarpment, southern Africa. **American Journal of Science**, 301: 326–358.

Bizerril, C. R. S. F. 1994. Descrição de uma nova espécie de *Trichomycterus* (Siluroidei, Trichomycteridae) do Estado de Santa Catarina, com uma sinopse da composição da família Trichomycteridae no leste brasileiro. **Arquivos de Biologia e Tecnologia**, 37 (3): 617-628.

Bockmann, F. A. & Sazima, I. 2004. *Trichomycterus maracaya*, a new catfish from the upper rio Paraná, southeastern Brazil (Siluriformes: Trichomycteridae), with notes on the *T. brasiliensis* species complex. **Neotropical Ichthyology**, 2(2): 61-74.

Bockmann, F. A.; Casatti, L. & de Pinna, M. C. C. 2004. A new species of trichomycterid catfish from the Rio Paranapanema basin, southeastern Brazil (Teleostei: Siluriformes), with comments on the phylogeny of the family. **Ichthyological Exploration of Freshwaters**, 15 (3): 225-242.

Buckup, P. A.; Brito, M.R.; Souza-Lima, R.; Pascoli, J.C.; Villa-Verde, L.; Ferraro, G.A.; Salgado, F.L.K. & Gomes, J.R. 2014. **Guia de identificação das espécies de peixes da bacia do rio das pedras município de Rio Claro, RJ**. Rio de Janeiro, The Nature Conservancy.

Burgess, W. E. 1989. **An atlas of freshwater and marine catfishes. A preliminary survey of the Siluriformes**. Neptune City, NJ., T.F.H. Publications. 784p., Pls. 1-285.

Cardoso, Y. P. & Montoya-Burgos J. I. 2009. Unexpected diversity in the catfish *Pseudancistrus brevispinis* reveals dispersal routes in a Neotropical center of endemism: the Guyanas Region. **Molecular Ecology**, 18: 947–964.

Carvalho, D.C.; Oliveira, D.A.; Pompeu, P.S; Leal, C.G.; Oliveira, C. & Hanner, R. 2011. Deep barcode divergence in Brazilian freshwater fishes: the case of the São Francisco River Basin. **Mitochondrial DNA**, 22(Suppl 1):1–7.

Carvalho, P.H.; Lima, M.Q.; Zawadzki, C.H.; Oliveira, C. & Pinna, M. 2015. Phylogeographic patterns in suckermouth catfish *Hypostomus ancistroides* (Loricariidae): dispersion, vicariance and species complexity across a Neotropical biogeographic region. **Mitochondrial DNA**, 27(5):3590-3596.

Castellanos-Morales, C.A. 2007. *Trichomycterus santanderensis*: a new species of troglomorphic catfish (Siluriformes, Trichomycteridae) from Colombia. **Zootaxa**, 1541: 49–55.

Cherem, L.F.S.; Varajão, C.A.C.; Braucher, R.; Bourlé, D.; Salgado, A.A.R. & Varajão, A.C. 2012. Long-term evolution of denudational escarpments in southeastern Brazil. **Geomorphology**, 173-174:118–127.

Chiachio, M. C.; Oliveira, C. & Montoya-Burgos J. I. 2008. Molecular systematics and historical biogeography of the armored Neotropical catfishes Hypoptopomatinae and Neoplecostominae (Siluriformes: Loricariidae). **Molecular Phylogenetics and Evolution**, 49: 606–617.

Clare, E. L.; Lim, B.K.; Engstrom, M.D.; Eger, J.L. & Herbert, P.D.N. 2007. DNA barcoding of neotropical bats: species identification and discovery within Guyana. **Molecular Ecology Notes**, 7: 184–190.

Cordeiro, L. M. 2014. **Distribuição, filogeografia dos bagres troglóbios do gênero *Trichomycterus* na área cárstica da Serra da Bodoquena, MS (Siluriformes:Trichomycteridae)**. Tese de Doutorado, Universidade de São Paulo, São Paulo.

Corin, S. E.; Lester, P.J.; Abbott, K.L. & Ritchie, P.A. 2007. Inferring historical introduction pathways with mitochondrial DNA: The case of introduced Argentine ants (*Linepithema humile*) into New Zealand. Diversity and Distributions, 13:510–518.

Costa, F. O. 2007. Biological identifications through DNA barcodes: the case of the Crustacea. **Canadian Journal of Fisheries and Aquatic Sciences**, 64: 272–295.

Costa, W. J. E. M. 1992. Description de huit nouvelles espèces du genre Trichomycterus (Siluriformes: Trichomycteridae), du Brésil oriental. **Revue Française d'Aquariologie et Herpetologie**, 18 (4): 101-110.

Costa, W. J. E. M. & Bockmann, F. A. 1993. Un nouveau genre neotropical de la famille des Trichomycteridae (Siluriformes: Loricarioidei). **Revue Française d'Aquariologie et Herpétologie**, 20(2): 43-46.

Costa-Silva G. J.; Rodriguez, M.S.; Roxo, F.F.; Foresti, F. & Oliveira, C. 2015. Using different methods to access the difficult task of delimiting species in a complex neotropical Hyperdiverse Group. **PLoS ONE**, 10(9): e0135075. doi:10.1371/journal. pone.0135075.

da Silva, A. M.; Belei, F.; Giongo, P. & Sampaio, W.M.S. 2013. Estado Da Conservação Da Ictiofauna Do Rio Guandu, Afluente Do Baixo Rio Doce, Espírito Santo, Sudeste Do Brasil. **Evolução e Conservação da Biodiversidade**, 4 (1): 8-13.

Dahl, G. 1960. Nematognathous fishes collected during the Macarena Expedition 1959. **Novedades Colombianas**, 1: 302-317.

Datovo, A. & Bockmann, F. A. 2010. Dorsolateral head muscles of the catfish families Nematogenyidae and Trichomycteridae (Siluriformes: Loricarioidei): comparative anatomy and phylogenetic analysis. **Neotropical Ichthyology**, 8(2): 193-246.

Dawnay, N.; McEwing, O.R.; Carvalho, G.R. & Thorpe, R.S. 2007. Validation of the barcoding gene COI for use in forensic genetic species identification. Forensic Science International, 173:1–6.

de Pinna M. C. C. 1989. A new sarcoglanidine catfish, phylogeny of its subfamily, and an appraisal of the phyletic status of the Trichomycterinae. **Americam Museum Novitates**, 2950: 1-39.

de Pinna, M. C. C. 1992a. *Trichomycterus castroi*, a new species of trichomycterid catfish from the Rio Iguaçu of southeastern Brazil (Teleostei: Siluriformes). **Ichthyological Exploration of Freshwaters**, 3 (1): 89-95.

de Pinna M. C. C. 1992b. A new subfamily of Trichomycteridae (Teleostei, Siluriformes), lower loricarioid relationships and a discussion on the impact of additional taxa for phylogenetic analysis. **Zoological Journal of the Linnean Society**, 106(3): 175-229.

de Pinna M. C. C. 1998. Phylogenetic relationships of Neotropical Siluriformes (Teleostei: Ostariophysi): historical overview and synthesis of hypotheses. *In*: Malabarba L. R.; Reis, R. E.; Vari, R. P.; Lucena, Z. M. & Lucena, C. A. S. (Eds.). **Phylogeny and classification of Neotropical Fishes**. Porto Alegre, Edipucrs. p. 279-330.

de Pinna M. C. C. 1999. Species concepts and phylogenetics. **Reviews in Fish Biology and Fisheries**, 9: 353–373.

de Pinna, M.C.C. & Wosiacki, W. 2003. Trichomycteridae. Pp. 270 – 290. In: Reis R.E., S.O. Kullander & C.J. Ferraris, Jr. (Eds.). Check list of the freshwater fishes of South and Central America. Edipucrs, Porto Alegre, Brazil, 729p.

de Queiroz, K. & Donoghue, M. J. 1990. Phylogenetic Systematics and species revisited. **Claidstics**, 6:83-90.

Dergam, J. A. S.; Ferreira F. F. & Machado, F. P. 2017. **Primeiro levantamento de ictiofauna da bacia do rio Doce após o rompimento da barragem de rejeito da Samarco, em Mariana-MG**. Viçosa, Universidade Federal de Viçosa.

DoNascimiento, C.; Prada-Pedreros S. & Guerrero-Kommritz, J. 2014a. *Trichomycterus venulosus* (Steindachner, 1915), a junior synonym of *Eremophilus mutisii* Humboldt, 1805 (Siluriformes: Trichomycteridae) and not an extinct species. **Neotropical Ichthyology**, 12(4): 707-715, 2014.

DoNascimiento, C.; Prada-Pedreros S. & Guerrero-Kommritz J. 2014b. A new catfish species of the genus *Trichomycterus* (Siluriformes: Trichomycteridae) from the río Orinoco versant of Páramo de Cruz Verde, Eastern Cordillera of Colombia. **Neotropical Ichthyology**, 12:717-728. DOI: 10.1590/1982-0224-20140005

Donoghue, M. J. 1985. A critique of the biological species concept and recommendations for a phylogenetic alternative. **The Bryologist**, 88(3): 172-181.

Eigenmann, C. A. 1918. The Pygidiidae, a family of South America Catfishes. **Memoirs of the Carnegie Museum**, 7(5):259-398.

Elias, M.. Hill, R. I.; Willmott, K. R.; Dasmahapatra, K. K.; Brower, A. V. Z.; Mallet, J. & Jiggins, C. D. 2007. Limited performance of DNA barcoding in a diverse community of tropical butterflies. **Proceedings of the Royal Society, B**, 274: 2881–2889.

Eschmeyer W. N. & Fong, J. D. 2018. **Species of Fishes by family Trichomycteridae**. On-line version dated 30 August 2016. http://research.calacademy.org/research/ichthyology/catalog/SpeciesByFamily.asp

Ferraris, Jr., C. J. 2007. Checklist of catfishes, recent and fossil (Osteichthyes: Siluriformes), and catalogue of siluriform primary types**. Zootaxa**, 1418: 1-628.

Ferrer, J. & Malabarba, L.R. 2013. Taxonomic review of the genus *Trichomycterus* Valenciennes (Siluriformes: Trichomycteridae) from the laguna dos Patos system, Southern Brazil. **Neotropical Ichthyology**, 11 (2): 217–246.

Fleming, A.; Summerfield, M.A.; Stone, J.O.H.; Fifield, L.K. & Cresswell, L.G. 1999. Denudation rates for the southern Drakensberg escarpment, SE Africa, derived from in-situproduced cosmogenic 36Cl: initial results. **Journal of the Geological Society**, 156 (2): 209–212.

García-Melo, L. J.; Villa-Navarro F. A. & DoNascimiento, C. 2016. A new species of *Trichomycterus* (Siluriformes: Trichomycteridae) from the upper río Magdalena basin, Colombia**.** **Zootaxa**, 4117 (2): 226-240.

Hebert, P.D.; Cywinska, A.; Ball, S.L. & deWaard, J.R. 2003. Biological identifications through DNA barcodes. **Proceedings Royal Society of London, B**, 270: 313–321.

Hebert, P. D. N.; Penton, E.H.; Burns, J.M.; Jansen, D.H. & Hallwachs, W. 2004a. Ten species in one: DNA barcoding reveals cryptic species in the neotropical skipper butterfly Astrapes fulgerator. **Proceedings National Academy of Science**, 101(42):1412-1417.

Hebert, P. D. N.; Stoeckle, M.Y.; Zemlack, T.S. & Francis, C.M. 2004b. Identification of birds through DNA barcodes. PLoS Biol. 2:e312. doi: 10.1371/ journal.pbio.0020312

Heimsath, A.M.; Chappell, J.; Dietrich, W.E.; Nishiizumi, K. & Finkel, R.C. 2001. Late Quaternary erosion in southeastern Australia: a field example using cosmogenic nuclides. **Quaternary International,** 83–85:169–185.

Heimsath, A.M.; Chappell, J.; Finkel, R.C.; Fifield, K. & Alimanovic, A. 2006. Escarpment erosion and landscape evolution in southeastern Australia. **GSA Special Papers,** 398: 173–190.

Henn, A. W. 1928. List of types of fishes in the collection of the Carnegie Museum on September 1, 1928. **Annals of the Carnegie Museum,** 19 (4): 51-99.

Hogg, I. D. & Hebert, P. D. N. 2004. Biological identification of springtails (Collembola: Hexapoda) from the Canadian Arctic, using mitochondrial DNA barcodes. **Canadian Journal of Zoology**, 82: 749–754.

Hubert, N.; Duponchelle, F.; Nuñez, J.; Garcia-Davila, C.; Paugy, D. & Renno, J.F. 2007. Phylogeography of the piranha genera Serrasalmus and Pygocentrus: Implications for the diversification of the Neotropical ichthyofauna. **Molecular Ecology**, 16:2115–2136.

Hubert, N.; Hanner, R.; Holm, E.; Mandrak, N.E.; Taylor, E.; Burridge, M.; Watkinson, D.; Dumont, P.; Curry, A.; Bentzen, P.; Zhang, J.; April, J. & Bernatchez, L. 2008. Identifying Canadian freshwater fishes through DNA barcodes. **PLoS One**, 3(6):e2490.

Ibarra, M. & Stewart, D. J. 1987. Catalogue of type specimens of Recent fishes in Field Museum of Natural History. **Fieldiana Zoology (New Series),** 35: 1-112.

Kashiwagi T, Marshall, A.D.; Bennett, M.B. & Ovenden, J.R. 2012. The genetic signature of recent speciation in manta rays (*Manta alfredi* and *M. birostris*). **Molecular phylogenetics and evolution,** 64:212–8. doi: 10.1016/j.ympev.2012.03.020 PMID: 22503670

Kimura, M. 1980. A simple method for estimating evolutionary rate of base substitutions through comparative studies of nucleotide sequences. **Journal of Molecular Evolution**, 16:111-120.

Krieger, J. & Fuerst, P.A. 2002. Evidence for a slowed rate of molecular evolution in the order Acipenseriformes. **Molecular Biology and Evolution**, 19: 891–897.

Kumar, S.; Stecher, G.; Li, M.; Knyaz, C. & Tamura, K. 2018. MEGA X: Molecular Evolutionary Genetics Analysis across computing platforms. **Molecular Biology and Evolution**, 35:1547-1549.

Lefebure, T.; Douady, C.J.; Gouy, M. & Gilbert, J. 2006. Relationship between morphological taxonomy and molecular divergence within Crustacea: proposal of a molecular threshold to help species delimitation. **Molecular Phylogenetics and Evolution**, 40: 435–447.

Lezama, A. Q.; Triques M. L. & Santos, P. S. 2012. *Trichomycterus argos* (Teleostei: Siluriformes: Trichomycteridae), a new species from the Doce River Basin, Eastern Brazil. **Zootaxa**, 3352: 60–68.

Lima S. M. Q. 2008. **Filogeografia e sistemática molecular de dois bagres das bacias costeiras da Serra do Mar, *Trichomycterus zonatus* (Eigenmann, 1983) e *Trichogenes longipinnis* Britski & Ortega, 1983 (Siluriformes: Trichomycteridae)**. Rio de Janeiro, UFRJ, phd thesis. Non-published.

Lima, S. M. Q. & Costa, W. J. E. M. 2004. *Trichomycterus giganteus* (Siluriformes: Loricarioidea: Trichomycteridae): a new catfish from the Rio Guandu basin, southeastern Brazil. **Zootaxa**, 761: 1-6.

Lima, S. M. Q.; Lazzarotto, H.; Costa, W. J. E. M. 2008. A new species of *Trichomycterus* (Siluriformes: Trichomycteridae) from lagoa Feia drainage, southeastern Brazil. **Neotropical Ichthyology**, 6(3):315-322.

Lundberg, J.G. 1982. The comparative anatomy of the toothless blindcat, *Trogloglanis pattersoni* Eigenmann, with a phylogenetic analysis of the ictalurid catfishes. **Miscelaneous Publications, Museum of Zoology, University of Michigan**, 163:1–85.

Mabragaña, E. *et al*., 2011. DNA Barcoding Identifies Argentine Fishes from Marine and Brackish Waters. PLoS One, 6:e28655.

Maldonado-Ocampo, J. A. & Albert, J. S. 2004. *Gymnotus ardilai*: a new species of Neotropical electric fish (Ostariophysi: Gymnotidae) from the Rio Magdalena Basin of Colombia. **Zootaxa**, 759: 1-10.

Marques, D.; Santos, F. & Silva, S. 2013. Cytogenetic and DNA barcoding reveals high divergence within the trahira, *Hoplias malabaricus* (Characiformes: Erythrinidae) from the lower Amazon River. **Neotropical Ichthyology,** 11:459–66.

Martin A. P. & Bermingham, E. 2000. Regional endemism and cryptic species revealed by molecular and morphological analysis of a widespread species of Neotropical catfish. **Proceedings Biological Sciences**, 1448 (267): 1135-1141.

Mayr, E. 1969. **Principles of systematic zoology**. New York, McGraw-Hill.

Melo, B.F.; Ochoa, L.E.; Vari, R.P. & Oliveira, C. 2016. Cryptic species in the Neotropical fish genus *Curimatopsis* (Teleostei, Characiformes). **Zoologica Scripta**, 45(5):650-658. doi:10.1111/zsc.12178.

Metcalf, J.L.; Pritchard, V.L.; Silvestri, S.M.; Jenkins, J.B.; Wood, J.S.; Cowley, D.E.; Evans, R.P.; Shiozawa, D.K. & Martin, A.P. 2007. Across the great divide: genetic forensics reveals misidentification of endangered cutthroat trout populations. **Molecular Ecology**, 16: 4445–4454. doi: 10.1111/j.1365-294X.2007.03472.x.

Miquelarena, A. M. & Fernández, L. A. 2000. Presencia de Trichomycterus davisi (Haseman, 1911) en la cuenca del Alto Paraná misionero (Siluriformes: Trichomycteridae). **Revista de Ictiología**, 8 (1/2): 41-45.

Miranda-Chumacero, G.; Alvarez, G.; Luna, V.; Wallace, R.B. & Painter, L. 2015. First observations on annual massive upstream migration of juvenile catfish *Trichomycterus* in an Amazonian River. **Environmental Biology of Fishes**, 98:1913–1926. DOI 10.1007/s10641-015-0407-3

Montoya-Burgos, J. I. 2003. Historical biogeography of the catfish genus Hypostomus (Siluriformes: Loricariidae), with implications on the diversification of Neotropical ichthyofauna. **Molecular Ecology**, 12: 1855–1867.

Nascimento, C. H. R.; Frantine-Silva, W.; Souza-Shibatta, L.; Sofia, S.H.; Ferrer, J. & Shibatta, O.A. 2017. Intrapopulational variation in color pattern of *Trichomycterus davisi* (Haseman, 1911) (Siluriformes: Trichomycteridae) corroborated by morphometrics and molecular analysis. **Zootaxa**, 4290 (3): 503–518.

Nei, M.; Maruyama T. & Chakraborty R. 1975. The Bottleneck Effect and Genetic Variability in populations. **Evolution,** 29: 1-10.

Nelson, G.J. & Platnick, N.I. 1981. Systematics and biogeography: cladistics and vicariance. New York, Columbia Univ. Press.

Nelson, L. A.; Wallman J. F. & Dowton, M. 2007. Using COI barcodes to identify forensically and medically important blowflies. **Medical and Veterinary Entomology**, 21:44–52.

Nixon, K.C. & Wheeler, Q. D. 1990. An amplification of the phylogenetic species concept. **Cladistics**, 6: 211–223.

Ochoa, L. E.; Silva, G.S.C.; Costa e Silva, G.J.; Oliveira C. & Datovo, A. 2017. New species of *Trichomycterus* (Siluriformes: Trichomycteridae) lacking pelvic fins from Paranapanema basin, southeastern Brazil. **Zootaxa**, 4319 (3): 550–560.

Ornelas-Garcia C.P.; Dominguez-Dominguez, O. & Doadrio, I. 2008. Evolutionary history of the fish genus *Astyanax* Baird & Girard (1854) (Actynopterigii, Characidae) in Mesoamerica reveals multiple morphological homoplasies. **BMC Evolutionary Biology**, 8 (340):1-17.

Perdices, A. Birmingham, E.; Montilla, A. & Doadrio, I. 2002. Evolutionary history of the genus Rhamdia (Teleostei: Pimelodidae) in Central America. **Molecular Phylogenetics and Evolution**, 25:172–189.

Perdices, A.; Doadrio, I. & Bermingham, E. 2005. Evolutionary history of the synbranchid eels (Teleostei: Synbranchidae) in Central America and the Caribbean islands inferred from their molecular phylogeny. **Molecular Phylogenetics and Evolution,** 37:460–473.

Pereira, L.H.; Maia, G.M.; Hanner, R.; Foresti, F. & Oliveira, C. 2011a. DNA barcodes discriminate freshwater fishes from the Paraíba do Sul River Basin, São Paulo, Brazil. **Mitochondrial DNA**, 22(Suppl. 1):71–79.

Pereira, L.H.; Maia, G.M.; Hanner, R.; Foresti, F. & Oliveira, C. 2011b. DNA barcoding reveals hidden diversity in the Neotropical freshwater fish *Piabina argentea* (Characiformes: Characidae) from the Upper Paraná Basin of Brazil. Mitochondrial DNA, 22(Suppl. 1):87–96.

Pereira, L.H.; Maia, G.M.; Hanner, R.; Foresti, F. & Oliveira, C. 2013. Can DNA barcoding accurately discriminate megadiverse Neotropical freshwater fish fauna? **BMC Genetics**, 14(20):1-14.

Pfenninger, M.; Nowak, C.; Kley, C.; Steinke, D. & Streit, B. 2007. Utility of DNA taxonomy and barcoding for the inference of larval community structure in morphologically cryptic Chironomus (Diptera) species. **Molecular Ecology**, 16:1957–1968.

Pons, J. 2006. DNA-based identification of preys from nondestructive, total DNA extractions of predators using arthropod universal primers. **Molecular Ecology Notes**, 6:623–626.

Reis, R. E.; Kullander, S. O. & Ferraris Jr., C. J. 2003. **Check list of the freshwater fishes of South and Central America**. Porto Alegre, Edipucrs. 742p.

Roldi, M. M. C.; Sarmento-Soares, L.M.; Pinheiro, R.F.M. & Lopes, M.M. 2011. Os Trichomycterus das drenagens fluviais no Espírito Santo, Sudeste do Brasil (Siluriformes: Trichomycteridae). **Boletim Sociedade Brasiliera de Ictiologia**, São Paulo, 103:1-3.

Rosso, J.J.; Mabragaña, E.; Castro, M.G. & de Astarloa, J.M. 2012. DNA barcoding neotropical fishes: recent advances from the pampa plain. Argentina. **Molecular Ecology Resources**, 12: 999–1011. doi: 10.1111/1755-0998.12010

Rubinoff, D.; Cameron, S. & Will, K. 2006. A genomic perspective on the shortcomings of mitochondrial DNA for ‘‘barcoding’’ identification. **Journal of Heredity**, 97: 581–594.

Saccone, C.; DeCarla, G.; Gissi, C.; Pesole, G. & Reynes, A. 1999. Evolutionary genomics in the Metazoa: the mitochondrial DNA as a model system. **Gene**, 238: 195–210.

Sales, S.M.; Salvador, G.N.; Pessali, T.C. & Carvalho, D.C. 2018. Hidden diversity hampers conservation efforts in a highly impacted Neotropical river system. **Frontiers in Genetics**, 9(271):1-11. doi: 10.3389/fgene.2018.00271

Santos J. F. 2012. **Revisão taxonômica do gênero *Trichomycterus* Valenciennes, 1832 (Siluriformes: Trichomycteridae) no sitema da laguna dos Patos**. Dissertação de mestrado. Porto Alegre, Universidade Federal do Rio Grande do Sul. 122p.

Sarmento-Soares, L.M.; Martins-Pinheiro, R.F.; Aranda, A.T. & Chamon, C.C. 2005. *Trichomycterus pradensis*, a new catfish from Southern Bahia coastal rivers, northeastern Brazil (Siluriformes: Trichomycteridae). **Ichthyological Explorations of Freshwaters**, 16(4):289-302.

Sarmento-Soares, L. M.; Zanata, A.M. & Martins-Pinheiro, R.F. 2011. *Trichomycterus payaya*, new catfish (Siluriformes: Trichomycteridae) from headwaters of rio Itapicuru, Bahia, Brazil. **Neotropical Ichthyology**, 9(2):261-271.

Sato L. R.; Oliveira, C. & Foresti, F. 2004. Karyotype description of five species of *Trichomycterus* (Teleostei: Siluriformes: Trichomycteridae). **Genetics and Molecular Biology**, 27(1): 45-50.

Shum P.; Moore, L.; Pampoulie, C.; Di Muri, C.; Vandamme, S. & Mariani, S. 2017. Harnessing mtDNA variation to resolve ambiguity in 'Redfish' sold in Europe. **PeerJ**., 2:1–18. doi: 10.7717/peerj.3746.

Silva, C.C.F.; Matta, L.S.F.; Hilsdorf, A.W.S.; Langeani, F. & Marceniuk, A.P. 2010. Color pattern variation in *Trichomycterus iheringi* (Eigenmann, 1917) (Siluriformes: Tricomycteridae) from Rio Itatinga and Rio Claro, São Paulo, Brasil. **Neotropical Ichthyology**, 8 (1): 49–56.

Sullivan, C.; Bierman, P.R.; Reusser, L.; Pavich, M.; Larsen, J. & Finkel, R.C. 2007. Cosmogenic erosion rates and landscape evolution of the Blue Ridge escarpment, southern Appalachian Mountains. *In*: Geological Society of America (Ed.). Geological Society of America. **Abstracts with Programs**. Colorado Convetion Center. p. 512.

Taylor, R. & Van Dyke, C. C. 1985. Revised procedures for staining and clearing small fishes and other vertebrates for bone and cartilage study. **Cybium**, 9: 107-119.

Tchernavin, V.V. 1944. A revision of some Trichomycterinae based on material in the British Museum (Natural History). **Proceedings of the Zoological Society of London**, 114: 234–275.

Triques M. L. & Vono, V. 2004. Three new species of Trichomycterus (Teleostei: Siluriformes: Trichomycteridae) from the Rio Jequitinhonha basin, Minas Gerais, Brazil. **Ichthyological Exploration of Freshwaters**, 15(2): 161-172.

Uieda, V. S. & Castro, R. M. C. 1999. Coleta e fixação de peixes de riachos. *In*: Caramaschi, E. P.; Mazzoni, R. & Peres Neto, P. R. (Eds). **Ecologia de peixes de riachos**. Rio de Janeiro, PPGE-UFRJ. (Série Oecologia Brasiliensis, vol. 06)

Valdez-Moreno, M.; Ivanova, N.V.; Elías-Gutiérrez, M.; Contreras-Balderas, S. & Hebert, P.D. 2009. Probing diversity in freshwater fishes from mexico and Guatemala with DNA barcodes. **Journal of Fish Biology**, 74: 377-402. doi: 10.1111/j. 1095-8649.2008.02077.x

Vanacker, V.; von Blanckenburg, F. & Hewaeasam, T. 2007. Constraining landscape development of the Sri Lankan Escarpment with cosmogenic nuclides in river sediment. **Earth and Planetary Science Letters**, 253: 402–414.

Vari, R. P. & Malabarba L. R. 1998. Neotropical Ichthyology: an overview. *In*: Malabarba, L. R.; Reis, R. E.; Vari, R. P.; Lucena, Z. M. S. & Lucena, C. A. S. (Eds.). **Phylogeny and classification of neotropical Fishes**. Porto Alegre, Edipucrs. p. 1-11.

Vieira, F. 2010. Distribuição, impactos ambientais e conservação da fauna de peixes da bacia do rio Doce. **MG-Biota**, 2(5):5-22.

Vinas, J. & Tudela, S. 2009. A validated methodology for genetic identification of tuna species (Genus Thunnus). **PLoS One,** 4:e7606. doi: 10.1371/journal.pone. 0007606.

Volpi, T. A. 2017. **Filogeografia de Trichomycterus (Siluriformes: Trichomycteridae) na Mata Atlântica**. Espírito Santo, UFES, Centro de Ciências Humanas e Naturais. Phd thesis not published.

Ward, R.D. 2009. DNA barcode divergence within species and genera of birds and fishes. **Molecular Ecology Resources**, 9:1077–1085.

Ward, R.D.; Zemlak, T.S.; Innes, B.H.; Last, P.R. & Hebert, P.D. 2005. DNA barcoding Australia's fish species. **Philosophical Transactions of the Royal Society B: Biological Sciences**, 360 (1462): 1847-1857.

Ward, R. D.; Hanner, R.; Hebert, P. D. N. 2009. The campaign to DNA barcode all fishes, FISH-BOL. **Journal of Fish Biology**, 74:329–356.

Ward, M.N. 2010. **Análise molecular e morfológica de exemplares de *Trichomycterus* Valenciennes, 1832 da chapada dos Guimarães (Bacia do Paraguai) e ensaio sobre o complexo de espécies *Trichomycterus brasiliensis* Lütken, 1874**. Disertação de Mestrado. Botucatu, UNESP - Universidade Estadual Paulista, Instituto de Biociências, 2010.

Weitzman, S. H. 1974. Osteology and evolutionary relationships of the Sternoptychidae, with a new classification of stomiatoid families. **Bulletin of the American Museum of Natural History**, 153(3):327-478 .

Wosiacki, W. B. 2002. **Estudo das relações filogenéticas de Trichomycterinae (Teleostei, Siluriformes, Trichomycteridae) com uma proposta de classificação**. Tese de Doutorado. São Paulo, Universidade de São Paulo, 324p. [não publicada]

Wosiacki, W. B. 2004. New species of catfish genus *Trichomycterus* (Siluriformes, Trichomycteridae) from the headwaters of rio São Francisco basin, Brazil. **Zootaxa**, 592: 1 – 12.

Wosiacki, W. B. 2005. A new species of *Trichomycterus* (Siluriformes: Trichomycteridae) from south Brazil and redescription of T. iheringi (Eigenmann). **Zootaxa**, 1040: 49–64.

Wosiacki, W. B. & Garavello, J. C. 2004. Five new species of Trichomycterus from the rio Iguaçu (rio Paraná basin), southern Brazil (Siluriformes: Trichomycteridae). **Ichthyological Exploration of Freshwaters,** 15 (1): 1-16.

Yoo, H.S.; Eah, J.-Y.; Kim, J. S.; Kim, Y.-J.; Min, Mi-S; Paek, W. K.; Lee, H. & Kim, C-B. 2006. DNA barcoding Korean birds. **Molecules and Cells**, 22(3): 323–327.

Yu, S.C.S. & Quilang, J.P. 2014. Molecular Phylogeny of Catfishes (Teleostei: Siluriformes) in the Philippines Using the Mitochondrial Genes COI, Cyt b, 16S rRNA, and the Nuclear Genes Rag1 and Rag2. **Philippine Journal of Science**, 143 (2): 187-198.

Table list

Table 01. Cytochrome Oxydase Sub-unity I (COI) primer used to produce distance analyses among species of *Trichomycterus* in the Rio Doce and adjacent basins in this dissertation.

Gene	Primer	Sequence (5'-3')	Literature
COI	FISH F1	TCA ACC AAC CAC AAA GAC ATT GGC AC	Ward *et al*., 2005
	FISH R2	TAG ACT TCT GGG TGG CCA AAG AAT CA	

Table 02. *Trichomycterus* specimens which the COI gene was successfully sequenced and used in this dissertation. Abbreviation: **URD**, upper Rio Doce; **MRD**, middle Rio Doce; **LRD**, lower Rio Doce; **MZUSP**, Museu de Zoologia da Universidade de São Paulo; **MZUFV**, Museu de Zoologia João Moojen da Universidade Federal de Viçosa; **MBML**, Museu de Biologia Melo Leitão; **UNESP**, Universidade Estadual Paulista; **PUCMG**, Pontifícia Universidade Católica de Minas Gerais; **MNRJ**, Museu Nacional do Rio de Janeiro.

#	Sample	Taxon	Drainage	Coordenades	Institution
1	MZUSP121709_CE3	*Trichomycterus alternatus*	Middel_Rio Doce	19°25'0.42"S 42°43'20.68"W	MZUSP
2	MZUSP121709_CE4	*Trichomycterus alternatus*	Middel_Rio Doce	19°25'0.42"S 42°43'20.68"W	MZUSP
3	MBML6822_AA80	*Trichomycterus alternatus*	Lower_Rio Doce	19°50'20,7"S 40°34'04,3"W	MBML
4	MBML6822_AA81	*Trichomycterus alternatus*	Lower_Rio Doce	19°50'20,7"S 40°34'04,3"W	MBML
5	MBML6822_AA86	*Trichomycterus alternatus*	Lower_Rio Doce	19°50'20,7"S 40°34'04,3"W	MBML
6	MBML6841_AB14	*Trichomycterus alternatus*	Lower_Rio Doce	19°53'20,3"S 40°34'32,8"W	MBML
7	MBML6207_AB16	*Trichomycterus alternatus*	Lower_Rio Doce	19°50'26,0"S 40°37'47,3"W	MBML
8	MBML4438_AB32-3	*Trichomycterus alternatus*	Lower_Rio Doce	19°47'02,1"S 40°38'52,0"W	MBML
9	MBML7641_AD18	*Trichomycterus alternatus*	Lower_Rio Doce	20°11'42"S 41°03'43"W	MBML
10	MBML7641_AD19	*Trichomycterus alternatus*	Lower_Rio Doce	20°11'42"S 41°03'43"W	MBML
11	MBML7641_AD20	*Trichomycterus alternatus*	Lower_Rio Doce	20°11'42"S 41°03'43"W	MBML

12	MBML7642_AD21-1	*Trichomycterus alternatus*	Lower_Rio Doce	20°10'59"S 41°04'46"W	MBML
13	MBML7642_AD22-2	*Trichomycterus alternatus*	Lower_Rio Doce	20°10'59"S 41°04'46"W	MBML
14	MBML7642_AD23	*Trichomycterus alternatus*	Lower_Rio Doce	20°10'59"S 41°04'46"W	MBML
15	MBML7665_AD24-1	*Trichomycterus alternatus*	Lower_Rio Doce	19°13'00"S 40°52'01"W	MBML
16	MBML7665_AD25-2	*Trichomycterus alternatus*	Lower_Rio Doce	19°13'00"S 40°52'01"W	MBML
17	MBML7665_AD26-3	*Trichomycterus alternatus*	Lower_Rio Doce	19°13'00"S 40°52'01"W	MBML
18	MBML7672_AD27	*Trichomycterus alternatus*	Lower_Rio Doce	19°13'46"S 40°48'52"W	MBML
19	MBML7672_AD29-3	*Trichomycterus alternatus*	Lower_Rio Doce	19°13'46"S 40°48'52"W	MBML
20	MBML7681_AD30-1	*Trichomycterus alternatus*	Lower_Rio Doce	19°52'57"S 40°41'24"W	MBML
21	MBML7681_AD31-2	*Trichomycterus alternatus*	Lower_Rio Doce	19°52'57"S 40°41'24"W	MBML
22	MBML6207_AG16-A	*Trichomycterus alternatus*	Lower_Rio Doce	19°50'26,0"S 40°37'47,3"W	MBML
23	MBML6207_AG17-B	*Trichomycterus alternatus*	Lower_Rio Doce	19°50'26,0"S 40°37'47,3"W	MBML
24	MBML6210_AG20-A	*Trichomycterus alternatus*	Lower_Rio Doce	19°52'41,6"S 40°36'48,5"W	MBML
25	MBML6210_AG21-B	*Trichomycterus alternatus*	Lower_Rio Doce	19°52'41,6"S 40°36'48,5"W	MBML

26	MBML6210_AG22	*Trichomycterus alternatus*	Lower_Rio Doce	19°52'41,6"S 40°36'48,5"W	MBML
27	MBML6210_AG23-A	*Trichomycterus alternatus*	Lower_Rio Doce	19°52'41,6"S 40°36'48,5"W	MBML
28	MBML6211_AG24-B	*Trichomycterus alternatus*	Lower_Rio Doce	19°53'49,2"S 40°36'10,9"W	MBML
29	MBML6211_AG25	*Trichomycterus alternatus*	Lower_Rio Doce	19°53'49,2"S 40°36'10,9"W	MBML
30	MBML6833_AG80	*Trichomycterus alternatus*	Lower_Rio Doce	19°53'04,4"S 40°34'30"W	MBML
31	MBML6833_AG81	*Trichomycterus alternatus*	Lower_Rio Doce	19°53'04,4"S 40°34'30"W	MBML
32	MBML6833_AG82	*Trichomycterus alternatus*	Lower_Rio Doce	19°53'04,4"S 40°34'30"W	MBML
33	MBML8191_AN76-2	*Trichomycterus alternatus*	Lower_Rio Doce	20°22'10,4"S 41°51'28,4"W	MBML
34	MBML8191_AN77-3	*Trichomycterus alternatus*	Lower_Rio Doce	20°22'10,4"S 41°51'28,4"W	MBML
35	MBML8191_AN78-4	*Trichomycterus alternatus*	Lower_Rio Doce	20°22'10,4"S 41°51'28,4"W	MBML
36	MBML8426_AP79-2	*Trichomycterus alternatus*	Lower_Rio Doce	19°57'52,5"S 40°44'20,4"W	MBML
37	MBML8426_AP80-3	*Trichomycterus alternatus*	Lower_Rio Doce	19°57'52,5"S 40°44'20,4"W	MBML
38	MBML8426_AP81-5	*Trichomycterus alternatus*	Lower_Rio Doce	19°57'52,5"S 40°44'20,4"W	MBML
39	MZUSP121709_CE2	*Trichomycterus alternatus*	Middle_Rio Doce	19°25'0.42"S 42°43'20.68"W	MZUSP

40	LBP12259_52186	*Trichomycterus alternatus*	Upper Rio Doce	21°09'09.7"S 43°31'37.9" W	UNESP
41	MBML6822_BC88	*Trichomycterus alternatus*	Lower_Rio Doce	19°50'20,7"S 40°34'04,3"W	MBML
42	MBML6822_BC89	*Trichomycterus alternatus*	Lower_Rio Doce	19°50'20,7"S 40°34'04,3"W	MBML
43	MBML6822_BD00	*Trichomycterus alternatus*	Lower_Rio Doce	19°50'20,7"S 40°34'04,3"W	MBML
44	MBML6822_BD001	*Trichomycterus alternatus*	Lower_Rio Doce	19°50'20,7"S 40°34'04,3"W	MBML
45	MZUSP121719_MZICT278	*Trichomycterus alternatus*	Middle Rio Doce	19°19'20.24"S 42°31'38.49"W	MZUSP
46	LBP8350_40416	*Trichomycterus alternatus*	Middle Rio Doce	19°40'53.8"S 43°00'50.1"W	UNESP
47	MZUSP121719_MZICT277	*Trichomycterus alternatus*	Middle Rio Doce	19°19'20.24"S 42°31'38.49"W	MZUSP
48	LBP12259_52186	*Trichomycterus alternatus*	Upper Rio Doce	21°09'09.7"S 43°31'37.9"W	UNESP
49	MZUSP121719_MZICT275	*Trichomycterus alternatus*	Middle Rio Doce	19°19'20.24"S 42°31'38.49"W	MZUSP
50	LBP8350_40415	*Trichomycterus alternatus*	Middle Rio Doce	19°40'53.8'S 43°00'50.1"W	UNESP
51	MZUSP121719_MZICT279	*Trichomycterus alternatus*	Middle Rio Doce	19°19'20.24"S 42°31'38.49"W	MZUSP
52	LBP12259_52190	*Trichomycterus alternatus*	Upper Rio Doce	21°09'09.7"S 43°31'37.9"W	UNESP
53	LBP12259_52189	*Trichomycterus alternatus*	Upper Rio Doce	21°09'09.7"S 43°31'37.9"W	UNESP

54	LGC3708	*Trichomycterus alternatus*	Middle Rio Doce	18º 57' 13" S 43º 26' 21" W	PUCMG
55	LGC5720	*Trichomycterus alternatus*	Middle Rio Doce	18° 48' 50" S 43° 24' 50" W	PUCMG
56	LGC5727	*Trichomycterus alternatus*	Middle Rio Doce	18° 46' 01" S 43° 25' 33" W	PUCMG
57	LGC5778	*Trichomycterus alternatus*	Middle Rio Doce	18° 55' 59" S 43° 26' 48" W	PUCMG
58	LGC5779	*Trichomycterus alternatus*	Middle Rio Doce	18° 55' 59" S 43° 26' 48" W	PUCMG
59	LGC5790	*Trichomycterus alternatus*	Middle Rio Doce	18° 55' 29" S 43° 27' 57" W	PUCMG
60	LGC5798	*Trichomycterus alternatus*	Middle Rio Doce	18° 59' 22" S 43° 22' 58" W	PUCMG
61	LGC5799	*Trichomycterus alternatus*	Middle Rio Doce	18° 59' 22" S 43° 22' 58" W	PUCMG
62	MBML6841_AB15	*Trichomycterus alternatus*	Lower_Rio Doce	19°53'20,3"S 40°34'32,8"W	MBML
63	MNRJ50893	*Trichomycterus alternatus*	Middle Rio Doce	18°21'20.00"S 43°10'12.00"W	MNRJ
64	MZUSP123357_I	*Trichomycterus alternatus*	Middle Rio Doce	18°56'2.50"S 42° 5'2.18"W	MZUSP
65	MZUSP123357_III	*Trichomycterus alternatus*	Middle Rio Doce	18°56'2.50"S 42° 5'2.18"W	MZUSP
66	MZUSP123397_I	*Trichomycterus alternatus*	Middle Rio Doce	19°51'20.22"S, 42° 8'24.63"O	MZUSP
67	MZUSP123397_II	*Trichomycterus alternatus*	Middle Rio Doce	19°51'20.22"S, 42° 8'24.63"O	MZUSP

68	MZUSP123761_I	*Trichomycterus alternatus*	Upper Rio Doce	20°14'13.05"S 42°56'53.65"W	MZUSP
69	MZUSP123763_VII	*Trichomycterus alternatus*	Upper Rio Doce	20°12'21.63"S 42°52'56.24"W	MZUSP
70	MZUSP123764_III	*Trichomycterus alternatus*	Upper Rio Doce	20°12'22.03"S 42°52'57.44"W	MZUSP
71	MZUSP123764_IV	*Trichomycterus alternatus*	Upper Rio Doce	20°12'22.03"S 42°52'57.44"W	MZUSP
72	MZUSP123764_V	*Trichomycterus alternatus*	Upper Rio Doce	20°12'22.03"S 42°52'57.44"W	MZUSP
73	MZUSP123764_VI	*Trichomycterus alternatus*	Upper Rio Doce	20°12'22.03"S 42°52'57.44"W	MZUSP
74	LBP12259_52188	*Trichomycterus alternatus*	Upper Rio Doce	21°09'09.7"S 43°31'37.9"W	UNESP
75	LGC5723	*Trichomycterus "astromycterus"*	Middle Rio Doce	18° 46' 33" S 43° 24' 34" W	PUCMG
76	LGC3017	*Trichomycterus "astromycterus"*	Middle_Rio Doce	18° 46' 33" S 43° 24' 34" W	PUCMG
77	LGC3018	*Trichomycterus "astromycterus"*	Middle_Rio Doce	18° 46' 33" S 43° 24' 34" W	PUCMG
78	MZUSP123361_I	*Trichomycterus "astromycterus"*	Middle Rio Doce	19°14'0.76"S 42°19'26.52"W	MZUSP
79	MZUSP123361_II	*Trichomycterus "astromycterus"*	Middle Rio Doce	19°14'0.76"S 42°19'26.52"W	MZUSP
80	MZUSP123361_III	*Trichomycterus "astromycterus"*	Middle Rio Doce	19°14'0.76"S 42°19'26.52"W	MZUSP
81	MZUSP123760_II	*Trichomycterus "astromycterus"*	Upper Rio Doce	20°11'40.32"S 42°51'8.47"W	MZUSP

82	MZUSP123760_III	*Trichomycterus "astromycterus"*	Upper Rio Doce	20°11'40.32"S 42°51'8.47"W	MZUSP
83	MZUSP123760_IV	*Trichomycterus "astromycterus"*	Upper Rio Doce	20°11'40.32"S 42°51'8.47"W	MZUSP
84	MZUSP123760_V	*Trichomycterus "astromycterus"*	Upper Rio Doce	20°11'40.32"S 42°51'8.47"W	MZUSP
85	MZUSP123365_IV	*Trichomycterus "astromycterus"*	Middle Rio Doce	19°14'0.76"S 42°19'26.52"W	PUCMG
86	MZUSP123365_V	*Trichomycterus "astromycterus"*	Middle Rio Doce	19°14'0.76"S 42°19'26.52"W	PUCMG
87	MZUFV3527_JD4057	*Trichomycterus brasiliensis*	São Francisco	-	MZUFV
88	MZUFV3527_JD4058	*Trichomycterus brasiliensis*	São Francisco	-	MZUFV
89	MZUFV3527_JD4059	*Trichomycterus brasiliensis*	São Francisco	-	MZUFV
90	MZUFV3527_JD4060	*Trichomycterus brasiliensis*	São Francisco	-	MZUFV
91	MZUFV 2565_JD1456	*Trichomycterus "tantalus"*	Upper Rio Doce	20° 9'32.47"S 42°24'9.57"W	MZUFV
92	MZUSP23369_MZICT3129	*Trichomycterus "tantalus"*	Middle Rio Doce	19° 1' 33.62"S 42° 7' 29.12"W	MZUSP
93	MZUSP23369_MZICT3130	*Trichomycterus "tantalus"*	Middle Rio Doce	19° 1' 33.62"S 42° 7' 29.12"W	MZUSP
94	MZUSP23369_MZICT3131	*Trichomycterus "tantalus"*	Middle Rio Doce	19° 1' 33.62"S 42° 7' 29.12"W	MZUSP
95	MZUSP121713_CL2	*Trichomycterus "melanopygius"*	Middle Rio Doce	19°23'42.63"S 42°42'51.30"W	MZUSP

96	MZUSP121713_CL4	*Trichomycterus "melanopygius"*	Middle Rio Doce	19°23'42.63"S 42°42'51.30"W	MZUSP
97	MZUSP123762_II	*Trichomycterus "melanopygius"*	Upper Rio Doce	20°12'21.63"S 42°52'56.24"W	MZUSP
98	LGC3687	*Trichomycterus "ipatinguensis"*	Middle Rio Doce	18° 58' 34" S 43° 22' 21" W	PUCMG
99	LGC3719	*Trichomycterus "ipatinguensis"*	Middle Rio Doce	18° 59' 22" S 43° 22' 58" W	PUCMG
100	LGC3721	*Trichomycterus "ipatinguensis"*	Middle Rio Doce	18° 58' 47" S 43° 23' 02" W	PUCMG
101	LGC5721	*Trichomycterus "ipatinguensis"*	Middle Rio Doce	18° 48' 50" S 43° 24' 50" W	PUCMG
102	LGC5736	*Trichomycterus "ipatinguensis"*	Middle Rio Doce	18° 58' 27" S 43° 22' 19" W	PUCMG
103	LGC5740	*Trichomycterus "ipatinguensis"*	Middle Rio Doce	18° 58' 27" S 43° 22' 19" W	PUCMG
104	LGC5745	*Trichomycterus "ipatinguensis"*	Middle Rio Doce	18° 58' 34" S 43° 22' 21" W	PUCMG
105	LGC5753	*Trichomycterus "ipatinguensis"*	Middle Rio Doce	18° 58' 40" S 43° 22' 26" W	PUCMG
106	LGC5797	*Trichomycterus "ipatinguensis"*	Middle Rio Doce	18° 59' 22" S 43° 22' 58" W	PUCMG
107	LGC3686	*Trichomycterus "ipatinguensis"*	Middle Rio Doce	18° 58' 27" S 43° 22' 19" W	PUCMG
108	MBML7503	*Trichomycterus pradensis*	Jucuruçu	16° 43' 48" S 40° 25' 48" W	MBML
109	MBML7512_I	*Trichomycterus pradensis*	Jucuruçu	16° 51' 00" S 40° 19' 48" W	MBML

110	MZUSP123750_IX	*Trichomycterus "vinnulus"*	Upper Rio Doce	20°12'21.63"S 42°52'56.24"W	MZUSP
111	MZUSP123750_VIII	*Trichomycterus "vinnulus"*	Upper Rio Doce	20°12'21.63"S 42°52'56.24"W	MZUSP
112	MZUSP123750_X	*Trichomycterus "vinnulus"*	Upper Rio Doce	20°12'21.63"S 42°52'56.24"W	MZUSP
113	MZUSP123750_XI	*Trichomycterus "vinnulus"*	Upper Rio Doce	20°12'21.63"S 42°52'56.24"W	MZUSP
114	MZUSP123750_XII	*Trichomycterus "vinnulus"*	Upper Rio Doce	20°12'21.63"S 42°52'56.24"W	MZUSP
115	MZUSP123757_I	*Trichomycterus "vinnulus"*	Upper Rio Doce	20°11'40.32"S 42°51'8.47"W	MZUSP
116	LGC3014	*Trichomycterus immaculatus*	Middle Rio Doce	19° 1'3.06"S 42° 7'16.31"W	PUCMG
117	LGC3015	*Trichomycterus immaculatus*	Middle Rio Doce	19° 1'3.06"S 42° 7'16.31"W	PUCMG
118	LGC3021	*Trichomycterus immaculatus*	Middle Rio Doce	19° 1'3.06"S 42° 7'16.31"W	PUCMG
119	CT505	*Trichomycterus immaculatus*	Upper Rio Doce	20°34'19.78"S 43° 0'35.10"W	MZUFV
120	CT506	*Trichomycterus immaculatus*	Upper Rio Doce	20°34'19.78"S 43° 0'35.10"W	MZUFV
121	CT527	*Trichomycterus immaculatus*	Upper Rio Doce	20°34'19.78"S 43° 0'35.10"W	MZUFV
122	CT555	*Trichomycterus immaculatus*	Upper Rio Doce	20°34'19.78"S 43° 0'35.10"W	MZUFV
123	CT556	*Trichomycterus immaculatus*	Upper Rio Doce	20°34'19.78"S 43° 0'35.10"W	MZUFV

124	CT575	*Trichomycterus immaculatus*	Upper Rio Doce	20°34'19.78"S 43° 0'35.10"W	MZUFV
125	MZUFV2565_JD1476	*Trichomycterus immaculatus*	Upper Rio Doce	20° 9'32.47"S 42°24'9.57"W	MZUFV
126	JD325	*Trichomycterus immaculatus*	Upper Rio Doce	20°41'26.64"S 42°37'8.09"W	MZUFV
127	MZUFV2953_JD431	*Trichomycterus immaculatus*	São Mateus	_	MZUFV
128	MZUSP123391_MZICT3105	*Trichomycterus immaculatus*	Middle Rio Doce	19° 1'3.06"S 42° 7'16.31"W	MZUSP
129	MZUSP123391_MZICT3106	*Trichomycterus immaculatus*	Middle Rio Doce	19° 1'3.06"S 42° 7'16.31"W	MZUSP
130	MZUSP123391_MZICT3107	*Trichomycterus immaculatus*	Middle Rio Doce	19° 1'3.06"S 42° 7'16.31"W	MZUSP
131	MZUSP123391_MZICT3111	*Trichomycterus immaculatus*	Middle Rio Doce	19° 1'3.06"S 42° 7'16.31"W	MZUSP
132	MZUSP123391_MZICT3112	*Trichomycterus immaculatus*	Middle Rio Doce	19° 1'3.06"S 42° 7'16.31"W	MZUSP
133	MZUSP123391_MZICT3116	*Trichomycterus immaculatus*	Middle Rio Doce	19° 1'3.06"S 42° 7'16.31"W	MZUSP
134	MZUSP123391_MZICT3117	*Trichomycterus immaculatus*	Middle Rio Doce	19° 1'3.06"S 42° 7'16.31"W	MZUSP
135	MZUSP123357_MZICT3134_II	*Trichomycterus immaculatus*	Middle Rio Doce	18°56'2.50"S 42° 5'2.18"W	MZUSP
136	MZUSP123357_MZICT3135_IV	*Trichomycterus immaculatus*	Middle Rio Doce	18°56'2.50"S 42° 5'2.18"W	MZUSP
137	MZUSP123357_MZICT3136_V	*Trichomycterus immaculatus*	Middle Rio Doce	18°56'2.50"S 42° 5'2.18"W	MZUSP

138	MZUSP123354_IV	*Trichomycterus immaculatus*	Middle Rio Doce	18°59'24.54"S 42°18'57.98"W	MZUSP
139	MZUSP123356_I	*Trichomycterus immaculatus*	Middle Rio Doce	18°57'10.39"S 42°21'39.81"W	MZUSP
140	MZUSP123356_II	*Trichomycterus immaculatus*	Middle Rio Doce	18°57'10.39"S 42°21'39.81"W	MZUSP
141	MZUSP123356_III	*Trichomycterus immaculatus*	Middle Rio Doce	18°57'10.39"S 42°21'39.81"W	MZUSP
142	MZUSP123762_I	*Trichomycterus immaculatus*	Upper Rio Doce	20°12'21.63"S 42°52'56.24"W	MZUSP
143	MZUFV 2565 _JD1474	*Trichomycterus immaculatus*	Upper Rio Doce	20° 9'32.47"S 42°24'9.57"W	MZUFV
144	LGC3020	*Trichomycterus immaculatus*	Middle Rio Doce	_	PUCMG
145	MBML7745_II	*Trichomycterus immaculatus*	Itaúnas	18° 11' 60" S 40° 02' 24" W	MBML
146	CZNC144_I	*Trichomycterus immaculatus*	São Mateus	18° 38' 24" S 40° 07' 12" W	CEUNES
147	LGC5732	*Trichomycterus "sordislutum"*	Middle Rio Doce	18° 45' 42" S 43° 25' 44" W	PUCMG
148	MZUSP123393_MZICT3132	*Trichomycterus* sp. 1	Middle Rio Doce	19° 1'3.06"S 42° 7'16.31"W	MZUSP
149	MZUSP123176_MZICT2661	*Trichomycterus* sp. 2	Cubatão	23°54'3.04"S 46°28'7.51"W	MZUSP
150	MZUSP123176_MZICT2662	*Trichomycterus* sp. 2	Cubatão	23°54'3.04"S 46°28'7.51"W	MZUSP
151	MZUSP123176_MZICT2663	*Trichomycterus* sp. 2	Cubatão	23°54'3.04"S 46°28'7.51"W	MZUSP

152	MZUSP123176_MZICT2670	*Trichomycterus* sp. 2	Cubatão	23°54'3.04"S 46°28'7.51"W	MZUSP

Table 03. Morphometric data of *Trichomycterus alternatus* based on comparative materials.

Trichomycterus alternatus Eignmann 1918				
	FMNH 58082 Holotype	Range (n = 658)	Mean	SD
Standard Length (mm)	65.6	66.61 - 33.3	46.2	-
% of standard length				
Anal fin base	8.4	9.65 - 6.70	8.4	0.8
Body depth	14.7	18.31 - 14.89	14.9	1.2
Caudal Peduncle depth	11.9	14.07 - 9.90	12.1	0.9
Dorsal fin base	10.2	13.00 - 8.16	10.8	1.2
First pectoral-fin length	18.7	17.18 - 12.41	14.3	1.3
Head length	17.7	20.65 -16.12	18.8	1.1
Preanal length	73.4	82.91 - 63.84	71.2	3.2
Predorsal length	66.4	70.29 - 55.44	63.4	3.4
Prepelvic length	54.4	70.86 - 52.82	56.9	5.1
% of head length				
Eye diameter	19.1	22.25 - 16.38	19.4	1.6
Interorbital width	26.4	31.62 - 21.59	26.3	2.9
Snouth length	50.7	57.89 - 30.06	44.4	5.0
Width of mouth	50.8	47.90 -26.96	35.8	4.6

Table 04. Average of conspecific barcoding divergence average (%) within *Trichomycterus* species analyzed in this dissertation, based on the model Kimura-Two-Parameters (K2P) using the COI data matrix.

Taxon	**K2P distance**
T. alternatus	0.017
T. "astromycterus"	0.001
T. brasiliensis	0.000
T. "ipatinguensis"	0.002
T. immaculatus	0.002
T. "melanopygius"	0.003
T. "tantalus"	0.002
T. "sordislutum"	n/c
T. "vinnulus"	0.000
Trichomycterus sp. 1	n/c
Trichomycterus sp. 2	0.000

Table 05. Morphometric data of *Trichomycterus argos* based on type materials.

Trichomycterus argos Lezama *et al.*, 2012			
	Range (n = 03)	Mean	SD
Standard Length (mm)	56.1 - 90.8	71.72	-
% of standard length			
Anal fin base	7.76 - 8.84	8.2	0.6
Body depth	15 - 16.15	15.6	0.6
Caudal Peduncle depth	14.81 - 15.31	15.1	0.3
Dorsal fin base	9.61 - 10.46	10.0	0.4
First pectoral-fin length	11.32 - 12.49	11.9	0.6
Head length	20.67 - 20.91	20.8	0.1
Preanal length	71.31 - 72.25	71.8	0.5
Predorsal length	63.90 - 65.37	64.8	0.8
Prepelvic length	59.52 - 60.58	59.9	0.6
% of head length			
Eye diameter	8.93 -10.80	10.2	1.1
Interorbital width	23.59 - 25	24.3	0.7
Snouth length	41.92 - 45.87	44.0	2.0
Width of mouth	40.68 - 46.02	42.5	3.0

Table 06. Morphometric data of *Trichomycterus "astromycterus"*, sp. nov. based on type materials.

Trichomycterus "astromicterus", sp. nov.				
	MZUSP 123760			
	Holotype	Range (n = 12)	Mean	SD
Standard Length (mm)	51.98	51.98 - 29.33	35.7	-
% of standard length				
Anal fin base	9.0	12.22 - 6.88	9.3	1.8
Body depth	15.4	16.68 - 13.13	14.8	1.5
Caudal Peduncle depth	10.4	10.41 - 8.48	9.3	0.6
Dorsal fin base	13.5	14.87 - 11.70	13.4	1.1
First pectoral-fin length	15.2	16.64 - 11.63	14.9	1.8
Head length	21.7	24.38 - 20.84	22.3	1.3
Preanal length	69.5	73.41 - 69.44	71.3	1.6
Predorsal length	58.5	60.69 - 56.59	58.7	1.6
Prepelvic length	51.9	69.31 - 51.48	55.6	6.1
% of head length				
Eye diameter	24.2	21.69 - 17.59	19.7	1.4
Interorbital width	24.7	24.05 - 20.15	22.1	1.7
Snouth length	56.5	56.41 - 48.40	52.8	3.2
Width of mouth	44.6	39.60 - 33.88	38.7	4.9

Table 07. Morphometric data of *Trichomycterus "barrocus"*, sp. nov. based on type materials.

Trichomycterus "barrocus", sp. nov.				
	MBML 2238			
	Holotype	Range (n = 06)	Mean	SD
Standard Length (mm)	78.9	78.88 - 55.86	71.2	-
% of standard length				
Anal fin base	6.7	9.27 - 4.90	6.9	2.2
Body depth	11.6	13.85 - 8.97	11.5	2.4
Caudal Peduncle depth	11.3	11.30 - 10.10	10.7	0.6
Dorsal fin base	7.7	10.08 - 7.37	8.4	1.5
First pectoral-fin length	12.6	14.34 - 8.70	11.9	2.9
Head length	19.2	19.23 - 18.68	19.0	0.3
Preanal length	61.7	69.03 - 48.98	59.9	10.1
Predorsal length	54.8	60.69 - 41.20	52.2	10.0
Prepelvic length	47.2	52.51 - 41.87	47.2	5.3
% of head length				
Eye diameter	15.3	17.47 - 14.81	15.9	1.4
Interorbital width	28.4	28.40 - 24.95	26.7	1.7
Snouth length	47.0	49.35 - 46.37	47.6	1.6
Width of mouth	31.5	39.11 - 21.41	30.7	8.9

Table 08. Morphometric data of *Trichomycterus "brucutu"*, sp. nov. based on type materials.

Trichomycterus "brucutu", sp. nov.				
	MZUSP 87834			
	Holotype	Range (n = 03)	Mean	SD
Standard Length (mm)	103.03	103.3 - 24.66		-
% of standard length				
Anal fin base	8.9	8.9 - 8.5	8.7	0.3
Body depth	19.9	19.94 - 19	19.5	0.6
Caudal Peduncle depth	14.8	15 - 14.76	14.9	0.2
Dorsal fin base	10.8	11.18 - 10.79	11.0	0.0
First pectoral-fin length	11.2	13.49 - 1122	12.4	1.6
Head length	16.2	17.31 - 16.21	16.8	0.8
Preanal length	70.3	72.08 - 70.32	71.2	1.2
Predorsal length	58.1	64.6 - 58.1	61.4	4.6
Prepelvic length	58.0	57.96 - 56.67	57.3	0.9
% of head length				
Eye diameter	18.8	18.80 - 18.5	18.7	0.2
Interorbital width	30.3	31.38 - 30.3	30.8	0.8
Snouth length	52.6	59.29 - 52.63	56.0	4.7
Width of mouth	40.7	40.71 - 36.28	38.5	3.1

Table 09. Morphometric data of *Trichomycterus brunoi* Barbosa & Costa, 2010. based on comparative materials.

Trichomycterus brunoi Barbosa & Costa 2010			
	Range (n = 06)	Mean	SD
Standard Length (mm)	85.75 - 29.65	47.7	-
% of standard length			
Anal fin base	11.91 - 7.13	8.5	2.3
Body depth	15.32 - 10.53	12.7	2.3
Caudal Peduncle depth	15.10 - 9.97	13.3	1.8
Dorsal fin base	12.72 - 7.83	10.5	2.2
First pectoral-fin length	14.67 - 8.08	11.3	2.8
Head length	23.24 - 17.76	20.5	1.7
Preanal length	71.77 - 49.43	60.9	10.9
Predorsal length	68.80 - 46.29	56.9	11.5
Prepelvic length	58.46 - 41.42	50.1	9.5
% of head length			
Eye diameter	15.44 - 10.81	13.4	1.9
Interorbital width	27.71 - 19.95	26.1	2.9
Snouth length	41.17 - 28.03	39.5	4.9
Width of mouth	42.52 - 24.82	35.0	8.6

Table 10. Morphometric data of *Trichomycterus "illuvies"*, sp. nov. based on type materials.

Trichomycterus "illuvies", sp. nov				
	MZUSP 112750 Holotype	Range (n = 11)	Mean	SD
Standard Length (mm)	45.0	45.04 - 32.17	39.6	-
% of standard length				
Anal fin base	9.0	8.99 - 4.37	7.8	1.7
Body depth	16.4	17.19 - 13.89	15.7	1.2
Caudal Peduncle depth	13.9	13.88 - 11.13	12.6	1.1
Dorsal fin base	12.3	12.26 - 9.83	10.5	0.9
First pectoral-fin length	13.5	15.76 - 13.04	14.6	1.1
Head length	22.6	22.56 - 18.91	20.7	1.2
Preanal length	71.2	72.96 - 70.66	71.5	0.9
Predorsal length	62.9	65.93 - 61.58	63.7	1.5
Prepelvic length	53.5	55.23 - 51.92	54.1	1.1
% of head length				
Eye diameter	16.0	19.98 - 13.09	17.5	2.3
Interorbital width	24.7	30.06 - 24.70	26.4	1.9
Snouth length	38.8	52.61 - 38.78	45.7	4.0
Width of mouth	30.2	34.07 - 27.92	30.5	2.2

Table 11. Morphometric data of *Trichomycterus immaculatus* (Eigenmann & Eigenmann, 1889) based on type and comparative materials.

Trichomycterus immaculatus (Eigenmann & Eigenmann, 1889)									
	Rio Doce basin			Type material of *T. immaculatus*			Type material of *T. pradensis*		
	Range (n = 883)	Mean	SD	Range (n = 09)	Mean	SD	Range (n = 12)	Mean	SD
Standard Length (mm)	104.15 - 42.76	68.98	-	164.97 - 51.55	123.2	-	109.71 - 39.91	71.2	-
% of standard length									
Anal fin base	9.81 - 6.89	8.2	0.7	9.66 - 5.84	7.3	1.0	9.28 - 7.80	8.6	0.4
Body depth	16.98 - 11.56	14.3	1.4	17.86 - 14.09	16.7	1.2	16.39 - 13.48	15.3	0.9
Caudal Peduncle depth	14.12 - 10.60	12.0	0.9	14.85 - 11.30	13.8	1.0	13.36 - 10.81	12.4	0.8
Dorsal fin base	12.36 - 9.94	11.2	0.8	11.02 - 9.23	9.9	0.6	12.56 - 8.31	11.0	1.2
First pectoral-fin length	15.06 - 11.02	13.4	1.1	16.09 - 10.36	13.1	1.6	15.85 - 12.10	14.3	1.1
Head length	21.09 - 17.01	19.6	1.0	19.33 - 15.74	18.3	1.1	20.82 - 18.44	19.6	0.7
Preanal length	75.96 - 55.86	73.2	1.4	82.14 - 74.46	78.2	2.2	75.77 - 55.86	71.2	5.1
Predorsal length	64.61 - 60.19	62.4	1.1	67.68 - 61.47	64.9	2.2	65.89 - 59.18	62.4	1.8
Prepelvic length	58.01 - 52.04	55.1	1.7	63.29 - 55.87	61.1	2.0	57.87 - 50.78	54.2	1.9
% of head length									
Eye diameter	19.72 - 14.04	17.1	1.7	15.76 - 12.28	13.9	1.1	21.42 - 13.84	18.0	2.3
Interorbital width	26.69 - 19.47	23.5	2.0	34.75 - 26.84	30.9	2.9	27.35 - 21.07	24.0	1.8
Snouth length	50.39 - 39.76	46.5	2.8	49.42 - 43.44	46.6	2.2	50.90 - 44.44	47.8	1.8
Width of mouth	36.95 - 27.24	32.3	2.4	48.85 - 34.82	40.8	4.2	40.66 - 26.14	33.2	4.3

Table 12. Average of congeneric barcoding divergence (%) between *Trichomycterus* species analyzed in this dissertation, based on the Kimura-Two-Parameters (K2P) model using the COI data matrix.

#	Taxon	1	2	3	4	5	6	7	8	9	10
1	*T. immaculatus*										
2	*T. brasiliensis*	0.062									
3	*Trichomycterus* sp. 1	0.053	0.066								
4	*Trichomycterus*_sp._2	0.060	0.079	0.036							
5	*T. alternatus*	0.050	0.065	0.031	0.032						
6	*T. "astromycterus"*	0.048	0.062	0.027	0.032	0.014					
7	*T. "sordislutum"*	0.050	0.067	0.060	0.063	0.048	0.046				
8	*T. "tantalus"*	0.039	0.061	0.052	0.056	0.043	0.045	0.029			
9	*T. "ipatinguensis"*	0.038	0.048	0.040	0.043	0.034	0.032	0.026	0.018		
10	*T. "melanopygius"*	0.038	0.055	0.046	0.046	0.033	0.033	0.023	0.015	0.008	
11	*T. "vinnulus"*	0.054	0.073	0.038	0.033	0.019	0.020	0.051	0.048	0.038	0.031

Table 13. Morphometric data of *Trichomycterus "ipatinguensis"*, sp. nov. based on type and comparative materials.

Trichomycterus "ipatinguensis", sp. nov.				
	MZUSP 112279			
	Holotype	Range (n = 23)	Mean	SD
Standard Length (mm)	67.57	112.64 -24.21	50.57696	-
% of standard length				
Anal fin base	6.1	10.61 - 7.53	9.1	0.9
Body depth	11.1	16.04 - 13.17	14.9	0.9
Caudal Peduncle depth	9.7	14.5 - 11.1	12.8	1.1
Dorsal fin base	7.2	11.71 - 10.17	10.8	0.5
First pectoral-fin length	8.2	17.28 - 11.31	13.9	1.7
Head length	11.1	20.4 - 14	18.5	1.7
Preanal length	46.3	85.15 - 66.52	71.8	5.8
Predorsal length	41.9	66.11- 57.54	62.2	2.2
Prepelvic length	36.7	68.90 - 51.87	57.4	5.3
% of head length				
Eye diameter	1.9	24.01 - 13.62	16.3	3.6
Interorbital width	3.2	38.22 - 28.65	30.8	2.7
Snouth length	6.1	71.85 - 43.86	56.6	8.7
Width of mouth	4.2	53.83 - 34.51	43.8	5.3

Table 14. Morphometric data of *Trichomycterus "melanopygius"*, sp. nov. based on type and comparative materials.

Trichomycterus "melanopigyus", sp. nov.				
	MZUSP110936			
	Holotype	Range (n = 10)	Mean	SD
Standard Length (mm)	97.7	100.71 - 28.29	50.4	-
% of standard length				
Anal fin base	19.2	10.03 - 8.32	9.2	0.7
Body depth	12.4	17.06 - 11.7	14.3	1.7
Caudal Peduncle depth	13.5	13.74 - 9.35	12.0	1.4
Dorsal fin base	9.0	14.55 - 9.1	11.6	1.9
First pectoral-fin length	12.4	14.9 - 10.93	13.1	1.4
Head length	18.7	21.59 - 17.99	20.1	1.2
Preanal length	69.6	73.99 - 65.89	70.6	2.6
Predorsal length	62.1	68.32 - 53.09	62.8	4.4
Prepelvic length	55.2	59.69 - 51.06	55.6	3.0
% of head length				
Eye diameter	3.2	20.47 - 14.97	18.1	1.9
Interorbital width	4.5	27.01 - 22.74	25.6	1.4
Snouth length	10.0	51.89 - 43.38	47.1	2.7
Width of mouth	7.3	40 - 32.63	36.6	2.7

Table 15. Morphometric data of *Trichomycterus "pussilipygius"*, sp. nov. based on type materials.

Trichomycterus "pusillipigyus", sp. nov				
	MZUSP 123339			
	Holotype	Range (n = 11)	Mean	SD
Standard Length (mm)	68.6	68.64 - 23.89	40.4	-
% of standard length				
Anal fin base	8.1	8.43 - 6.45	7.8	0.6
Body depth	16.2	16.43 - 13.85	15.2	1.0
Caudal Peduncle depth	11.6	11.57 - 9.48	10.9	0.7
Dorsal fin base	9.8	12.69 - 9.16	10.4	1.2
First pectoral-fin length	12.5	16.40 - 11.57	13.1	1.6
Head length	16.6	18.81 - 16.61	17.6	1.0
Preanal length	72.5	73.23 - 69.15	71.4	1.4
Predorsal length	64.0	64.27 - 59.70	62.4	1.7
Prepelvic length	57.9	58.99 - 58.54	57.1	1.3
% of head length				
Eye diameter	17.8	21.56 - 16.59	18.9	1.8
Interorbital width	33.2	33.76 - 27.25	29.7	2.7
Snouth length	43.1	52.14 - 41.20	47.1	4.0
Width of mouth	37.2	43.11 - 29.98	35.7	4.5

Table 16. Morphometric data of *Trichomycterus "sordislutum"*, sp. nov. based on type materials.

Trichomycterus "sordislutum", sp. nov.				
	MZUSP 80309 Holotype	Range (n = 04)	Mean	SD
Standard Length (mm)	78.3	92.77 - 78.28	87.5	-
% of standard length				
Anal fin base	6.6	9.68 - 8.48	9.0	0.6
Body depth	12.6	17.8 - 15.68	16.6	0.9
Caudal Peduncle depth	8.9	15.38 - 11.33	12.7	1.8
Dorsal fin base	8.2	11.53 - 10.48	11.1	0.5
First pectoral-fin length	10.3	13.16 - 12.05	12.7	0.5
Head length	13.6	20.89 - 17.31	19.1	1.5
Preanal length	56.1	72.05 - 71.33	71.7	0.3
Predorsal length	47.9	63.72 - 61.00	62.3	1.4
Prepelvic length	41.4	55.38 - 52.87	54.1	1.2
% of head length				
Eye diameter	1.8	14.40 - 12.18	13.3	0.9
Interorbital width	3.8	28.04 - 23.48	25.7	1.9
Snouth length	6.6	52.73 - 46.18	49.6	2.8
Width of mouth	4.9	38.07 - 31.73	34.8	2.7

Table 17. Morphometric data of *Trichomycterus "tantalus"*, sp. nov. based on type materials.

Trichomycterus ""tantalus"", sp. nov				
	MZUSP 123369 Holotype	Range (n = 10)	Mean	SD
Standard Length (mm)	74.8	155 - 81.33	82.9	-
% of standard length				
Anal fin base	8.7	8.69 - 7.16	8.0	0.4
Body depth	14.5	17.20 - 13.27	14.4	1.2
Caudal Peduncle depth	10.7	12.53 - 9.40	10.5	0.9
Dorsal fin base	8.9	12.05 - 8.89	10.1	0.9
First pectoral-fin length	12.7	14.96 - 12.19	13.6	0.9
Head length	20.9	22.14 - 19.80	20.8	0.8
Preanal length	71.0	73.38 - 69.09	71.5	1.5
Predorsal length	62.1	64.45 - 57.42	60.8	2.3
Prepelvic length	53.4	56.30 - 50.60	53.7	1.6
% of head length				
Eye diameter	16.9	17.05 - 13.37	15.2	1.2
Interorbital width	24.0	27.33 - 23.42	25.1	1.2
Snouth length	45.8	51.37 - 42.98	45.4	2.3
Width of mouth	30.4	42.83 - 30.37	34.0	3.5

Table 18. Morphometric data of *Trichomycterus "vinnulus"*, sp. nov. based on type materials.

Trichomycterus "vinnulus", sp. nov				
	MZUSP123750			
	Holotype	Range (n = 10)	Mean	SD
Standard Length (mm)	55.8	60.96 - 21.21	49.7	-
% of standard length				
Anal fin base	8.0	9.52 - 6.64	7.7	0.9
Body depth	11.9	14.59 - 11.53	13.1	1.0
Caudal Peduncle depth	10.2	12.00 - 10.13	10.9	0.7
Dorsal fin base	10.8	12.23 - 8.69	10.8	1.1
First pectoral-fin length	14.3	15.21 - 10.50	12.9	1.5
Head length	19.3	21.23 - 18.26	19.6	1.0
Preanal length	69.1	73.45 - 69.08	71.7	1.5
Predorsal length	62.9	63.51 - 59.97	62.3	1.2
Prepelvic length	51.6	55.05 - 51.54	52.5	1.2
% of head length				
Eye diameter	22.1	22.91 - 18.55	21.2	1.4
Interorbital width	21.8	25.54 - 21.04	23.4	1.6
Snouth length	55.3	58.94 - 50.05	53.8	2.6
Width of mouth	35.5	40.52 - 30.38	35.9	3.0

Figure List

Fig. 01 – Hydrographic map of Rio Doce basin and the hydrographic region of Barra Seca river. Source: IBGE and Agência Nacional de Águas (ANA): Hidrografia e limites das bacias.

Fig. 02 – *Trichomycterus alternatus*, topotypes (right, lateral view; left, dorsal view): (A) MZUSP123764_IV, 42.97 mm SL; (B) MZUSP123764_III, 44,42 mm SL; (C) MZUSP123763, 45.42 mm SL; (D) MZUSP 123761, 50.98 mm SL. Brazil, State of Minas Gerais: Rio Doce municipality. Photos by V. J. C. Reis.

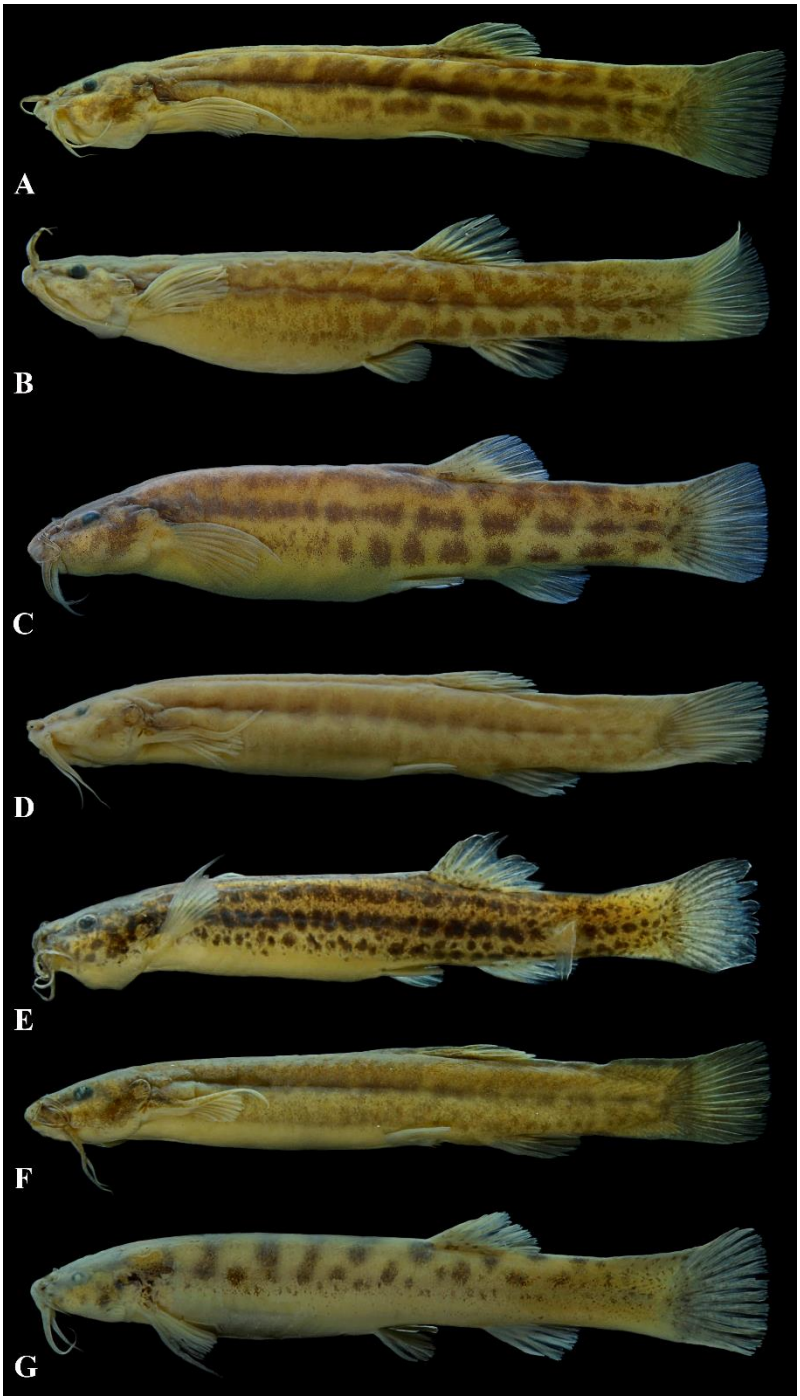

Fig. 03 – Color pattern and morphology variation in *Trichomycterus alternatus*: (A) MZUSP110937, 65.24 mm SL; (B) MZUSP87832, 58.18 mm SL; (C) MZUSP94564, 58.46 mm SL; (D) MZUSP109311, 49.30 mm SL; (E) MZUSP121719, 40.94 mm SL; (F) MZUSP 109302, 53.55 mm SL; (G) MBML6200, 47.00 mm SL. Photos by V. J. C. Reis.

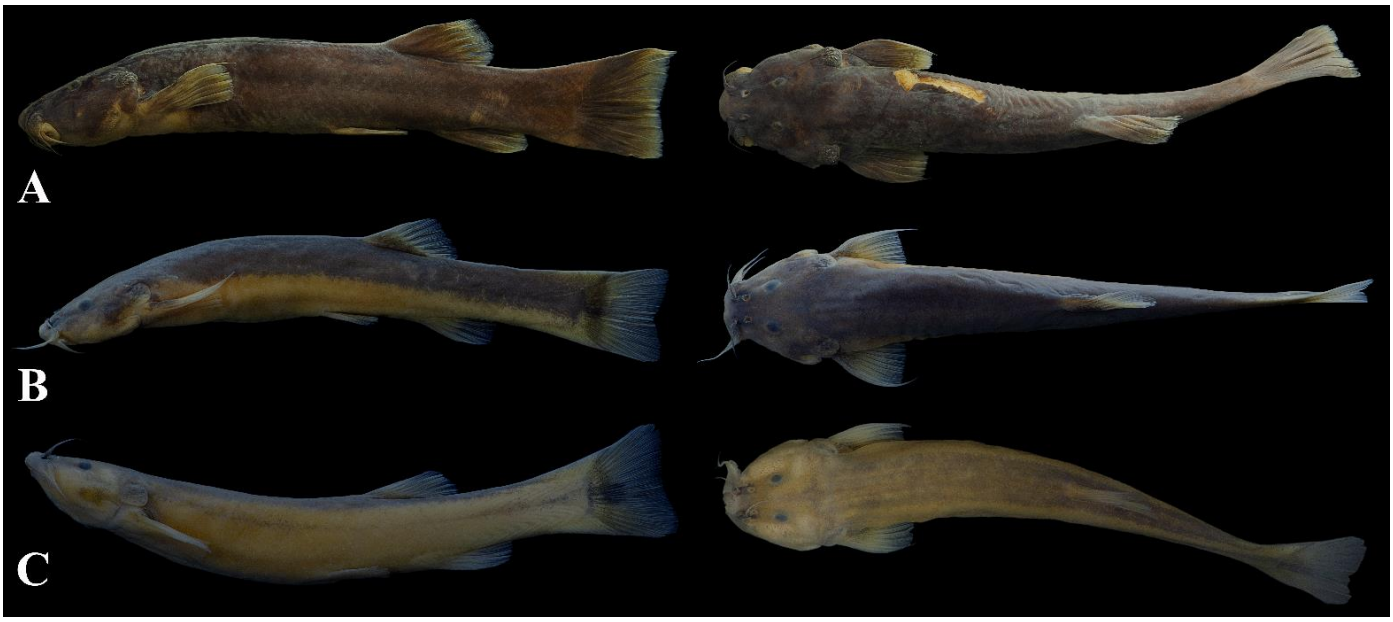

Fig. 04 – Color pattern and morphology variation in *Trichomycterus "tantalus"*, sp. nov. (right, lateral view; left, dorsal view): (A) MZUFV2565, 154.01 mm SL; (B) MZUSP123369 (holotype), 75.98 mm SL; (C), MZUSP123369, 74.82 mm SL. Photos by V.J. C. Reis.

Fig. 05 - Color pattern and morphology variation in *Trichomycterus "ipatinguensis"*, sp. nov. (right, lateral view; left, dorsal view): (A) MZUSP104702, 67.57 mm SL; (B) MZUSP 112277 92.86 mm SL; (C) MBML6223, 68.68 mm SL. Photos by V.J. C. Reis.

Fig. 06 - Color pattern and morphology variation in *T. immaculatus* as represented in paratypes of *Trichomycterus pradensis* (right, lateral view; left, dorsal view): (A) MNRJ28484, 48.44 mm SL; (B) MNRJ28485, 39.80 mm SL; (C) MNRJ28488, 67.42 mm SL; (D) MNRJ28490, 67.44 mm SL. Photos by V. J. C. Reis.

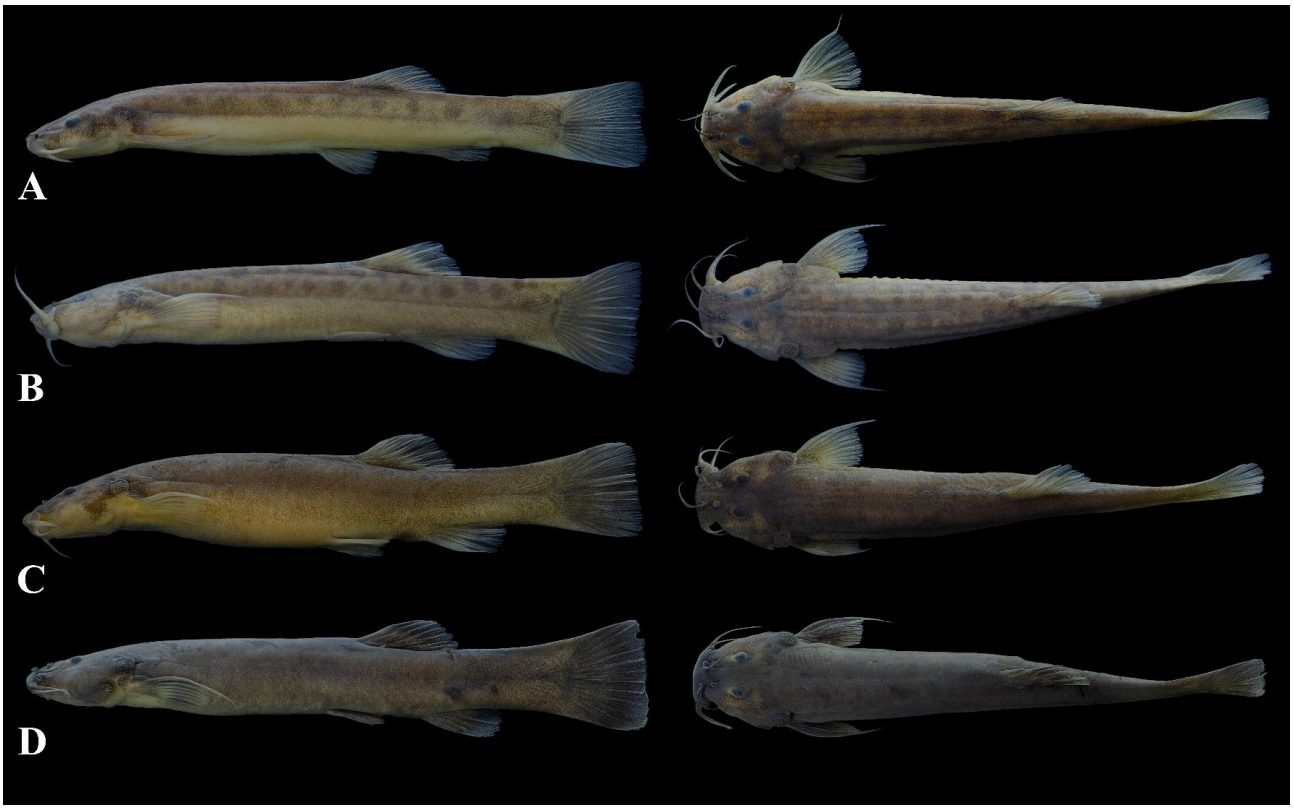

Fig. 07 - Color pattern and morphology variation in *Trichomycterus immaculatus* from the Rio Doce basin (right, lateral view; left, dorsal view): (A) MZUSP123368, 56.25 mm SL; (B) MZUSP123357, 69.41 mm SL; (C) MZUSP123762, 91.03 mm SL; MZUSP123353, 69.72 mm SL. Photos by V.J.C. Reis.

Fig. 08 - Color pattern and morphology variation in *Trichomycterus "pussilipygius"*, sp. nov. (A) MZUSP 123339, 33.69 mm SL; (B) MZUSP123339, 35.29 mm SL; (C) MZUSP123339, 70.04 mm SL. Photos by V.J. C. Reis.

Fig. 09 - Color pattern and morphology variation in *Trichomycterus "vinnulus"*, sp. nov. (right, lateral view; left, dorsal view): (A) MZUSP123750, 38.91 mm SL; (B) MZUSP123750, 47.07 mm SL; (C) MZUSP123750, 54.00 mm SL; (D) MZUSP123750, 60.60 mm SL. Photos by V.J.C. Reis.

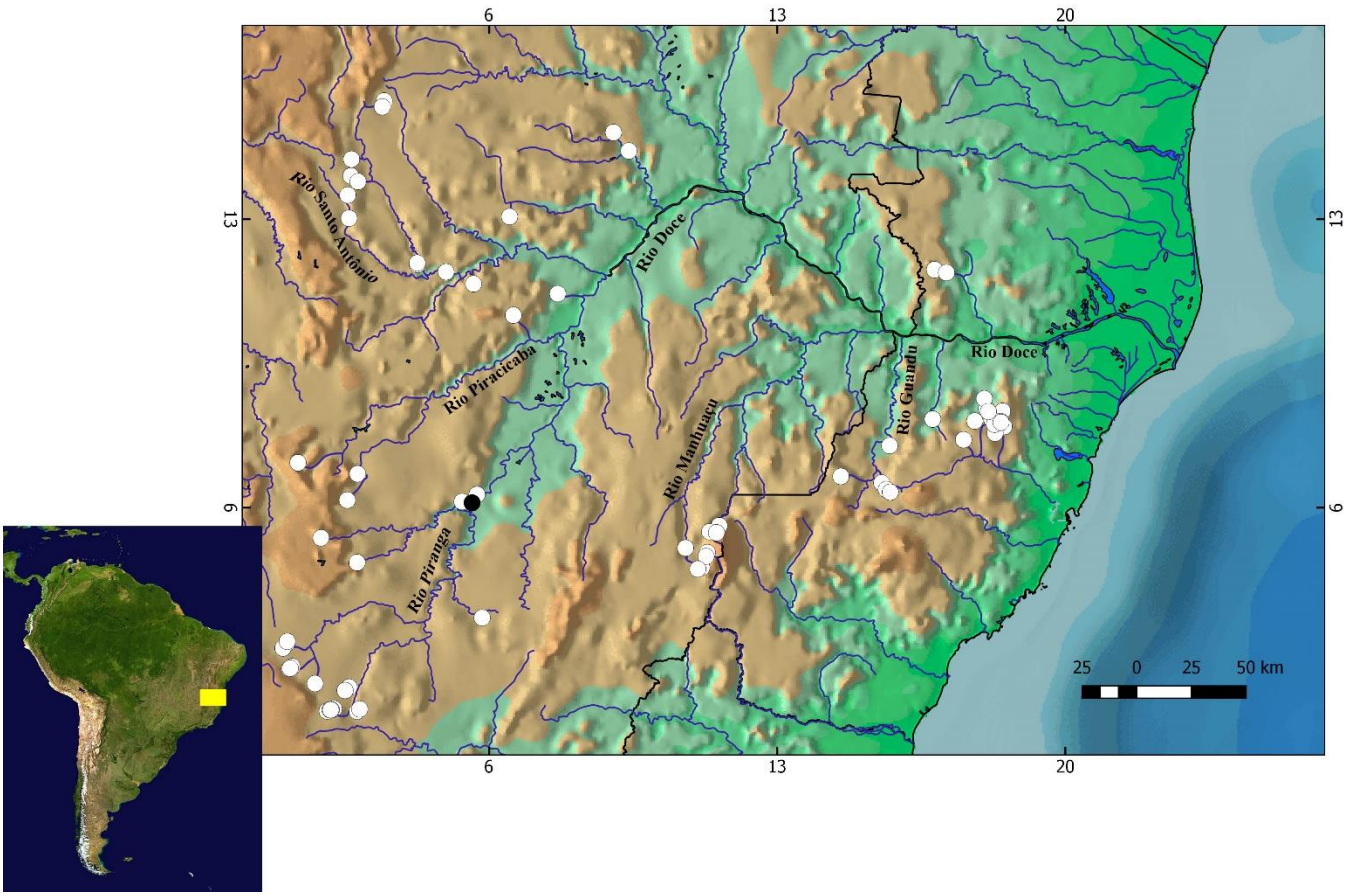

Fig. 10 – Geographical distribution of *Trichomycterus alternatus* in the Rio Doce basin; **Black circle** - type locality; **white circle** – non-type localities.

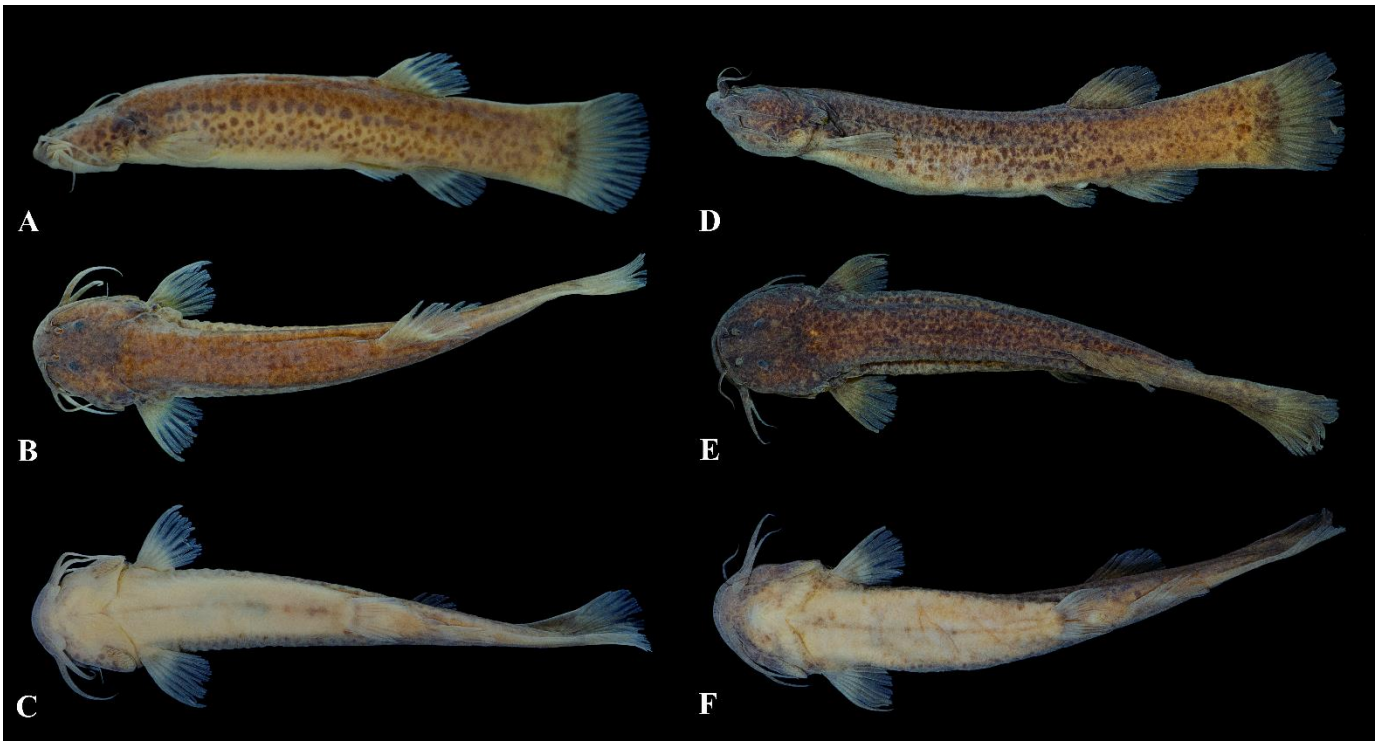

Fig. 11 – *Trichomycterus argos*. MZUSP 106274, paratype, (A, lateral; B, dorsal; C, ventral) 56.75 mm SL and (D, lateral; E, dorsal; F, ventral) 90.81 mm SL. Brazil, State of Minas Gerais: Araponga municipality, Parque Estadual da Serra do Brigadeiro. Photo by V.J.C. Reis.

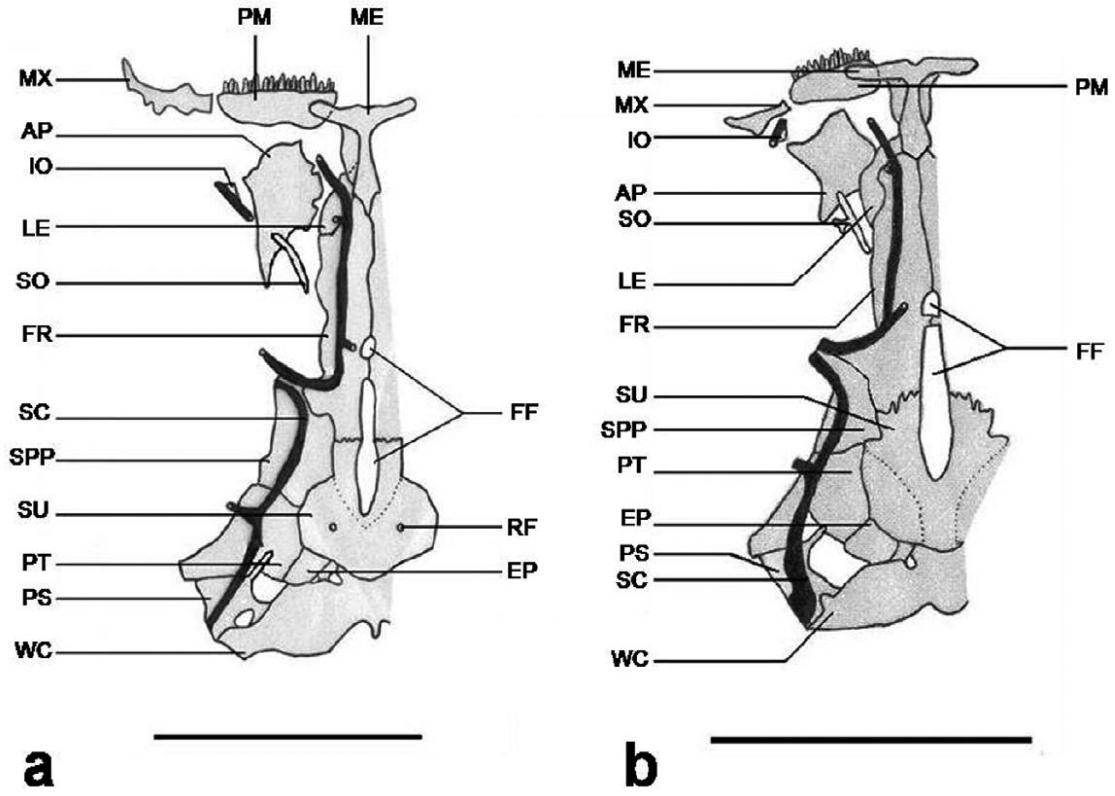

Fig. 12 - Dorsal views of the cranium and Weberian complex of a) *Trichomycterus argos* (DZUFMG 067, 101 mm SL, paratype) and b) *Trichomycterus brasiliensis* (DZUFMG 064, 102,1 mm SL). Abbreviations: **AP**, autopalatine; **EP**, epioccipital; **FF**, frontal fontanels; **FR**, frontal; **IO**, tendon-bone infraorbital; **LE**, lateral ethmoid; **ME**, mesethmoid; **MX**, maxilla; **PM**, premaxilla; **PS**, posttemporosupracleithrum; **PT**, pterotic; **RF**, foramen for the ramus lateralis accessorius facialis; **SC**, cephalic sensory canal; **SO**, tendon-bone supraorbital; **SPP**, sphenotic-prootic-pterosphenoid compound bone; **SU**, parietosupraoccipital; **WC**, Weberian capsule. Scale bar: 1cm. From Lezama *et al*., 2012.

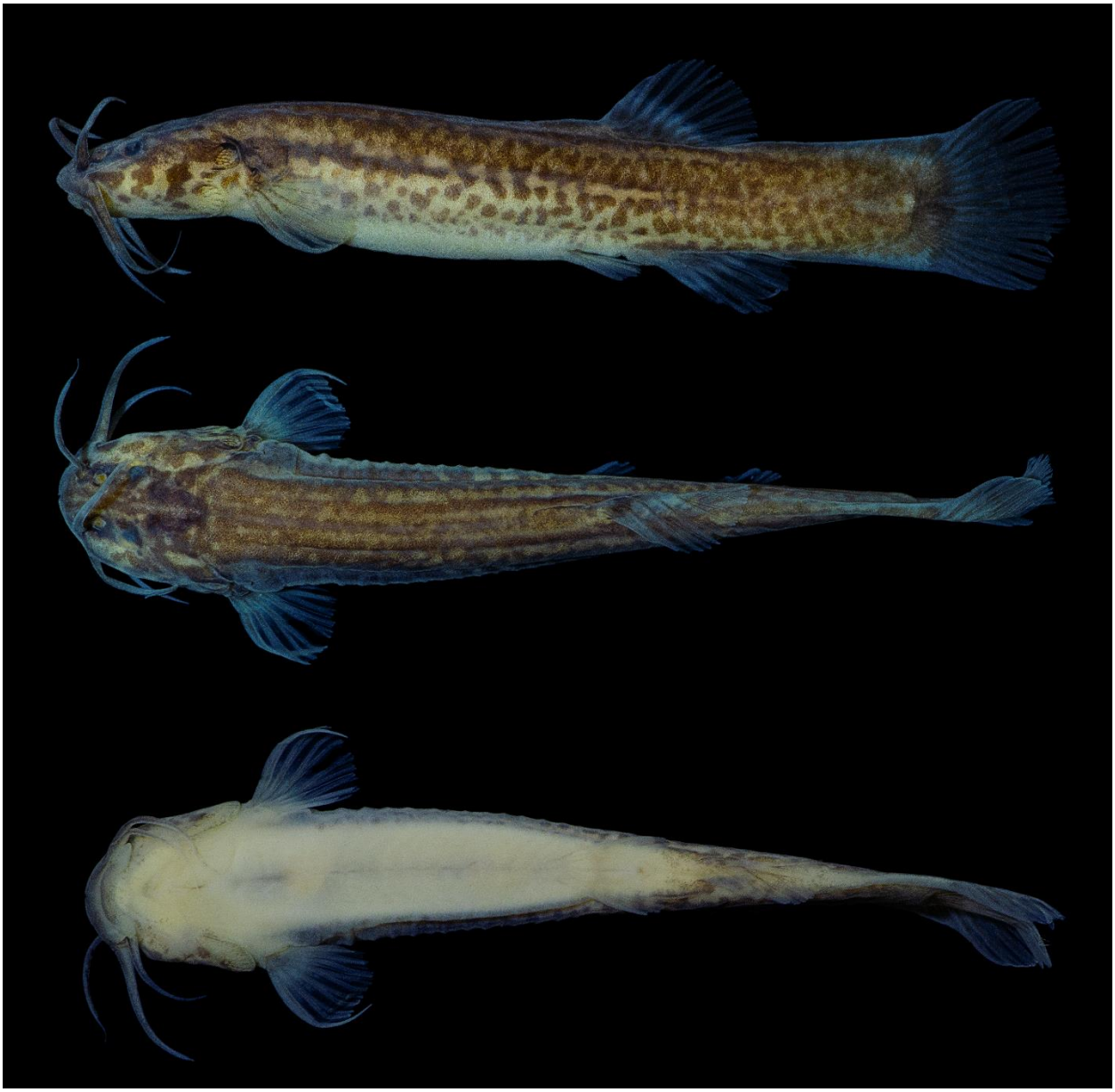

Fig. 13 – *Trichomycterus brunoi*. MBML4308, 41.83 mm SL. Brazil, State of Minas Gerais: Alto Caparaó. Photos by V.J.C.R Reis.

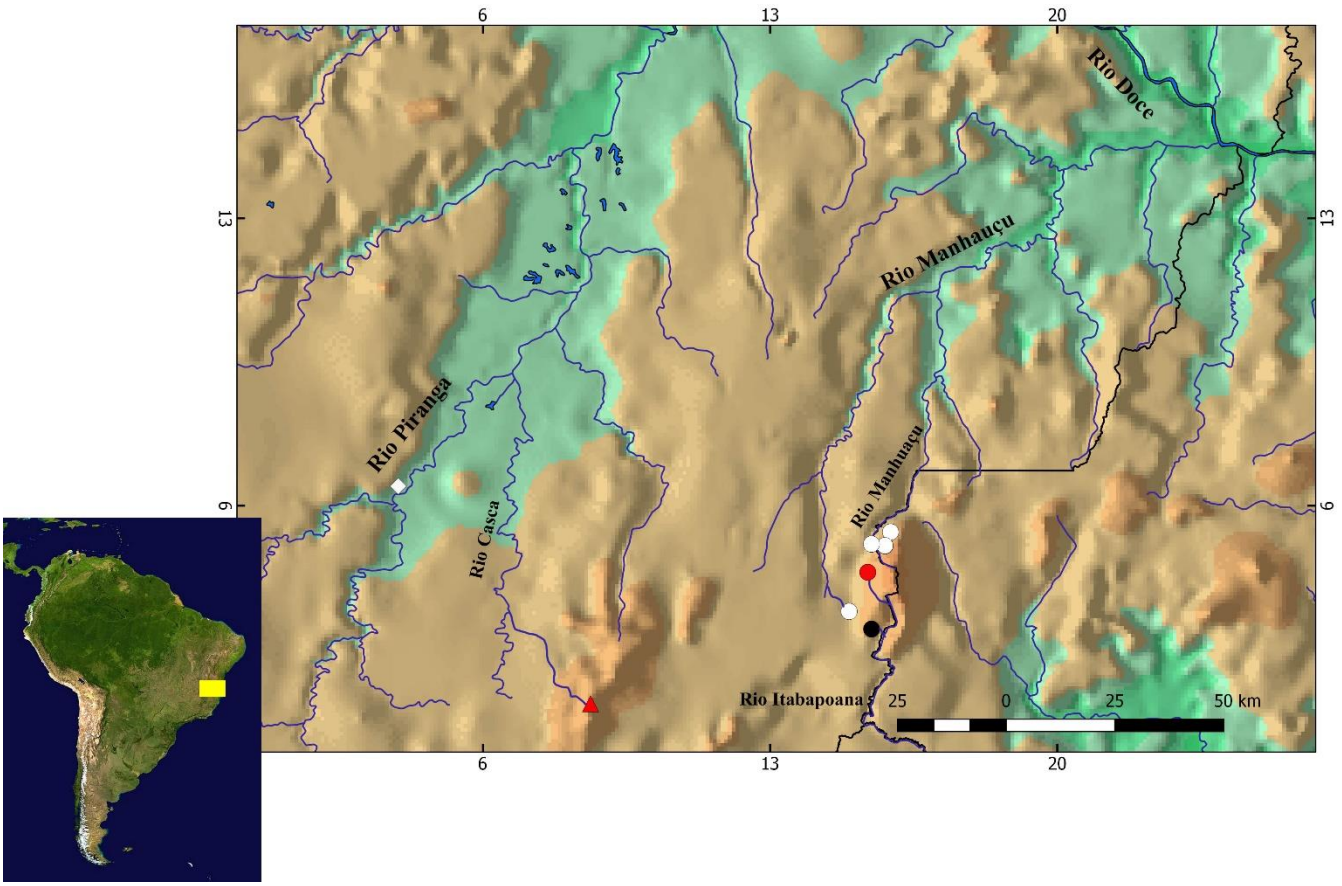

Fig. 14 - Geographical distribution of *Trichomycterus argos*, *Trichomycterus brasiliensis* and *T. brunoi* in the Rio Doce basin. **Red triangle -** type locality of *T. argos*; **white square -** non-type locality of *T. brasiliensis*; **red circle -** holotype and paratype locality of *T. brunoi*; **black circle -** paratype locality of *T. brunoi*; **white circle -** non-type localities of *T. brunoi*.

Fig. 15 – *Trichomycterus "astromycterus"*, sp. nov. MZUSP123760, holotype, 51.47 mm SL. Brazil, Minas Gerais: Rio Doce municipality. Photos by V.J.C. Reis.

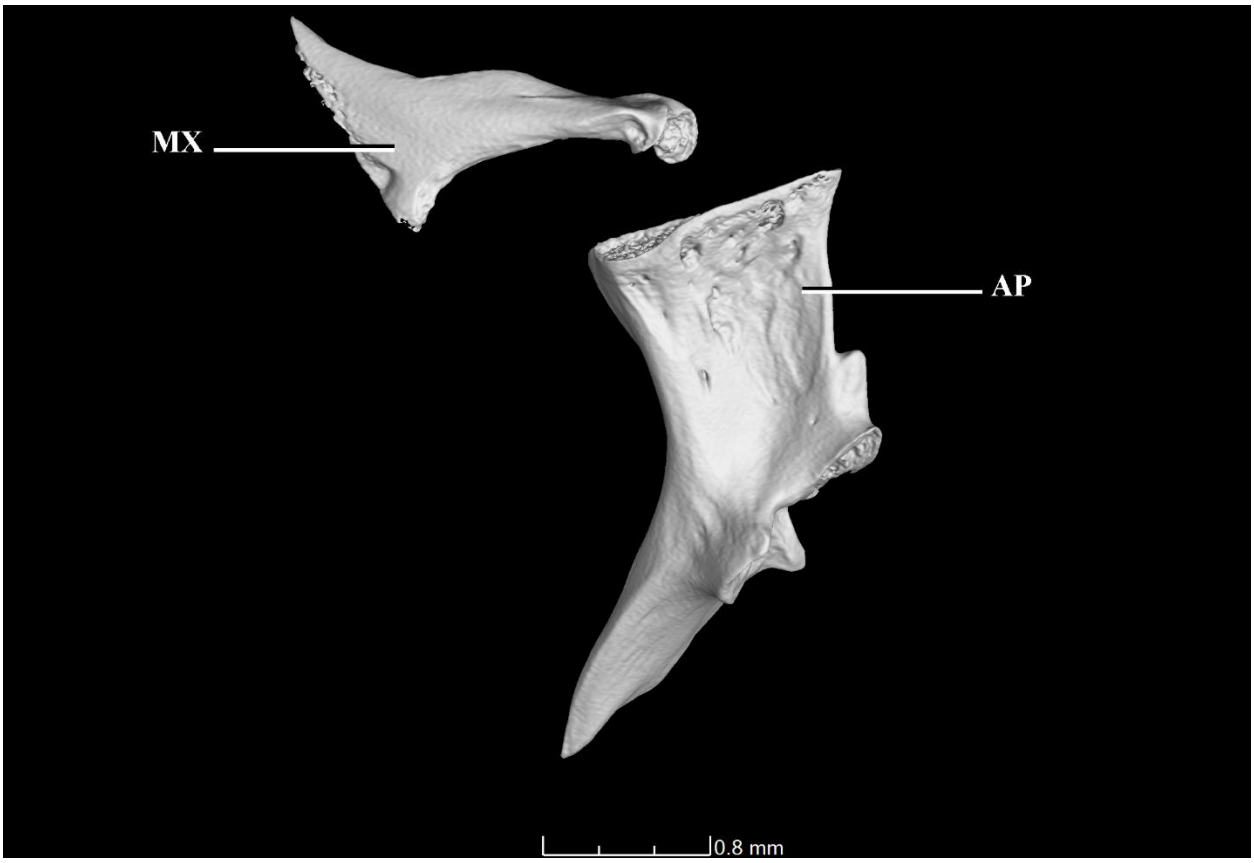

Fig. 16 – CT-Scan images of maxilla and palatine of *Trichomycterus "astromycterus"*, sp. nov., paratype, MZUSP123341; dorsal view, left side. Abbreviation: **MX,** maxila; **AP,** autopalatine.

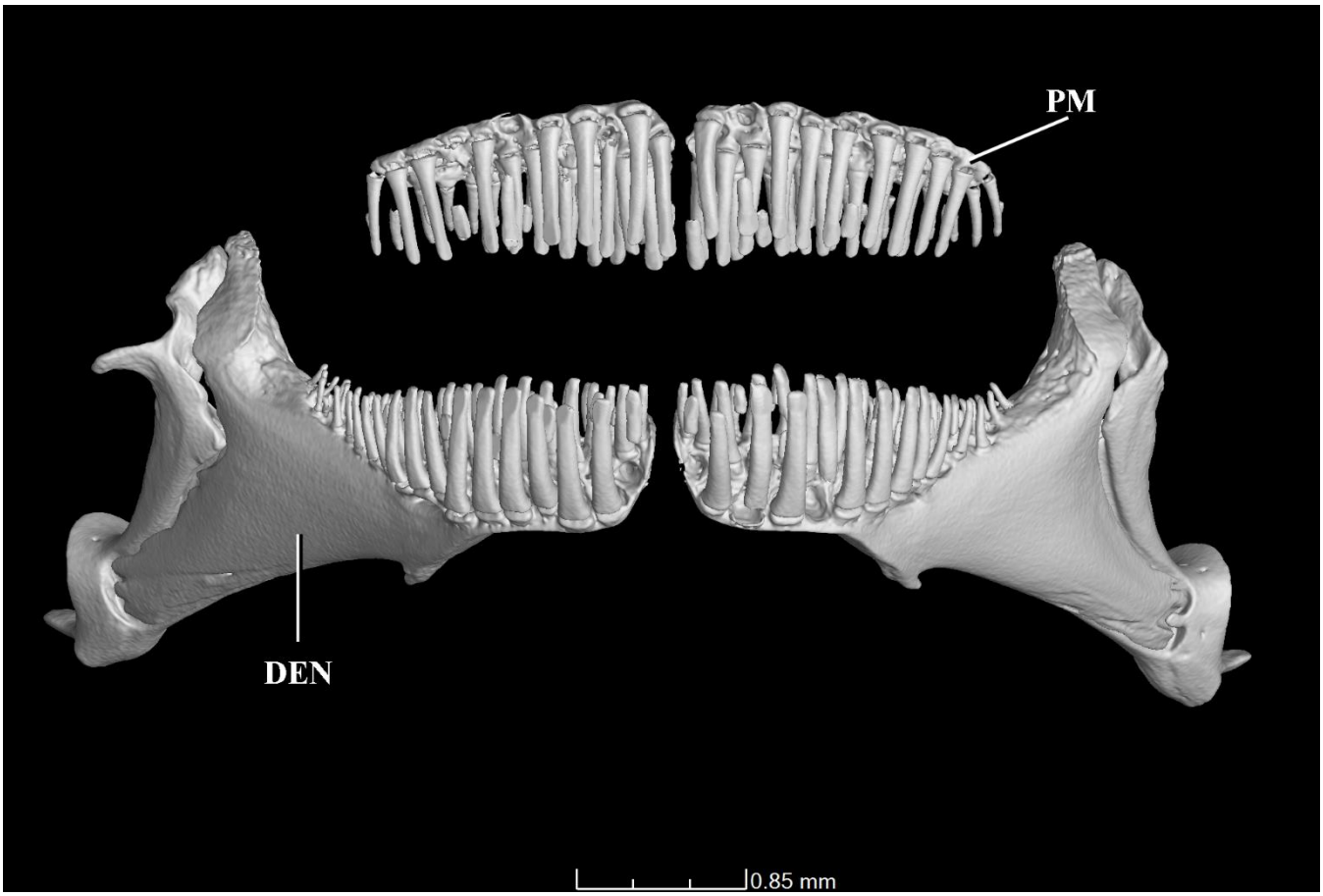

Fig. 17 – CT-Scan images of jaws of *Trichomycterus "astromycterus"*, sp. nov., paratype, MZUSP123341. Anteroventral view. Dentary teeth, first row mostly narrowly incisiform near symphysis, with remaining teeth conical. Abbreviation: **DEN**, dentary; **PM**, premaxilla.

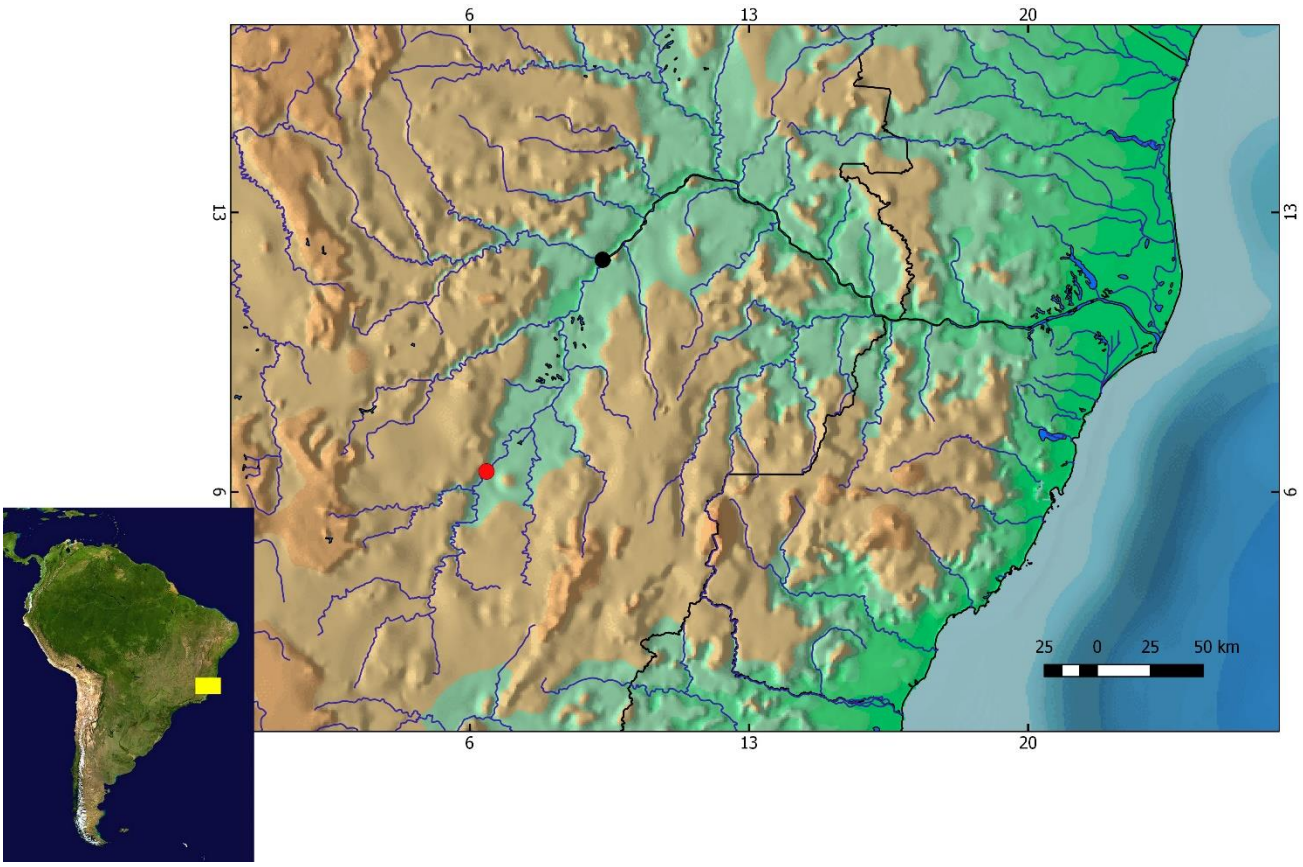

Fig. 18 - Geographical distribution of *Trichomycterus "astromycterus"*, sp. nov. in the Rio Doce basin. **Red circle** – holotype (MZUSP123760) and paratypes (ex-MZUSP123760); **black circle** - paratypes MZUSP 123341.

Fig. 19 – *Trichomycterus "barrocus"*, sp. nov. MBML2238, holotype, 79.83 mm SL. Brazil, State of Espírito Santo, Afonso Cláudio municipality. Photos by V.J.C. Reis.

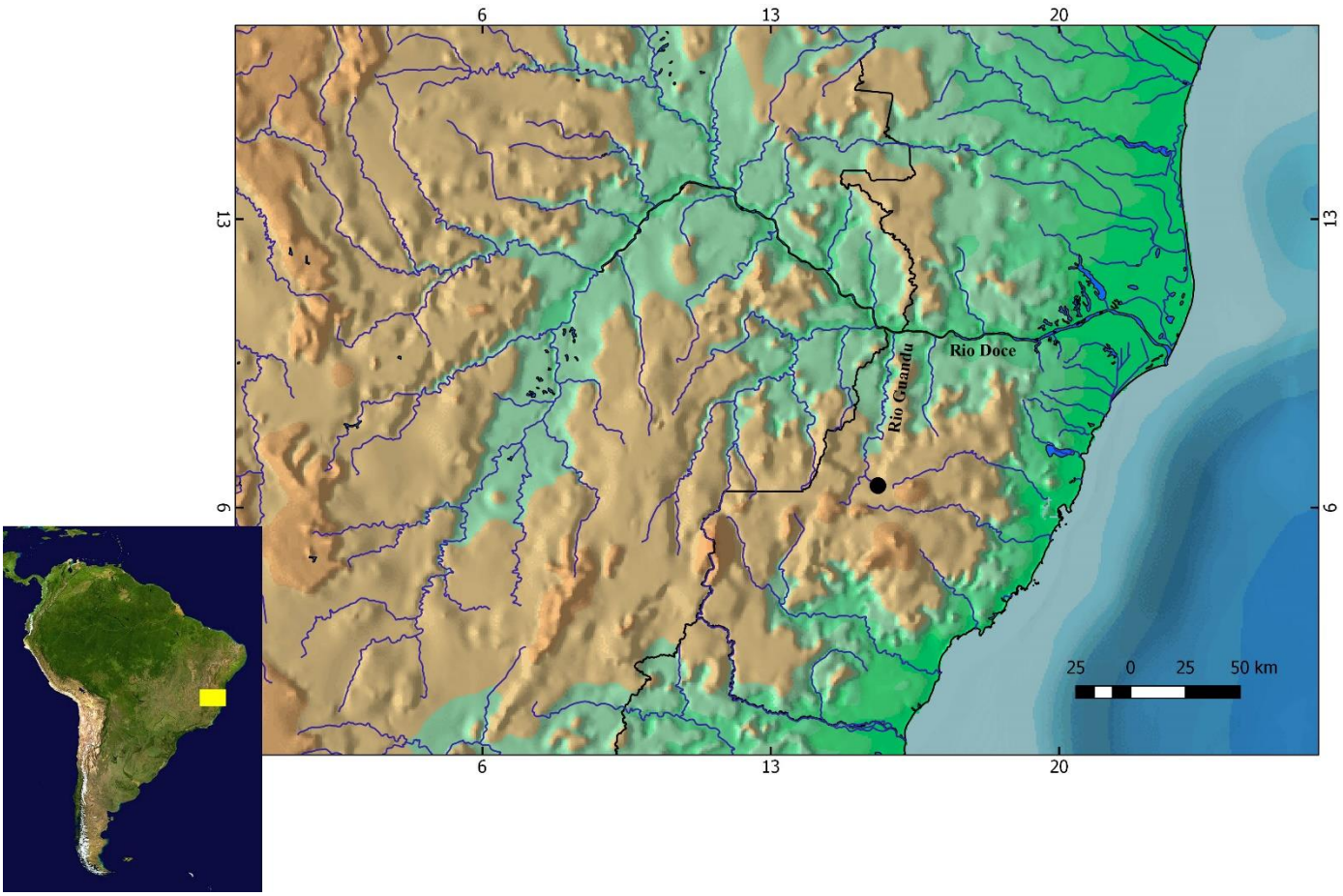

Fig. 20 – Geographical distribution of *Trichomycterus "barrocus"*, sp. nov. in the Rio Doce basin.

Black circle - holotype (MBML 2238) and paratypes (ex-MBML 2238).

Fig. 21 - *Trichomycterus "brucutu"*, sp. nov. MZUSP 87834, holotype, 103 mm SL. Brazil, State of Minas Gerais, Santo Antônio de Itambé municipality. Photo by V. J. C. Reis.

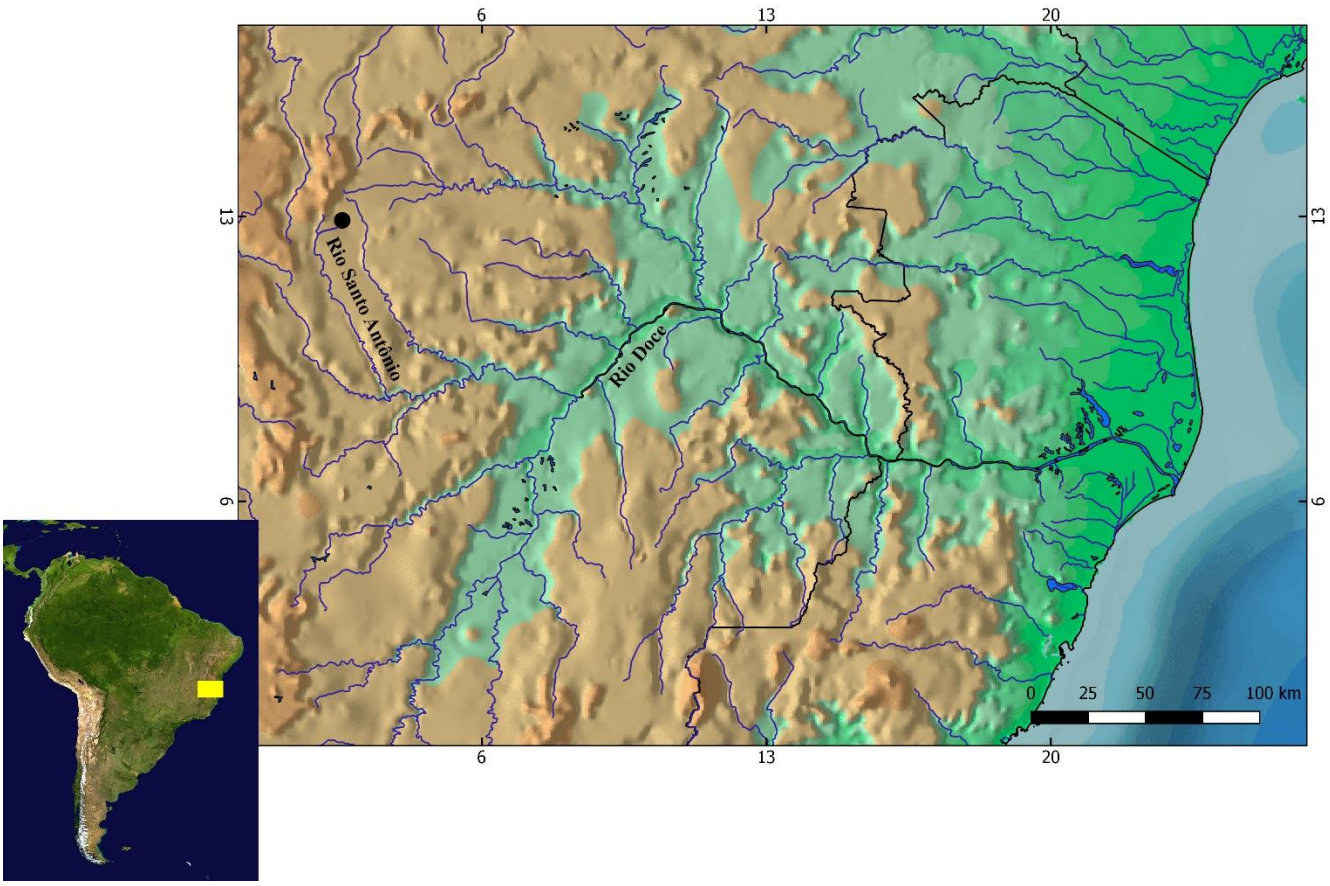

Fig. 22 – Geographical distribution of *Trichomycterus "brucutu"*, sp. nov. in the Rio Doce basin.

Black circle - holotype (MZUSP 87834) and paratypes (ex-MZUSP 87834).

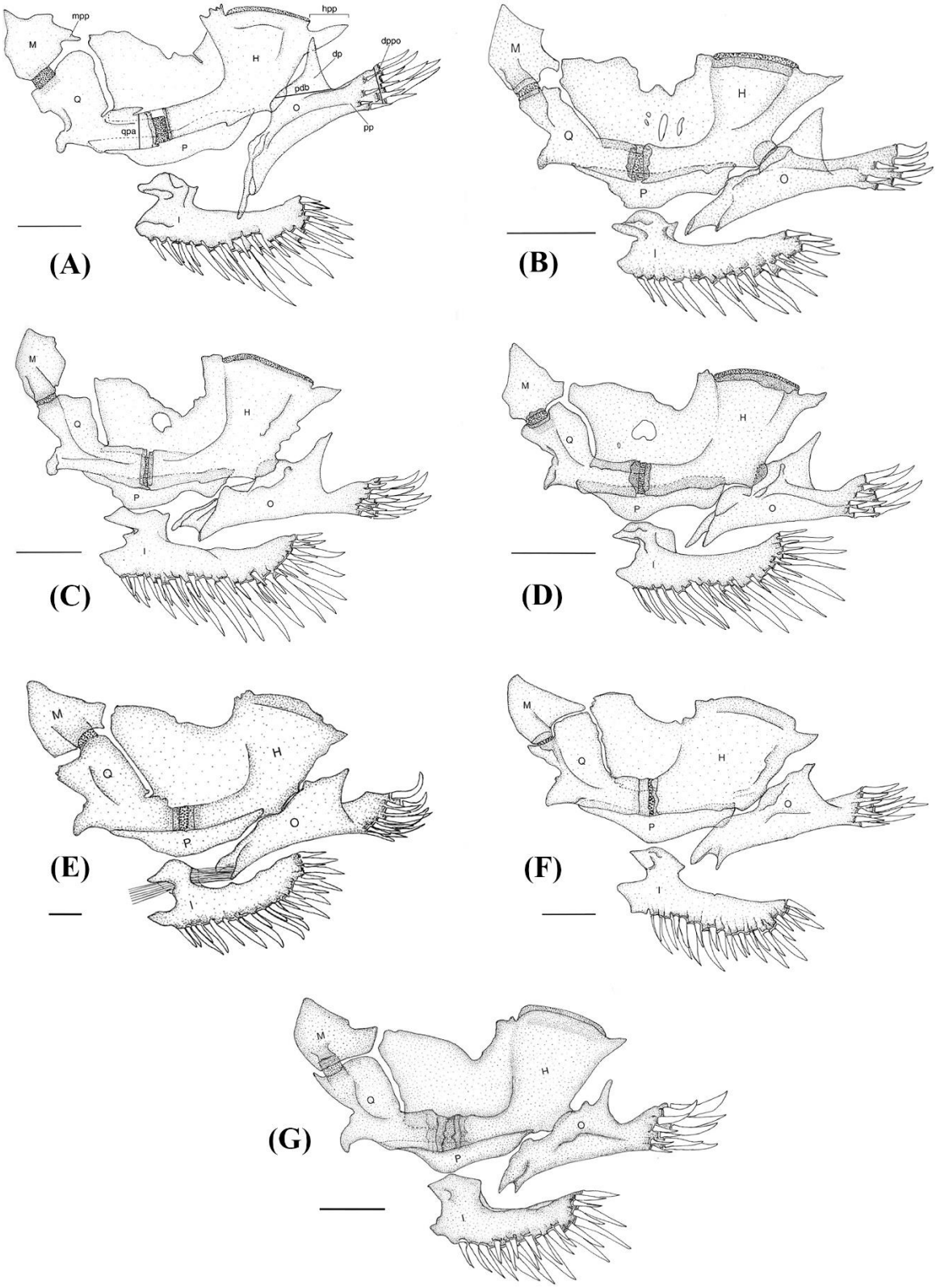
mpp
hpp
dppo
dp
pdb
pp
qpa
M
H
Q
P
O
I
(A)
(B)
(C)
(D)
(E)
(F)
(G)

Fig. 23 – (A) *Trichomycterus brunoi* (UFRJ5658); (B) *Trichomycterus fuliginosus* (MN18177); (C) *Trichomycterus claudiae* (UFRJ5685); (D) *Trichomycterus mariamole* (UFRJ5400); (E) *Trichomycterus novalimensis* (MZUSP37145); (F) *Trichomycterus rubiginosus* (MZUSP34168); (G) *Trichomycterus brasiliensis* (UFRJ4834). Left jaw suspensorium and opercular series, lateral view. Abbreviations: **H**, hyomandibula; **I**, interopercle; **M**, meta pterygoid; **0**, opercle; **P**, preopercle; **Q**, quadrate. Scale bar 1 mm. From Barbosa & Costa, 2010.

Fig. 24 - *Trichomycterus "illuvies"*, sp. nov. MZUSP 112750, holotype, 45.04 mm SL; Brazil, Minas Gerais, Ferros municipality. Photo by V. J. C. Reis.

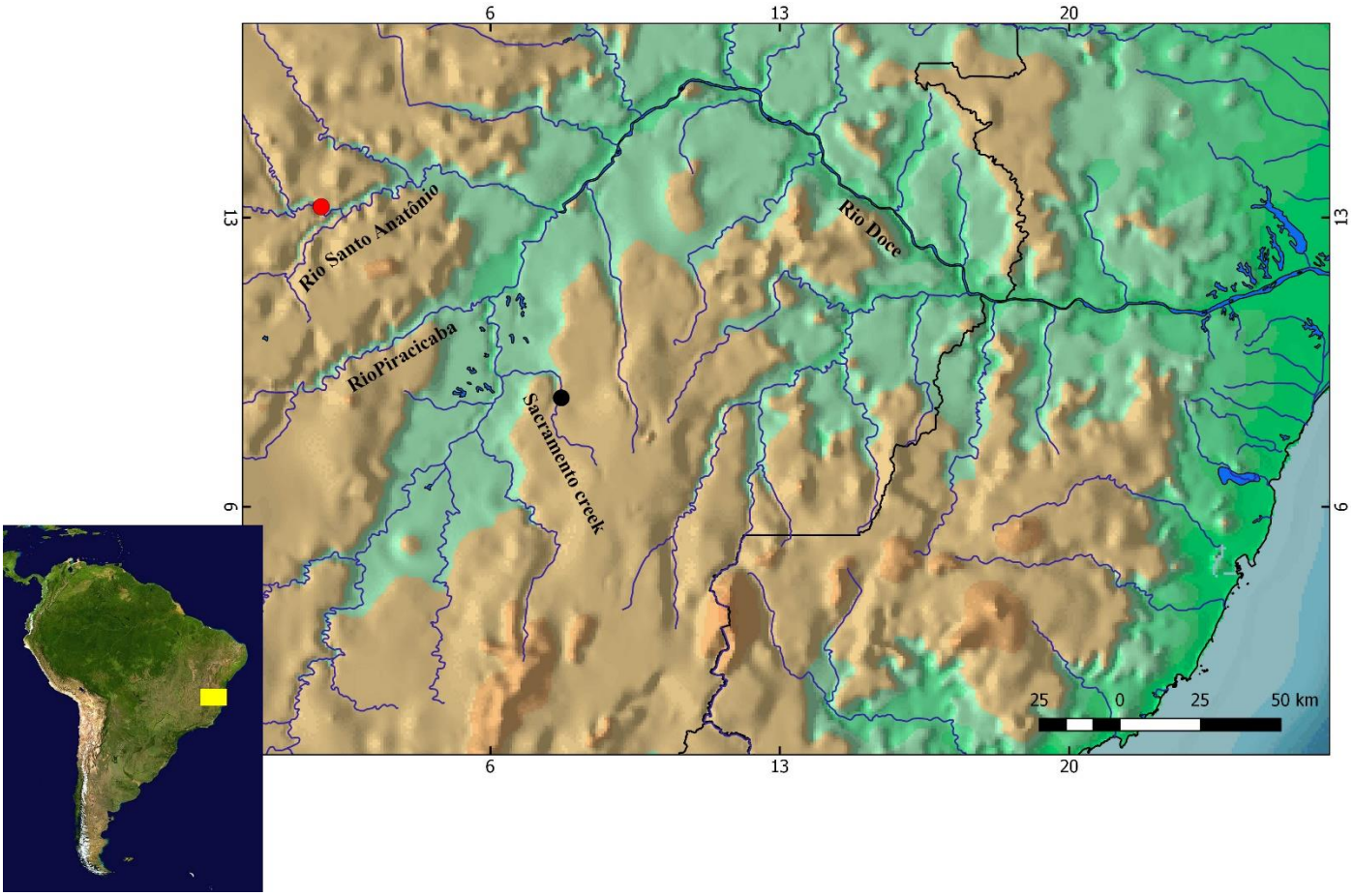

Fig. 25 - Geographical distribution of *Trichomycterus "illuvies"*, sp. nov. in the Rio Doce basin. Legend: **Red circle** - holotype (MZUSP 112750) and paratype (ex-MZUSP 112750) localities; **black circle** – paratype (MZUSP 110720).

Fig. 26 - *Trichomycterus immaculatus* MCZ 8300_4, lectotype, 123.2mm SL; Brazil, Minas Gerais, Juiz de Fora municipality. Photo by V. J. C. Reis.

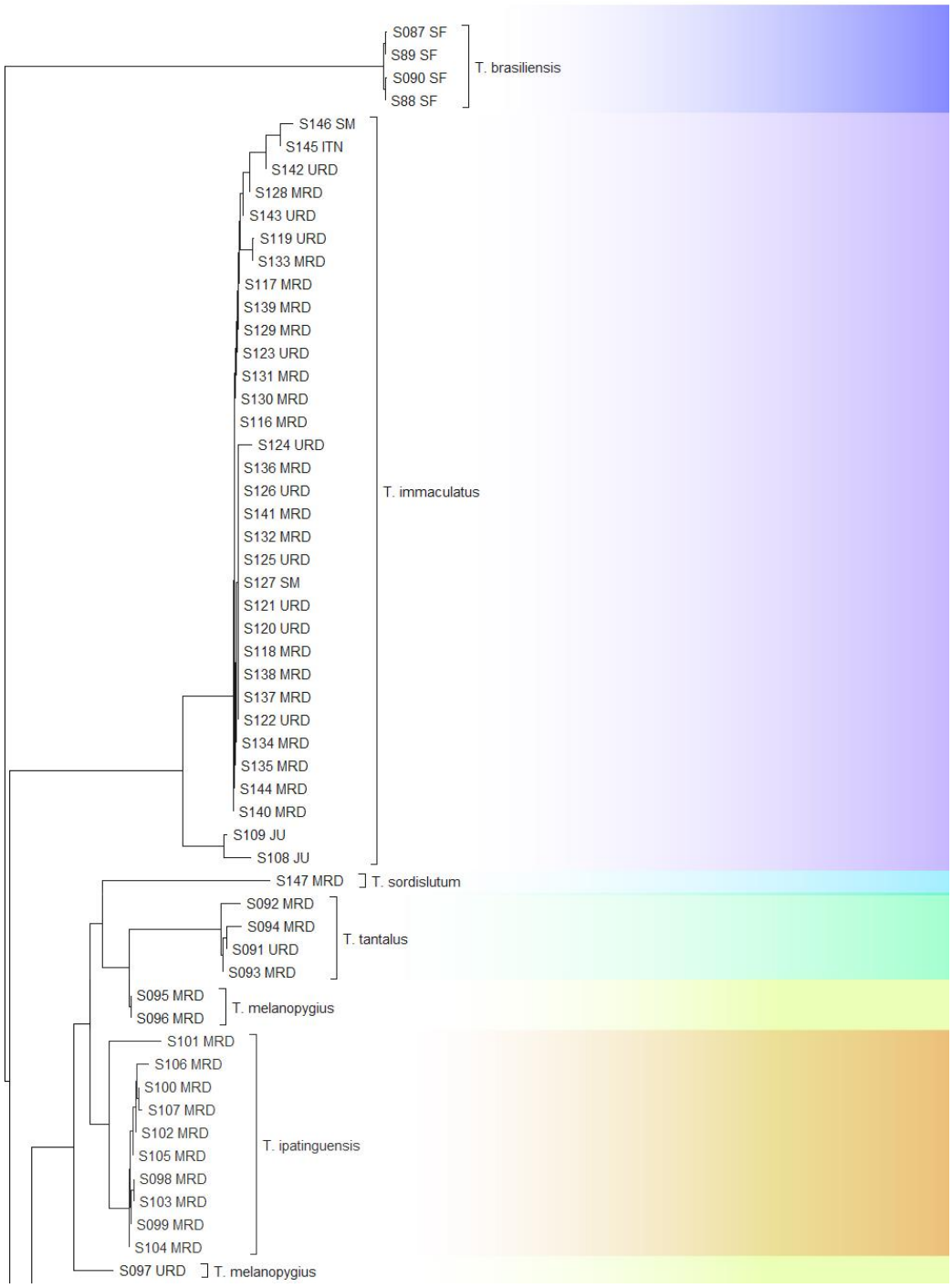

Fig. 27 – Neighbor-Joining (NJ) dendrogram (continued on next page) with K2P distance of the *Trichomycterus* species from the Rio Doce and some related basins (Jucuruçu, Itaúna, São Mateus, São Francisco, and Cubatão). Terminals composed by code of specimens (see Table 02) and drainage origin. Abbreviations: **URD**, upper Rio Doce; **MRD**, middle Rio Doce; **LRD**, lower Rio Doce; **JU**, Jucuruçú; **ITN**, Itaúna; **SM**, São Mateus; **SF**, São Francisco; **CT**, Cubatão.

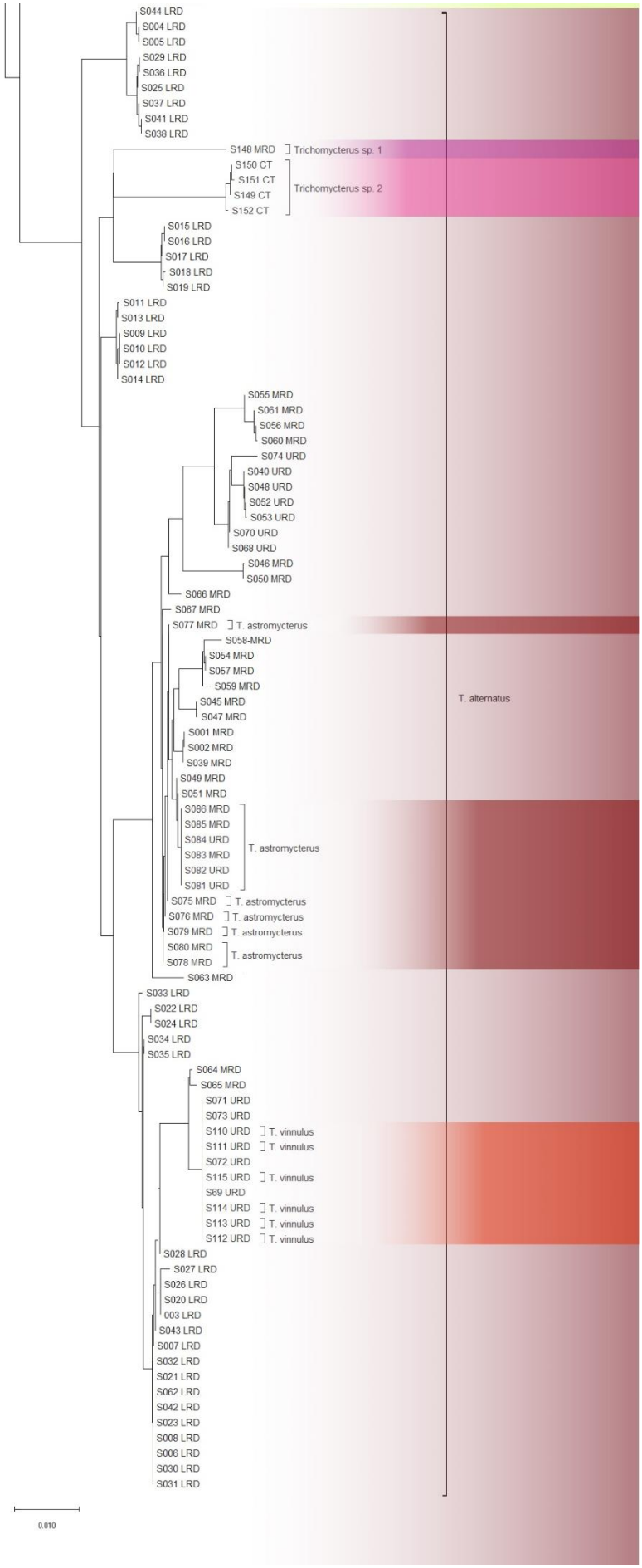
S044 LRD
S004 LRD
S005 LRD
S029 LRD
S036 LRD
S025 LRD
S037 LRD
S041 LRD
S038 LRD
S148 MRD
Trichomycterus sp. 1
S150 CT
S151 CT
S149 CT
S152 CT
Trichomycterus sp. 2
S015 LRD
S016 LRD
S017 LRD
S018 LRD
S019 LRD
S011 LRD
S013 LRD
S009 LRD
S010 LRD
S012 LRD
S014 LRD
S055 MRD
S061 MRD
S056 MRD
S060 MRD
S074 URD
S040 URD
S048 URD
S052 URD
S053 URD
S070 URD
S068 URD
S046 MRD
S050 MRD
S066 MRD
S067 MRD
S077 MRD
T. astromycterus
S058-MRD
S054 MRD
S057 MRD
S059 MRD
S045 MRD
S047 MRD
S001 MRD
S002 MRD
S039 MRD
S049 MRD
S051 MRD
S086 MRD
S085 MRD
S084 URD
S083 MRD
S082 URD
S081 URD
T. astromycterus
S075 MRD
T. astromycterus
S076 MRD
T. astromycterus
S079 MRD
T. astromycterus
S080 MRD
S078 MRD
T. astromycterus
S063 MRD
T. alternatus
S033 LRD
S022 LRD
S024 LRD
S034 LRD
S035 LRD
S064 MRD
S065 MRD
S071 URD
S073 URD
S110 URD
T. vinnulus
S111 URD
T. vinnulus
S072 URD
S115 URD
T. vinnulus
S69 URD
S114 URD
T. vinnulus
S113 URD
T. vinnulus
S112 URD
T. vinnulus
S028 LRD
S027 LRD
S026 LRD
S020 LRD
003 LRD
S043 LRD
S007 LRD
S032 LRD
S021 LRD
S062 LRD
S042 LRD
S023 LRD
S008 LRD
S006 LRD
S030 LRD
S031 LRD
0.010

Fig. 27 – Neighbor-Joining (NJ) dendrogram (continued from previous page) with K2P distance of the *Trichomycterus* species from the Rio Doce and some related basins (Jucuruçu, Itaúna, São Mateus, São Francisco, and Cubatão). Terminals composed by code of specimens and drainage origin. Abbreviations: **URD**, upper Rio Doce; **MRD**, middle Rio Doce; **LRD**, lower Rio Doce; **JU**, Jucuruçú; **ITN**, Itaúna; **SM**, São Mateus; **SF**, São Francisco; **CT**, Cubatão.

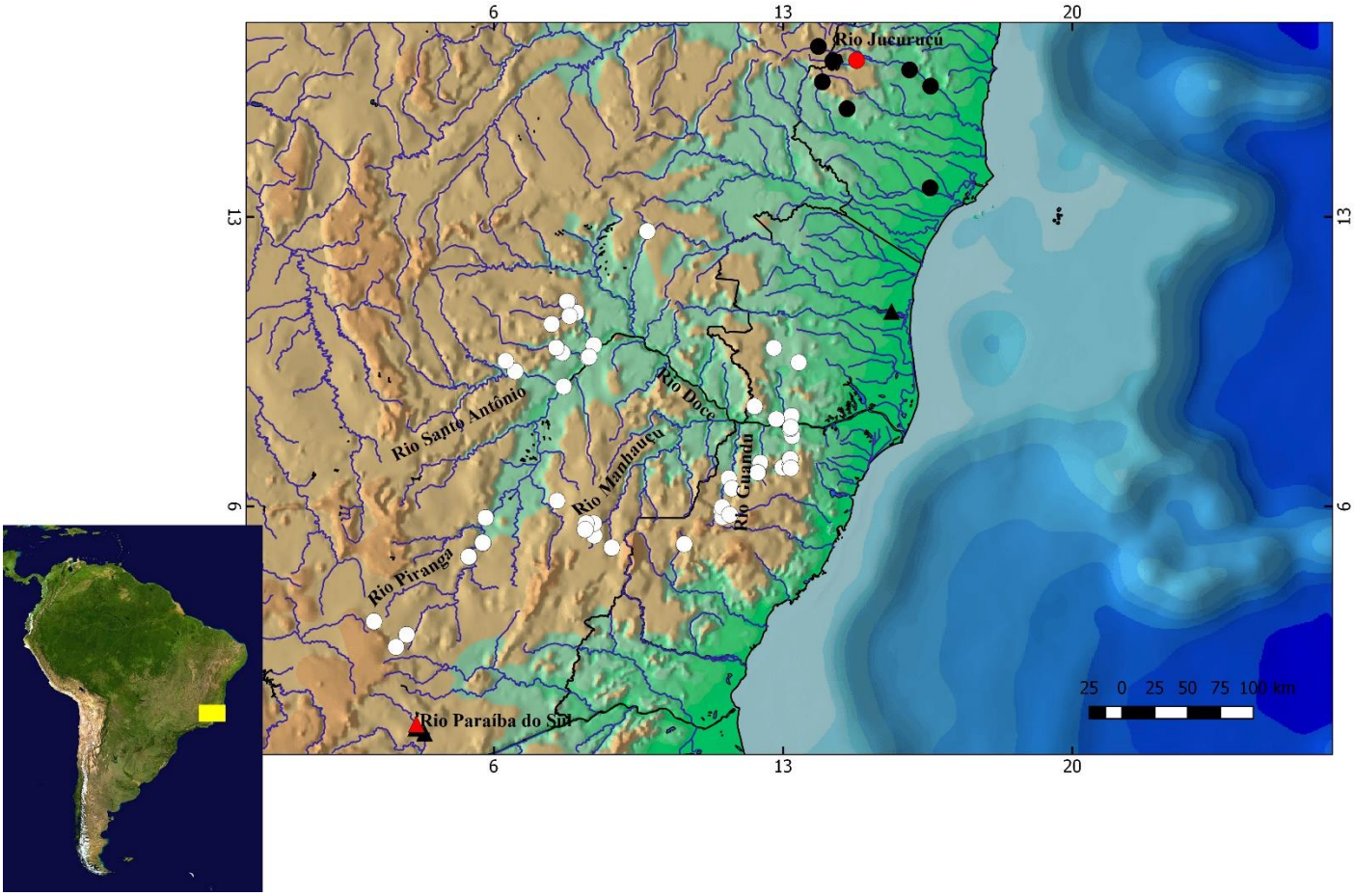

Fig. 28 - Geographical distribution of *Trichomycterus immaculatus* in the Rio Doce, Paraíba do Sul, São Mateus, and Jucuruçú basins. Legend: **Red triangle -** lectotype and paralectotype locality of *T. immaculatus*; **black triangle -** paralectotype locality of *T. immaculatus*; **red circle -** Jucuruçu locality of *T. immaculatus* (holotype of *T. pradensis*); **black circle -** Jucuruçu localities of *T. immaculatus* (paratypes of *T. pradensis*); **white circle -** Rio Doce localities of *T. immaculatus*.

Fig. 29 - *Trichomycterus "ipatinguensis"*, sp. nov. MZUSP 112279, holotype, 67.57 mm SL; Brazil, State of Minas Gerais, Conceição do Mato Dentro municipality. Photo by V. J. C. Reis.

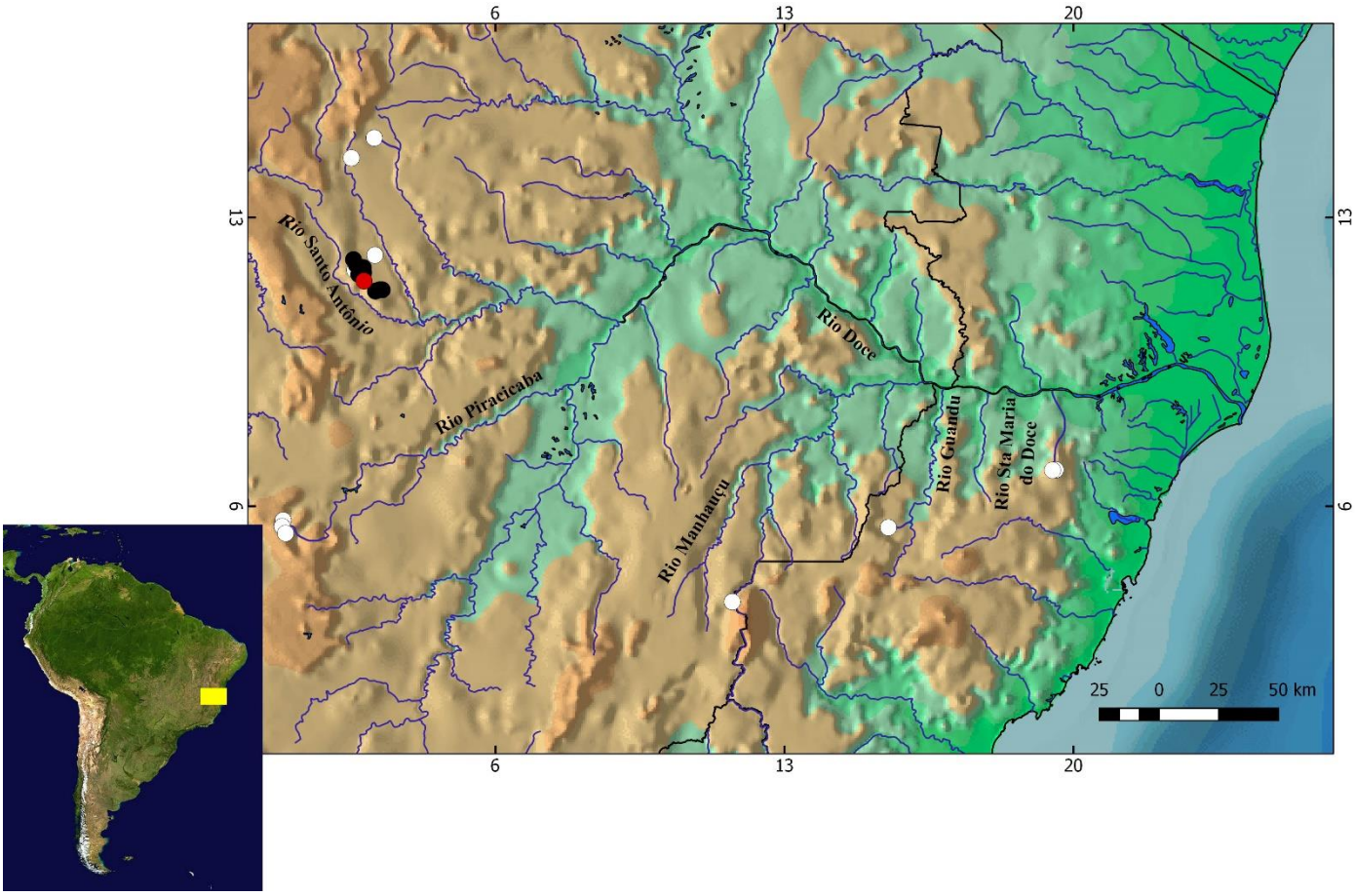

Fig. 30 - Geographical distribution of *Trichomycterus "ipatinguensis"*, sp. nov. in the Rio Doce basin. Legend: **Red circle -** holotype and paratype localities; **black circle** – paratype localities; **white circle -** non-type localities.

Fig. 31 - *Trichomycterus "melanopygius"*, sp. nov. MZUSP 110936, holotype, 97.7 mm SL; Brazil, State of Minas Gerais, Mariana municipality. Photo by V. J. C. Reis.

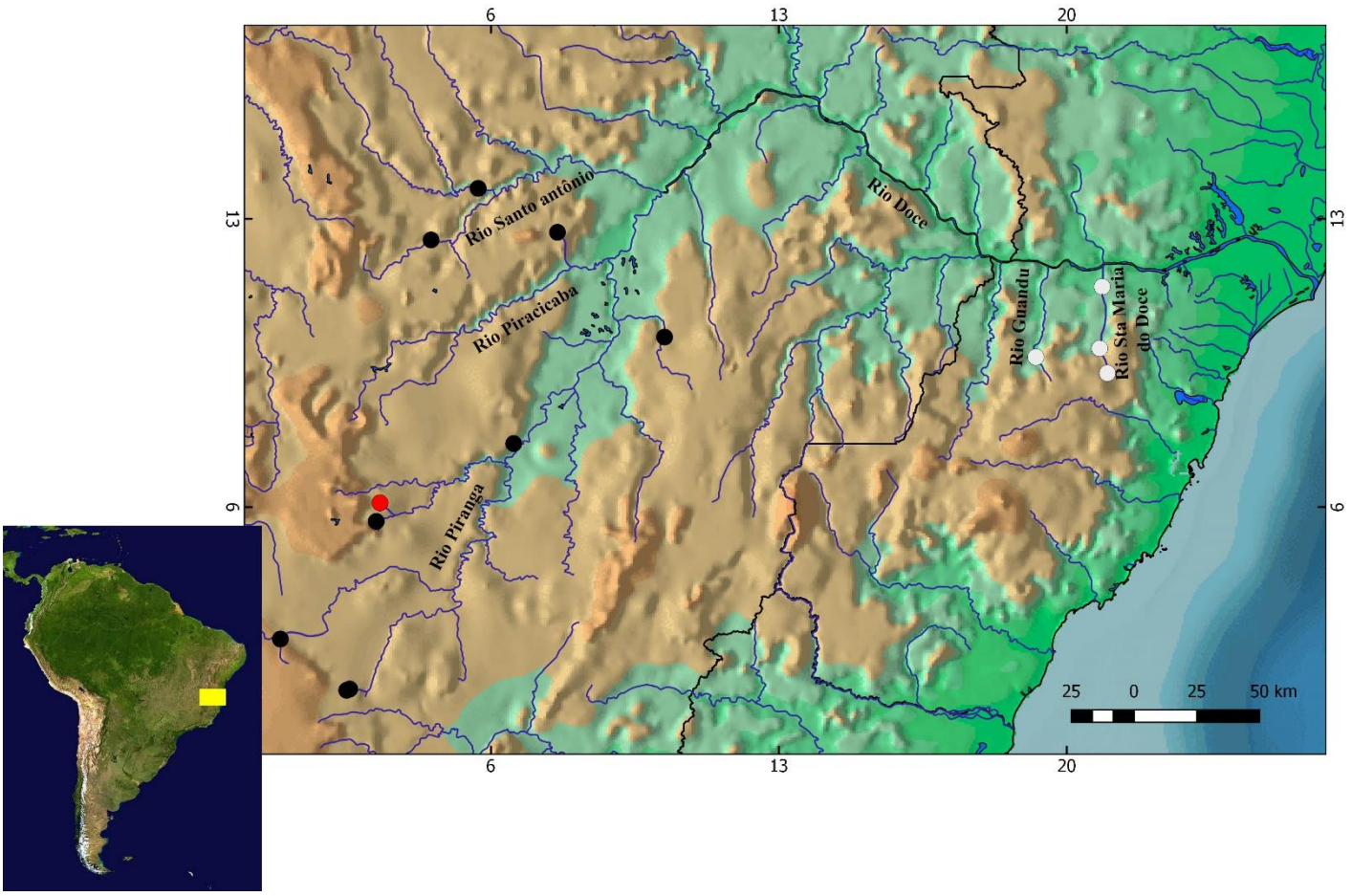

Fig. 32 - Geographical distribution of *Trichomycterus "melanopygius"* sp. nov. in the Rio Doce basin. Legend: **Red circle -** holotype and paratype localities; **black circle** – paratype localities; **white circle -** non-type localities.

Fig. 33 - *Trichomycterus "pussilipygius"*, sp. nov., holotype, MZUSP 123339, 68.8 mm SL; Brazil, State of Minas Gerais, Santa Rita de Minas municipality. Photo taken by V. J. C. Reis.

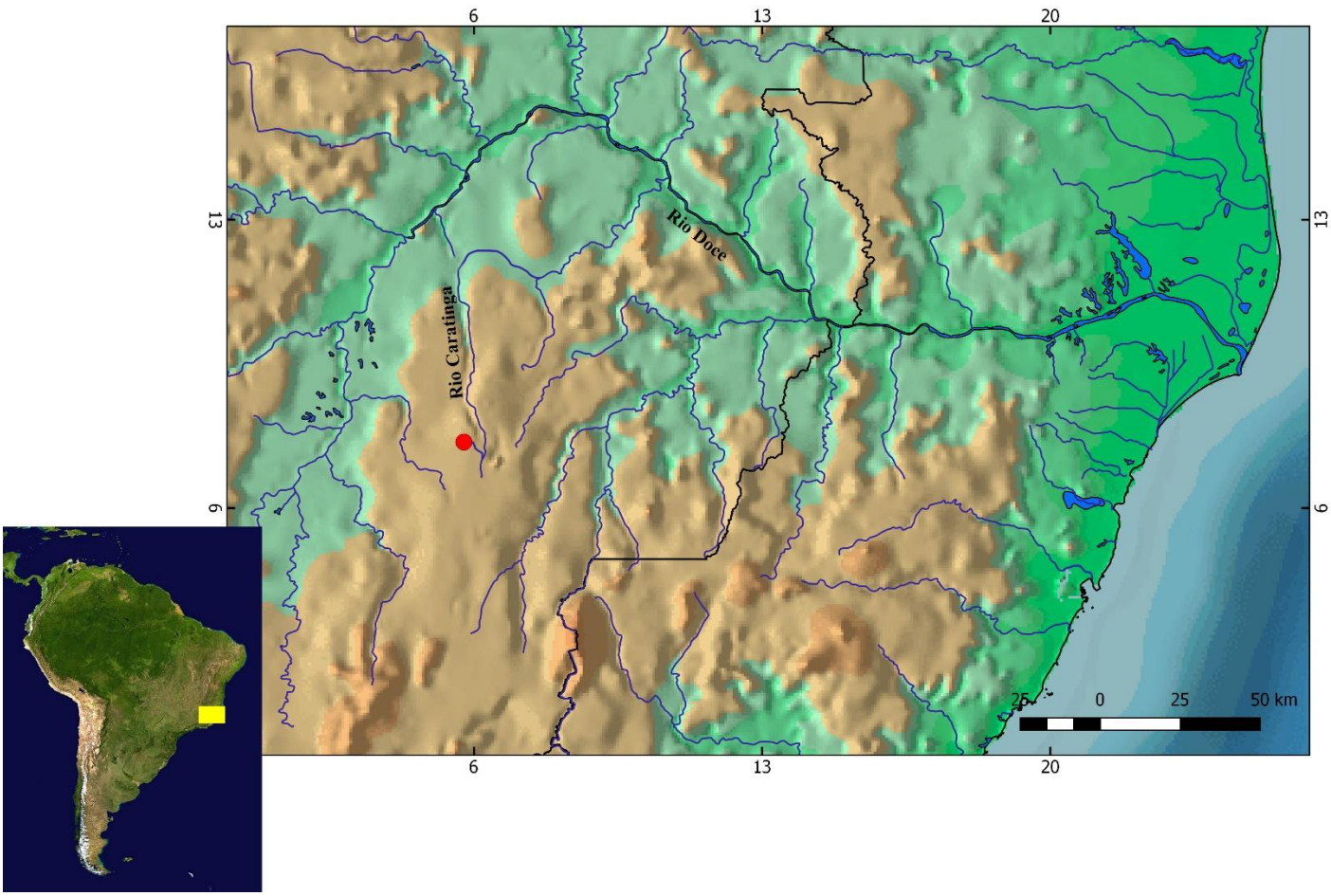

Fig. 34 - Geographical distribution of *Trichomycterus "pussilipygius"*, sp. nov. in the Rio Doce basin. Legend: **Red circle** - holotype and paratype localities.

Fig. 35 - *Trichomycterus "sordislutum"*, sp. nov., holotype, MZUSP 73162, 78.3 mm SL, Brazil, State of Minas Gerais, Conceição do Mato Dentro municipality. Photo by V. J. C. Reis.

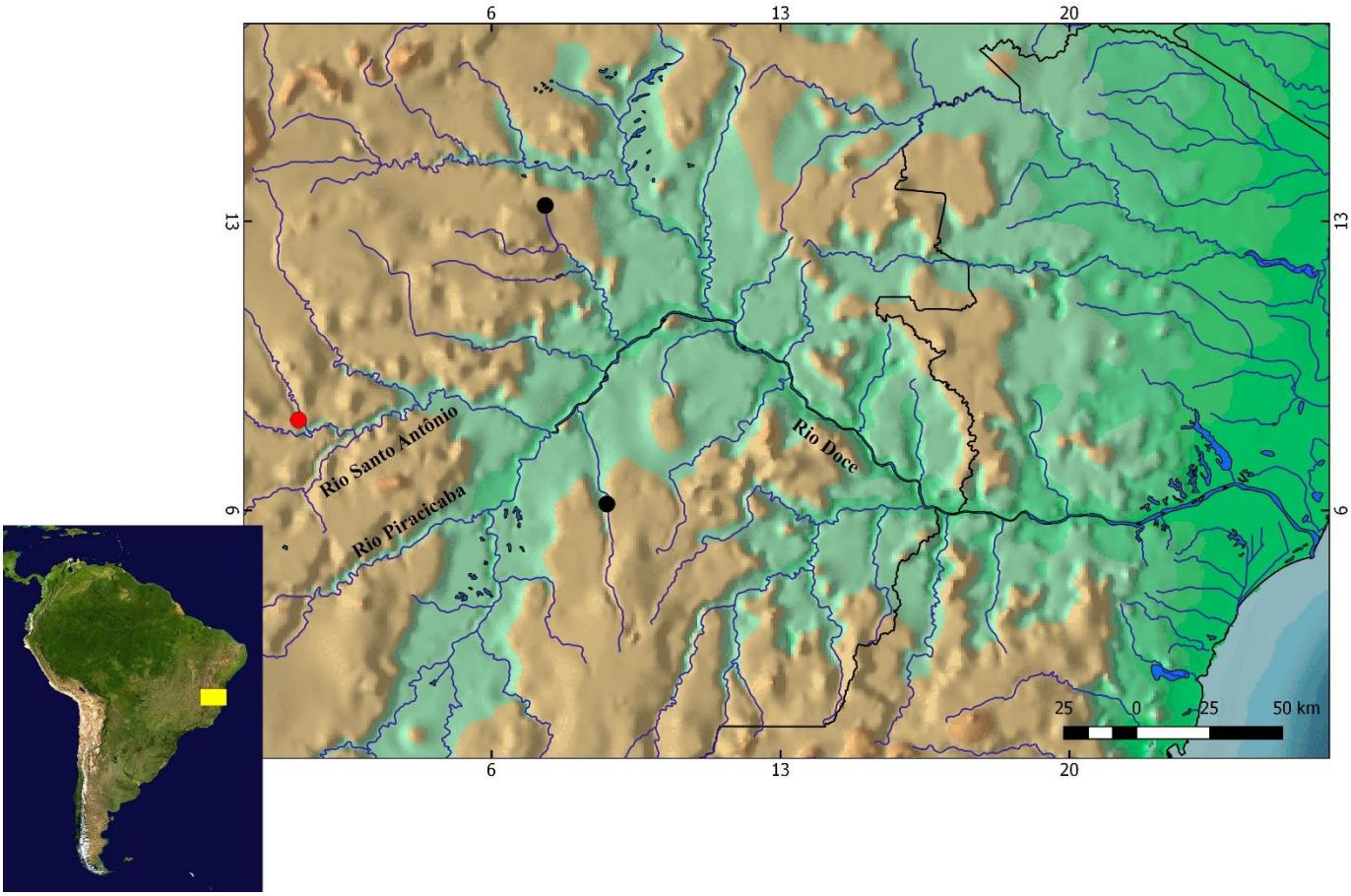

Fig. 36 - Geographical distribution of *Trichomycterus "sordislutum"*, sp. nov in the Rio Doce basin. Legend: **Red circle** - holotype locality; **black circle** – paratype localities.

Fig. 37 – *Trichomycterus "tantalus"*, sp. nov., holotype, MZUSP 123369, 75.98 mm SL; Brazil, Minas Gerais, Baguari municipality. Photo by V. J. C. Reis.

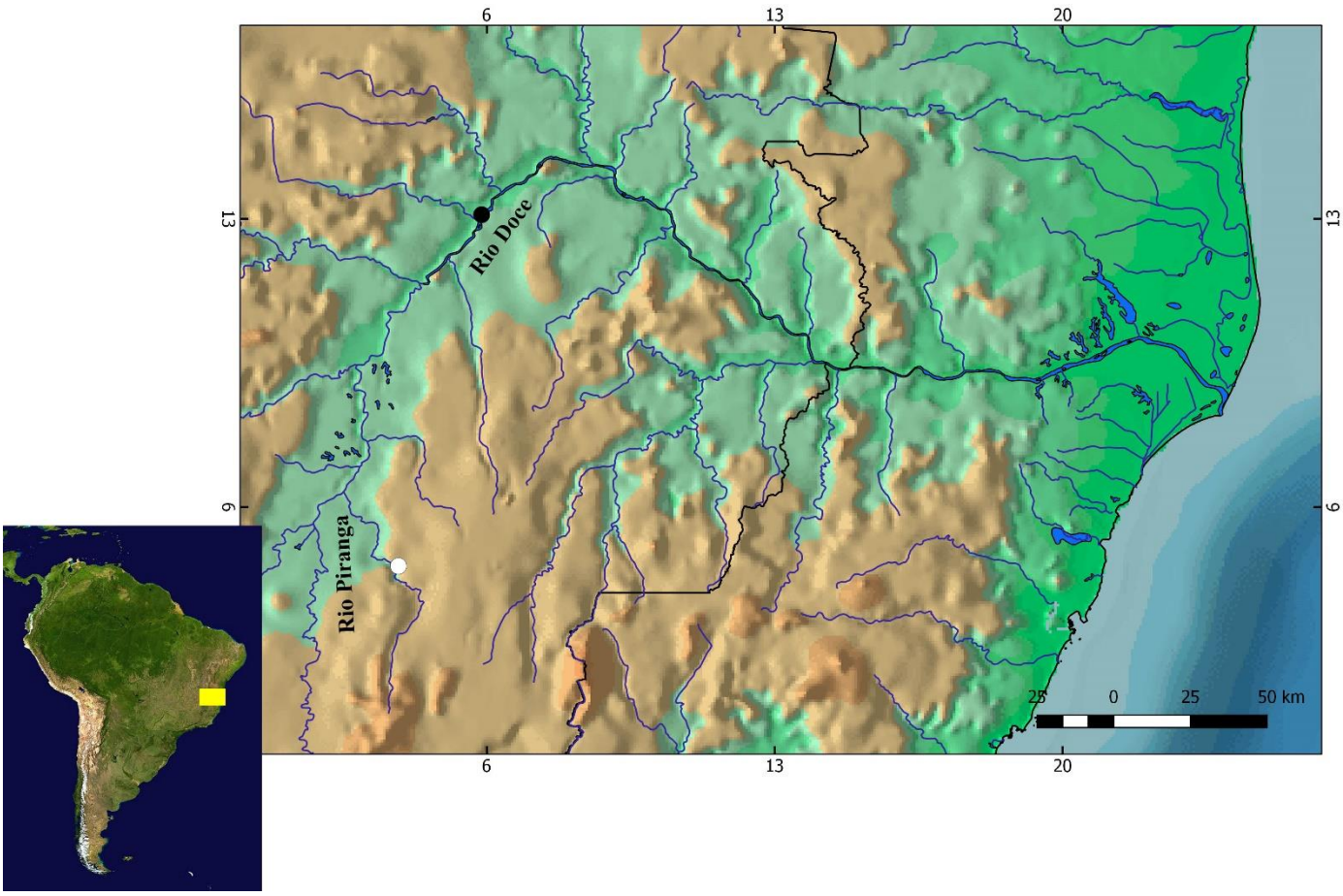

Fig. 38 - Geographical distribution of *Trichomycterus "tantalus"*, sp. nov. in the Rio Doce basin. Legend: **Black circle** - holotype (MZUSP123369) and paratype (1 ex. MZUSP123369) localities; **white circle** – paratype (MZUFV2565).

Fig. 39 - *Trichomycterus "vinnulus"*, sp. nov. MZUSP 123750, holotype, 54.0 mm SL; Brazil, State of Minas Gerais, Rio Doce municipality. Photo by V. J. C. Reis.

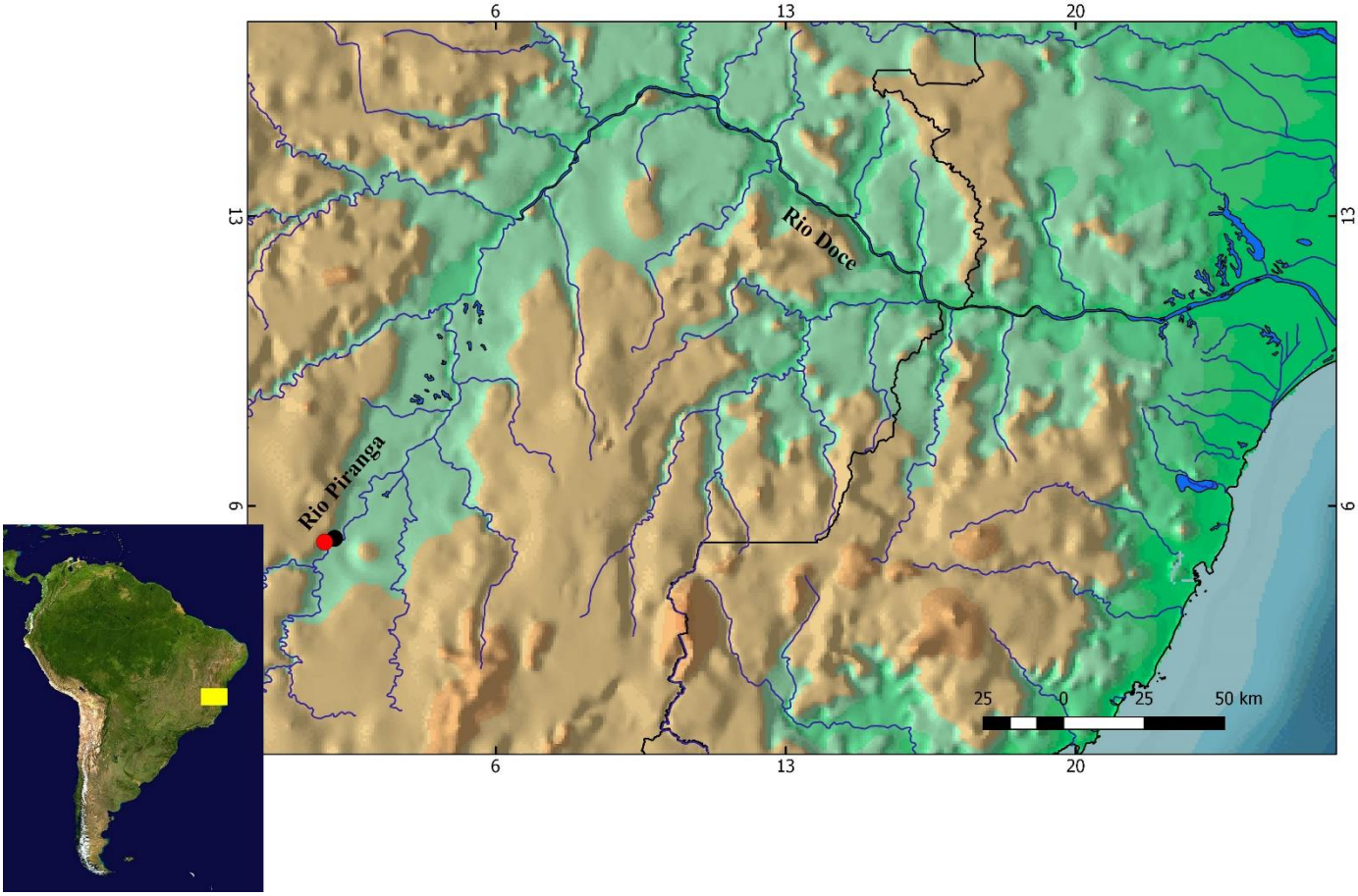

Fig. 40 - Geographical distribution of *Trichomycterus "vinnulus"*, sp. nov. in the Rio Doce basin. Legend: **Red circle** – holotype MZUSP 123750, and paratype ex-MZUSP 123750; **black circle** – paratype MZUSP 123757.

Fig. 41 – Mass concentration of *Trichomycterus* (*T. immaculatus*, *T. "tantalus"*, sp. nov, and *Trichomycterus* sp. 1) captured in the fish transposition system at the Baguari Hydroelectric plant, main channel of middle Rio Doce river. Photo by Tiago Pessali.

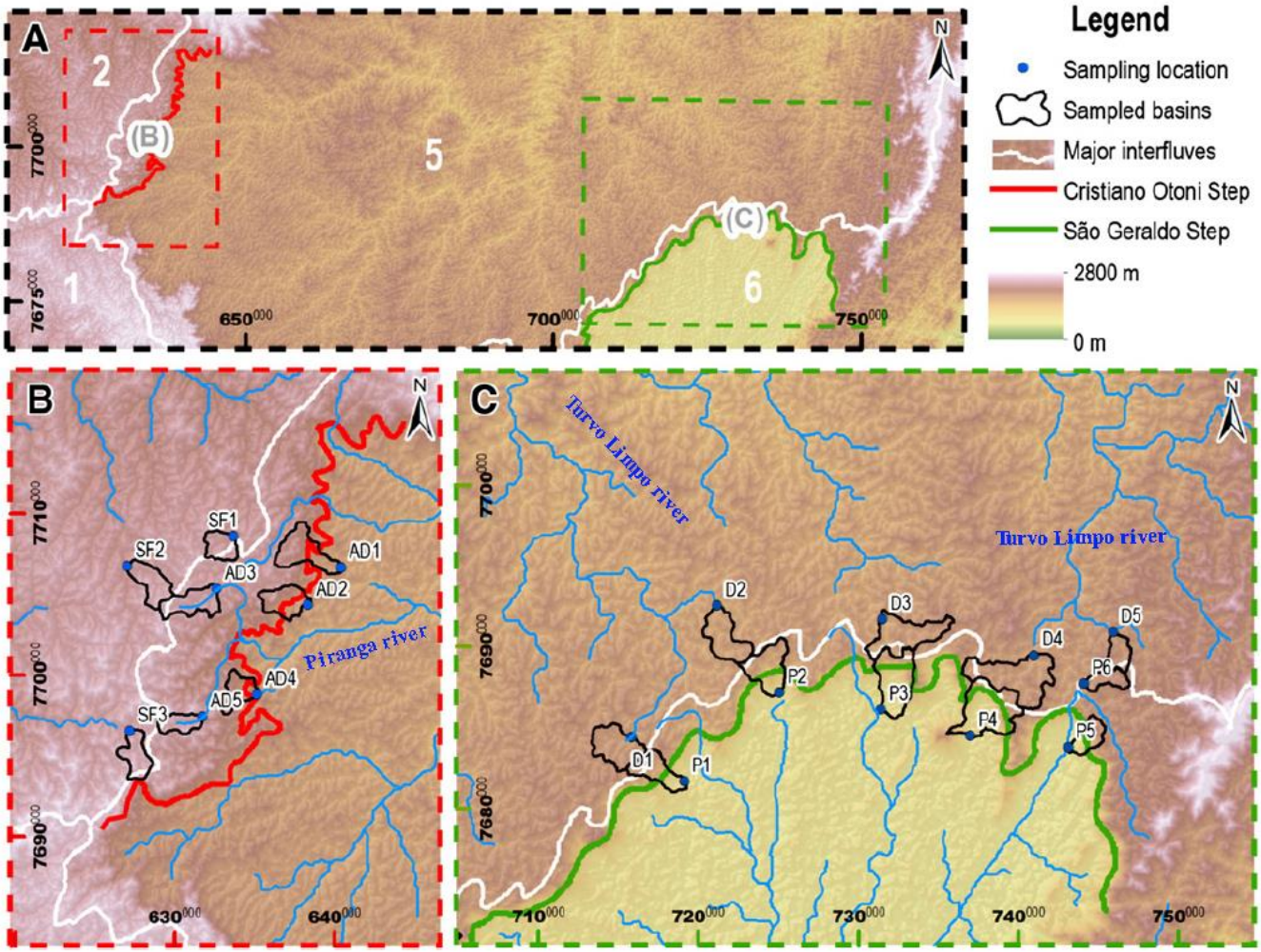

Fig. 42 – Hydrographic basin limits of 1 - Paraná; 2 - São Francisco; 5 - Rio Doce; 6 - Paraíba do Sul; showing the studied drainages that bordering 2 with 5, and 5 with 6. **(A)** Overview of studied area; sampled streams along the **(B)** Cristiano Otoni Step and the **(C)** São Geraldo Step. Modified figure extracted from Cherem *et al*., 2012.

Chapter 2. – The type specimens of *Trichomycterus alternatus* (Eigenmann, 1917) and *Trichomycterus zonatus* (Eigenmann, 1918), with elements for future revisionary work (Teleostei, Siluriformes, Trichomycteridae).

Abstract

Among the most pervasive elements in mid- to high-elevation coastal streams of Southeastern Brazil are the trichomycterid catfish species *Trichomycterus alternatus* Eigenmann, 1917 and *Trichomycterus zonatus* Eigenmann, 1918. Despite their abundance and ecological ubiquity, uncertainty still reigns in the applicability of their names. Examination of the type material of the two species reveals that part of the confusion stems from a mixing of species in the *T. zonatus* type-series. Such situation triggered a long-lasting chain of taxonomic misinterpretations and erroneous identification protocols and traditions. We disentangle this situation, providing detailed information on the holotypes and remaining type specimens of each species by classical and pioneering (Stereo Triplet) morphology analyses for data obtention. This will allow further taxonomic work to proceed on a firm nomenclatural basis. We also clarify and map the reported localities of the type material and offer comments into the validity of *T. alternatus* and *T. zonatus*, along with that of possibly related forms.

Resumo

Dentre as espécies de peixes neotropicais mais bem distribuídas entre médias e elevadas altitudes para as regiões costeiras do sudeste brasileiro, duas espécies de bagres da família Trichomycteridae se destacam, *Trichomycterus alternatus* Eigenmann, 1917 e *Trichomycterus zonatus* Eigenmann, 1918. Apesar da abundância e presença em diversos ecossistemas, diversas incertezas ainda permeiam a taxonomia dessas duas espécies. O exame detalhado dos respectivos materiais tipos revelou que a complexidade taxonômica provem em parte da presença de uma segunda espécie no material tipo de *T. zonatus*. Este fato provavelmente resultou em uma longa cascata de interpretações taxonômicas equivocadas e protocolos de identificação errôneos. Esta questão é resolvida a partir de informações detalhadas sobre a morfologia interna e externa dos materias tipos de *T. alternatus* e *T. zonatus*, utilizando análises morfológicas clássicas e pioneiras (Stereo Triplet) para a obtenção de dados. Com base nas informações prestadas, trabalhos futuros poderão prosseguir em bases nomenclaturais sólidas determinando a aplicabilidade dos nomes das respectivas espécies. Também são esclarecidas e mapeadas as localidades-tipo dessas espécies, com comentários a respeito da validade de *T. alternatus* e *T. zonatus.* Finalmente, as duas espécies, em suas concepções revisadas, são comparadas a formas já descritas para o sudeste brasileiro.

Introduction

Trichomycterus alternatus and T. zonatus are two of the most abundant catfish species in coastal freshwaters of Southeastern Brazil (Triques & Vono, 2004; Sato *et al*., 2004; Vieira, 2010; Da Silva *et al.*, 2013; Sales *et al*., 2018). They occur in cool, fast flowing, clear water streams and rivers, on rocky, sandy and mixed substrates, from just above sea level to over 1000 m altitude (de Pinna, 1998). Forms related to those taxa are nearly always present in biological inventories, ecological studies, faunistic surveys and freshwater samples in suitable habitats in that region (Sato *et al*., 2004; Vieira, 2010; Da Silva, 2013; Sales *et al*., 2018). Despite that, the two species remain poorly defined taxonomically and their identification is still confusing. As a consequence, their exact geographical range is yet uncharted and their degree of intraspecific variation remains undetermined. Numerous new species have been, and continue to be proposed for forms which are obviously related to *T. alternatus* and *T. zonatus* (e.g. *T. auroguttatus* Costa, 1992; *T. caudofasciatus* Alencar & Costa, 2004; *T. florensis* (Miranda Ribeiro 1943); *T. gasparinii* Barbosa, 2013; T. *longibarbatus* Costa, 1992; *T. mimosensis* Barbosa, 2013; *T. pantherinus* Alencar & Costa, 2004; *T. travassosi* (Miranda Ribeiro 1949)). Their validity depends on critical information about the delimitation and applicability of those two names, which have priority over most other species names assignable to *Trichomycterus* in Southeastern Brazil.

It is clear that information about the type material of *T. alternatus* and *T. zonatus* is critical for progress on that issue. Curiously, however, data from the types have rarely been considered in taxonomic publications discussing issues related to those species, even though they are in relatively good preservation condition and readily available for study. Most subsequent authors have simply relied on information provided in original publications by C. Eigenmann (e.g. Costa, 1992; Alencar & Costa, 2004; Barbosa, 2013). That information is quite limited when compared

to current descriptive standards and fail to provide comparative data critically needed today for taxonomic decisions. Besides, the type series of the two species reveals a number of problems related to localities, non-conspecificity between paratypes and holotypes, and inaccuracies in published data. Our aim in this paper is to disentangle that situation and to provide a clear picture of the situation of the type material, along with detailed morphological information on existing type specimens. We also refine and map the reported localities of the type material, offer data on recently-collected topotypes, and discuss the validity of *T. alternatus* and *T. zonatus*, along with that of possibly related forms.

We believe that accurate information on the relevant type material of *T. alternatus* and *T. zonatus* is tantamount for further research on the biological entities concerned and will allow upcoming contributions to proceed on a sound nomenclatural basis. This is necessary for increasing knowledge on the biodiversity of *Trichomycterus* in the Southeastern Brazilian region and ultimately to help untangling the broad-scale taxonomic maze of the genus.

Material and Methods

Meristics and morphometrics

All measurements were straight-line, taken with Mitutoyo digital calipers to the nearest 0.1 mm, on the left side of specimens whenever possible. From Tchernavin (1944) the measurements were: Standard Length; depth of the body; depth of the caudal peduncle; anteventral length; head width; interorbital width; length of nasal, maxillary, and rictal barbels. From de Pinna (1992b) the measurements were: Head length; caudal peduncle length; dorsal and anal-fin base lengths; length of the interopercular patch of odontodes; and eye diameter. From Bockmann & Sazima (2004) we used the length of pectoral and pelvic fins. In this paper, we propose the update of the following

measurements: Antedorsal length, from the anteriormost mesial point of upper lip to the base of the last conspicuous and segmented, but not branched, dorsal-fin ray visible without dissection; anteanal length, from the anteriormost mesial point of upper lip to the base of the last, conspicuous and segmented, but not branched, anal-fin ray visible without dissection; snout length, from the anteriormost mesial point of upper lip to the center of the interorbital width.

Data on meristic for fin-rays followed Bockmann & Sazima (2004). The posteriormost dorsal- and anal-fin rays were counted separately as branched segmented rays. Remain counts followed Pinna (1992). Vertebral counts included only free vertebrae (thus not including the Weberian complex) and the compound caudal centrum (PU1+U1) as one.

Osteology and the Stereo Triplet

Data on osteology, fin position and meristic characters were obtained from X-rays using (x-ray panel: Paxscan 4030E; x-ray tube: PXS5-927EA Microfocus X-Ray Source) at the Fish Division, National Museum of Natural History, Smithsonian Institution. Stereo-images were produced by radiographing specimens at slightly different angles and then searching various pairwise combinations for optimal stereo effect (Westheimer, 2011). We introduce here the concept of stereo triplet, as far as we know for the first time in fish morphology (a similar technique was used to illustrate computerized protein structure by Ratnaparkhi *et al.*, (2000) and Berry & Baker (2010), called therein "triplet stereo plot"). On radiographic imaging, the stereo triplet effect is obtained by producing first a stereo pair by the usual method. This will naturally result in either a dorsal or ventral view effect to the observer. If the relative positions of the pair components are reversed, that original view will be inverted (dorsal to ventral or vice versa). Thus it is possible to have both dorsal and ventral view effects on a single plate by duplicating one of the images and positioning it at the other extreme of the pair, as a third element. This forms a stereo triplet where

the two left elements when combined, produce a dorsal view effect and the two right elements, a ventral view (or the opposite, depending on how the original images are arranged). In practice, both dorsal end ventral effects are visible simultaneously, as the middle two elements in a set of four. The stereo-triplet effect allows a much enhanced grasp of the tridimensional structure of the anatomy and is particularly useful in obtaining anatomical information from unique types as in the present case.

Research institutions

Institutional abbreviations are: National Museum of Natural History – Smithsonian Institution, Washington, DC (NMNH), Field Museum of Natural History, Chicago (FMNH), and Museu de Zoologia, Universidade de São Paulo, São Paulo (MZUSP).

Material examined

Trichomycterus alternatus – **Holotype FMNH 58082**, 65.6 mm SL; Rio Doce, near the village of Rio Doce, Minas Gerais, Brazil, Rio Doce basin; col. J. Haseman, 25 May 1908; **Paratype FMNH 58083**, 62, 30.4 - 57.9 mm SL; same data from holotype. **Topotipic material - MZUSP 123761**, 01, 50.9 mm SL; Rio Doce, Córrego da Laje creek near town of Rio Doce, tributary of main channel of Rio Doce basin (20°14'13.05"S 42°56'53.65"W); col. V. J. C. Reis, M. C. C. de Pinna, G. F. de Pinna & G. Ballen, 23 Jun 2018. **MZUSP 123763**, 1, 46.25 mm SL; Rio Doce, creek bordering the hidropower dam resevouir Risoleta Neves, Rio Doce basin (20°12'21.63"S 42°52'56.24"W); col. V. J. C. Reis, M. C. C. de Pinna, G. F. de Pinna & G. Ballen, 24 Jun 2018. **MZUSP 123764**, 4, 47.29 – 42.65 mm SL; Rio Doce, creek bordering the hidropower dam resevouir Risoleta Neves, Rio Doce basin (20°12'22.03"S 42°52'57.44"W); col. V. J. C. Reis, M. C. C. de Pinna, G. F. de Pinna & G. Ballen, 24 Jun 2018.

Trichomycterus zonatus – **Holotype: FMNH 58573**, 52.31 mm SL; São Paulo, Água Quente, Iporanga; Ribeira do Iguape river; col. Haseman, 27 November 1908. **Paratypes: FMNH 58572**, 1, 50.69 mm SL; São Paulo, Cubatão, seven miles west from Santos; Cubatão river; col. Haseman, 1th August 1908; **FMNH 58574**, 2, 42.83 – 46.85 mm SL, São Paulo, Água Quente, Iporanga; Ribeira do Iguape river; col. Haseman, 27 November 1908. Type localities of both species published in Haseman (1911). **Topotype MZUSP 83139**, 8, 28.42 - 53.38 mm SL, (C&S) 2, 35.24 - 41.2 mm SL; Brazil, State of São Paulo, Iporanga, Betari river (Água Quente), tributary of Ribeira do Iguape basin; col. Sonia Buck & P. Gerhard, 5 Feb. 1998. **MZUSP 123175**, 10, 35.86 – 56.32 mm SL, Brazil, State of São Paulo, Cubatão, Cubatão rive, prainha perto da ponte (23°54'3.04"S 46°28'7.51"W); col. M. de Pinna, V. C. Reis, F. Carvalho, L. Donin, 09 Nov. 2017.

Cartography and image records

Photographs of dorsal and lateral view of all specimens were done by a NIKON P700 camera. Images were edited using software photoshop. Global Positioning System (GPS) data were obtained from topotype specimens, plotted into GoogleEarth Pro® in order to create a KML files. These files were then used within the free software QGIS 2.16 to create a map showing the geographical distribution of both species.

Results

Type localities

Although *T. alternatus* and *T. zonatus* are often confused in efforts at identification, their respective type material comes from widely disjunct localities. The holotype of *T. alternatus* is from the Rio Doce, a major system draining the Brazilian States of Espírito Santo and Minas Gerais. *Trichomycterus zonatus*, on the other hand, is based on material from much further south, the Rio Ribeira de Iguape in the State of São Paulo (Fig. 01). The type material of both species was collected by J. Haseman in the course of an expedition to Southeastern Brazil sponsored by the Carnegie Museum. Although their published type localities are rather brief, information on the itineraries of Haseman´s travels (Eigenmann, 1911) permits a more precise delimitation of the respective locations.

The type locality of *T. alternatus* is stated simply as "Rio Doce", with collection date 25th May 1908. Rio Doce can refer either to the river of that name, which covers a vast area of the States of Minas Gerais and Espírito Santo, or to a village with the same name located in the upper sector of the rio Doce, near the main channel of the river in the State of Minas Gerais. Haseman´s travel notes not always distinguish the village from the river, but it is possible to bracket the locality according to the points visited before and after May 25th. The village is today the Municipality of Rio Doce (20º14'41" S 42º53'45" W) and its name has been the same since September 6, 1886 years (riodoce.mg.gov.br). There is no name ambiguity and thus little doubt remains that the village of Rio Doce visited by Haseman corresponds to today´s municipality of Rio Doce. According to Haseman (1911), on May 24th his recorded location explicitly distinguished the river from the village: "Rio Doce and creek near village of Rio Doce". On May 25th, date of collection of the types of *T. alternatus*, Haseman was at a "rocky mill race at Rio Doce" (not specified

whether the river itself or some tributary near the village). The day of May 26th was spent at "creeks, pools and river", supposedly in the surroundings of the locality of the previous day. On May 27th he was again at "Rio Doce", with some of the lots specified as "whirlpool two miles below village of Rio Doce". So, the type specimens of *T. alternatus* were collected in the surroundings of the Village of Rio Doce, either in the Rio Doce itself or in some tributary at a sector close to the main river. This is a substantial narrowing of the type locality, when compared to the entire Rio Doce basin. Haseman collected 67 specimens in total, which indicates that the species was then locally abundant. In the elapsing 110 years, the region around the village of Rio Doce has been heavily impacted by damming, pollution, mining disasters and introduced species (Barros *et al*., 2012).

The main water course running through the village of Rio Doce is the Ribeirão da Laje, a tiny stream, now polluted and channeled in its urban sector. Its upper course is not heavily polluted and runs through farmland, mostly pastures, with small pockets of secondary gallery forest. The water flow in the headwaters of the Ribeirão da Laje is very small, and the creek was at most 1.5m wide and 15cm deep at the time of our visit. Specimens of *Trichomycterus alternatus* are rare in that locality, where we managed to secure a single specimen during a recent field trip. Additional specimens were found at larger tributaries near the village, also fitting the general type locality, as listed in the Material Examined.

The type material of *T. zonatus* comes from two different localities. The holotype **(**FMNH 58573**)** and two paratypes (FMNH 58574) are reported simply as from "Água Quente" in the original description. According to Eigenmann (1911), on Nov 27th 1908, Haseman was at "Água Quente, into Rio Ribeira da[sic] Iguape, eight miles from Iporanga in small mountain creeks near caves". The locality probably refers to a place in the Rio Betari, itself tributary to the Rio Ribeira

de Iguape, Municipality of Iporanga, Southern São Paulo State. The only nontype material we located of *T. zonatus* from that locality is MZUSP 83139. A third paratype specimen (FMNH 58572) comes from a widely disjunct locality: "Cubatão, seven miles west of Santos, São Paulo, Brazil" as per the original description. In this case, Eigenmann (1911) provides no further information since the collection date of Aug 1st is not recorded as an entry. The nearest recorded date, Jul 31st, states that Haseman was at "Rio Pilao, near Santos. From torrent 100 feet broad, one foot deep, fifteen miles southwest of Santos, near water-works" and "Cubatão, Rio Cubatão. Clear, swift, and rocky creeks, seven miles west of Santos". "Rio Pilao" probably refers to the Rio Pilões, a small tributary to the Rio Cubatão. Thus, the paratype FMNH 58572 comes from the Rio Cubatão or one of its tributaries in the neighborhood of the cities of Santos and Cubatão. As discussed below (see Discussion), this particular specimen is not conspecific with the holotype and remaining paratypes. We have examined recently-collected material from the Rio Cubatão (MZUSP 123175) and the specimens indeed are not conspecific with *T. zonatus*. In fact, no specimens from that locality so far examined correspond to *T. zonatus*.

The type locality of *T. zonatus* is listed by Wosiacki & de Pinna (2003) as "Água Quente [Cubatão, seven miles west of São Paulo (Eigenmann, 1918) = 23 40'S 46 25'W], São Paulo, Brazil." This report is mistaken, and was induced by a misreading of the locality records in Eigenmann (1918: 330-331), where the locality is listed as a place called Água Quente for the holotype and two paratypes and then Cubatão, São Paulo, Brazil for the third paratype. As seen above, the real locality of the holotype of *T. zonatus* is Iporanga, in the Rio Ribeira do Iguape basin, 304 km from the city of Cubatão.

Taxonomical accounts

Trichomycterus alternatus (Eigenmann, 1917)

(Fig.02)

Pygidium alternatum Eigenmann, 1917: 700 Rio Doce, Brazil [holotype**:** FMNH 58082 (ex CM 7079), paratypes**:** CAS 64575 (4), FMNH 58083 (62)]; Henn 1928:79 [type catalog]; Ibarra & Stewart 1987:72 [type catalog]; Ferraris 2007:414 [checklist];

*Trichomycterus alternatu*m Eigenmann, 1917; Burgess 1989:321 [list];

Trichomycterus alternatus Eigenmann, 1917; Costa, 1992:104 [comparisons]; Bizerril 1994:623 [list]; Miquelarena & Fernández 2000:44 [list]; de Pinna & Wosiacki, 2003:279 [checklist]; Wosiacki, 2004 [type catalog]; Wosiacki & Garavello 2004:5 [list]; Triques & Vono 2004:170 [comparisons]; Bockmann & Sazima 2004:71 [discussion on its relationships]; Bockmann *et al*. 2004:227 [cited]; Alencar & Costa 2004:3 [comparisons]; Wosiacki, 2005:51 [comparisons]; Lima *et al.*, 2008 [comparisons]; Barbosa & Costa 2010:120 [comparisons]; Sarmento-Soares *et al*., 2011:262 [comparisons]; Roldi *et al*., 2011:02 [comparisons]; Barbosa & Costa 2011:308 [comparisons]; Barbosa & Costa 2012:155 [comparisons]; Barbosa 2013:274 [comparisons], DoNascimiento *et al*., 2014:709 [comparisons]; García-Melo *et al*. 2016:238 [comparisons]; Sales *et al*., 2018 [comparisons].

Descriptions – Morphometric data for holotype and paratypes in Table 01, asterisk on number means the holotype value. See Figs. 02 and 03 for general external aspect. Body cross-section oval near head, becoming gradually compressed posteriorly towards caudal fin. Head depressed, approximately as long as wide. Head width increasing slightly from snout to end of opercle, parabolic to trapezoid in dorsal view. Body elongate with dorsal and ventral profiles slightly

convex on trunk and nearly straight along caudal peduncle. Body depth approximately even along entire body, only slightly decreasing posterior to dorsal-fin origin.

Anterior nostril closer to upper lip than to anterior margin of eye, surrounded by membrane forming short and slender tube continuous posterolaterally with base of nasal barbel. Posterior nostril anteriorly surrounded by thin and short flap of integument. Eye large, without free orbital rim, located at anterior half of head length and on dorsolateral region of head. Elliptical ocular capsule formed by thin and translucent skin not adhered to surface of eyeball. Interorbital space slightly convex and equivalent to twice orbital diameter.

Opercular patch of odontodes dorsolaterally located on head, surrounded by fold of integument, with posterior margin almost reaching vertical through anterior margin of base of first pectoral-fin ray, with 15 [1], 16* [2], 17 [4], 20 [2], 21 [1], 23 [1] claw-like odontodes. Interopercular patch of odontodes large, ventrolaterally located on head, about two thirds as deep as opercular patch, with 27 [1], 30 [2], 31 [2], 33 [1], 34 [2], 38* [2], 40 [1] Claw-like odontodes. Mouth subterminal. Upper lip convex, covered with numerous small, short papillae on internal and external surfaces. Premaxillary teeth arranged in three or four well-defined and roughly regular rows. Dentary teeth arranged in one regular inner row, with two additional irregular rows near symphysis. Lower lip well developed, convex, with lateral fleshy folds adjacent to base of rictal barbel. Fleshy fold slender than, and half overall size of, lower lip, its insertion anterior to origin of rictal barbel. Branchiostegal membranes narrowly joined to isthmus medially and forming large free fold. Branchiostegal rays 6 [1], 7* [9], with bigger ones partly visible in outline on surface of skin. Maxillary barbel reaching to base of pectoral fin or slightly beyond. Rictal barbel reaching middle of interopercular patch of odontodes or posteriormost margin of gill opening. Nasal barbel extending to anterior margin of opercular patch of odontodes.

Pectoral-fin rays I + 7. Distal margin of pectoral fin straight or slightly convex; first ray prolonged as a long filament. Anterior portion of pectoral-fin base not covered by branchial membrane. Axillary pore dorsal to base of first pectoral-fin ray, anteroventral to first lateral-line pore, bigger and adjacent to lateral-line pores. Pelvic-fin rays I+4. Distal margin of pelvic fin entirely covering anus. Base of pelvic fin separated by one eye diameter. Dorsal-fin rays iii+II+7* [6], ii+II+7 [3], II+7 [2]. Dorsal fin convex distally, on posterior half of SL, its origin slightly anterior to vertical through origin of anal fin. Dorsal-fin pterygiophores eight. First dorsal pterygiophore anterior to neural spine of 13th [1], 15th* [15], 16th [35], 17th [2] post-Weberian vertebrae. Anal-fin rays iii+II+5* [4], ii+II+5 [4], II+5. Distal margin of anal fin convex. Anal-fin pterygiophore six. First anal pterygiophore anterior to hemal spine of 17th [1], 18th [5], 19th*[32], 20th [13] post-Weberian vertebrae. Caudal-fin rays 6+7. Caudal fin shape variable, with margin ranging from truncate to slightly convex, in all cases with round corners.

Post-Weberian vertebrae 32 [1], 33 [1], 34 [11], 35 [35], 36* [15], First post-Weberian vertebrae nearly half the length of subsequent ones. Second post-Werberian vertebrae, short and transversal hemal process, with a wide in tip. Ribs 8 [1], 9 [2], 10* [29], 11 [21], 12[8]. Mesethmoid with slightly concave anterior margin with an anterior concave neck. Maxilla bone slender and fin. Ventro-medial process of maxilla articulating with antero-lateral process of autopalatine. Autopalatine anteriorly concave with long triangular postero-lateral process, with a wide base, almost the same length of this bone. Anterior and posterior cranial fontanel present. Posterior cranial fontanel goes until the middle of parieto-supraoccipital. Postorbital process of sphenotic-prootic-pterosphenoid complex bone directed anteriorly. Uroyal anteriorly deep concave with a concave constriction in its neck, its lateral process as a relative high width in compare to its length, making its posterior border slight concave or straight. Short and fin posterior

process of the uroyal. All osteological characters from head can be better observed in the stereo triplet (Fig. 04). Upper caudal plate formed by uroneural and two elements, hypural 3, and the fused hypural 4, and 5. Lower caudal plate consisting of single element presumably consisting of fusion of parhypural with hypurals 1 and 2. Epural absent.

Cephalic lateral-line canals with simple, non-dendritic tubes ending in single pores. Supraorbital canal mostly within frontal bone. Supraorbital pores: s1, mesial to nasal-barbel base; s3 mesial to posterior nostril; and s6 median and posteromedial to eye and at midlength of frontal. Infraorbital canal incomplete, with four pores, i1 (ventro-lateral to nasal-barbel base) and i2 (ventro-lateral to posterior nostril), i10 (posteroventral to eye) and i11 (posterior to eye). Otic canal without pores. Postotic pores po1 (anteromedial to opercular patch of odontodes), and po2 (medial to opercular patch of odontodes). Lateral line of trunk anteriorly continuous with postotic canal and reduced to short, tube in all specimens analyzed. Lateral line pores ll1 and ll2 present dorsomedial to pectoral-fin base and posterior to posttemporo-supracleithrum.

Coloration in ethanol (Fig. 02 and 03). - Pigmentation severely faded in all specimens due to long preservation history, but general features still visible. Dark chromatophores distributed into inner and outer skin layers. Those on inner skin layer forming large roundish maculae responsible for the main color features of the body. Basic arrangement of maculae in four variably arranged rows. One row along mid-dorsal line from occiput, through entire dorsum, into dorsal edge of caudal peduncle and to base of caudal fin. Second row ventrolateral to that, extending from base of head through upper part of flanks, dorsal portion of caudal peduncle, to base of caudal fin. Third row running along mid-lateral line, from immediately posterior to opercle to base of caudal fin. Fourth and ventralmost row shorter, extending from mid-length of abdomen through ventral margin of caudal peduncle to base of caudal fin. Basic four-row pattern disrupted by fusions

(mostly along anterior part of body) and unaligned maculae, resulting in varied configurations. Mid-lateral line mostly independent but occasionally fused on dorsum. Head darkest on region corresponding to neurocranium, outlined by brain pigment seen by transparency. Dark spot normally at base of opercular patch of odontodes, with additional dark markings on cheeks. Light teardrop-shade area extending from posterior margin of eye to base of opercular patch of odontodes, corresponding to levator operculi muscle. Base of nasal barbels surrounded with concentration of dark pigment, extending posteriorly as elongate dark field to anterior margin of eyes. Distal margin of integument fold of opercular patch of odontodes darkly-pigmented. Interopercular patch of odontodes white. Ventral side of the body lacking dark pigment. Fins with small brownish spots randomly distributed on fin-rays.

Trichomycterus zonatus (Eigenmann, 1918)

(Fig. 05)

Pygidium zonatum Eigenmann, 1918:330, Agua Quente, Cubatao, 7 miles west of Santos, São Paulo, Brazil. [Holotype: FMNH 58573 (ex CM 7596), paratypes: FMNH 58572 (1), 58574 (2)]; Henn 1928:81 [type catalog], Ibarra & Stewart 1987:73 [type catalog], Ferraris 2007:425 [checklist].

Trichomycterus zonatum Eigenmann, 1918; Burgess 1989:323 [list].

Trichomycterus zonatus Eigenmann, 1918; Bizerril 1994:623 [comparisons]; de Pinna & Wosiacki 2003:285 [checklist]; Triques & Vono 2004:170 [list]; Bockmann & Sazima 2004:71 [comparisons]; Bockmann *et al.* 2004:228 [comparisons]; Wosiacki, 2004 [type catalog]; Wosiacki, 2005:51 [comparisons]; Ferraris 2007:425 [checklist]; Lima *et al.*, 2008 [comparisons];

Barbosa & Costa 2010:121 [comparisons]; Barbosa & Costa 2011:308 [comparisons]; Barbosa & Costa 2012:82 [comparisons]; Barbosa 2013:270 [comparisons]; Katz & Barbosa 2014:3 [comparisons]; DoNascimiento *et al*., 2014:709 [comparisons]; García-Melo *et al.* 2016:237 [comparisons].

Description - Morphometric data for holotype and paratypes in Table 02, asterisk on number means the holotype value. See Figs. 05 and 06 for general external aspect. Body cross-section oval, becoming increasingly compressed posteriorly mainly along caudal peduncle. Head dorsal-ventrally compressed having its length and width very similar. Width of the head slightly increase from the most-anterior portion of the mouth to the end of the opercle, parabolic to trapezoid in dorsal view. *Levator mandibulae* well-developed and bigger than those from the paratypes. Body elongate with dorsal and ventral profiles slightly convex on trunk and nearly straight until the caudal peduncle. Body depth slightly the same in all body, slightly decreasing its depth after the dorsal fin origin.

Anterior nostril closer to upper lip than to anterior margin of eye, surrounded by membrane forming short tube continuous with nasal-barbel base. Posterior nostril anteriorly surrounded by thin, crescent flap of integument. Eye big, without free orbital rim, located at anterior half of head length and on dorsolateral region of head. Elliptical ocular capsule formed by thin and translucent skin not adhered to eyeball's surface. Interorbital space slightly convex transversally and about the double or smaller than orbital diameter.

Opercular patch of odontodes dorsolaterally located, posteriorly surrounded by fold of integument, with posterior margin almost reaching vertical through anterior margin of base of first pectoral-fin ray, and 10 [1], 14* [2], 15 [1] conical odontodes. Interopercular patch of odontodes

ventrolaterally located, large, about twice deeper than opercular patch, with 15 [1], 17 [1], 27 [1] conical odontodes. Mouth convex and subterminal. Upper lip convex, covered with various small and short papillae internally and externally. Premaxillary teeth arranged in three well-defined and almost regular rows. Dentary teeth arranged in one regular inner row with two additional irregular rows gradually appearing towards dentary symphysis. Lower lip well developed, convex and covered with small and short papillae internal and externally, with lateral fleshy folds adjacent to rictal-barbel base. Branchiostegal membranes thick, narrowly joined to isthmus medially and forming large free fold. Branchiostegal rays eight in holotype FMNH58573, paratype FMNH 58574 specimens, and seven in paratype FMNH 58572, big most rays most been visualized through skin. Maxillary barbell not reaching pectoral-fin origin, but reaches gill opening. Rictal barbell not reaching posterior margin of interopercular patch of odontodes. Nasal barbel extending to perpendicular through posterior margin of opercular patch of odontodes but not transposing it.

Pectoral-fin rays I + 6 in holotype FMNH58573, paratype FMNH 58574 specimens, and I+7 in paratype FMNH 58572. Distal margin of pectoral fin straight or slightly convex; first ray not prolonged as a filament. Anterior portion of pectoral-fin base not covered by branchial membrane. Axillary pore dorsal to base of first pectoral-fin ray, anteroventral to first lateral-line pore, bigger than the lateral line pores. Pelvic-fin rays I+4 in all specimens. Distal margin of pelvic fin extending posterior to anus. Base of pelvic fin close together in FMNH58573, FMNH 58574, and separated by one eye diameter in FMNH 58572. Dorsal-fin rays iii+II+7 [3]*, ii+II+7 [1]. Dorsal fin convex distally, on posterior half of the body, with origin slightly ahead vertical through origin of anal fin. Dorsal-fin pterygiophores always eight. First pterygiophore usually just anterior to neural spine of 17th post-Weberian vertebrae, except for the specimen FMNH 58572, 16th. Anal-fin rays iii+II+5 [1]*, ii+II+5 [2], i+II+5 [1]. Distal margin of anal fin convex. Anal-fin

pterygiophore always six. First pterygiophore usually just anterior to hemal spine of 21th post-Weberian vertebrae, except for the specimen FMNH 58572, 20th. Caudal-fin rays always 6+7. Caudal fin with posterior margin ranging from straight to slightly convex and rounded dorsal and ventral corners. Post-Weberian vertebrae 38 [3]*, 36 [1]. First post-Weberian vertebrae nearly half the length of the subsequent one. Second vertebrae post-Werberian vertebrae with a wide, short and transversal hemal process. Ribs 11 [2], 13 [2]*.

Mesethmoid with anterior margin slightly concave. Autopalatine robust and laterally wide with long latero-posterior process, almost the same length of this bone. Anterior and posterior cranial fontanel present. Posterior cranial fontanel usually goes until the posterior region of parieto-supraoccipital. Postorbital process of sphenotic-prootic-pterosphenoid complex bone directed anteriorly. Uroyal anteriorly concave, anterolateral process wide and long with a concave constriction in its neck, its lateral process as a relative high width in compare to its length. Short and fin posterior process of the uroyal. All osteological characters from head can be better observed in the stereo triplet (Fig.07). Upper caudal plate formed by uroneural and two elements, hypural 3, and the fused hypural 4, and 5. Lower caudal plate consisting of single element presumably consisting of fusion of parhypural with hypurals 1 and 2. Epural absent.

Cephalic lateral line canals with simple, non-dendritic tubes ending in single pores. Supraorbital canal mostly within frontal bone. Supraorbital pores invariably present: s1 medial to nasal-barbel base and autopalatine, s3 medial to posterior nostril and anterior to frontal, and s6 paired posteromedial to eye and at medium length of frontal. A single lot of paratype with just one specimen (FMNH 58572) anomalously exhibiting just one S6 pore. Infraorbital canal consisting of posterior segment only, lacking associated ossification. Infraorbital pores present: i10 and i11 posterior to eye, and anterolateral to postorbital process of sphenotic-prootic-pterosphenoid. A

single lot of paratype with just one specimen (FMNH 58572) anomalously exhibiting i1 and i2. Otic canal without pores. Postotic pores present: po1 anteromedial to opercular patch of odontodes and lateral to joint between sphenotic-prootic-pterosphenoid and pterotic, and po2 medial to opercular patch of odontodes and lateral to joint between pterotic and posttemporo-supracleithrum. Lateral line of trunk anteriorly continuous with postotic canal and reduced to short, usually non-ossified tube. Lateral line pores invariably present: ll1 and ll2 dorsomedial to pectoral-fin base and posterior to posttemporo-supracleithrum.

Coloration in ethanol (Figs.5 and 6). Unpigmented body background pale yellow. Melanophores distributed into inner and outer skin layers. Dark brown to dark grey melanophores on inner skin layer forming maculae without defined shape. These maculae can be fused creating stripes along the body or being separated creating randomly distributed blotches in the body. This strip, in some specimens, creates the same pigmentation impression as in Trichomycterus itatiayae, occupying almost all the space of the caudal peduncle in some specimens, as can be seem in the holotype. On the fins there was possible to see some lighter pigmentations creating small lighter brownish spots randomly distributed on the fin-rays. There is no pigmentation in the ventral side of the body.

Discussion

The data provided above leave little doubt that the respective type material of *T. alternatus* and *T. zonatus* refer to different species (in the latter, one of the paratypes is a different species and comparisons that follow refer to the holotype and two conspecific paratypes; see explanation below). There are several morphological differences which are taxonomically relevant. For example, *T. alternatus* has two anterior infraorbital sensory canal pores (i1 and i3) while none is present in *T. zonatus* (Fig. 08). The number of pectoral-fin rays also differs significantly between the two holotypes, with *T. alternatus* having I+7 and *T. zonatus*, I+6. Also the first pectoral-fin ray is prolonged as a filament in the former and entirely absent in the latter. Vertebral number is another characteristic which readily distinguishes the two type specimens, with *T. alternatus* having 32-36 and *T. zonatus*, 38. The position of the first dorsal-fin pterygiophore also varies significantly, with *T. alternatus* having it inserted anterior to the 13th-17th neural spine (modally 16th, n=35) and *T. zonatus* to the 18th (in holotype and conspecific paratypes; for the third paratype, see below). The same differences apply to the anal-fin pterygiophore, which in *T. alternatus* inserts anterior to the 17th-20th (modally 19th, n=32) while in *T. zonatus* it is anterior to the 21st. Branchiostegal ray number is another meristic trait where the two species differ, with 6-7 in T. alternatus and 8 in *T. zonatus*. Additional differences exist, but they are less conclusive taxonomically because of intraspecific variation with overlapping values for the two species. In the latero-sensory canal system, the holotype of *T. alternatus* has one S6 pore (median), which in *T. zonatus* has two (paired) s6 pores (Fig. 08). Additional differences exist in morphometrics, with *T. alternatus* having a wider head (87.0-100.1%HL; vs. 82-89.5 in T. zonatus). Although the head in *T. zonatus* is clearly longer visually in a comparison between holotypes and many other specimens of the respective type series, such difference show overlap in values, thus not being

absolute criteria to distinguish the two taxa. Finally, the two species differ also in color pattern, a difference which is subtle yet consistent if the necessary details are observed. *Trichomycterus alternatus* will be distinguished by a line of dark and round maculae, dorsally and laterally on the mid-line in the body, usually not fusing with others in the mid-line. In the other hand, *T. zonatus* maculae is more randomly distributed fusing with other maculae not always organized in line as observed in fig. 05. Such differences are not obvious from an examination of Eigenmann´s Plate 51, fig. 1, which is not the holotype but instead a paratype, corresponding to specimen in Fig. 05C. This specimen is particularly close to the color of *T. alternatus*, though still typically *T. zonatus*-like. The difference in coloration is more pronounced in the holotype, which has massively confluent maculae, especially in the caudal peduncle region (Fig.05A).

The summation of all the differences above leave little doubt that the type material of *T. alternatus* and *T. zonatus* represent different species. Their distinguishing characteristics equal or surpass, in kind and degree, those normally seen between different species of *Trichomycterus* (Triques & Vono, 2003; Bockmann & Sazima, 2004; Wosiacki & de Pinna, 2008). This is a straightforward conclusion in face of the data provided above. However, it differs considerably from conceptions widespread in the literature about the identity of *T. zonatus* (Lima, 2008), which apply the name indiscriminately to many *T. alternatus*-like forms of *Trichomycterus* in the coastal basins in the region between the Rio Doce and Ribeira de Iguape. In reality, *T. zonatus* is a rather rare species in collections and for this study we located a single lot additional to the type series (MZUSP83139). Therefore, *T. zonatus* is a species in reality not present in most of the geographical range where it has been allegedly reported, such as the Rio Paraíba do Sul, Rio Doce and all smaller coastal basins in the intervening region (Lima, 2008; de Oliveira, 2011). While its

absence in the northern Southeastern Brazilian basins is likely, the southern range of T. zonatus is still undetermined.

The type series of *T. zonatus* poses a singular problem. One of the paratypes (FMNH 58572) clearly represents a different species from the holotype and two remaining paratypes. That specimen differs from the remainder of its type series by several relevant traits, such as the presence of a median (single) s6 supraorbital sensory pore (vs. paired in other types); presence of two anterior infraorbital sensory pores (i1, i3) (Fig.08); I+7 pectoral fin-rays, with the first ray prolonged as filament; 36 free vertebrae; the first dorsal-fin pterygiophore inserted anterior to the neural spine of 16th vertebra; the first anal-fin pterygiophore inserted anterior to the hemal spine of 20th vertebra; and 7 branchiostegal rays. As seen above, all those conditions contrast with those reported for the remaining type specimens of *T. zonatus*. In fact, they agree closely with those for *T. alternatus*. The color pattern of paratype FMNH 58572 also differs from that of its co-type specimens, matching that described for *T. alternatus*, with brownish rounded unfused maculae disposed along the midline of the body. The taxonomic status of that paratype is yet uncertain, since there are other names to be considered in the problem which lies beyond the scope of this paper. Still, it seems to correspond either to T. alternatus or to a form more closely related to the latter than to *T. zonatus*.

The lack of information on the type specimens of *T. alternatus* and *T. zonatus* have led to a number taxonomic uncertainties which on occasion have resulted in skewed biodiversity assessments. Alencar & Costa (2004), in describing *Trichomycterus caudofaciatus*, compared that species with *T. alternatus* saying that it differed from the latter by the presence of a fused s6 pore. However, as seen above, the s6 pore is also fused in both the holotype and paratypes of *T. alternatus*. Another case that deserves mention is that of *T. cubataonis* Bizerril, 1994. De Pinna &

Wosiacki (2003) considered this species as a junior synonym of *T. zonatus*, a decision later contested by Katz & Barbosa (2014). The original proposal of synonymy by Wosiacki & de Pinna was based on preliminary data on the types of *T. zonatus*, now expanded into the present paper. Under common yet erroneous concepts of *T. zonatus*, indeed *T. cubataonis* looks like a distinctive species. However, as seen above, *T. zonatus* is actually a rather different species from the Trichomycterus forms north of the Rio Ribeira de Iguape. The actual *T. zonatus* is quite similar in shape and coloration to the species described as *T. cubataonis*. We find it likely that *T. cubataonis* is closely related or synonymous with *T. zonatus*, rather than to forms north of their range. Resolution of this problem will have to await more data and specimens from the relevant localities.

The prospective delimitation of *T. alternatus* and *T. zonatus* opens interesting questions about the validity of other names applied to taxa in the region between the two type localities. The oldest of those is *Trichomycterus goeldii* Boulenger, 1896, described from "Colonia Alpina, Therezopolis", today the city of Teresópolis in the State of Rio de Janeiro. The entire city is drained by the rio Paquequer drainage, a tributary to the rio Paraíba do Sul, thus leaving no doubt about the hydrographic origin of the type specimen. Specimens subsequently collected from that drainage are certainly similar in general aspect to *Trichomycterus* samples from other regions in the Paraíba do Sul. It is possible that the name *T. goeldii* is the correct name to many such forms, and not *T. zonatus* or *T. alternatus* as commonly applied. A most likely junior synonym of *T. goeldii* is *T. paquequerense* (Miranda Ribeiro, 1943), from exactly the same drainage, the rio Paquequer. Other names that fit into the same general problems are *T. florensis* (Miranda Ribeiro, 1943) and *T. travassosi* (Miranda Ribeiro, 1949) (the latter two synonymized into *T. alternatus* by Wosiacki & de Pinna (2003). The latter three names have been proposed with little consideration for previously available names and require careful reevaluation. The diagnostic characters offered

are details known to undergo substantial intraspecific variation in species of *Trichomycterus* and in themselves provide no empirical support for taxonomic distinctiveness. Additionally, they have all been based on single specimens, further casting doubt on their validity. More recently, various additional species have been described from the Paraíba do Sul and basins adjacent to the Rio Doce whose distinctiveness from *T. zonatus*, *T. alternatus* or *T. goeldi* also needs to be reinvestigated. Those include forms such as *T. albinotatus* Costa, 1992, *T. auroguttatus* Costa, 1992 and *T. longibarbatus* Costa, 1992.

The case of *T. alternatus* and *T. zonatus* is very specific considering the great diversity of Trichomycterus species in Southeastern Brazilian drainages. Nonetheless, we believe that the lessons to be learned from them are general and bring to surface widespread problems and vices which plague the taxonomy of the genus as a whole. Such traditions include the description of species without consideration for geographical, intraspecific and ontogenetic variation, and the lack of attention to information on type specimens of older yet obscure names which may have priority. We believe that detailed study will reveal similar situations with species of other species groups of *Trichomycterus* in southeastern Brazil, such as *T. immaculatus* (Eigenmann, 1889), *T. brasiliensis* Lütken 1874.

References

Alencar, A. R. & Costa, W. J. E. M. 2004. Description of two new species of the catfish genus *Trichomycterus* from southeastern Brazil (Siluriformes: Trichomycteridae). **Zootaxa**, 744: 1–8.

Arratia, G. 1990. The South American Trichomycterinae (Teleostei: Siluriformes), a problematic group, In: Peters, G. & Hutterer, R. (Eds.). **Vertebrates in the tropics**. Bonn, Museum Alexander Koening. p. 395–403.

Barbosa, M. A. & Costa, W. J. E. M. 2010. Seven new species of the catfish genus *Trichomycterus* (Teleostei: Siluriformes: Trichomycteridae) from Southeastern Brazil and redescription of *T. brasiliensis*. **lchthyological Exploration of Freshwaters**, 21(2): 97-122.

Barbosa, M. A. 2013. Description of two new species of the catfish genus Trichomycterus (Teleostei: Siluriformes: Trichomycteridae) from the coastal river basins, southeastern Brazil. **Vertebrate Zoology**, 63 (3): 269 – 275.

Barbosa, M. A. & Costa, W. J. E. M. 2011. Description of a new species of the catfish genus Trichomycterus (Teleostei: Siluriformes: Trichomycteridae) from the rio de Contas basin, northeastern Brazil. **Vertebrate Zoology**, 61 (3): 307-312.

Barbosa, M. A. & Costa, W. J. E. M. 2012. *Trichomycterus puriventris* (Teleostei: Siluriformes: Trichomycteridae), a new species of catfish from the rio Paraíba do Sul basin, southeastern Brazil. **Vertebrate Zoology**, 62 (2): 155-160.

Barbosa, M.A. & Costa, W.J.E.M. 2003. *Trichomycterus potschi* (Siluriformes: Loricarioidei): a new trichomycterid catfish from coastal streams of southeastern Brazil. **Ichthyological Exploration of Freshwaters**, 14: 281 – 287.

Berry, Colin & Baker, Matthew D. 2010. Multimedia in Biochemistry and Molecular Biology Education Inside Protein Structures. Teaching in three dimensions. Biochemistry and Molecular Biology Education. Vol. 38, No. 6, pp. 425–429.

Bizerril, C. R. S. F. 1994. Descrição de uma nova especie de Trichomycterus (Siluroidei, Trichomycteridae) do Estado de Santa Catarina, com uma sinópse da composição da familia Trichomycteridae no leste Brasileiro. **Arquivos de Biologia e Tecnologia**, 37 (3): 617-628.

Bockmann, F. A. & Sazima, I. 2004. *Trichomycterus maracaya*, a new catfish from the upper rio Paraná, southeastern Brazil (Siluriformes: Trichomycteridae), with notes on the *T. brasiliensis* species complex. **Neotropical Ichthyology**, 2(2): 61-74.

Bockmann, F. A.; Casatti, L.& de Pinna, M. C. C. 2004. A new species of trichomycterid catfish from the Rio Paranapanema basin, southeastern Brazil (Teleostei: Siluriformes), with comments on the phylogeny of the family. **Ichthyological Exploration of Freshwaters,** 15 (3): 225-242.

Boulenger, G. A. 1896. Description of a new siluroid fish from the Organ Mountains, Brazil. **Annals and Magazine of Natural History, Series 6,** 18 (23): 154.

Burgess, W. E. 1989. An atlas of freshwater and marine catfishes. A preliminary survey of the Siluriformes. Neptune City, N.J., T.F.H. Publications, 784p. Pls. 1-285.

Chardon, M. 1968. Anatomie compareé de I'appareil de Weber et des structures connexes chez les Siluriformes. **Annales de Musee Royale de I'Afrique Centrale. Serie No. 8, Sceances Zoologiques**, 169: 1-277.

Costa, W. J. E. M. 1992. Description de huit nouvelles espèces du genre *Trichomycterus* (Siluriformes: Trichomycteridae), du Brésil oriental. **Revue française d' Aquariologie**, 18: 101-110.

da Silva, A. M.; Belei, F.; Giongo, P. & Sampaio, W. M. S. 2013. Estado da conservação da Ictiofauna Do Rio Guandu, Afluente Do Baixo Rio Doce, Espírito Santo, Sudeste Do Brasil. **Evolução e Conservação da Biodiversidade**, 4 (1): 8-13.

de Oliveira, M. L. M. 2011. Mapeamento físico dos genes ribosomais 18S e 5S em peixes do gênero *Trichomycterus* (Teleostei, Trichomycteridae). Botucatu, UNESP. Trabalho de conclusão de curso não publicado.

Datovo, A. & Bockmann, F. A. 2010. Dorsolateral head muscles of the catfish families Nematogenyidae and Trichomycteridae (Siluriformes: Loricarioidei): comparative anatomy and phylogenetic analysis. **Neotropical Ichthyology**, 8(2): 193-246.

de Pinna, M. C. C. 1992. A new subfamily of Trichomycteridae (Teleostei, Siluriformes), lower loricarioid relationships and a discussion on the impact of additional taxa for phylogenetic analysis. **Zoological Journal of the Linnean Society**, 106(3): 175-229.

de Pinna M. C. C. 1998. Phylogenetic relationships of Neotropical Siluriformes (Teleostei: Ostariophysi): historical overview and synthesis of hypotheses. *In*: Malabarba, L. R.; Reis, R. E.; Vari, R.P.; Lucena, Z.M. & Lucena, C. A. S. (Eds.). **Phylogeny and classification of neotropical fishes**. Porto Alegre, Edipucrs. p. 279-330

de Pinna M. C. C. 1999. Species concepts and phylogenetics. **Reviews in Fish Biology and Fisheries,** 9: 353–373.

de Pinna, M.C.C. & Wosiacki, W. 2003. Trichomycteridae. *In*: Reis, R.E.; Kullander, S.O. & Ferraris Jr., C.J. (Eds.). **Check list of the freshwater fishes of South and Central America**. , Porto Alegre, Edipucrs. p. 270-290.

DoNascimiento, C.; Prada-Pedreros S.; Guerrero-Kommritz J. 2014. *Trichomycterus venulosus* (Steindachner, 1915), a junior synonym of *Eremophilus mutisii* Humboldt, 1805 (Siluriformes: Trichomycteridae) and not an extinct species. **Neotropical Ichthyology**, 12(4): 707-715.

Eigenmann, C. 1917. Desciptions of sixteen new species of pygidiidae. **Proceedings American Philosophical Society**, 56: 690 – 703.

Eigenmann, C. 1918. The Pygidiidae, a family of South American cat-fishes. **Memoirs of Carnegie Museum**, 7: 259-373.

Ferraris Jr., C. J. 2007. Checklist of catfishes, recent and fossil (Osteichthyes: Siluriformes), and catalogue of siluriform primary types. **Zootaxa**, 1418: 1-628.

García-Melo, L.J.; Villa-Navarro, F.A. & DoNascimiento, C. 2016. A new species of *Trichomycterus* (Siluriformes: Trichomycteridae) from the upper río Magdalena basin, Colombia. **Zootaxa**, 4117 (2): 226-240.

Henn, A. W. 1928. List of types of fishes in the collection of the Carnegie Museum on September 1, 1928. **Annals of the Carnegie Museum**, 19(4): 51-99.

Ibarra, M. & Stewart, D. J. 1987. Catalogue of type specimens of Recent fishes in Field Museum of Natural History. **Fieldiana Zoology (New Series),** 35: 1-112.

Kartz, A. M. & Barbosa, M. A. 2014. Re-description of *Trichomycterus cubataonis* Bizerril, 1994 (Siluriformes: Trichomycteridae) from the Cubatão river basin, southern Brazil. **Vertebrate Zoology,** 64 (1): 3- 8.

Lima, S. M. Q.; Lazzarotto, H. & Costa, W. J. E. M. 2008. A new species of *Trichomycterus* (Siluriformes: Trichomycteridae) from lagoa Feia drainage, southeastern Brazil. **Neotropical Ichthyology**, 6(3):315-322.

Lundberg, J.G. & Baskin, J.N. 1969. The caudal skeleton of the catfishes, order Siluriformes. **American Museum Novitates**, 2398:1-49.

Miquelarena, A. M. & Fernández, L. A. 2000. Presencia de Trichomycterus davisi (Haseman, 1911) en la cuenca del Alto Paraná misionero (Siluriformes: Trichomycteridae). **Revista de Ictiologia**, 8 (1/2): 41-45.

Miranda Ribeiro, P. 1943. Dois novos pigidídeos brasileiros. **Boletim do Museu Nacional**, Rio de Janeiro, 9: 1-3.

Miranda Ribeiro, P. de. 1949. Duas novas espécies de peixes na coleção ictiológica do Museu Nacional (Pisces, Callichthyidae et Pygidiidae). **Revista Brasileira de Biologia**, 9: 143-145.

Ratnaparkhi, G. R; Awasthi S. K.; Rani, P.; Balaram, P.; Varadarajan, R. 2000. Structural and thermodynamic consequences of introducing aminoisobutyric acid in the S peptide of ribonuclease S. **Protein Engineering,** 13 (10): 697 – 702.

Roldi, M. M. C.; Sarmento-Soares, L.M.; Pinheiro, R.F.M. & Lopes, M.M. 2011. Os Trichomycterus das drenagens fluviais no Espírito Santo, Sudeste do Brasil (Siluriformes: Trichomycteridae). **Boletim Sociedade Brasiliera de Ictiologia**, São Paulo, 103:1-3.

Sales, N.G.; Mariani, S.; Salvador, G.N.; Pessali, T.C. & Carvalho, D.C. 2018. Hidden diversity hampers conservation efforts in a highly impacted Neotropical river system. Frontiers in Genetics, 9(271):1-11. doi: 10.3389/fgene.2018.00271

Sarmento-Soares, L. M.; Zanata, A.M. & Martins-Pinheiro, R.F. 2011. *Trichomycterus payaya*, new catfish (Siluriformes: Trichomycteridae) from headwaters of rio Itapicuru, Bahia, Brazil. **Neotropical Ichthyology**, 9(2):261-271.

Sato, L. R.; Oliveira, C. & Foresti F. 2004. Karyotype description of five species of *Trichomycterus* (Teleostei: Siluriformes: Trichomycteridae). **Genetics and Molecular Biology**, 27(1): 45-50.

Tchernavin, V.V. 1944. A revision of some Trichomycterinae based on material in the British Museum (Natural History). **Proceedings of the Zoological Society of London**, 114: 234-275.

Triques, M. L. & Vono, V. 2004. Three new species of Trichomycterus (Teleostei: Siluriformes: Trichomycteridae) from the Rio Jequitinhonha basin, Minas Gerais, Brazil. **Ichthyological Exploration of Freshwaters,** 15(2):161-172.

Vieira, F. 2010. Distribuição, impactos ambientais e conservação da fauna de peixes da bacia do rio Doce. MG-Biota, Belo Horizonte, 2(5): 5-22.

Westheimer, G. 2011. Three-dimensional displays and stereo vision. **Proc. R. Soc. B**, 278: 2241–2248. doi:10.1098/rspb.2010.2777

Wosiacki, W.B. 2004. New species of catfish genus Trichomycterus (Siluriformes, Trichomycteridae) from the headwaters of rio São Francisco basin, Brazil. **Zootaxa**, 592: 1-12.

Wosiacki, W. B. 2005. A new species of *Trichomycterus* (Siluriformes: Trichomycteridae) from south Brazil and redescription of T. iheringi (Eigenmann). **Zootaxa**, 1040: 49–64.

Wosiacki, W. B. & Garavello, J. C. 2004. Five new species of Trichomycterus from the rio Iguaçu (rio Paraná basin), southern Brazil (Siluriformes: Trichomycteridae). **Ichthyological Exploration of Freshwaters,** 15 (1): 1-16.

Wosiacki, W. B. & de Pinna, M. 2008. A new species of the neotropical catfish genus *Trichomycterus* (Siluriformes: Trichomycteridae) representing a new body shape for the family. **Copeia**, 2: 273–278.

Table List

Table 01. – Morphometric and meristic data of *Trichomycterus alternatus* (Eigenmann, 1917) based on type materials.

***Trichomycterus alternatus* (Eigenmann, 1917)**			
	Holotype FMNH 58082	**Paratypes FMNH 58083**	
		Range (n = 10)	**Mean**
Standard length (mm SL)	65.6	42.53 - 57.12	50.1
Head length (mm HL)	11.6	8.74 - 10.29	9.6
% of SL			
Head length	17.7	18.10 - 20.55	23.1
Predorsal length	66.4	62.89 - 67.09	65.0
Prepelvic length	54.4	55.22 - 59.10	57.2
Preanal length	73.4	71.78 - 76.57	74.3
Pectoral-fin length*	18.7	20.25 - 23.48	21.1
Pelvic-fin length	11.8	9.61 - 12.13	10.7
Distance of pelvic-fin base to anus	7.5	6.31 - 9.03	7.3
Caudal peduncle length	19.9	19.21 - 21.84	20.4
Caudal peduncle depth	11.9	9.89 - 12.38	11.2
Body depth	14.7	11.17 - 15.99	13.8
Dorsal-fin base length	10.2	9.30 - 11.63	10.6
Anal-fin base length	8.4	7.14 - 9.61	8.1
% of pectoral-fin length			
Filament of first pectoral-fin ray	29.0	19.88 - 39.024	31.7
% of HL			
Head width	107.8	86.98 - 100.11	93.1
Nasal barbel length	84.6	76.92 - 99.41	80.7
Maxillary barbel length	82.3	80.82 - 102.80	90.8
Rictal barbel length	61.2	56.28 - 72.05	63.8
Snout length	50.7	41.83 - 48.51	44.6
Interorbital width	26.4	22.06 - 30.73	25.9
Mouth width	50.8	35.41 - 44.14	38.7
Eye diameter	19.1	16.72 - 22.52	19.3
Opercle diameter	22.2	19.31 - 21.60	20.4
Interopercle length	37.6	30.22 - 39.92	34.3
Counting			**Mode**
Dorsal-fin rays	iii+II+7	[(ii - iii) + (II)+7]	iii + II + 7
Pectoral-fin rays	I+7	I+7	I+7
Pelvic-fin rays	I+4	I+4	I+4
Anal-fin rays	iii+II+5	[(ii - iii) + (II)+5]	iii+II+5

Caudal-fin rays	6+7	6+7	6+7
Ribs	10	10 - 12	10
Free vertebrae**	15D_19A/36	[(15 - 16 D)_(19A) 35 - 36]	15D_19A/36
Dorsal pterygiophore rays	8	8	8
Ventral pterygiophore rays	6	6	6
Dorsal procurrent rays	xix	xviii - xx	xviii
Ventral procurrent rays	xiv	xii - xiv	xiii
Ondontodes opercle	16	15 - 23	17
Odontodes interopercle	38	27 - 40	30
Lateral line pores	2	2	2
Pore of postotic sensory canal	2	2	2
Pores of infraorbital sensory canal	4	4	4
Pores of supraorbital sensory canal	3	3	3
S6 pore	1	1	1

* Full length of first pectoral-fin ray

** First dorsal and ventral pterygiophore anteriorly inserted in the free vertebra plus number of free vetebrae

Table 02. - Morphometric and meristic data of *Trichomycterus zonatus* based on type materials.

	***Trichomycterus zonatus* (Holotype)** FMNH58573	***Trichomycterus zonatus* (Paratype) 1/2** FMNH 58574	***Trichomycterus zonatus* (Paratype) 2/2** FMNH 58574	***Trichomycterus zonatus* (Paratype)*** FMNH 58572	**Trichomycterus zonatus (Holoype and 2 Paratypes) Mean**
Standard length (mm SL)	52.3	42.8	46.9	50.7	47.3
Head length (mm HL)	10.5	7.5	9.0	10.5	9.0
% of SL					
Head length	20.0	17.4	19.2	20.8	18.9
Predorsal length	67.2	64.5	63.4	63.7	65.0
Prepelvic length	57.6	54.1	54.9	53.7	55.5
Preanal length	73.0	70.1	70.7	71.6	71.3
Pectoral-fin length**	15.0	15.3	13.2	16.9	14.5
Pelvic-fin length	9.3	9.8	9.2	11.1	9.4
Distance of pelvic-fin base to anus	7.3	7.7	8.9	7.6	8.0
Caudal peduncle length	18.8	20.6	21.5	19.2	20.3
Caudal peduncle depth	12.7	10.8	11.4	11.3	11.6
Body depth	15.9	13.4	15.5	13.2	14.9
Dorsal-fin base length	10.9	11.0	12.6	12.6	11.5
Anal-fin base length	9.5	8.3	8.2	9.3	8.7
% of pectoral-fin length					
Filament of the first pectoral-fin ray	/n	/n	/n	21.1	/n
% of HL					
Head width	89.5	86.1	82.0	86.2	85.9
Nasal barbel length	62.5	64.1	48.2	56.3	58.3
Maxillary barbel length	68.4	73.1	63.7	47.2	68.4
Rictal barbel length	56.3	55.8	52.7	38.0	54.9
Snout length	42.2	46.3	39.7	44.7	42.7
Interorbital width	21.0	24.1	21.1	24.8	22.1

Mouth width	40.9	35.5	43.0	31.3	39.8
Eye diameter	16.4	19.9	14.4	12.9	16.9
Opercle diameter	18.3	20.7	19.9	17.7	19.6
Interopercle length	26.4	35.5	26.8	33.3	29.5
Counting					**Mode**
Dorsal rays	iii+II+7	iii+II+7	ii+II+7	iii+II+7	iii+II+7
Pectoral rays	I+6	I+6	I+6	I+7	I+6
Pelvic rays	I+4	I+4	I+4	I+4	I+4
Anal rays	iii+II+5	ii+II+5	ii+II+5	I+II+5	ii+II+5
Caudal rays	6+7	6+7	6+7	6+7	6+7
Ribs	13	11	13	11	13
Vertebrae***	18D_21V/38	18D_21V/38	18D_21V/38	16D_20V/36	18D_21V/38
Dorsal pterygiophore rays	8	8	8	8	8
Ventral pterygiophore rays	6	6	6	6	6
Dorsal procurrent rays	xvi	xiii	xiii	xx	xiii
Ventral procurrent rays	xii	xi	x	xii	xiii
Ondontodes opercle	14	10	14	15	14
Odontodes interopercle	-	15	17	27	16
Lateral line pores	2	2	2	2	2
Pore of postotic sensory canal	2	2	2	2	2
Pores of infraorbital sensory canal	2	2	2	4	2
Pores of supraorbital sensory canal	3	3	3	3	3
S6 pore	2	2	2	1	2

* *Trichomycterus* sp.

** Full length of first pectoral-fin ray

*** First dorsal and ventral pterygiophore anteriorly inserted in the free vertebra plus number of free vetebrae

Figure List

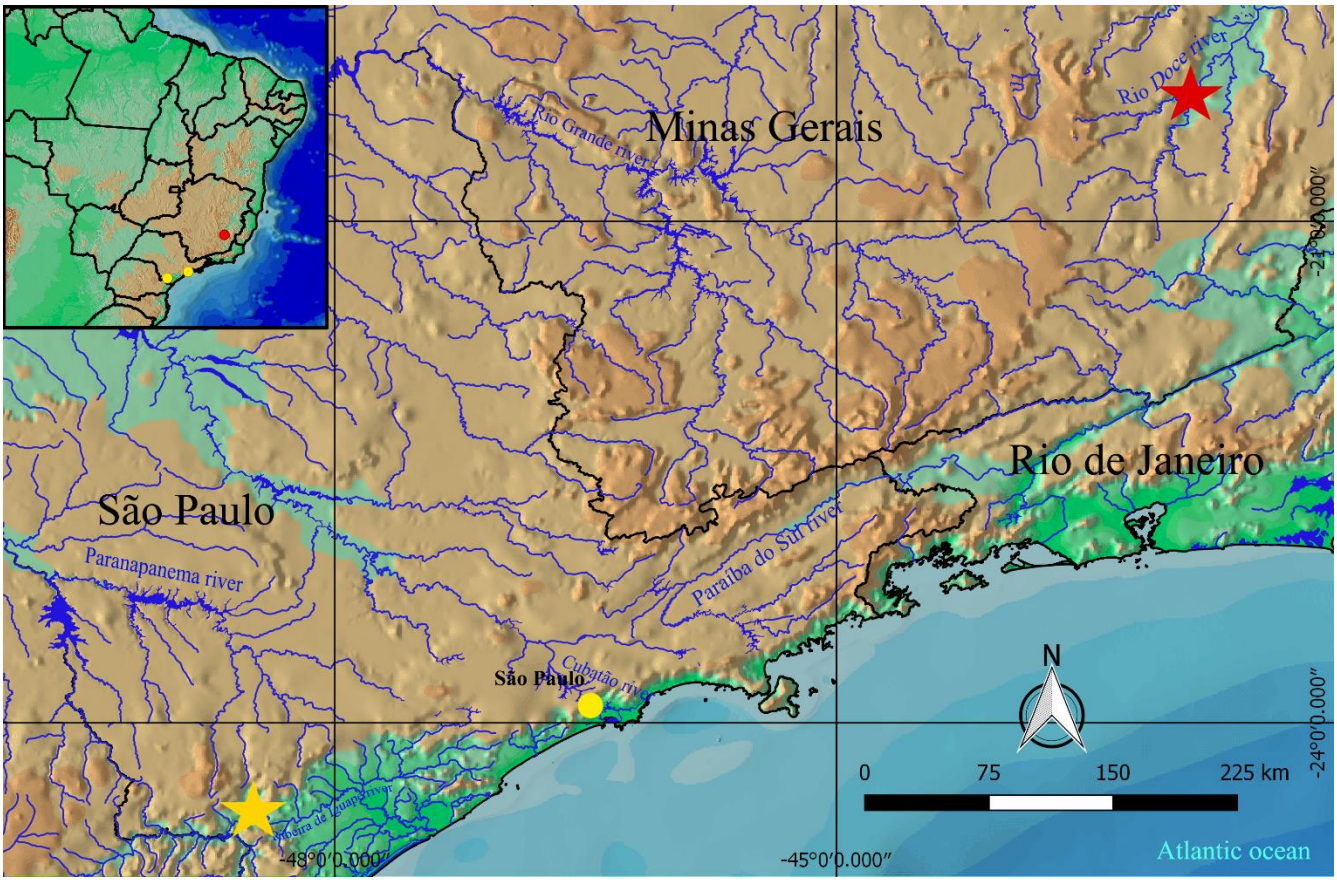

Fig. 01. - Geographical distribution of *Trichomycterus alternatus* and *Trichomycterus zonatus* type material. **Red star** – *T. alternatus*, holotype FMNH 58082 and paratype FMNH 58083; **yellow star** – *T. zonatus*, holotype FMNH58573 and paratype FMNH 58574; **yellow circle** - *T. zonatus* paratype FMNH 58572.

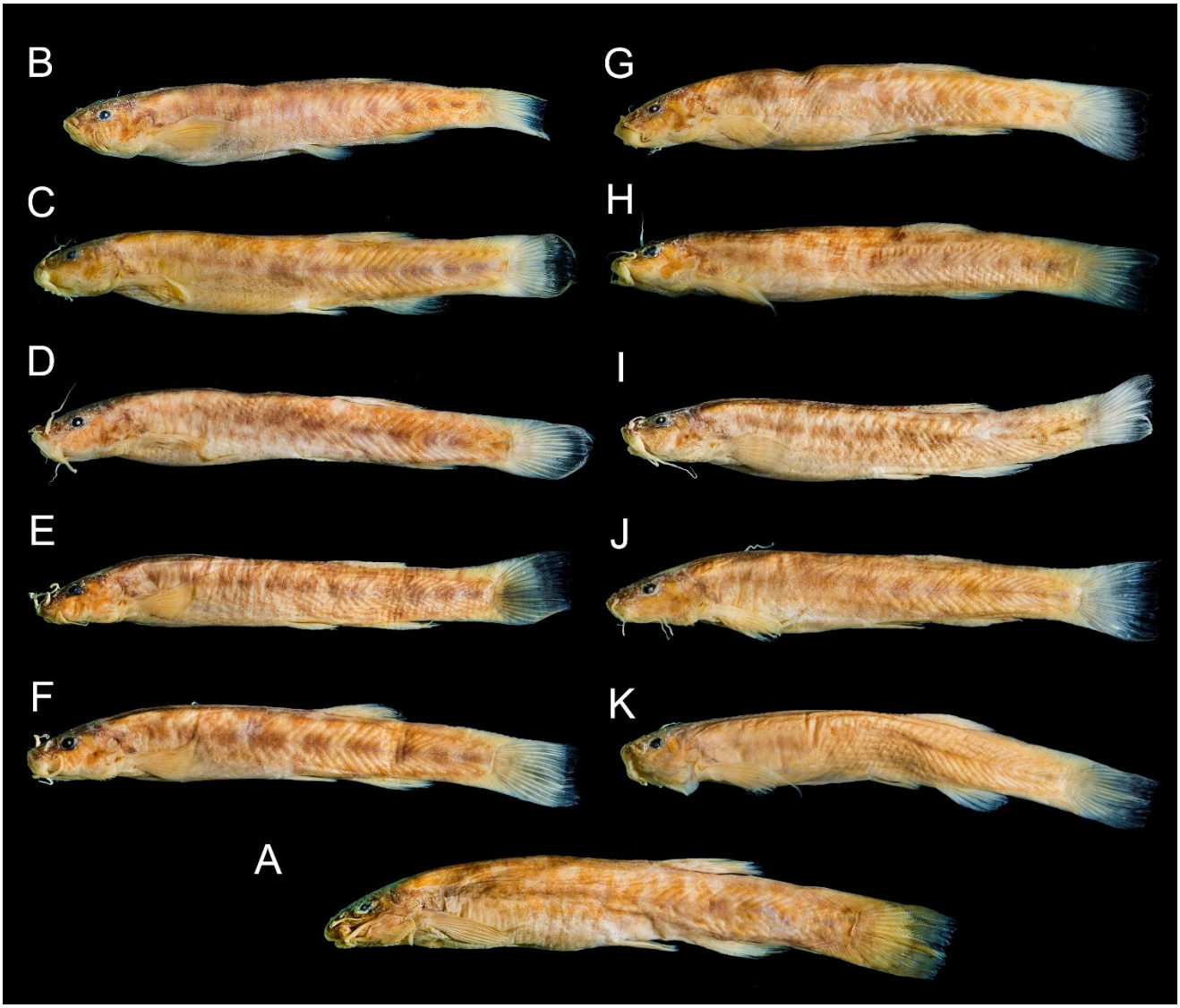

Fig. 02. - *Trichomycterus alternatus*. Lateral view of holotype FMNH 58082, (A) 65.57 mm SL and FMNH 58083, paratype, (B - K) 42.53 - 57.12 mm SL. Brazil, Minas Gerais: Rio Doce municipality. Photo by V. J. C. Reis.

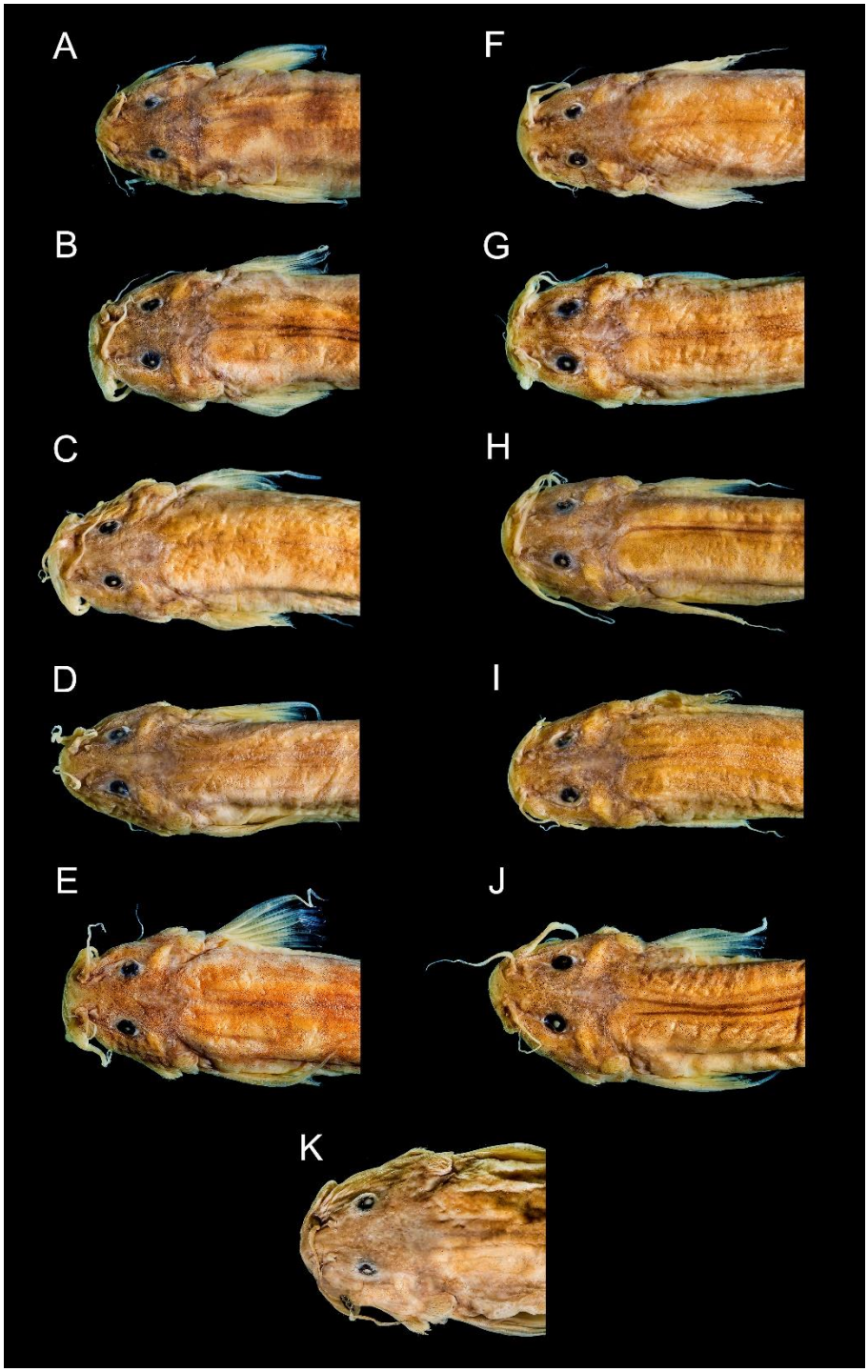

Fig. 03 - *Trichomycterus alternatus*. Dorsal head view of FMNH 58082, holotype, (K) 65.57 mm SL and FMNH 58083, paratype, (A-J) 42.53 - 57.12 mm SL. Brazil, Minas Gerais: Rio Doce municipality. Photo by V. J. C. Reis.

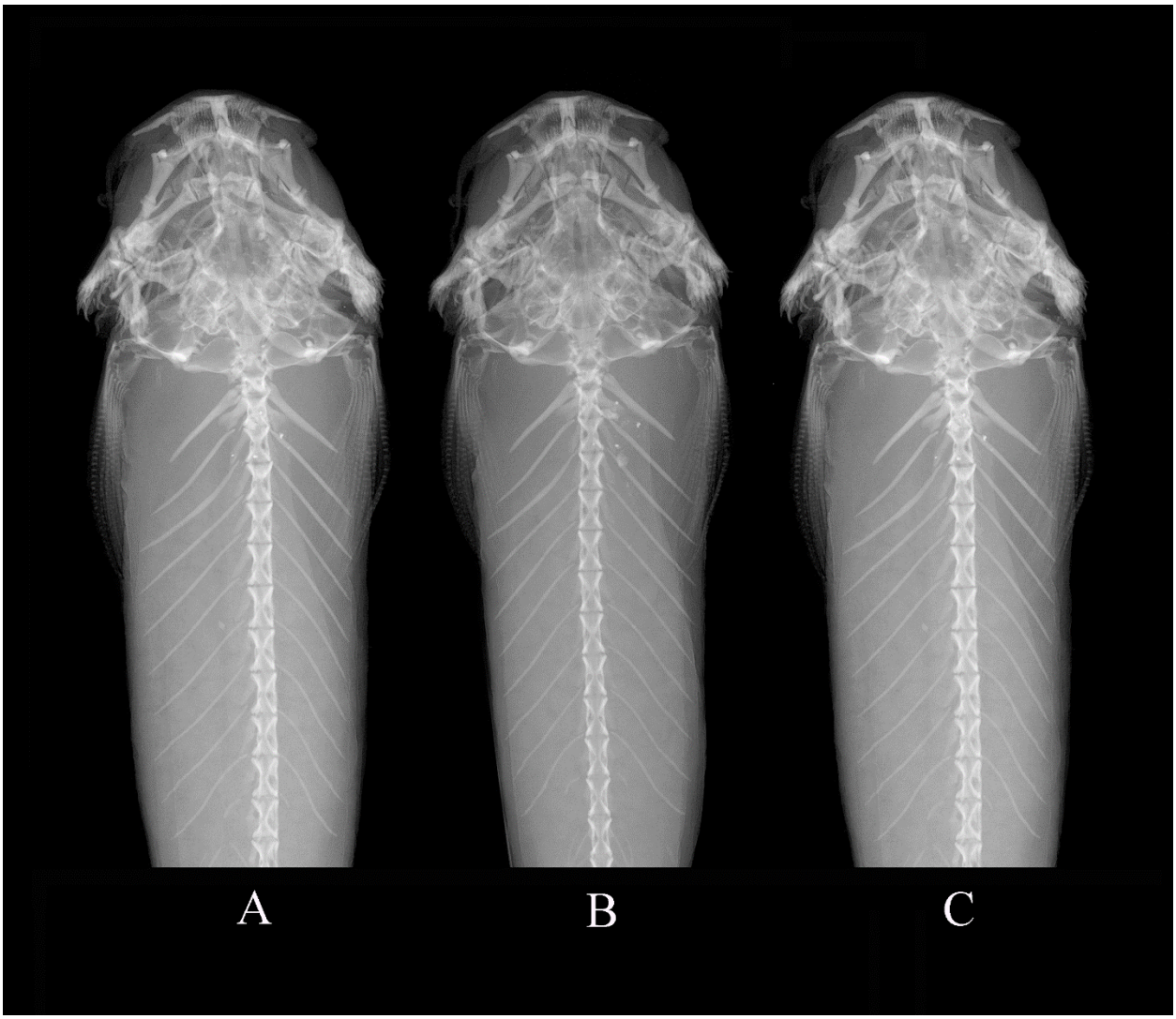

Fig. 04 - Stereo triplet of *Trichomycterus alternatus* holotype FMNH 58082. 3D image of ventral view formed on the right side and 3D image of dorsal view formed on the left side.

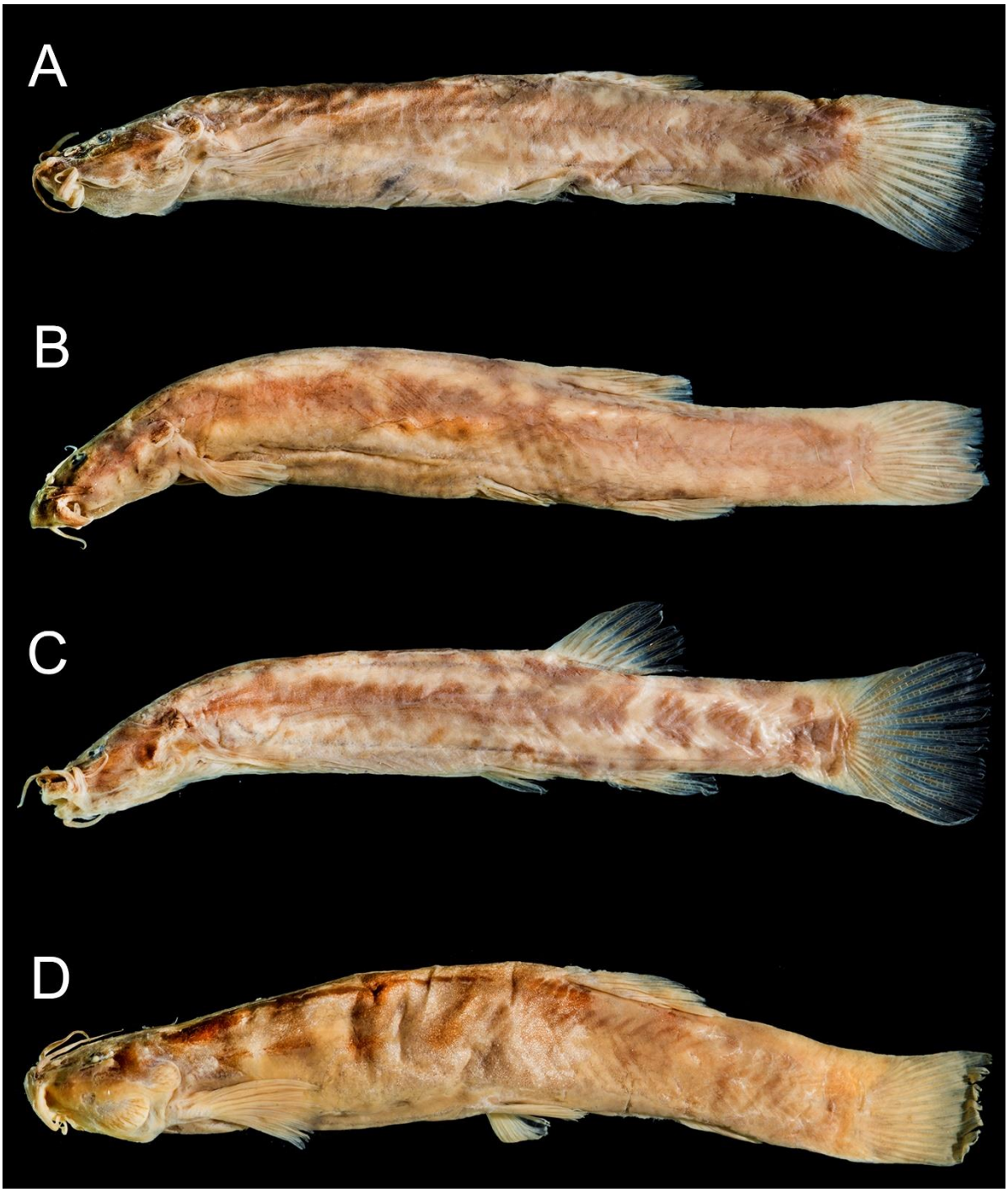

Fig. 05. - *Trichomycterus zonatus*. Lateral view of holotype FMNH58573, (A) 52.31 mm SL; FMNH 58574, paratype, (B and C) 42.83 - 46.85 mm SL, (both holotype and paratype from Água Quente); and FMNH 58572, paratype, (D) 50.69 mm SL., Cubatao, 7 miles west of Santos, São Paulo, Brazil. Photo by V. J. C. Reis.

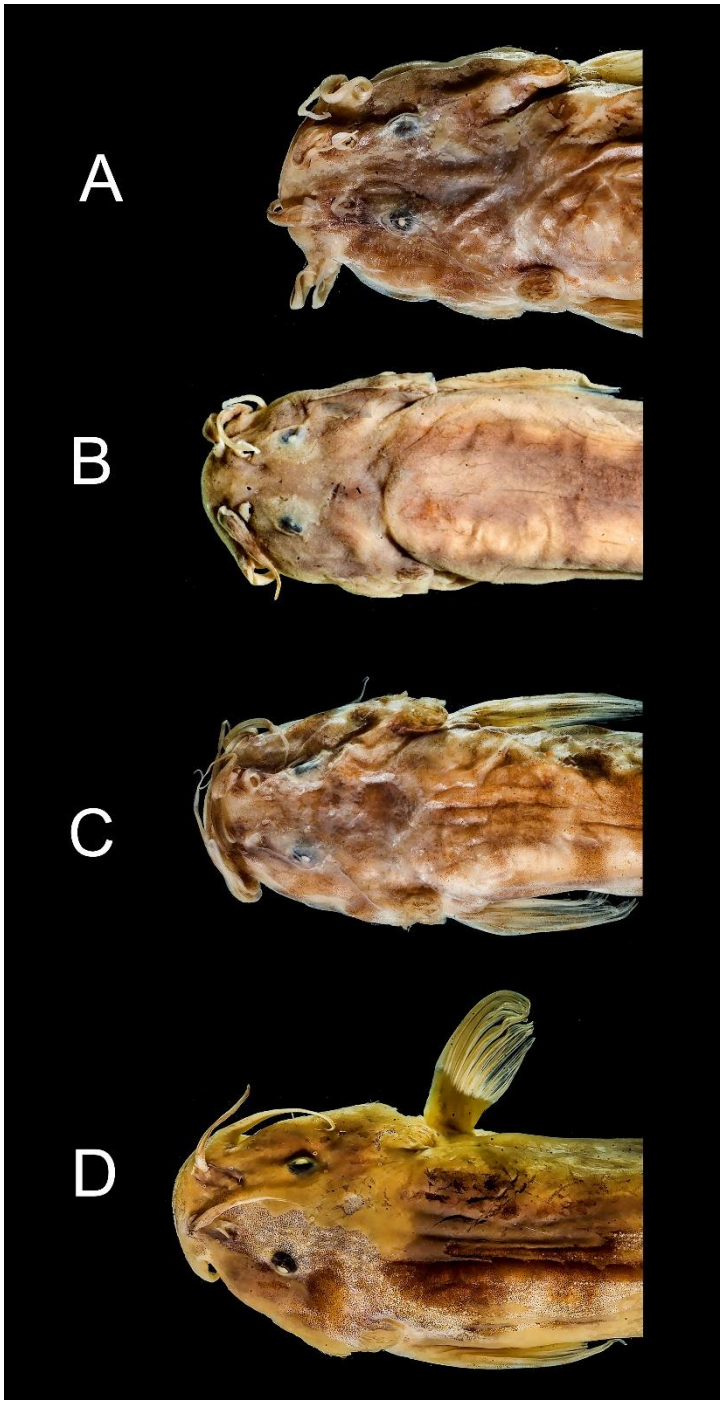

Fig. 06. - *Trichomycterus zonatus*. Dorsal head view of holotype FMNH58573, (A) 52.31 mm SL; FMNH 58574, paratype, (B and C) 42.83 - 46.85 mm SL, (both holotype and paratype from Água Quente); and FMNH 58572, paratype, (D) 50.69 mm SL., Cubatao, 7 miles west of Santos, São Paulo, Brazil. Photo by V. J. C. Reis.

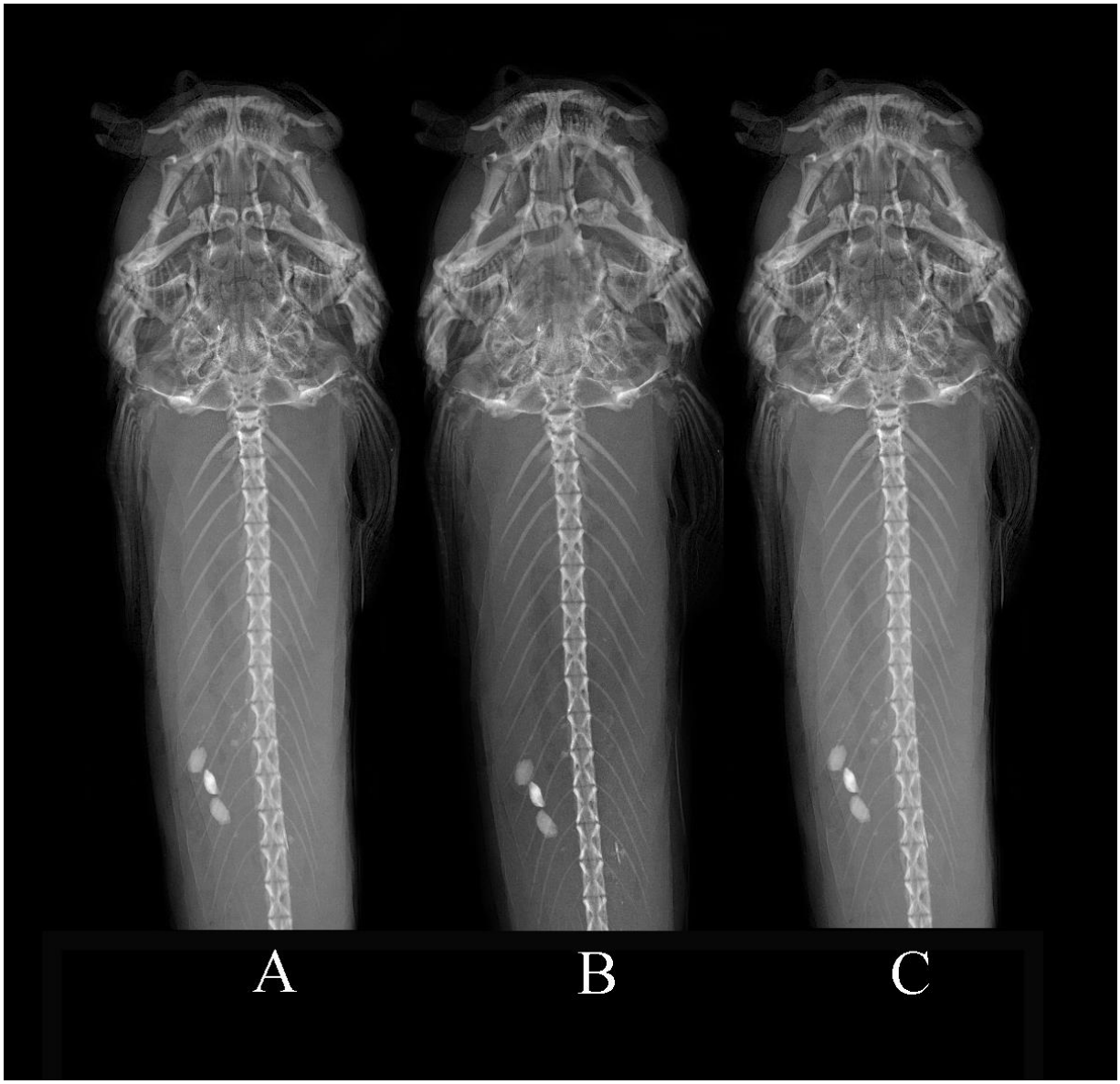

Fig. 07 - Stereo triplet of *Trichomycterus zonatus* holotype FMNH58573. 3D image of ventral view formed on the right side and 3D image of dorsal view formed on the left side.

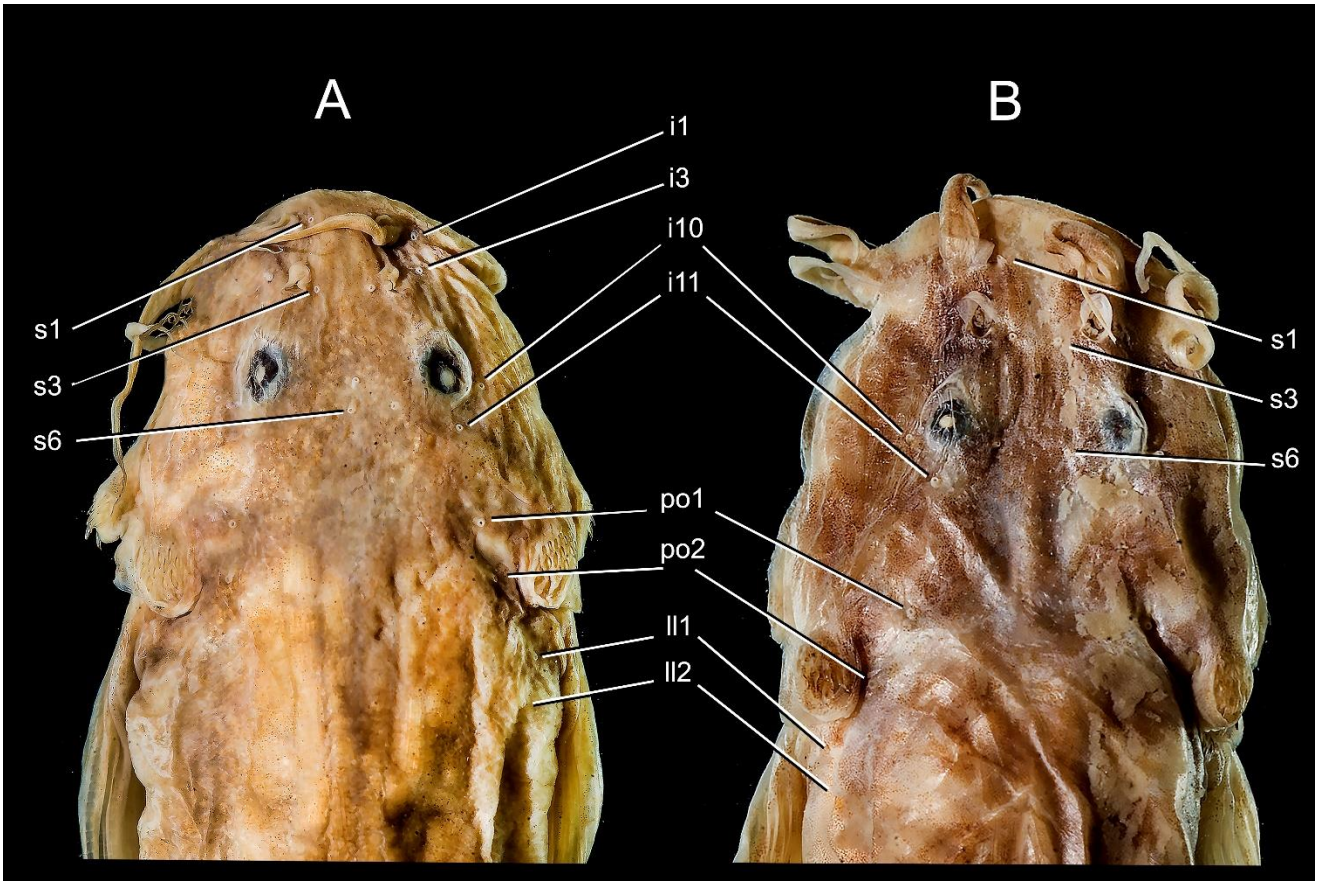

Fig. 08 – Sensory pores of head in (A) - *Trichomycterus alternatus* (holotype FMNH58082), and in (B) - *Trichomycteus zonatus* (holotype FMNH58573). Abbreviations: **i1**, infraorbital sensory pore 1; **i3**, infraorbital sensory pore 3; **i10-11**, infraorbital sensory pore 10 and 11; **ll1-2**, lateral line sensory pore 1 (supracleithral sensory branch) and 2; **po1-2**, postotic sensory pore 1 and 2; **s1**, supraorbital sensory pore 1; **s3**, supraorbital sensory pore 3; **s6**, supraorbital sensory pore 6 (epiphyseal branch).